ARABIDOPSIS THALIANA CARBOXYL-TERMINAL DOMAIN PHOSPHATASE-LIKE1 (CPL1) MEDIATES RESPONSES TO IRON DEFICIENCY AND CADMIUM TOXICITY

A Dissertation

by

EMRE AKSOY

Submitted to the Office of Graduate and Professional Studies of
Texas A&M University
in partial fulfillment of the requirements for the degree of

DOCTOR OF PHILOSOPHY

Chair of Committee,	Hisashi Koiwa
Committee Members,	Keyan Zhu-Salzman
	Alan E. Pepper
	Kendal D. Hirschi
	Scott A. Finlayson
Intercollegiate Faculty Chair,	Dirk B. Hays

May 2014

Major Subject: Molecular and Environmental Plant Sciences

ABSTRACT

The expression of genes that control iron (Fe) uptake and distribution (i.e., Fe utilization-related genes) is under a strict regulation. Fe deficiency strongly induces Fe utilization-related gene expression; however, little is known about the mechanisms that regulate this response in plants. In this dissertation, a RNA metabolism factor, *RNA POLYMERASE II CTD-PHOSPHATASE-LIKE1* (*CPL1*) was shown to localize to the root stele, and to be involved in the regulation of Fe deficiency responses in *Arabidopsis thaliana*. An analysis of multiple *cpl1* alleles established that *cpl1* mutations enhanced transcriptional responses of Fe utilization-related genes, e.g. *IRON-REGULATED TRANSPORTER1* (*IRT1*), to low Fe availability. In addition to the lower Fe content in the roots, but higher Fe content in the shoots of *cpl1-2* plants, the root growth of *cpl1-2* showed improved tolerance to Fe deficiency. Genetic data indicated that *cpl1-2* likely activates Fe deficiency responses upstream of both FE–DEFICIENCY-INDUCED TRANSCRIPTION FACTOR (FIT)-dependent and -independent signaling pathways. Interestingly, various osmotic stress/ABA-inducible genes were up-regulated in *cpl1-2*, and the expression of some ABA-inducible genes was controlled by Fe availability.

Unlike Fe, accumulation of the heavy-metal cadmium (Cd) in plants is toxic and it is absorbed by the roots due to the low selectivity of metal transporters such as AtIRT1. In this dissertation, CPL1 was also shown to regulate the transcriptional responses to Cd toxicity. *cpl1-2* showed higher tolerance to the Cd toxicity by enhancing the root-to-shoot translocation of Cd by an unknown mechanism. A knowledge-based screening resulted in identification of a putative metal transporter, *OLIGOPEPTIDE TRANSPORTER (OPT)*, which was highly induced in *cpl1-2* upon exposure to Cd. OPT was localized to the plastids, indicating a role of plastids in Cd transport and accumulation. The root growth of *opt* mutants showed higher tolerance to the Cd toxicity, and the mutants accumulated less Cd, Fe and Zn, indicating the involvement of OPT in the transport of these metals.

This presented dissertation suggests that 1) CPL1 functions as a negative regulator of the Fe deficiency signaling at the crosstalk with a branch of the osmotic stress/ABA signaling pathway, and 2) CPL1 regulates the Cd distribution in plants by repressing the expression of *OPT*.

ACKNOWLEDGEMENTS

Foremost, I would like to thank to my Ph.D. advisor, Dr. Hisashi Koiwa, for providing me the opportunity to work on this project as well as others to understand the molecular mechanisms of RNA metabolism regulator(s) in various environmental stresses, including Fe deficiency and Cd toxicity. I owe Dr. Koiwa a debt of gratitude for his systematic scientific support and encouragement to complete my dissertation in five years. I also thank my committee members, Drs. Keyan Zhu-Salzman, Kendal D. Hirschi, Alan E. Pepper and Scott A. Finlayson for their guidance and suggestions in experimentation and writing of the dissertation.

I thank all the past and present members of the Koiwa's and Zhu-Salzman's labs for their critical discussions in the lab meetings, support in the experiments and friendship not only in the lab, but also in other occasions. I believe they will be among my future collaborators. I also appreciate the tremendous support of the interdisciplinary MEPS program for providing travel grants and the Department of Horticultural Sciences for providing teaching assistantships for two and a half years. I also would like to thank Dr. William D. James in the Elemental Analysis Laboratory for his guidance in ICP-MS analyses.

I would like to acknowledge The Scientific and Technological Research Council of Turkey (TUBITAK) for providing me a scholarship in the first year of my Ph.D. education.

Last but not least, I thank my family and friends for their support. This dissertation work would not have been accomplished without their prayers.

NOMENCLATURE

Fe	Iron
Cd	Cadmium
Zn	Zinc
Mn	Manganase
Na	Sodium
K	Potassium
Cu	Copper
FIT	FER-LIKE IRON DEFICIENCY-INDUCED TRANSCRIPTION FACTOR
bHLH	Basic-Helix-Loop-Helix
FRO	FERRIC CHELATE REDUCTASE
IRT1	IRON-REGULATED TRANSPORTER1
FRD3	FERRIC REDUCTASE DEFECTIVE3
FER	FERRITIN
YSL	YELLOW STRIPE-LIKE
HMA	HEAVY METAL ATPASE
PCR	PLANT CADMIUM RESISTANCE
OPT	OLIGOPEPTIDE TRANSPORTER
TDT	TRIDENT
LEA	LATE EMBRYOGENESIS ABUNDANT
DUO1	DUO POLLEN1
NA	nicotianamine
PC	phytochelatin
GSH	glutathione
PCS	PCS SYNTHETASE
RNAPII	RNA polymerase II
CTD	C-TERMINAL DOMAIN

CPL1	CTD PHOSPHATASE-LIKE1
LUC	luciferase
GUS	β-glucuronidase
GFP	Green Fluorescent Protein
ABA	abscisic acid
ICP-MS	inductively coupled plasma–mass spectrometry

TABLE OF CONTENTS

Page

Page

Page

LIST OF FIGURES

FIGURE Page

FIGURE Page

LIST OF TABLES

CHAPTER I

INTRODUCTION AND LITERATURE REVIEW

1.1 Iron: An Essential Micronutrient

Iron (Fe) is an essential metal element for nearly all organisms and its deficiency causes serious problems. In plants, iron is present as a cofactor in many metallo-proteins and is found in active sites of photosynthetic and respiratory Fe-S clusters. Fe is also required for DNA and hormone biosynthesis, nitrogen fixation, sulfate assimilation, and chlorophyll biosynthesis (Hell and Stephan, 2003). On the other hand, Fe is highly reactive and excess Fe can trigger the production of reactive oxygen species (ROS) via Fenton reactions (Moller et al., 2007). In soil, the predominant form of Fe is Fe(III), which is abundantly present as insoluble ferric oxides and ferric hydroxides in aerobic environments (Guerinot and Yi, 1994; Palmer and Guerinot, 2009). The concentration of soluble form of iron, Fe(II), in aerated soils is lower than the iron concentration essential for plant survival (Marschner and Marschner, 1995; Marschner and Marschner, 2011). Therefore, plants suffer from Fe deficiency when grown on well-aerated calcareous or alkaline soils. One third of agricultural land all over the world is covered by these types of soils and is potentially Fe deficient (Driessen et al., 2000; White and Brown, 2010). Fe deficiency in plants induces intercostal/interveinal leaf chlorosis due to limited chlorophyll biosynthesis. This in turn causes significant yield losses of crops in the field. Since the main source of Fe in human diet is plants, low Fe levels in plants also compromises human health. Indeed, it is one of the most frequently deficient elements in human diet. Being the most common cause of anemia worldwide, Fe deficiency in humans is one of the crucial problems of both developed and developing countries. It is estimated that Fe deficiency anemia affects approximately two billion people, causing almost one million deaths each year (WHO, 2002). Therefore, understanding novel regulatory

mechanisms of Fe utilization in plants is essential for the bio-fortification of crop plants as better iron sources.

1.2 Iron Uptake and Distribution in Plants

1.2.1 Iron Uptake

Plants utilize two separate mechanisms to solubilize the insoluble ferric Fe [Fe(III)] in the rhizosphere and transport it through the plasma membrane (PM): reduction-based strategy (strategy I) and chelation-based strategy (strategy II) (Romheld, 1987; Marschner and Romheld, 1994; Welch, 1995; Schmidt, 1999; Gross et al., 2003; Grotz and Guerinot, 2006; Puig et al., 2007; Buckhout et al., 2009; Kobayashi et al., 2010; Conte and Walker, 2011; Schmidt and Buckhout, 2011; Thomine and Lanquar, 2011; Ivanov et al., 2012; Kobayashi and Nishizawa, 2012; White, 2012; Thomine and Vert, 2013).

1.2.2 Strategy I: The Reduction Strategy

In Strategy I plants, all dicots and non-graminaceous monocots such as *Arabidopsis thaliana*, Fe acquisition consists of three activities on PM of root epidermal cells: 1) rhizosphere acidification by PM-localized H^+-ATPase (AHA)-mediated proton extrusion, 2) reduction of insoluble Fe(III) to soluble ferrous [Fe(II)] by the PM-localized oxidoreductase, named FERRIC CHELATE REDUCTASE (FRO), and 3) consequent transport of Fe(II) ion into the root cells by a member of the ZINC (Zn)–Fe-REGULATED TRANSPORTER (ZIP) family of metal transporters.

There are many redundant isoforms of PM H^+-ATPases in plants. For instance, AHA family contains 12 members in Arabidopsis and some of them are regulated by Fe (Colangelo and Guerinot, 2004; Li W et al., 2007). Two of these, AHA2 and AHA7, have

roles in the Fe-deficiency response in the roots. AHA2 functions in the acidification of the rhizosphere after Fe deficiency, while AHA7 plays a role in the development of root hairs in response to Fe deficiency (Santi and Schmidt, 2009).

In Arabidopsis, the FRO family consists of eight members (Jeong and Connolly, 2009). Members of the FRO family show various specificities of tissue expression and subcellular localization (Guerinot, 2010). The first identified member of the family, FRO2, is localized to the PM of root epidermal cells (Robinson et al., 1999; Connolly et al., 2003; Feng et al., 2006; Mukherjee et al., 2006; Jeong et al., 2008; Jeong and Connolly, 2009), whereas FRO6 and FRO7 are expressed in the shoots (Wu et al., 2005; Mukherjee et al., 2006). As for the subcellular localizations, different FROs are found on PM, chloroplastic or mitochondrial membranes, or predicted to be localized to the secretory pathway (Heazlewood et al., 2004; Mukherjee et al., 2006; Jeong et al., 2008). Because of the diverse tissue and organelle specificities of FRO family proteins it is believed that reduction-based Fe transport is an essential component of iron uptake and homeostasis in plants. As a membrane electron transporter, FRO2 protein contains eight transmembrane domains and predicted binding sites for NADPH and FAD (Schagerlöf et al., 2006). AtFRO2 homologs are also well-characterized in various strategy I plants such as tomato (Li et al., 2004), pea (Waters et al., 2002) and cucumber (Waters et al., 2007). Arabidopsis FRO2 knock-out mutant, *frd1-1* (*ferric reductase defective 1-1*), does not show FRO activity and is chlorotic under Fe deficiency (Yi and Guerinot, 1996). Moreover, Arabidopsis, rice, soybean and tobacco plants overexpressing *FRO2* show tolerance to Fe-deficiency-induced chlorosis (Connolly et al., 2003; Oki et al., 2004; Vasconcelos et al., 2006; Ishimaru et al., 2007).

The reduced Fe is transported across the root PM by a member of the ZIP family transporters, IRON-REGULATED TRANSPORTER1 (IRT1) (Eide et al., 1996; Henriques et al., 2002; Varotto et al., 2002; Vert et al., 2002). IRT1 is a high-affinity transporter, which is strongly expressed in root epidermal cells and is localized to the PM

(Eide et al., 1996; Vert et al., 2002). Arabidopsis IRT1 can functionally complement yeast defective in Fe uptake, and is essential for Fe uptake as the *irt1-1* knock-out mutant is chlorotic and requires high levels of soluble Fe for survival (Eide et al., 1996). IRT1 is a non-selective Fe transporter since it can also transport manganese (Mn), zinc (Zn), cobalt (Co), nickel (Ni) and cadmium (Cd) in functional yeast complementation experiments (Vert et al., 2002). A paralog of IRT1 in Arabidopsis, IRT2, can also transport Fe and Zn in the same yeast complementation experiments (Vert et al., 2001). Although IRT2 is also induced under Fe deficiency and expressed in the root epidermis, its overexpression in *irt1-1* mutant cannot recover the iron uptake defect of *irt1* (Varotto et al., 2002; Vert et al., 2009). Moreover, an *irt2* mutant does not show chlorosis when Fe is limited, and unlike IRT1, IRT2 is localized to intracellular vesicles when transiently expressed in cultured cells (Vert et al., 2009). These data indicate that IRT1 is the primary Fe(II) uptake route in plants.

1.2.3 Strategy II: The Chelation Strategy

In Strategy II plants, which include Graminaceous plants such as wheat, rice and maize, phytosiderophores (PSs) are released into the rhizosphere, where they solubilize Fe(III) by forming a complex with it, and then the Fe(III)-PS complex is taken up into the root cells via the YELLOW STRIPE (YS) family of transporters, named for maize (*Zea mays*) ZmYS1 transporter (Takagi, 1976; Takagi et al., 1984; Curie et al., 2001; Kim and Guerinot, 2007; Curie et al., 2009; Kobayashi and Nishizawa, 2012). Phytosiderophores, such as mugineic acids (MAs), are synthesized from L-methionine in four sequential enzymatic reactions (Mori and Nishizawa, 1987; Shojima et al., 1990; Ma et al., 1999; Bashir et al., 2006; Ueno et al., 2007). L-methionine is generated as an end product of the sulfur assimilation pathway (Ravanel et al., 1995; Amir et al., 2002; Anjum et al., 2008). L-methionine is converted into S-ADENOSYL-L-METHIONINE (SAM) by SAM synthetase. Then, three molecules of SAM are converted first into nicotinamine (NA) by NICOTIANAMINE SYNTHASE (NAS), then by NICOTIANAMINE

AMINOTRANSFERASE (NAAT) to a 3'-keto acid, which is subsequently converted into 2'-deoxymugineic acid (DMA) by DEOXYMUGINEIC ACID SYNTHASE (DMAS) (Higuchi et al., 1999; Takahashi et al., 1999; Bashir et al., 2006). DMA is used as the precursor of nine types of MAs characterized to date. In barley and rye, two dioxygenases, IRON DEFICIENCY–SPECIFIC CLONE2 (IDS2) and IDS3 add further hydroxyl groups to DMA in order to generate MAs (Nakanishi et al., 2000; Kobayashi et al., 2001). There is a recycling mechanism, called Yang cycle, to provide methionine for the production of MAs (Ma et al., 1995). Fe deficiency induces the expression of genes encoding enzymes involved in the MA biosynthetic pathway, Yang cycle and the sulfur assimilation pathway (Kobayashi et al., 2005; Nagasaka et al., 2009).

Similar to Strategy I plants, some grasses can also acquire Fe(II) in addition to Fe(III)-PS by help of a Fe(II) transporter. Rice IRT1 functions in Fe(II) uptake as similar to its counterpart in Arabidopsis (Ishimaru et al., 2006). A mutation in the rice NAAT gene does not affect the plant growth as long as Fe(II) is supplied although the mutant cannot synthesize PS (Cheng et al., 2007). Interestingly, unlike Strategy I plants, rice H^+-ATPase and FRO activities are not induced by Fe deficiency. This suggests an adaptation of rice to its growth environment, where Fe(II) is highly accessible in submerged and anaerobic conditions (Itai et al., 2000; Ishimaru et al., 2006).

1.2.4 Iron Distribution

Once Fe(II) is absorbed into the roots, various transporters and chemicals are involved in its inter- and intracellular mobilization for storage and utilization. Even though Fe uptake mechanisms have been extensively studied in recent decades, less is known about the mechanisms involved in Fe distribution at the cellular and the organismal levels.

1.2.5 Intercellular Fe Distribution

Fe(II) can be chelated by nicotianamine (NA) and transported intercellularly by YELLOW STRIPE-LIKE (YSL) transporters (DiDonato et al., 2004; Waters et al., 2006; Waters and Grusak, 2008; Chu et al., 2010). NA is the biochemical precursor of PS in grasses. It can chelate Fe(II), Fe(III) and other divalent metal ions (Stephan and Scholz, 1993; von Wirén et al., 1999). NA is present both in roots and shoots (Stephan et al., 1990), and its concentration is much higher in phloem than in xylem, suggesting its probable function as the Fe chelator in phloem (Schmidke and Stephan, 1995; Pich and Scholz, 1996). A tomato mutant, *chloronerva* (*chln*) (Rudolph et al., 1985; Higuchi et al., 1996), defective in NA biosynthesis shows Fe deficiency symptoms such as interveinal chlorosis and high constitutive expression of Fe utilization-related genes (Stephan and Scholz, 1993), expression of which is reduced upon exogenous application of NA (Pich et al., 2001). Arabidopsis genome contains four NAS genes, among which NAS2 and NAS4 are induced in the roots under Fe deficiency (Klatte et al., 2009). Single mutants of all four NAS genes have wild-type levels of NA, indicating a functional redundancy among NAS family (Guerinot, 2010). Low levels of NA production, similar to tomato *chln* mutant, is only observed when all four NAS genes are mutated in a quadruple mutant of *nas4x-1* (Klatte et al., 2009). The Fe signaling is disrupted in the *nas4x-1* mutant since it displays Fe deficiency symptoms in shoots, roots and flowers, and accumulates low levels of Fe in flowers and seeds, suggesting NA functions in Fe deficiency responses and seed Fe accumulation. In addition to its function in metal transport in plants, increased NA accumulation has been used as a tool to improve the biofortification of Fe, Zn and Cu in the seeds of Arabidopsis, tobacco, barley and rice (Kim et al., 2005; Lee et al., 2009; Masuda et al., 2009; Usuda et al., 2009; Wirth et al., 2009; Zheng et al., 2010; Johnson et al., 2011).

Aforementioned ZmYS1 transporter is the first identified protein of the YSL family. It functions in root Fe-PS uptake from the rhizosphere, and it is suggested that YS1 may also

be involved in root-to-shoot distribution of Fe since it is upregulated in both roots and shoots under Fe deficiency (Curie et al., 2001). It is strongly believed that the YSL family of proteins transport Fe(II)-NA in both grasses and non-grasses, and Fe(III)-PS specifically in grasses. They function in Fe(III)-PS uptake from the rhizosphere into the roots in grasses, and Fe(II)-NA distribution in graminoids as well as non-graminoids (Curie et al., 2009). YSL family belongs to a novel family of OLIGOPEPTIDE TRANSPORTERS (OPTs) and have been shown to function in transit metal movements through the plasma membrane (Inoue et al., 2009; Lee et al., 2009). The OPT family belong to the peptide transporting protein families (Lubkowitz, 2006). Thus far, the YSL-family transporters has only been found in bacteria, archaea, fungi and plants, but not in animals (Lubkowitz, 2011). The Arabidopsis genome contains eight *YSL* genes (*YSL1-8*), which are shown to transport Fe(II)-NA complexes in yeast functional complementation experiments (DiDonato et al., 2004). The expression of *AtYSL2* is regulated by the availability of Fe and Cu, and it is believed to be involved in lateral movement of metal ions in vascular tissue (DiDonato et al., 2004; Schaaf et al., 2005). Although the single null mutants of *AtYSL1* and *AtYSL3* do not show any visible phenotypes (Jean et al., 2005), *ysl1ysl3* double mutant shows acute interveinal chlorosis due to lower Fe accumulation in the roots, leaves, and seeds. It also presents metal mobilization defects from leaves during senescence (Waters et al., 2006). These suggest that YSL1 and YSL3 play redundant roles in metal movement from leaves into developing seeds.

In addition to YSLs, OPT3 may also function as a transporter of Fe-chelates in Arabidopsis (Wintz et al., 2003; Stacey et al., 2008). Expression of *OPT3* is induced both in roots and shoots of Arabidopsis under Fe deficiency (Stacey, 2006; Buckhout et al., 2009). In *opt3-2* mutant, *AtOPT3* expression is decreased resulting in the accumulation of excessive levels of Fe in roots and shoots, but not in the seeds, in Fe sufficient conditions. In agreement with the *opt3-2* mutant phenotype of low Fe accumulation in the seeds, the loss-of-function *opt3-1* allele exhibits an embryo-lethal phenotype (Stacey et al., 2002). Since the movement of Fe to non-transpirating organs, such as seeds, is hypothesized to

take place exclusively thru phloem transport, it was suggested that the *opt3-2* mutation is involved in the transport of a peptide Fe-chelator via the phloem (Stacey et al., 2008). Another signature phenotype of *opt3-2* mutant is the induction of Fe deficiency responsive genes, *IRT1* and *FRO2*, in mutant roots even in Fe sufficient conditions. This indicates that OPT3 mediates long-distance signaling between shoots and roots (Lubkowitz, 2011).

In the vasculature, citrate, which is exuded by a FERRIC REDUCTASE DEFECTIVE3 (FRD3) transporter (Durrett et al., 2007), forms a tri-Fe(III), tri-citrate complex, first identified in tomato xylem sap, for long-distance transport (Rogers and Guerinot, 2002; Green and Rogers, 2004; Rellan-Alvarez et al., 2010). FRD3 is a member of the MULTIDRUG AND TOXIN EFFLUX (MATE) family of transporters, and is localized to the PM of the pericycle and the vasculature of roots in Arabidopsis (Roschzttardtz et al., 2011). The *frd3* mutant accumulates less Fe in the leaves, less Fe and citrate in the xylem exudate, and exhibits chlorosis even under Fe sufficient conditions (Green and Rogers, 2004). Fe-responsive genes such as *IRT1* and *FRO2* are constitutively activated in the roots of *frd3* mutant although it accumulates Fe in the roots (Green and Rogers, 2004). Interestingly, application of external Fe to the leaves of *frd3* mutant inhibits the constitutive activation of *IRT1* and *FRO2* in the roots, indicating a negative signaling transported from shoots to roots under Fe repletion (Lucena et al., 2006). Recently, FRD3 was presented as an essential cross-regulator of the Fe and Zn homeostasis in a Zn tolerance quantitative trait loci (QTL) analysis (Pineau et al., 2012).

1.2.6 Subcellular Fe Distribution

Chloroplasts and mitochondria are the major Fe usage sites within plant cells (Nouet et al., 2011). In the form of Fe-S clusters, chloroplast Fe makes up 70–90% of cellular iron in the mesophyll cells (Nouet et al., 2011). Besides chloroplasts and mitochondria, Fe is also found in nucleolus in Arabidopsis leaves and pea embryo (Roschzttardtz et al., 2011).

However, excess Fe is sequestered in the vacuole for long-term storage as it is highly reactive, and it can trigger the production of ROS within the cell (Moller et al., 2007).

Vacuole

Fe is mainly accumulated in globoid structures of protein storage vacuoles in endodermal cells of Arabidopsis and wheat embryos (Roschzttardtz et al., 2009). VACUOLAR IRON TRANSPORTER1 (VIT1) is responsible for Fe(II) transport into the vacuole in the Arabidopsis embryo (Kim et al., 2006). Yeast ortholog of AtVIT1, CCC1p (Ca2+-sensitive cross-complementer 1) can also transport Fe and Mn into the vacuoles, and its overexpression in yeast causes Fe accumulation in vacuoles (Li et al., 2001). AtVIT1 can functionally complement Δ*ccc1* yeast mutant by reducing the sensitivity of the mutant to toxic levels of Fe (Kim et al., 2006). VIT1 is expressed in the Arabidopsis vasculature and seed, with the highest expression observed during the development of embryo. Rice VIT1 homologs, OsVIT1 and OsVIT2, are highly expressed in flag leaves and are localized to the vacuolar membrane (Zhang et al., 2012). In addition to VIT1, IREG2/FPN2 (IRON REGULATED2/ FERROPORTIN2) also contributes to Fe sequestration in the root vacuoles (Morrissey et al., 2009). *IREG2/FPN2* is highly expressed upon Fe deficiency, and *fpn2* mutant shows a diminished Fe deficiency response. Interestingly, a member of MATE family, ZINC-INDUCED FACILITATOR1 (ZIF1), is responsible for Zn sequestration into the vacuole by transporting nicotinamine into the vacuole (Haydon and Cobbett, 2007). As nicotinamine may complex with Fe as well, it is expected to be transported into vacuole by ZIF1 (Haydon et al., 2012). Both ZIF1 overexpression and *zif1* loss-of-function mutants are hypersensitive to Fe deficiency, indicating the proper expression of *ZIF1* is required for Fe homeostasis. In contrast to VIT1 and ZIF1, AtNRAMP3 and AtNRAMP4 play a role in Fe export from vacuole to the cytoplasm both during germination and in other developmental stages (Lanquar et al., 2005).

Fe can also be sequestered in vesicles in addition to the central vacuole. AtIRT2 can function in Fe transport into the vesicles in order to protect the cell against Fe toxicity due to high FRO2/IRT1-mediated Fe acquisition into the root cells (Vert et al., 2001; Vert et al., 2009).

Plastids and Mitochondria

PERMEASE IN CHLOROPLASTS1 (PIC1) is localized to the inner membrane of chloroplasts and functions in Fe transport into the chloroplasts (Duy et al., 2007). In Arabidopsis *pic1* loss-of-function mutants, Fe accumulates more in the cytosol, and genes involved in photosynthesis are down-regulated, indicating the necessity of this transporter for plant growth and development (Duy et al., 2011). PIC1 interacts with NiCo, a predicted Ni or Co transporter, and forms an Fe import complex in the plastid envelope (Duy et al., 2011). It was speculated that PIC1 could work together with the protein translocon on chloroplast membranes in order to deliver Fe for the formation of Fe-S clusters (Teng et al., 2006). Localization of AtFRO7 (FERRIC-CHELATE REDUCTASE OXIDASE7) in the chloroplast envelope suggests the potential role of reduction machinery in Fe translocation into the chloroplasts (Jeong et al., 2008). Additionally, MAR1/IREG3 (MULTIPLE ANTIBIOTIC RESISTANCE1/IRON-REGULATED PROTEIN3) may be involved in Fe-NA complex transport into the plastids because of the sequence similarity to other IREG family of proteins, and the reversible leaf chlorosis of MAR1 overexpression plants by Fe application (Conte et al., 2009; Conte and Lloyd, 2010).

In Arabidopsis, one of the ABC family of proteins, ATP-BINDING CASSETTE TRANSPORTERS OF MITOCHONDRIA3 (ATM3), is suggested to function in the export of Fe-S clusters from mitochondria (Kushnir et al., 2001; Bernard et al., 2009). The homolog of yeast *ATM1*, *ATM3* is also named *STA1* and *AtABCB25 (Verrier et al., 2008)*. It is localized to the mitochondria and it can functionally complement the yeast *atm1* phenotype (Kushnir et al., 2001; Chen et al., 2007). The loss-of-function mutant of

AtATM3 presents a dwarf, chlorotic phenotype with altered leaf morphology and cell nuclei (Kushnir et al., 2001). Cytosolic Fe-S proteins and molybdenum cofactor activities are also reduced in the mutant (Bernard et al., 2009; Teschner et al., 2010), suggesting its involvement in the transport of a molecule necessary for the synthesis of both proteins. MITOCHONDRIAL FE TRANSPORTER (MIT)/MITOFERRITIN functions in Fe influx into the mitochondria in rice (Bashir et al., 2011). MIT complements the growth of yeast defective in mitochondrial Fe transport. The loss-of-function mutant of MIT is lethal whereas a weak mutant allele shows a reduction in the activity of aconitase, mitochondrial and cytosolic Fe-S enzyme, indicating the requirement of MIT for proper Fe loading into the mitochondria.

YSL isoforms localize to diverse organelles. HvYSL5 is localized to the vesicles or the tonoplast in barley (Zheng et al., 2011); OsYSL6 signals indicate a cytosolic localization in rice (Sasaki et al., 2011); Arabidopsis AtYSL4 and AtYSL6 are localized to the plastids in one study (Divol et al., 2013), or to the vacuolar membranes/the internal membranes similar to the endoplasmic reticulum in another study (Conte et al., 2013).

Fe-binding proteins, ferritins, function in sequestration of excess Fe (Waldo et al., 1995; Briat et al., 2010). They are the major storage form of Fe in the seeds and function in controlled release of Fe after germination (Goto et al., 1999). n the leaves, they can also function as Fe storage molecules in aiding the production of iron-containing proteins involved in photosynthesis (Lobreaux and Briat, 1991). Among 4 *FERRITIN (FER)* genes in Arabidopsis, *AtFER2* is the only one expressed in the seeds, whereas other *AtFERs* are expressed in vegetative and reproductive tissues (Petit et al., 2001; Petit et al., 2001). In *fet1-3-4* triple mutant devoid of ferritins, Fe homeostasis is altered in the reproductive organs, and Fe transport between the organs is disrupted, causing to Fe toxicity (Ravet et al., 2009; Briat et al., 2010). Interestingly, the expression of *AtFER1*, the most highly expressed ferritin gene in response to extra Fe, is under the control of various pathways. These include oxidative stress (Baruah et al., 2009), nitric oxide (NO) (Kim and Ponka,

2003; Arnaud et al., 2006), the ubiquitinylation (Ub) followed by 26S proteasome-dependent degradation of a repressor (Farrás et al., 2001), and dephosphorylation events occurring during Fe treatment Moreover, the central oscillator of the circadian clock and *TIME FOR COFFEE (TIC)*, circadian-clock regulator that is necessary to maintain clock period and rhythmic amplitude, also regulates the expression of *AtFER1* (Hall et al., 2003; Ding et al., 2007; Duc et al., 2009). Likewise, AtFER2 proteins is under post-translational regulation in response to intracellular iron levels in Arabidopsis (Ravet et al., 2009).

In addition to Fe transporters found in vacuole, chloroplast and mitochondria, one of the members of MATE family of proteins, BCD1 (BUSH-AND-CHLOROTIC-DWARF1), localizes to the Golgi complex and contributes to iron homoeostasis during stress responses and senescence in Arabidopsis (Seo et al., 2012).

1.3 Regulation of Fe Utilization-related Genes in Strategy I Plants

Plants have developed various ways to regulate the Fe homeostasis in cellular and organismal levels since its toxicity as well as deficiency cause deleterious consequences. One of those ways is the transcriptional regulation of genes involved in Fe uptake, mobilization, and signaling, collectively named as "Fe utilization-related genes" (Kobayashi et al., 2009).

The expression level of genes encoding components of the Fe acquisition mechanism, such as *FRO2* and *IRT1*, are under transcriptional regulation in Fe-limited conditions, as their mRNA levels increase in response to Fe deficiency (Eide et al., 1996; Robinson et al., 1999; Connolly et al., 2002; Vert et al., 2002). Central to this regulation are basic helix-loop-helix (bHLH) transcription factors, FER in tomato (Ling et al., 2002) and FER-LIKE IRON DEFICIENCY-INDUCED TRANSCRIPTION FACTOR (FIT) in Arabidopsis (Bauer et al., 2004; Colangelo and Guerinot, 2004; Jakoby et al., 2004; Yuan et al., 2005; Bauer et al., 2007). Similar to FER, FIT is located in the nucleus. In Arabidopsis, the

expression of *FIT* is induced only in the roots upon Fe deficiency. According to the microarray analysis of *FIT* loss-of-function mutant (*fit*), FIT regulates various Fe utilization-related genes, including *IRT1*, *FRO2*, and *NAS1* (Colangelo and Guerinot, 2004; Jakoby et al., 2004). Fe levels in roots and shoots of *fit* mutants is less than the levels in the wild-type plants. Shoots of the mutants show chlorosis and they need excess Fe supply for proper growth on soil (Colangelo and Guerinot, 2004).

Interestingly, constitutive overexpression of *FIT* does not induce *FRO2* and *IRT1* in the roots under Fe deficiency (Colangelo and Guerinot, 2004; Jakoby et al., 2004). This suggests that FIT requires some interacting factor(s) for its proper functioning in the regulation of Fe utilization-related genes. FIT dimerizes with group-Ib bHLH family transcription factors, bHLH38 or bHLH39, and directly activates the transcription of *IRT1* and *FRO2* (Yuan et al., 2008). While the induction of *FIT* expression during the Fe deficiency response is moderate (Bauer et al., 2004; Colangelo and Guerinot, 2004; Jakoby et al., 2004), *bHLH38*, *bHLH39*, *bHLH100*, and *bHLH101* are strongly up-regulated in both roots and shoots (Wang et al., 2007), most probably via signaling pathways separate from those regulating *FIT*. Because of the redundancy of their functions, single loss-of-function mutations in *bHLH* genes do not show any phenotypes (Wang et al., 2007). Co-overexpression of *FIT* together with *bHLH038* or *bHLH039* leads to the constitutive expression of *IRT1* and *FRO2*, and accumulation of their proteins even under Fe-sufficient conditions (Yuan et al., 2008). It has been proposed that the dimerization of FIT with different bHLHs determines the target specificity of Fe deficiency-induced transcriptional activation (Yuan et al., 2008). Despite the high homology to bHLH38 and bHLH39, the dimerization of bHLH100 and bHLH101 with FIT has not been shown yet. Moreover, *bhlh100/bhlh101* double mutant does not affect the expression of FIT-regulated transcripts, indicating bHLH100 and bHLH101 regulates the Fe homeostasis through a FIT-independent pathway (Sivitz et al., 2012). To date, little is known about the upstream mechanisms that sense cellular Fe levels and regulate the early signals that lead to the expression of *FIT* and group Ib *bHLH* genes.

In addition to the central pathway, there is another cell-specific regulatory mechanism mediated by the bHLH transcription factors POPEYE (PYE) and IAA-LEUCINE RESISTANT3 (ILR3), and the DNA-binding E3 ubiquitin–protein ligase BRUTUS (BTS) that operates in the root pericycle Fe response, controls root development, and regulates the internal Fe mobilization in the root and its root-to-shoot transport (Long et al., 2010). *pye-1* mutant has a chlorotic phenotype with retarded growth under Fe deficiency. Several Fe utilization-related genes, such as *bHLH39, bHLH101, FRD3, OPT3, ZIF1, NAS4, FRO3* and *NRAMP4*, are induced in the mutant roots. Among these genes, *ZIF1, NAS4* and *FRO3* are direct targets of PYE. Moreover, PYE can interact with ILR3, which connects auxin metabolism to metal homeostasis (Rampey et al., 2006). Interestingly, BTS contains several potential Fe binding sites and can interact with bHLH transcription factors related to PYE. Hence, it is speculated that BTS acts as a Fe sensor, which then can dimerize with PYE and regulate the Fe homeostasis in plants (Samira et al., 2013). Moreover, repression of *FER1* gene in the absence of excess Fe is mediated by the cis-element IDRS (iron-dependent regulatory sequence) (Petit et al., 2001). Overall, these regulators control specific branches of Fe deficiency signaling; however, the mechanisms that sense Fe availability and fine-tune the signal throughput of individual pathways have yet to be determined.

Fe utilization-related genes are not only controlled transcriptionally, but their protein products are also under post-translational regulation under changing Fe conditions. For instance, in addition to the control at the transcription level, FIT is also regulated post-translationally by differential activity and stability of FIT protein via proteasomal degradation (Lingam et al., 2011; Sivitz et al., 2011). Although not proven by experimentation yet, it is hypothesized that FIT is ubiquitinated by a lysine-63-linked ubiquitin conjugase, UBC13A or UBC13B, and then it is destined to 26S proteasome for degradation (Li and Schmidt, 2010). Moreover, FIT is stabilized by binding to ETHYLENE INSENSITIVE3 (EIN3) and ETHYLENE INSENSITIVE 3-LIKE1 (EIL1) transcription factors, which are activated by the activity of ethylene (Lingam et al., 2011).

Interestingly, NO works as a signal downstream of ethylene to further promote both the transcription of FIT gene, and the stability of FIT protein (Garcia et al., 2010; García et al., 2011; Meiser et al., 2011; Romera et al., 2011). Similar to FIT, IRT1 is also under post-translational control via ubiquitination and degradation. There are two separate routes of IRT1 degradation. First, PM-localized IRT1 can be conjugated with monoubiquitin and then internalized via endocytosis to be sorted into the vacuole for degradation. Second, a RING-type E3 ligase, *IRT1 DEGRADATION FACTOR1 (IDF1)*, can bind to and ubiquinate PM-localized IRT1, whereby it is degraded by the 26S proteasome (Shin et al., 2013). Rapid turnover of FIT and IRT1 is necessary for allowing the plants to rapidly react to changing conditions to maintain Fe homeostasis.

In addition to the transcriptional and posttranslational modifications, proper control of Fe utilization-related gene products, and in turn the Fe homeostasis is proposed to be highly complex with several layers of regulations, including alternative splicing, RNA processing, microRNAs and other post-translational modifications (Kong and Yang, 2010; Lan et al., 2011; Salvail and Massé, 2012; Samira et al., 2013). As far as RNA-binding proteins that can function in RNA metabolism and processing are concerned, abundance of several of them increases under Fe deficiency (Lan et al., 2011). For instance, elongation factor 5A (eIF5A) protein is abundantly found in Fe deficiency-treated Arabidopsis root proteome, and is thought to be essential for the control of RNA metabolism under Fe deficiency (Lan and Schmidt, 2011).

Among the various genes that affect the expression of Fe utilization-related genes, *TRIDENT* (*TDT*) is unique as it encodes a subunit of an RNA decapping enzyme that is involved in RNA metabolism (Goeres et al., 2007). The RNA metabolic pathway is a major mechanism in the co-/post-transcriptional regulation of diverse developmental and environmental responses (Kuhn and Schroeder, 2003; Gregory et al., 2008; Nakaminami et al., 2012). While ABA signaling is a prototypical target of RNA metabolism-mediated regulation, many transcripts are regulated by small RNAs, such as miRNAs and siRNAs

(Ramachandran and Chen, 2008). The *tdt* mutation has been shown to repress the expression of Fe utilization-related genes; however, whether this is due to severe growth defects in the mutant or to specific Fe signaling defects has not been elucidated (Goeres et al., 2007).

A wide range of physiological and molecular signals influence Fe signaling in Arabidopsis. In contrast to the positive regulation of ethylene, cytokinin and ABA repress the expression of *IRT1, FRO2,* and *FIT* (Seguela et al., 2008). Environmental stresses, such as salt/osmotic stress, attenuate Fe deficiency responses (Seguela et al., 2008), whereas phosphate starvation triggers the Fe deficiency responses (Hirsch et al., 2006; Thibaud, 2010). Moreover, volatiles emitted by soil microbes can up-regulate the expression of Fe utilization-related genes (Zhang et al., 2009). The molecular mechanisms that facilitate multiple inputs into Fe signaling have not been determined; however, the plasticity of Fe signaling implies the presence of diverse regulatory components that are coordinated to achieve proper levels of cellular Fe.

1.4 Cadmium: A Non-essential Transition Metal

Cadmium (Cd) is a non-essential transition metal classified as a heavy metal due to its potential harmful effects on living organisms even at very low concentrations (Duffus, 2002). Unlike essential metals, such as Fe, Mn and Zn, Cd does not have any known biological functions even though it is shown to function as a micronutrient in the marine alga *Thalassiosira weissflogii* by replacing Zn as a cofactor in the carbonic anhydrase CDCA1 under insufficient Zn availability near the surface of the sea (Price and Morel, 1990; Lane et al., 2005). Interestingly, heavy metals can enhance the plant defense mechanisms against herbivores and pathogens (Boyd et al., 2002; Hanson et al., 2003; Poschenrieder et al., 2006). As an example, Cd hyperaccumulation protects Noccaea *caerulescens* (previously known as *Thlaspi caerulescens*) leaves against feeding damage by thrips (Jiang et al., 2005).

Cadmium is emitted to the biosphere from both natural (geogenic) and industrial (anthropogenic) sources (Singh and McLaughlin, 1999; Garrett, 2000; NCM, 2003). In contrast to the natural sources of Cd mobilization from the crust of the earth, such as volcanoes and weathering of rocks, Cd extraction and extensive usage in technology by humans causes elevated contamination in air, water and soil. Massive areas of top soil in the world have been contaminated with Cd since the industrial revolution, mainly due to mining, metal industry activities, sewage sludge disposal, uncontrolled disposal of batteries and car tires, and the intensive use of phosphate fertilizers rich in Cd (Buchauer, 1973; Fergusson et al., 1980; McBride et al., 1997; Polle and Schützendübel, 2004; Leitenmaier and Küpper, 2013). It is estimated that Cd contamination in top soil in countries including the UK, Austria, Denmark, Greece and Ireland will increase 4 – 43% by the end of the century (NCM, 2003; Programme, 2008).

Among heavy metals, Cd is very phytotoxic since it is highly soluble in water and it is readily phytoavailable in the soil for plant absorption (Singh and McLaughlin, 1999; Traina, 1999). Hence, Cd is promptly absorbed by the plants, accumulated in the edible parts, and contaminates the food chain, which consequently causes severe health risks to humans including diabetic renal complications, hypertension, osteoporosis, leukaemia and cancer (Alfvén et al., 2000; Nordberg, 2003; Satarug et al., 2003; Bernard, 2008; Nordberg, 2009; Satarug et al., 2011).

Even at low concentrations, cadmium can result in severe problems in non-tolerant plant species. It can alter the redox status, and in turn metabolism of the cell by highly reacting with the sulphydryl groups of proteins (Appenroth, 2010). Genotoxic effects of Cd in plants include competition for the binding sites of essential divalent metals such as iron (Fe^{2+}), zinc (Zn^{2+}), magnesium (Mg^{2+}) and calcium (Ca^{2+}) and formation of ROS, which consequently results in lipid peroxidation, protein degradation and genome instability (Siedlecka and Krupa, 1996; Das et al., 1997). Cd also causes reduction in water and nutrient uptake (Sanita di Toppi and Gabbrielli, 1999). Consequently, Cd exposure

induces leaf chlorosis and malnutrition, and inhibits photosynthesis, respiration, nitrate metabolism and overall plant growth (Yadav, 2010).

1.4.1 Strategies to Cope with Cd Toxicity in Plants

As sessile organisms, plants have adapted various strategies to cope with the adverse effects of heavy metals. Plants can be divided into three main categories according to their abilities to cope with heavy metals (Alloway, 2013; Smolders, 2013):

1) Sensitive (Indicator) plants, such as *Arabidopsis thaliana* and *Brassica juncea* (Indian mustard), cannot tolerate even low levels of heavy metals and show lower bioaccumulation of toxic metals (Smolders, 2013). They adjust the metal uptake in order to balance the internal concentration of the metal with its external levels.

2) Tolerant plants, maintain low and constant metal concentration in their shoots by either preventing the uptake of heavy metals into the roots (in case of avoiders), or sequestering heavy metals into root vacuole, or transporting excess amounts of heavy metals back into the rhizosphere, which is seen in excluders (Ernst, 2006).

3) Hyperaccumulator plants can tolerate extreme levels of metal(s) in roots and shoots as a result of vacuolar compartmentalization and chelation. They show higher rates of metal uptake and its root-to-shoot translocation (Chaney et al., 1997). Moreover, these plants also have developed strategies for reducing the toxic side effects of heavy metals, such as enhanced detoxification systems.

1.5 Cd Uptake, Complexation, and Distribution

1.5.1 Cd Uptake into the Roots

There are two phases of Cd uptake into the roots: apoplastic binding and symplastic uptake (Hart et al., 1998; Zhao et al., 2002; Lin and Aarts, 2012). Chemically resembling Zn, Fe and Ca, Cd enters the root cells as a cation non-selectively through ZIP (ZRT-IRT like protein; Zinc-regulated transporter/Iron-regulated transporter-like Protein) transporters, e.g. AtIRT1 (Cohen et al., 1998; Connolly et al., 2002; Vert et al., 2002), NcZNT1/NcZIP4 (Plaza et al., 2007), and wheat TaLCT1 (Clemens et al., 1998; White and Broadley, 2003; White, 2005), or Ca channels, e.g. depolarization-activated calcium channels (DACC), hyperpolarization activated calcium channels (HACC), and voltage-insensitive cation channels (VICC) (Verbruggen et al., 2009), or as Cd-chelators via YSL transporters (Curie et al., 2009). IRT1 may especially cause the accumulation of Cd under Fe deficiency because of its broad range of metal specificity (Rodecap et al., 1994; Cohen et al., 1998; Korshunova et al., 1999; Vert et al., 2002; Schaaf et al., 2006). Moreover, overexpression of *IRT1* leads to a Cd-sensitive phenotype in transgenic plants (Connolly et al., 2002).

1.5.2 Cd Complexation

Once entered the roots, Cd ions can complex with thiol and non-thiol ligands. Thiol ligands include metallothioneins (MTs), glutathione (GSH) and phytochelatins (PCs), and whereas non-thiol ligands include organic acids (Küpper, 2004; Leitenmaier and Küpper, 2013).

Metallothioneins (MTs) are cysteine-rich peptides that can complex with metals (García-Hernández et al., 1998; Cobbett and Goldsbrough, 2002). They are induced in Cd/Zn hyperaccumulator *N. caerulescens* even though they generally do not complex with stored

metals (Papoyan and Kochian, 2004). On the other hand, they function in the detoxification of copper (Cu), which is highly accumulated in Cd/Zn hyperaccumulator due to its unavoidable transport by overexpressed Cd/Zn transporters (Walker and Bernal, 2004). Hence, MTs were reported to bind to the excessive Cu accumulated in Cd/Zn hyperaccumulator *N. caerulescens* (Mijovilovich et al., 2009). Interestingly, they are also induced under abiotic stresses in rice and wheat (Cobbett and Goldsbrough, 2002). Moreover, transgenic tobacco plants overexpressing mouse MT show higher Cd tolerance (Pan et al., 1994), whereas ectopic expression of *Brassica juncea* MT2 in Arabidopsis results in increased Cd and Cu tolerance (Zhigang et al., 2006).

PCs are small peptides derived from reduced glutathione in a dipeptidyltransferase reaction catalyzed by cytosolic PC SYNTHETASE (PCS) (Grill et al., 1989; Ha et al., 1999; Vatamaniuk et al., 1999; Cobbett and Goldsbrough, 2002). They can form low-molecular-weight (LMW) complexes with heavy metals, especially with Cd, with molecular weights in the range of 2500-3600 Da. To protect the cytosol from free Cd^{2+} ions, these complexes are sequestered into the vacuole, where they ultimately procedure high-molecular-weight (HMW) complexes (Cobbett, 2000; Cobbett and Goldsbrough, 2002). There are two *PCS* genes in *A. thaliana* genome. A loss-of-function mutant of *AtPCS1* (*cad1*) cannot produce PCs, and thus is Cd hypersensitive (Howden et al., 1995). Moreover, biochemical inhibition of PCS enhances the hypersensitivity of non-hypertolerant plants towards Cd toxicity due to inhibited PC production (Schat et al., 2002). Involvement of *PCS1* in Cd detoxification was also shown by heterologous expression of *AtPCS1* and wheat *TaPCS1* in native PCS-deficient yeast species of *Saccharomyces cerevisiae (Clemens et al., 1999)*. *AtPCS2*, on the other hand, did not show a strong Cd tolerance in yeast complementation experiments even though it functions in PCs production (Cobbett et al., 1998; Cazalé and Clemens, 2001). *PCS* genes, especially *PCS1*, are highly induced in non-hyperaccumulators even under low concentrations of Cd, indicating the necessity of PC accumulation in response to Cd toxicity (Clemens et al., 1999; Ha et al., 1999; Vatamaniuk et al., 1999; Andresen et al., 2013). Overexpression

studies on *PCS* genes gave contradictory findings such that the expression of *AtPCS1* in *B. juncea*, and the expression of *Thlaspi caerulescens PCS* in tobacco enhanced the Cd tolerance, whereas the overexpression of *AtPCS1* in Arabidopsis caused Cd hypersensitivity (DalCorso et al., 2013). Interestingly, the levels of PCs were found to be lower in hyperaccumulators than non-accumulators (Ebbs et al., 2002; Mijovilovich et al., 2009), and the chemical inhibition of PCS in hyperaccumulators did not affect the Cd tolerance, indicating the main function of PCs in hyperaccumulators might be more towards metal translocation than sequestration (Schat et al., 2002). PCs also have a role in root-to-shoot translocation of metals since more Cd is accumulated in the shoots and less in the roots of Arabidopsis plants that expressed wheat *PCS1* specifically in the roots (Gong et al., 2003).

Besides being the precursor of PCs, GSH can bind to Cd as a low affinity ligand. It also functions in scavenging of ROS, which are highly produced under Cd toxicity (Ogawa, 2005). GSH levels were reported to be induced (Pietrini et al., 2003; Sun et al., 2005; Sun et al., 2007) or repressed (Xiang et al., 2001; Ahner et al., 2002; Küpper, 2004) in different species under Cd treatments, representing the multiple functional layers of GSH in Cd toxicity.

1.5.3 Cd Distribution

Sequestration into the Vacuole

In the root cells, Cd-thiol complexes are either sequestered into the vacuole in non-hyperaccumulators (DalCorso et al., 2008), or reach the stele via apoplastic and/or symplastic pathways in hyper-accumulators (Salt et al., 1995; Leitenmaier and Kuepper, 2011). Metal transporters involved in vacuole Cd sequestration include CPX-(=P_{1B})-type heavy metal ATPase (HMA), Cation Diffusion Facilitator (CDF), Cation Exchanger

(CAX), ATP-binding cassette (ABC), and Natural Resistance-associated Macrophage Proteins (NRAMP) families (Chaffai and Koyama, 2011).

P-type ATPases, i.e., HMA transporters have roles in the ATP-dependent transmembrane transport of essential and nonessential metal ions (Lee et al., 2007; Morel et al., 2009). Among eight HMA proteins found in Arabidopsis, AtHMA2, AtHMA3, and AtHMA4 function in transport of Zn, Cu, Pb, Co and Cd (Leitenmaier and Küpper, 2013). AtHMA3 and rice OsHMA3 localized to the tonoplast, where they pump metal ions into the vacuole against their electrochemical gradients (Krämer et al., 2007; Morel et al., 2009; Ueno et al., 2010; Miyadate et al., 2011). Its overexpression in Arabidopsis or rice confers tolerance to Cd as well as other heavy metals, by reducing the root-to-shoot Cd distribution and shoot Cd accumulation (Morel et al., 2009; Ueno et al., 2010). OsHMA3 was identified as the major locus responsible for a shoot Cd accumulation QTL in rice (Ueno et al., 2010; Miyadate et al., 2011). Recently, AtHMA3 was also identified as the main locus responsible for the leaf Cd level variation in 149 *A. thaliana* accessions (Chao et al., 2012). Remarkably, higher shoot Cd accumulation is related to the reduced function of HMA3 caused by a nonsense mutation and polymorphisms that change two specific amino acids. In a study on Zn/Cd hyperaccumulator *Noccaea caerulescens* (previously known as *Thlaspi caerulescens*), NcHMA3 was reported to be expressed constitutively in the roots and the shoots, similar to its ortholog in Arabidopsis (Ueno et al., 2011). However, AtHMA3 is localized to the final destination of the transpiration system in the leaves, such as vascular tissue, hydathodes and guard cells, whereas NcHMA3 is mainly expressed in the mesophyll cells of the leaves, where the heavy metals are primarily stored in leaves of hyperaccumulators (Küpper et al., 2000; Cosio et al., 2004). Moreover, NcHMA3 expresses thousands of times more than its Arabidopsis ortholog, indicating the significance of HMA3 expression in Cd sequestration and tolerance in plants (Ueno et al., 2011). Interestingly, even though an ortholog of AtHMA3 in Zn hyperaccumulator species, *Arabidopsis halleri*, shows a constitutive high expression in the shoots, it can only transport Zn, but not Cd, in yeast functional complementation analyses (Becher et al.,

2004). On the contrary, a QTL analysis indicated that *AhHMA3* is not related to Zn hyperaccumulation in *A. halleri* (Filatov et al., 2007). More studies are required to find the mode of function of HMA3 in *A. halleri*.

CDF (CATION DIFFUSION FACILITATOR) transporter family of proteins, also named METAL TRANSPORTER PROTEINS (MTPs) in plants, function in divalent metal, including Zn, Mn, Fe and Cd, transport into subcellular compartments, such as vacuole and Golgi network, or extracellular space (Haney et al., 2005; Ricachenevsky et al., 2013). In Arabidopsis, some MTPs (AtMTP1 and AtMTP3) mainly transport Zn while others predominantly transport Mn into subcellular compartments. AtMTP1 (formerly known as ZAT - ZINC TRANSPORTER) displayed Zn transport activity in heterologous system, and its mutant is sensitive to Zn (Bloß et al., 2002; Kobae et al., 2004). AtMTP1 orthologs are also characterized in non-hyperaccumulators, such as *Medicago truncatula* (MtMTP1) (Chen et al., 2009), rice (OsMTP1) (Yuan et al., 2012), as well as hyperaccumulators, such as *A. halleri* (AhMTP1) (Dräger et al., 2004), and *N. goesingense* (NgMTP1) (Kim et al., 2004). There are five copies of *MTP1* in the genome of *A. halleri*, resulting in constitutive high expression of the gene in both roots and shoots (Dräger et al., 2004; Shahzad et al., 2010). Moreover, it is linked to a QTL responsible for Zn hyperaccumulation and tolerance in *A. halleri (Willems et al., 2007).* AtMTP3 also functions in vacuolar Zn sequestration in the roots (Arrivault et al., 2006). In contrast to AtMTP1 and AtMTP3, AtMTP11 transports Mn into the pre-vacuolar compartment or the Golgi network (Delhaize et al., 2007; Peiter et al., 2007). Even though no evidence of Cd transportation activity of MTPs have been shown to date, in theory they may function in Cd sequestration into the vacuole because of the chemical similarity of Cd and Zn ions (Leitenmaier and Küpper, 2013). Overexpression of a CDF family of protein, *AtMHX*, in tobacco leaf tonoplasts causes increased sensitivity to Cd as well as Zn and Mn, and reduction in plant size, indicating the contribution of CDF transporters in vacuolar Cd sequestration (Berezin et al., 2008).

CAX family of proteins also functions in vacuolar metal transport through Ca^{2+}/H^{+} exchange. In *A. thaliana*, AtCAX2 and AtCAX4 transport Cd into the vacuole and overexpression increases the vacuolar accumulation of Cd whereas root growth in *cax* mutants is altered in response to Cd (Hirschi et al., 2000; Koren'kov et al., 2007; Korenkov et al., 2007; Mei et al., 2009).

Root-to-shoot Translocation

As a non-hyperaccumulator species, in *A. thaliana*, cadmium is mainly accumulated in the roots suggesting the root-to-shoot Cd translocation is restricted at the xylem loading step (Thapa et al., 2012). Up to date, two members of the HMA transporters, AtHMA2 and AtHMA4, and some YSL transporters have been shown to be responsible for Cd loading into the xylem (Wong and Cobbett, 2009). Both AtHMA2 and AtHMA4 are localized to the plasma membrane and specifically express in the root stele, and their knock-out mutants in Arabidopsis present sensitivity to Cd (Eren and Argüello, 2004; Hussain et al., 2004; Verret et al., 2004; Mills et al., 2005; Verret et al., 2005; Wong et al., 2009). Expression of AtHMA4 in yeast results in Cd tolerance (Mills et al., 2003). In contrast, overexpression of AtHMA4 in Arabidopsis results in an increase in the root-to-shoot translocation of Zn and Cd, and confers Cd sensitivity due to the lack of mechanisms detoxifying the Cd and Zn accumulating in the shoots (Verret et al., 2004; Hanikenne et al., 2008). In rice, OsHMA2 is localized to the plasma membrane and is expressed in the root stele, where it functions in efflux of Zn and Cd into xylem for root-to-shoot translocation of those metals (Nocito et al., 2011; Satoh-Nagasawa et al., 2012; Takahashi et al., 2012; Takahashi et al., 2012). When expressed in yeast, AtHMA4 orthologs in Zn/Cd hyperaccumulators *A. halleri* and *N. caerulescens*, namely AhHMA4 and NcHMA4, confer Cd tolerance (Bernard et al., 2004; Papoyan and Kochian, 2004). Hyperaccumulation and hypertolerance of Cd and Zn in *A. halleri* are related to the enhanced promoter activity, due to the evolution of cis-regulatory elements, and increased gene copy number of AhHMA4 (Talke et al., 2006; Hanikenne et al., 2008). Similar to *A.*

halleri, tandem quadruplication of NcHMA4 also reflects the hypertolerance of Cd and Zn in *N. caerulescens* (Lochlainn et al., 2011).

PLANT CADMIUM RESISTANCE (PCR) proteins are efflux transporters involved in Zn or Cd translocation. PCR family consists of 12 and 21 members in Arabidopsis and rice, respectively (Lin and Aarts, 2012). *PCR1* overexpressing Arabidopsis plants are more tolerant to Cd whereas *PCR1* antisense plants show Cd sensitivity (Song et al., 2004). Moreover, loss-of-function of *PCR2* causes both Cd and Zn sensitivities, indicating their importance in metal distribution and detoxification in Arabidopsis (Song et al., 2010).

1.6 Family of Oligopeptide Transporters (OPT)

Members of Oligopeptide Transporters (OPTs) function in transit metal movements through the plasma membrane (PM). OPT family of proteins belongs to the peptide transporting protein superfamily that also includes ABC transporter family, consisting of more than 120 members in Arabidopsis, and PEPTIDE TRANSPORTER/ NITRATE TRANSPORTER (PTR/NTR) family, with over 50 putative genes in the Arabidopsis genome (Stacey et al., 2002; Tsay et al., 2007; Lubkowitz, 2011). Peptide transporters utilize the electrochemical potential to move peptides and their derivatives across the membranes (Lubkowitz et al., 1997; Lubkowitz et al., 1998). This electrochemical potential is generated by the hydrolysis of ATP in case of plant ABC transporter family (Rea, 2007), or by the proton-motive force in case of PTR and OPT families (Hauser et al., 2001). ABC transporters transport their substrates mainly out of cytosol (Kang et al., 2011), whereas PTR/NTR and OPT family of transporters function as symporters to transport their substrates into the cytosol (Hauser et al., 2000; Schaaf et al., 2004; Osawa et al., 2006). Various peptide transporters including the ABC transporters AtMRP3 (Bovet et al., 2003), AtATM3 (Kim et al., 2006) and AtPDR8 (Kim et al., 2007) are involved in root-to-shoot movement of nutrients and transition metals such as Cd and Pb. In yeast

(Lubkowitz et al., 1997; Lubkowitz et al., 1998), OPTs function in various biological processes, including nitrogen mobilization (Williams and Miller, 2001), heavy metal sequestration (Cagnac et al., 2004), and glutathione transport (Zhang et al., 2004), in addition to long distance movement of metals (Cao et al., 2011).

OPTs are very hydrophobic and contain 12-14 transmembrane domains (Koh et al., 2002; Wiles et al., 2006; Vasconcelos et al., 2008). Phylogenetic analysis revealed two distantly related sub-families of YSL and Oligopeptide Transporter (PT) (Lubkowitz, 2011). YSL genes are found in all organisms, except for animals while PT genes are only been identified in fungi and plants (Lubkowitz, 2011). The proteins in PT clade are more closely related to their fungal orthologs than they are to YSL proteins in maize (Yen et al., 2001). There are eight and nine YSL isoforms (AtYSL1-AtYSL8) and nine PT isoforms (AtOPT1-AtOPT9), respectively, in the *A. thaliana* genome (Koh et al., 2002; DiDonato et al., 2004). Sequence comparison of OPT proteins from Arabidopsis, rice, Populus and Vitis identified 20 distinct motifs, 14 of which were found in many PT-clade proteins whereas 9 were found in YSL clade (Cao et al., 2011). Conserved motifs in each clade may represent a functional diversification of OPT proteins in plants.

OPTs have a wide range of substrate specificity for small peptides of 2-8 amino acids in length, tetra-/penta-peptides being the most common (Lubkowitz et al., 1997; Stacey et al., 2002; Reuß and Morschhäuser, 2006). Five OPT isoforms in Arabidopsis (OPT1, 4, 5, 6, and 7) were shown to transport tetra- and penta-peptide in yeast functional complementation assays (Koh et al., 2002; Osawa et al., 2006). They can also transport metal-chelates composed of mugeneic acids, nicotinamine, and glutathione (Curie et al., 2001; Koh et al., 2002; Bogs et al., 2003; Zhang et al., 2004) in addition to the role of ZmYS1 in Fe(III)-PS uptake into the roots (Curie et al., 2001). For instance, AtOPT6 can transport glutathione derivatives (Cagnac et al., 2004) and signaling peptides derived from mammals and plants (Pike et al., 2009), whereas rice YSL2 (OsYSL2) (Koike et al., 2004), OsYSL15 (Inoue et al., 2009; Lee et al., 2009), and OsYSL18 (Aoyama et al., 2009), and

T. caerulescens YSL3 (TcYSL3) (Gendre et al., 2007) can transport metal-NA. Five Arabidopsis OPTs (OPT1, OPT5, YSL3, YSL7, and YSL8) confer sensitivity to Syringolin A (SylA), a virulence factor secreted by certain strains of the plant pathogen *Pseudomonas syringae* pv. *syringae*, when expressed in yeast, indicating the potential functions of OPT proteins in uptake of virulence factors into the plant cells and future biotechnological targets to improve the plant resistance against pathogens (Hofstetter et al., 2013). Variety of substrate specificities of OPT family of transporters may represent a functional diversification of OPT proteins in plants.

1.6.1 Cellular and Subcellular Localization of OPT Family of Proteins in Plants

OPT family of proteins show a diversity of expression patterns both in Arabidopsis and rice. Tissue specific transcript accumulation revealed that many *AtOPT* genes were expressed in the roots except for *AtOPT5*, which was only expressed in the flowers (Koh et al., 2002). Moreover, promoter-*GUS* reporter analyses (Stacey, 2006) found that *AtOPT1*, *AtOPT3*, *AtOPT4*, *AtOPT6*, *AtOPT7* and *AtOPT8* were highly expressed in the vasculature, whereas *AtOPT1*, *AtOPT3* and *AtOPT8* were exclusively expressed in the pollens. *AtOPT6* was expressed in the ovules (Stacey et al., 2006). *AtOPT3* was also shown to be expressed during embryo development (Stacey et al., 2002). In rice, transcripts of *OsOPT2, OsOPT3, OsOPT4, OsOPT7, OsOPT8, OsOPT9, OsYSL2, OsYSL9, OsYSL12, OsYSL13* and *OsYSL16* accumulate in all tissues (Liu et al., 2012). Interestingly, *OsOPT1*, *OsOPT3*, *OsOPT4*, and *OsOPT7* also express in the embryos (Vasconcelos et al., 2008). These localization analyses led to the hypothesis that specific OPTs, including AtOPT1, AtOPT3, AtOPT6, AtOPT8, OsOPT1, OsOPT3, OsOPT4, and OsOPT7, may function in transporting essential nutrients during embryogenesis (Liu et al., 2012), in addition to their functions in metal uptake, sequestration and long distance transportation.

Majority of the YSL transporters are shown to localize to the PM in maize (Ueno et al., 2009), Arabidopsis (DiDonato et al., 2004; Waters et al., 2006; Chu et al., 2010), rice (Koike et al., 2004; Aoyama et al., 2009; Inoue et al., 2009; Lee et al., 2009; Lee et al., 2012), barley (Murata et al., 2006) and others. Interestingly, ZmYS1 is localized to the distal side of the epidermal cells, and AtYSL3 and AtYSL2 localize exclusively to the lateral PMs indicating their potential function in lateral movement of metals (DiDonato et al., 2004; Waters et al., 2006; Chu et al., 2010). Some YSLs, on the other hand, do not localize to the PM. For instance, HvYSL5 localizes to the vesicles or the tonoplast (Zheng et al., 2011). As an interesting observation, OsYSL6 signals indicate a cytosolic localization in rice (Sasaki et al., 2011) whereas Arabidopsis AtYSL4 and AtYSL6 localize to the plastids (Divol et al., 2013). In a latest study, Conte *et al.* (2013) showed AtYSL6 localized to vacuolar membranes when transiently expressed, or to the internal membranes similar to the endoplasmic reticulum. Despite the difficulties in determining the correct *in planta* localization of some OPT family of proteins, taken together these findings indicate the potential functions of OPT proteins in both inter- and intracellular metal translocation. In contrast to YSLs, our knowledge of *in planta* subcellular localization of OPT proteins is limited to PM localization of AtOPT1, AtOPT5 and TcOPT3 (Hu et al., 2012; Hofstetter et al., 2013).

1.6.2 Known Functions of OPT Family of Transporters in Heavy Metal Transport

The recent studies indicate OPTs transport heavy metals in addition to essential metals. Transporters from non-hyperaccumulators such as AtOPT6 and AtOPT7, and OsOPT3 (OsGT1), as well as hyperaccumulators such as BjGT1, and TcOPT3 were shown to be involved in heavy metal tolerance (Bogs et al., 2003; Cagnac et al., 2004; Zhang et al., 2004; Pike et al., 2009; Hu et al., 2012). When expressed in yeast, AtOPT6 and AtOPT7 can transport Cd or Cd-glutathione complex (Cagnac et al., 2004), whereas the expression of AtOPT3 in *S. cerevisiae opt2* mutants causes higher Cd sensitivity and Cd uptake (Zhai et al., 2010). However, overall, only limited functional characterization of plant OPTs in

heavy metal transport has been reported. For instance, *A. thaliana opt3-3* mutant shows either Cd tolerance at maturity, or extreme sensitivity to Cd toxicity in young seedling stage (Zhai et al., 2010; Zhai, 2011). On the other hand, *AtOPT6* overexpression plants showed hypersensitivity to Cd, and accumulated higher level of Cd, GSH and PCs in the roots and lower levels of Cd and PCs in the shoots, indicating the involvement of AtOPT6 in long-distance translocation of Cd from roots to shoots in forms of Cd-GSH and/or Cd-PCs complexes (Patel, 2007). Taken together, these experimental results show the probable role of OPTs in heavy metal transport in plants.

1.7 RNA Polymerase II CTD Regulates Transcription

In eukaryotes, the transcription of all protein encoding genes as well as small nuclear RNAs (snRNAs) is mediated by RNA polymerase II (RNAPII). RNAPII contains a distinctive domain made of heptapeptide repeats with the consensus sequence of Tyr1–Ser2–Pro3–Thr4–Ser5–Pro6–Ser7 at the C-terminal domain (CTD) of its largest subunit (Rpb1) (Phatnani and Greenleaf, 2006; Chapman et al., 2008). The heptapeptide consensus sequence is highly conserved among yeast, human and plants (Allison et al., 1988; Nawrath et al., 1990). The CTD of Arabidopsis contains 15 consensus and 19 divergent heptapeptide repeats (Koiwa, 2002). During different stages of gene transcription, the recruitment of factors to the elongating RNAPII and to the nascent transcript is coordinated by the dynamic phosphorylation and dephosphorylation of serine residues in CTD by kinases and phosphatases, respectively (Egloff and Murphy, 2008. These factors are required for transcription, co-transcriptional RNA processing, chromatin remodeling, and RNA export (Egloff and Murphy, 2008; Buratowski, 2009; Egloff et al., 2012; Hsin and Manley, 2012). Moreover, phosphorylation status of the Ser2 and Ser5 in the CTD is important for the recycling of the RNAPII (Hajheidari et al., 2013) since recycling of RNAPII requires dephosphorylation of the CTD. Ser7 is also phosphorylated in yeast and animals, and is required for the interaction with the snRNA gene–specific Integrator complex (Chapman et al., 2007; Egloff et al., 2007). More recently, Tyr1 and

Thr4 were also shown to be phosphorylated throughout the transcription cycle (Hsin et al., 2011; Hintermair et al., 2012; Mayer et al., 2012). Tyr1 phosphorylation impairs the recruitment of transcription termination factor to RNAPII; however, Thr4 phosphorylation is necessary for histone mRNA 3′ end processing. Several CTD phosphatases are known to function in the dephosphorylation process.

1.7.1 CTD Phosphatases in Yeast and Mammals

Protein phosphatase superfamily is divided into four families: Serine/Threonine (Ser/Thr)-specific phosphoprotein phosphatase (PPP), metal-dependent protein phosphatase (PPM), protein tyrosine phosphatase (PTP), and Aspartate (Asp)-based metal- dependent phosphatase/Asp-based catalysis (AMP) families (Kerk et al., 2008; Hajheidari et al., 2013). PPPs and PPMs phosphatases generally dephosphorylate phosphoserines and phosphothreonines whereas PTPs can additionally dephophorylate phosphotyrosines. PTPs contain a common signature motif (CX_5R) in their catalytic domains (Tonks, 2006), and can dephosphorylate glycogen (Cohen, 2002), mRNA (Kennelly, 2003) or phosphoinositides (Tonks, 2006), but not proteins (Moorhead et al., 2009). PPPs contain three signature motifs (-GDXHG-, -GDXVDRG- and -GNHE-) within a 280 amino acid catalytic domain, and include PP (PROTEIN PHOSPHATASE) 1, PP2A, PP2B (orPP3), PP4, PP5, PP6 and PP7 (Moorhead et al., 2009). PPMs include PP2C and pyruvate dehydrogenase phosphatase.

AMP family of proteins contains the signature motif of ΨΨ(DXDXT/V)ΨΨ, where Ψ represents a hydrophobic residue, in the catalytic domain, which is commonly found in phosphotransferases and hydrolases (Collet et al., 1998; Kobor et al., 1999). The family is grouped into three sub-categories of the transcription factor IIF (TFIIF)-associated RNAPII CTD phosphatase (FCP), the small CTD phosphatase (SCP), and the haloacid dehalogenase (HAD) enzymes (Moorhead et al., 2009). TFIIF-stimulated CTD phosphatase I (Fcp1) is first identified in fission yeast *Schizosaccharomyces pombe*. Fcp1

contains N-terminus-localized phosphatase domain called Fcp1 homology (FCPH) domain, important for the catalytic activity, C-terminus-localized breast cancer 1 (BRCA1) protein-related carboxyl-terminal (BRCT) domain (Zhang et al., 1998), necessary for the interaction with phosphorylated RNAPII CTD (Kobor et al., 1999), and an Fcp1 specific helical domain (Ghosh et al., 2008). With a 6-fold higher preference for Ser2, Fcp1 dephosphorylates both Ser2 and Ser5 of the CTD *in vitro* and *in vivo* (Hausmann and Shuman, 2002). Highly conserved among eukaryotes, Fcp1 activity is pivotal for transcription both *in vivo* and *in vitro* due to the dynamic phosphorylation of CTD is necessary for Pol II recycling, and transcription elongation (Cho et al., 1999; Kobor et al., 1999; Corden, 2013). In *Drosophila Fcp1* knock-out mutant, nonchromatin bound phosphorylated Pol II accumulates without altering the chromatin bound Pol II phosphorylation state (Fuda et al., 2012). Recently, Fcp1 is shown to function in mitosis exit in human cells (Visconti et al., 2012).

In addition to Fcp1, there is another related family of SCPs encoded by various genes in animal cells. The SCPs contain the catalytic signature motif of DXDXT/V, in the FCPH domain, but lacks the BRCT domain (Yeo et al., 2003). In contrast to Fcp1, Scp1 shows a 60-fold preference for Ser5P over Ser2P (Zhang et al., 2006) due to the specific arrangement of amino acids in the active site groove and the occurrence of extra domains in Fcp1 (Ghosh et al., 2008). Interestingly, the expression of neuronal genes are negatively regulated by Scp1 in non-neuron cells (Yeo et al., 2005).

1.7.2 CTD Phosphatases in Arabidopsis thaliana

There are more than 20 CTD phosphatases identified in the Arabidopsis genome by homology search for the phosphatases similar to the fungal and metazoan FCP1 phosphatases (Koiwa et al., 2002), and the first identified Arabidopsis CTD phosphatases were given the name of *CTD PHOSPHATASE-LIKE1* (*CPL1), CPL2, CPL3* and *CPL4* (Koiwa, 2002). CPL family is divided into three categories based on the structure.

Belonging to Group I, AtCPL1 and AtCPL2 contain a catalytic FCPH domain and double-stranded RNA (ds-RNA)-binding motif(s) (DRMs), two in AtCPL1 and one in AtCPL2 structure. The DRMs can function in the protein-protein interaction and/or dsRNA-binding, and could be targeted by regulatory RNA molecules, such as miRNAs, and RNA binding proteins that function in transcriptional and posttranscriptional regulation of gene expression (Isel and Karn, 1999; Van Trung Nguyen et al., 2001; Yang et al., 2001; Koiwa, 2006; Manavella et al., 2012; Jeong et al., 2013; Jiang et al., 2013; Zhang et al., 2013; Guan et al., 2014). CPL1 and CPL2 are unique to plants since they are the only known examples of proteins with both DRM and phosphatase domains. AtCPL3 and AtCPL4 belong to Group II and they contain a FCPH and a BRCT domain, thus resemble to the yeast Fcp1 (Koiwa, 2002; Bang et al., 2006). SCP1-like small CTD phosphatases (SSPs) make up the Group III (Koiwa, 2006). They are homologous to SCP1 since they contain only the FCPH domain, but not the BRCT domain. There are 18 predicted SSPs in Arabidopsis genome. Included in this group, AtCPL5 contains two FCPH domains similar to CTD small phosphatase-like 2 in humans (Jin et al., 2011). AtCPLs show different substrate specificities. AtCPL1 and AtCPL2 specifically dephosphorylate CDT Ser5P residues (Koiwa et al., 2004), whereas AtCPL5 dephosphorylates CTD Ser2P *in vitro* (Jin et al., 2011). Additionally, AtSSP4 and AtSSP4b dephosphorylate Ser2P and Ser5P residues, although AtSSP5 dephosphorylates only Ser5P residues of the CTD *in vitro (Feng et al., 2010)*. Unfortunately, *in vivo* CTD phosphatase activity of CPL proteins have not been reported yet. Interestingly, unlike FCP1, catalytic FCPH domain of AtCPL1 is enough for CTD Ser5 phosphatase activity, suggesting the DRMs of AtCPL1 are not necessary for the catalytic function of the protein (Koiwa et al., 2004).

Phylogenetic analyses of CPLs in plant species other than Arabidopsis are limited. A homology search of AtCPLs predicts new CPLs in *Oryza sativa*, *Populus trichocarpa* and green algae *Chlamydomonas reinhardtii*, indicating their importance in various lineages of evolution (Kerk et al., 2008; Moorhead et al., 2009). Recently, two genes of *O. sativa Os07g10690* (Ji et al., 2010) and *Os02g0639000* (Undan et al., 2012), renamed as *OsCPL1*

and *OsLMS*, respectively, are identified as homologs of *AtCPL1* and *AtCPL2*. OsCPL1 consists of a CTD phosphatase domain whereas OsLMS contains a CTD phosphatase activity domain and two DRMs. Although not confirmed experimentally, *ToCPL1* containing a CTD phosphatase domain is proposed to be the candidate gene for the *jointless-2* locus in tomato (Budiman et al., 2004; Lewis et al., 2006).

In silico analysis indicates that *AtCPL2* expresses mainly in the seed endosperm and coat, the sperm cell in addition to the root and the guard cell protoplasts. *AtCPL3* expresses in the seed endosperm and coat as well as the root protoplast, the vasculature and the senescent leaf. *AtCPL4* is predicted to express in the seed endosperm and coat, the pistil, the root protoplast and the shoot apex. *AtCPL1* and *AtCPL2* express in the root tip, and both root and shoot vasculature (Ueda et al., 2008; Aksoy et al., 2013), whereas *AtCPL5* expresses in seed coat, flower buds, stems, stamens, carpels, funiculi of siliques, cotyledons, hypocotyl, rosette leaves and roots, with highest expression in the vasculature (Jin et al., 2011). Moreover, *OsCPL1* is mostly expressed in the panicles, the vasculature of the panicle and the region adjacent to the abscission layer in young spikelets, with strongest expression in the abscission layer (Ji et al., 2010).

As the subcellular localizations are concerned, all CPLs identified from Arabidopsis and rice localize in the nucleus, except for AtCPL2, which is localized in cytosol (Koiwa et al., 2004; Bang et al., 2006; Bang et al., 2008; Ji et al., 2010; Jin et al., 2011). Interestingly, under specific conditions, AtCPL1 localizes to speckles in the nucleus (Chen et al., 2013; Jeong et al., 2013; Jiang et al., 2013), where pre-mRNA splicing machinery and active transcription takes place (Lorković et al., 2008).

1.7.3 Known Functions of CTD Phosphatase-Like Proteins (CPLs) in Plants

Studies of CPLs in Arabidopsis and rice demonstrated that CTD phosphatases play roles in various signaling pathways, and plant growth and development (Koiwa, 2002; Xiong et al., 2002; Hajheidari et al., 2013). AtCPL1 and AtCPL3 are negative regulators of the drought-responsive/C-repeat (DRE/CRT) class of stress-responsive genes, including *COR15A, COR47, DREB2A, KIN1,* and *CBF3* under different stresses. AtCPL2 regulates various pathways related to plant growth, stress response and auxin signaling (Ueda et al., 2008). Notably, even though both AtCPL3 and AtCPL4 interact with RAP74, the large subunit of TFIIF, in the nucleus, AtCPL3 regulates ABA signaling, whereas AtCPL4 is required for normal plant growth since loss-of-function mutant of *AtCPL4* is lethal (Bang et al., 2006). There are other functions of AtCPL1. Recently, it was shown that AtCPL1 functions downstream of both JA-dependent and -independent mechanisms as a negative regulator of wound signaling (Matsuda et al., 2009). One of the SSPs, in contrast to the other characterized CPLs, AtCPL5 positively controls the expression of specific ABA- or drought-responsive genes, including those encoding the DREB-type AP2/ERF transcription factors, such as *RAP2.4, RAP2,* and *QRAP2,* which can contribute to ABA-mediated drought tolerance and development in Arabidopsis (Jin et al., 2011).

Besides the dephosphorylation of CTD Ser5P, AtCPL1 and perhaps AtCPL2 can regulate the phosphorylation of other proteins by binding to them through the DRMs. Mediated by the zing finger protein SE, the interaction of CPL1 with dsRNA binding protein HYL1 and concurrent CPL1-dependent dephophorylation of HYL1 is essential for precise and efficient miRNA processing (Manavella et al., 2012). Involvement of CPL1 in miRNA biogenesis has been verified by Jeong et al. (2013), where CPL1 was shown to regulates DNA methylation by interacting with the proteins important for miRNA biogenesis. Additionally, it was also shown that CPL1 was involved in the RNA-directed DNA methylation pathway without reducing siRNA production (Jeong et al., 2013). On the other hand, CPL1 can interact with a putative chromosome architecture protein,

DEFECTIVE IN MERISTEM SILENCING3 (DMS3) or INVOLVED IN DE NOVO1 (IDN1) (Bang et al., 2008), which can potentially link nucleic acids in facilitating an RNA1-mediated epigenetic modification involving secondary siRNA and spreading of DNA methylation (Stroud et al., 2013). However, it has to be proven that the interaction of CPL1 with DMS3/IDN1 is necessary for the epigenetic modification involving secondary siRNA.

Recently, it was shown by four independent groups that CPL1 interacts with a K-homology (KH) domain containing RNA binding protein REGULATOR OF CBF GENE EXPRESSION3 (RCF3), co-named SHINY1 [SHI1], and HIGH OSMOTIC STRESS GENE EXPRESSION5 [HOS5]), in the nucleus, and this interaction is necessary for the co-localization of the two proteins in the speckles after stress treatment (Chen et al., 2013; Guan et al., 2013; Jeong et al., 2013; Jiang et al., 2013). CPL1-(RCF3/SHI1/HOS5) interaction is required for proper pre-mRNA splicing under stress conditions (Chen et al., 2013), as well as co-transcriptional processes such as mRNA 5'-capping and polyadenylation (Jiang et al., 2013). There are additional CPL1-interacting partners, including transcription factors, ANAC019 and AtMYB3, which have functions in stress and ABA signaling (Bang et al., 2008). CPL1 also interacts with a ubiquitin ligase, XB3 ORTHOLOG1 IN ARABIDOPSIS THALIANA (XBAT31), expressed in the root vasculature and involved in lateral root initiation via its role in ethylene biosynthesis (Nodzon et al., 2004; Prasad et al., 2010). Finally, Feng et al. (2011) demonstrated a biotechnological application of cpl1 mutant in anthocyanin accumulation in plants. By using *cpl1-2* mutant in a three-component gene expression system, the anthocyanin levels have increased up to 30 folds under cold treatment. This indicates the potential future interest in developing new biotechnological tools to improve the plants.

CHAPTER II

LOSS OF FUNCTION OF *ARABIDOPSIS C-TERMINAL DOMAIN PHOSPHATASE-LIKE1* (*CPL1*) ACTIVATES IRON DEFICIENCY RESPONSES AT THE TRANSCRIPTIONAL LEVEL[1]

2.1 Summary

The expression of genes that control iron (Fe) uptake and distribution (i.e., Fe utilization-related genes) is tightly regulated. Fe deficiency strongly induces Fe utilization-related gene expression; however, little is known about the mechanisms that regulate this response in plants. Transcriptome analysis of an *Arabidopsis thaliana* mutant defective in *RNA polymerase II CTD-phosphatase-like 1* (*CPL1*) revealed significant up-regulation of Fe utilization-related genes, e.g., *IRON-REGULATED TRANSPORTER1*, suggesting the importance of RNA metabolism in Fe signaling. An analysis using multiple *cpl1* alleles established that *cpl1* mutations enhanced specific transcriptional responses to low Fe availability. Changes in protein level were less prominent than those in transcript level, indicating that *cpl1-2* mainly affects the Fe deficiency response at the transcriptional level. However, Fe content was significantly increased in the roots and decreased in the shoots of *cpl1-2* plants, indicating that the *cpl1* mutations do indeed affect Fe homeostasis. Furthermore, root growth of *cpl1-2* showed improved tolerance to Fe deficiency and cadmium (Cd) toxicity. *cpl1-2* plants accumulated more Cd in the shoots, suggesting that Cd toxicity in the roots of this mutant is averted by the transport of excess Cd to the shoots.

---

[1] Used with permission from **Aksoy E, Jeong IS, Koiwa H** (2013) Loss of Function of Arabidopsis C-Terminal Domain Phosphatase-Like1 Activates Iron Deficiency Responses at the Transcriptional Level. Plant Physiology **161:** 330-345. www.plantphysiol.org, Copyright American Society of Plant Biologists.

Genetic data indicate that *cpl1-2* likely activates Fe deficiency responses upstream of both FE–DEFICIENCY-INDUCED TRANSCRIPTION FACTOR (FIT)-dependent and -independent signaling pathways. Interestingly, various osmotic stress/ABA-inducible genes were up-regulated in *cpl1-2,* and the expression of some ABA-inducible genes was controlled by Fe availability.We propose that the *cpl1* mutations enhance Fe deficiency signaling and promote crosstalk with a branch of the osmotic stress/ABA signaling pathway.

2.2 Introduction

Iron (Fe) is an essential metal element for nearly all organisms. In plants, Fe is present as a cofactor in many metallo-proteins and is found in the active sites of photosynthetic and respiratory Fe-S clusters. Fe is also required for RNA and hormone biosynthesis, nitrogen fixation, sulfate assimilation, and chlorophyll biosynthesis (Broadley et al., 2012). On the other hand, Fe is highly reactive and excess Fe can produce reactive oxygen species via Fenton reactions (Moller et al., 2007). In soil, the predominant form of Fe is Fe(III), which is abundantly present as insoluble ferric oxides and ferric hydroxides in aerobic environments (Guerinot and Yi, 1994; Palmer and Guerinot, 2009). The solubility of Fe(III) in aqueous solution is an order of magnitude less than the Fe concentration needed for survival; therefore, a large portion of agricultural land is Fe deficient (Guerinot and Yi, 1994). Fe deficiency in plants induces intercostal/interveinal leaf chlorosis due to limited chlorophyll biosynthesis and results in significant yield loss of crops.

Plants have developed two distinct mechanisms, i.e., strategy I (reduction strategy) and II (chelation strategy), to mobilize insoluble Fe(III) in the rhizosphere and transport it through the plasma membrane (PM) (Romheld, 1987; Welch, 1995; Schmidt, 1999; Gross et al., 2003; Grotz and Guerinot, 2006; Puig et al., 2007; Conte and Walker, 2011; Schmidt and Buckhout, 2011; Ivanov et al., 2012; White, 2012). *Arabidopsis thaliana* and other dicots rely on strategy I. In this strategy, the rhizosphere is first acidified by a PM-localized

H^+-ATPase, AHA2 (Santi and Schmidt, 2009). Then, FERRIC CHELATE REDUCTASE2 (FRO2) reduces Fe(III) to soluble Fe(II) (Yi and Guerinot, 1996; Robinson et al., 1999). Finally, the reduced Fe is taken up by a high-affinity transporter, IRON-REGULATED TRANSPORTER1 (IRT1) (Eide et al., 1996; Henriques et al., 2002; Varotto et al., 2002; Vert et al., 2002), which is strongly expressed in root epidermal cells and is localized to the PM (Eide et al., 1996; Vert et al., 2002). Once the Fe(II) is absorbed, various transporters and chemicals mobilize it. Fe(II) can be chelated by nicotianamine and transported intercellularly by YELLOW STRIPE-LIKE (YSL) transporters (DiDonato et al., 2004; Waters et al., 2006; Waters and Grusak, 2008; Chu et al., 2010). In the vasculature, citrate, which is exuded by a FERRIC REDUCTASE DEFECTIVE3 (FRD3) transporter (Durrett et al., 2007), forms a tri-Fe(III), tri-citrate complex for long-distance transport (Rogers and Guerinot, 2002; Green and Rogers, 2004; Rellan-Alvarez et al., 2010). In addition, OLIGOPEPTIDE TRANSPORTER3 (OPT3) may also function as a transporter of Fe-chelates (Wintz et al., 2003; Stacey et al., 2008). In contrast, excess Fe is sequestered in plastids by Fe-binding proteins named ferritins (Waldo et al., 1995). Here, we collectively refer to genes that are involved in Fe uptake, mobilization, and signaling, as "Fe utilization-related genes", according to Kobayashi et al. (2009).

The expression level of genes encoding components of the Fe acquisition mechanism, such as *FRO2 and IRT1*, are under transcriptional regulation in Fe-limited conditions, as their mRNA levels increase in response to Fe deficiency (Eide et al., 1996; Robinson et al., 1999; Connolly et al., 2002; Vert et al., 2002). Central to this regulation are basic helix-loop-helix (bHLH) transcription factors, FER in tomato (Ling et al., 2002) and FER-LIKE IRON DEFICIENCY-INDUCED TRANSCRIPTION FACTOR (FIT) in Arabidopsis (Colangelo and Guerinot, 2004; Jakoby et al., 2004; Yuan et al., 2005; Bauer et al., 2007). In Arabidopsis, FIT regulates various Fe utilization-related genes, including *IRT1, FRO2*, and *NICOTINAMINE SYNTHASE1* (*NAS1*) (Colangelo and Guerinot, 2004; Jakoby et al., 2004). FIT dimerizes with group-Ib bHLH family transcription factors, bHLH38 or

bHLH39, and directly activates the transcription of *IRT1* and *FRO2* (Yuan et al., 2008). While the induction of *FIT* expression during the Fe deficiency response is moderate (Bauer et al., 2004; Colangelo and Guerinot, 2004; Jakoby et al., 2004), *bHLH38, bHLH39, bHLH100,* and *bHLH101* are strongly up-regulated (Wang et al., 2007). It has been proposed that dimerization of FIT with different bHLHs determines the target specificity of Fe deficiency-induced transcriptional activation (Yuan et al., 2008). To date, little is known about the upstream mechanisms that sense cellular Fe levels and regulate the early signals that lead to the expression of *FIT* and group Ib *bHLH* genes. In addition to the central pathway, a recent study reported the existence of a cell-specific regulatory mechanism mediated by the bHLH transcription factors *POPEYE* (*PYE*) and *IAA-LEUCINE RESISTANT3* (*ILR3*), and the E3 ligase *BRUTUS* (*BTS*) that operates in the root pericycle Fe response and controls root development (Long et al., 2010). Repression of *FERRITIN1* (*FER1*) genes in the absence of excess Fe is mediated by the *cis*-element IDRS (iron-dependent regulatory sequence) (Petit et al., 2001). These regulators control specific branches of Fe deficiency signaling; however, the mechanisms that sense Fe availability and fine-tune the signal throughput of individual pathways have yet to be determined.

A wide range of physiological and molecular signals influence Fe signaling in Arabidopsis. Ethylene regulates the expression of *IRT1, FRO2,* and *FIT,* perhaps via the activity of EIN3 and EIL1, which stabilize FIT (Lingam et al., 2011). In contrast, cytokinin and ABA repress the expression of *IRT1, FRO2,* and *FIT* (Seguela et al., 2008). Environmental stresses, such as salt/osmotic stress, attenuate Fe deficiency responses (Seguela et al., 2008), whereas phosphate starvation triggers the Fe deficiency responses (Hirsch et al., 2006; Thibaud et al., 2010). Moreover, volatiles emitted by soil microbes can up-regulate the expression of Fe utilization-related genes (Zhang et al., 2009). The molecular mechanisms that facilitate multiple inputs into Fe signaling have not been determined; however, the plasticity of Fe signaling implies the presence of diverse regulatory components that are coordinated to achieve proper levels of cellular Fe.

Among the various genes that affect the expression of Fe utilization-related genes, *TRIDENT* (*TDT*) is unique as it encodes a subunit of an RNA decapping enzyme that is involved in RNA metabolism (Goeres et al., 2007). The RNA metabolic pathway is a major mechanism in the co-/post-transcriptional regulation of diverse developmental and environmental responses (Kuhn and Schroeder, 2003; Gregory et al., 2008; Nakaminami et al., 2012). While ABA signaling is a prototypical target of RNA metabolism-mediated regulation, many transcripts are regulated by small RNAs, such as miRNAs and siRNAs (Ramachandran and Chen, 2008). The *tdt* mutation has been shown to repress the expression of Fe utilization genes; however, whether this is due to severe growth defects in the mutant or to specific Fe signaling defects has not been elucidated (Goeres et al., 2007).

Here, an isoform of RNA metabolism regulators, CPL1 [RNA polymerase II C-terminal domain (pol II CTD) phosphatase-like 1], is identified as a novel regulator of the Fe deficiency responses. CPL family proteins are known to dephosphorylate pol II CTD (Koiwa et al., 2004), which is the regulatory domain of pol II. Of the more than 20 CPL isoforms present in the *Arabidopsis* genome, CPL1 is a negative regulator of stress-responsive gene expression under various osmotic stresses (Koiwa et al., 2002; Xiong et al., 2002). In this report, CPL1 is determined to function also in the plant Fe deficiency response. Microarray analysis of the c*pl1* transcriptome found that both the osmotic stress/ABA response and the Fe deficiency response are activated in *cpl1*. *cpl1* mutant plants exhibited various hallmarks of the Fe deficiency response, such as altered metal profiles, and increased tolerance to Fe deficiency and cadmium toxicity. These results suggest that *CPL1* is a previously uncharacterized regulator of the Fe deficiency response. In addition, the data suggest that a subset of ABA/osmotic stress-induced genes are co-regulated by Fe deficiency signals and are targets of CPL1 regulation.

2.3 Materials & Methods

2.3.1 Chemicals & Primer Information

All chemicals were obtained from Sigma. Sigma agar E was used for all plant growth experiments. Primer sequences used in this study are shown in Appendix A.

2.3.2 Plant Materials

The *Arabidopsis thaliana* ecotypes Col-0 and C24 were used in this study. The *cpl1-1* and *cpl1-2* lines were described previously (Koiwa et al., 2002; Xiong et al., 2002). *cpl1-5* (GK-590C07) and *cpl1-6* (GK-165H09) were obtained from the Nottingham Arabidopsis Stock Center (NASC) and *frd3-1* was obtained from Arabidopsis Biological Resource Center. *fit-2* seeds were provided by Dr. Paul Paré.

For general growth and microarray analyses, seeds were sown on media containing 1/4 Murashige and Skoog (MS) salts, 0.5% sucrose, and 0.8% agar. After stratification for 2 days at 4^{o}C, the plates were kept in a growth incubator under a long-day photoperiod (16 h light, 8 h darkness) at 25^{o}C for 10 days.

2.3.3 RNA Extraction

Total RNA was isolated using TRIzol reagent (Chomczynski and Sacchi, 1987) and treated with DNase I (Promega, WI) to remove genomic DNA contamination.

2.3.4 Microarray Analyses

Total RNA was extracted from 10-day-old wild-type C24 and *cpl1-2* mutant seedlings. Quality tests of the RNA samples, complementary RNA (cRNA) synthesis, biotin

labeling, hybridization to Affymetrix ATH1 GeneChips, and scanning were performed by the Affymetrix Service at the Nottingham Arabidopsis Stock Centre (NASC). After chip hybridization and scanning, triplicate data were obtained for each genotype and data were processed using GeneSpringGX 11.0.2 software (Agilent, CA). Raw intensity values, computed from .CEL files, were processed first by Robust Multiarray Analysis (RMA) (Irizarry et al., 2003). Filtering on expression levels and fold changes (≥2) were performed using the GeneSpring package and differentially expressed genes were determined. Statistical analyses were performed using one-way ANOVA at $p < 0.05$ (with asymptotic *p*-value computation) followed by the Tukey HSD post hoc test and Benjamini Hochberg FDR multiple testing correction. A fold change of at least 2 was considered indicative of differential expression, where a *p* value of 0.05 or under was considered indicative of significant alteration in expression. All microarray data from this study were deposited in the NASC Database under accession number 611.

For hierarchical clustering of up-regulated genes, raw gene expression data for abiotic stresses and hormone treatments were first obtained from the AtGenExpress project (http://www.arabidopsis.org/portals/expression/microarray/ATGenExpress.jsp). The CEL file names are NASCarray 176 (ABA), 140 (salt), and 139 (mannitol)]. The CEL file for the Fe deficiency experiment (GSE15189) was obtained from the GEO database (Buckhout et al., 2009). All data were clustered by Pearson correlation distance and the average linkage rule (Eisen et al., 1998).

2.3.5 Gene Set Enrichment Analysis

Gene Set Enrichment Analysis (GSEA) was performed using GeneTrail (Backes et al., 2007; Schuler et al., 2011). Briefly, 22811 probes on ATH1 microarray datasets obtained from public databases were ranked and sorted according to fold change from the most induced to the most suppressed by each stress treatment. Subsequently, GSEA analyses were performed for each sorted dataset, using gene sets created from an analysis of the

cpl1-2 microarray. As a reference, gene sets consisting of constitutively expressed genes in Arabidopsis were analyzed (Czechowski et al., 2005). False Discovery Rate was used as the *p*-value adjustment (Benjamini and Hochberg, 1995).

2.3.6 RT-qPCR Analysis

Total RNA samples (2 µg) were reverse-transcribed using random hexamers and the Superscript III Reverse Transcriptase (Life Technology, CA) in a total volume of 20 µl. One-twentieth of the reverse transcription products was analyzed using ABI 7900 Sequence Detectors and SYBR Green Master Mix (Life Technologies, CA). The amplification reaction and data analysis were performed as described (Salzman et al., 2005). Each reaction was run in technical duplicate and the melting curves were analyzed by SDS2.2.2 software (Life Technologies, CA) to verify that only a single product was amplified. TUB8 (At5g23860) was used as an internal control for normalization of data.

2.3.7 Preparation and Analysis of the FIT-LUC Reporter Gene

A 1324-bp genomic DNA fragment of the *FIT* promoter was amplified by PCR using a primer pair [1047,1048] and BAC clone F24D13 as template. The PCR product was digested by HindIII and EcoRV, and ligated into pEnEL2Ω-LUC (GenBank Accession No. JN570503) digested with HindIII and SnaBI. A Gateway LR reaction was performed according to the manufacturer's instructions, using pBSVirHygGW as the destination vector (Ueda et al., 2008). Transformation of *Agrobacterium tumefaciens* GV3101(pMP90RK), floral transformation of *cpl1-6*, and hygromycin selection of transformants were performed as described previously (Ueda et al., 2008). The homozygous *cpl1-6 FIT-LUC* line was crossed with the Col-0 wild type and *fit-2*, and homozygous Col-0 *FIT-LUC, fit-2 FIT-LUC,* and *cpl1-6 fit-2 FIT-LUC* lines were identified in the segregating F2 population and confirmed in the F3 generation. The expression level of *LUC* in each line was determined by RT-qPCR.

2.3.8 Preparation and Analysis of the CPL1-GUS Reporter Gene

A genomic fragment (8.1 kb) of the *CPL1* locus encoded by an 8.4-kb BlpI fragment of BAC clone F17L22 was cloned in SmaI-digested pENTR2B (Life Technologies, CA). Subsequently, a ß-glucuronidase-coding sequence of pBI101was inserted immediately before the stop codon of *CPL1*. The resulting entry clone was then recombined with pBSVirHygGW binary plasmid (Ueda et al., 2008) using LR recombinase (Life Technologies, CA) to produce pBSVirHygCPL1-GUS, which was introduced into *Agrobacterium tumefaciens* GV3101(pMP90RK) and then used for flower transformation of Col-0 plants (Koiwa et al., 2002). Hygromycin-resistant transgenic plants were selected on medium containing 1/4x MS salts, 30 µg/ml hygromycin, 100 µg/ml cefotaxime, and 0.8% agar.

Five-day-old Col-0 *CPL-GUS* plants germinated on basal medium were grown for an additional three days on Fe-sufficient or -deficient basal medium (see below). For high-resolution GUS staining, plants were fixed in ice cold 90% acetone for 15 min and then incubated at 37°C for 4 h in a solution containing 2 mM 5-bromo-4-chloro-3-indolyl glucuronide, 5 mM $K_3Fe(CN)_6$, 5 mM $K_4Fe(CN)_6$, 100 mM sodium phosphate buffer (pH 7.0), and 0.1% Triton X-100. After incubation, the samples were rinsed with 100 mM phosphate buffer.

For embedding, GUS-stained plants were fixed in 2% glutaraldehyde using cold microwave technology in a BioWave^{TM} microwave with a 6-min vacuum cycle (2 min on/ 2 min off) at 200 W. After washing in the 100 mM sodium phosphate buffer (pH 7.0), the sample was dehydrated in a MeOH/water graded series at 10% MeOH increments (from 50% to 90%) for 1 min (30 s on/ 30 s off) at 200 W followed by 3 cycles in 100% MeOH. Samples were rinsed in propylene oxide and then 2 ml of fresh propylene oxide was added to each sample. Samples were infilterated with Quetol 651-low viscosity resin by the stepwise addition of 10% (V:V) resin to each sample (Ellis, 2006). After each addition of

resin, samples were allowed to infiltrate for several hours to overnight before additional resin was added. After two changes of 100% resin, samples were again vacuum infiltrated for 6 min (2 min on/ 2min off) at 200 W and then embedded. Five-micrometer sections were prepared and mounted onto slides, and stained with toluidine blue before observation.

2.3.9 Stress Treatments

For testing plant responses to various Fe regimens, seeds were sown on basal medium containing 1/4 x MS salts, 50 µM Fe-EDTA, 0.5% sucrose, and 1.5% agar. Fe deficiency was applied by transferring 7-day-old seedlings to basal medium without Fe-EDTA but containing 300 µM ferrozine [3-(2-pyridyl)-5,6-diphenyl-1,2,4-triazine sulfonate] (0_{FZN} basal media). Total RNA was isolated at the indicated times. For growth analysis, 4-day-old seedlings grown on basal medium were transferred to the 0_{FZN} basal medium and plants were photographed 5 days after the transfer. Primary root lengths were analyzed using Image J software.

To determine cadmium sensitivity, seedlings of the C24 wild type and *cpl1-2* mutant were grown on basal medium adjusted to the indicated concentration of Fe-EDTA and in the presence or absence of 60 µM $CdCl_2$. Seedlings were photographed after 11 days of growth and primary root lengths were analyzed.

For ABA treatment, seven-day-old plants grown on basal medium were transferred to basal medium with or without 1 µM ABA.

2.3.10 Determination of Ferric Chelate Reductase Activity

Root ferric chelate reductase activity was measured spectrophotometrically as described (Yi and Guerinot, 1996). The assay solution was composed of 0.1 mM Fe(III)-EDTA and

0.3 mM ferrozine in distilled water. Roots of five plants were soaked in assay solution for 30 minutes in darkness and then the absorbance of the assay solution was determined. An identical assay solution without any plants was used as blank. Purple-colored Fe(II)-ferrozine complex formation was quantified using a molar extinction coefficient of 28.6 mM^{-1} cm^{-1} at 562 nm. The experimental results were the mean of three biological repeats with six technical replicates each.

2.3.11 IRT1 Accumulation

Total root protein was extracted from both C24 wild-type and *cpl1-2* mutant plants grown either in Fe-sufficient or Fe-deficient conditions. Extracts were prepared by grinding tissues in extraction buffer on ice, followed by centrifugation at 4°C for 15 min at 14,000 x g. Twenty micrograms of total protein extracts was resolved on a 10% SDS–polyacrylamide gel and electroblotted onto polyvinylidene fluoride (PVDF) membrane (Millipore, MA). After blocking with 6% skim milk in Tris-buffered saline (TBS), the membrane was incubated with affinity-purified rabbit anti-IRT1 antibodies (diluted to 1/5000 in Tris-Tween buffered saline (TTBS)) prepared as described previously (Vert et al., 2002) (Genscript, CA) and then goat anti-rabbit IgG-HRP conjugate (Thermo Scientific, MA) diluted to 1/100,000 in TTBS. The blot was developed using a Supersignal West Femto Kit (Thermo Scientific, MA) and documented using a Cascade II CCD camera (Photometrics, AZ). Anti-actin antibody (A2066: Sigma, MO) was used as the loading control.

2.3.12 Determination of Metal Content

Tissue element analysis of Na, K, Ca, Fe, Mn, Zn, and Cd using inductively coupled plasma–mass spectrometry (ICP-MS) was performed as described (Baxter et al., 2007). Briefly, shoots were washed thoroughly with distilled water. Roots were washed first in 2 mM $CaSO_4$ and 10 mM EDTA for 10 minutes, and were then rinsed twice in distilled

water. Then, tissues were blot-dried, divided into three replicates of about 100 mg fresh weight, dried in a 65˚C oven for 48 h, and reweighed. The dried samples were digested completely using 0.6 ml of concentrated ultrapure grade HNO_3 (JT Baker, Netherlands) at 110˚C for 4 h. Each sample was diluted to 6 ml with nanopure water (18.2 MΩ) and analyzed on a PerkinElmer NexION 300D ICP-MS in the reaction mode. Indium (EMD Millipore, Germany) was used as an internal standard. The National Institute of Standards and Technology traceable calibration standards (Alfa Aesar, MA) were used for the calibration. Each sample was read five times in the pulse detector mode. Three biological replicates were performed per analysis.

2.3.13 Perls Staining of Fe

Perls staining of Arabidopsis seedlings was performed as described (Stacey et al., 2008) with slight modifications. Ten-day-old wild type C24 and *cpl1-2* mutant seedlings were first washed with 10 mM EDTA (pH 8.0) solution for 5 minutes, then with distilled water three times. Next, seedlings were vacuum infiltrated with equal volumes of 4% (v/v) HCl and 4% (w/v) potassium ferrocyanide (Perls solution) for 30 minutes at room temperature and then incubated for 30 min at 53°C. Seedlings were then rinsed several times with distilled water and observed under BX51 microscope (Olympus, PA).

2.3.14 Statistical Analysis

Statistical analyses were performed with MINITAB 16 software (Minitab, PA). Statistical significances of differences between mean values were determined using Student's *t*-test or one-way analysis of variance (ANOVA) followed by Tukey's HSD post hoc test. Differences were considered significant when the *p*-value was less than 0.05.

2.3.15 Accession Numbers

Sequence data from this article can be found in the Arabidopsis Genome Initiative or the GenBank/EMBL data libraries under the following accession numbers: CPL1 (AT4G21670), CPL2 (AT5G01270), CPL3 (AT2G33540), IRT1 (AT4G19690), FIT (AT2G28160), FRO2 (AT1G01580), BHLH38 (AT3G56970), BHLH39 (AT3G56980), BHLH100 (AT2G41240), BHLH101 (AT5G04150), FER1 (AT5G01600), ICL (AT3G21720), BGLU29 (AT2G44460), OPT3 (AT4G16370), AHP4 (AT3G16360), NAS4 (AT1G56430), LSU2 (AT5G24660), PPCK1 (AT1G08650), OPR (AT1G17990), HVA22b (AT5G62490), LEA4-2/LEA18 (AT2G35300), LEA4-5 (AT5G06760), BGLU30 (AT3G60140), ADC2 (AT4G34710), PAP17 (AT3G17790), TUB8 (AT5G23860), ACT2 (AT3G18780), AT5G26220, AT3G15670, AT3G02480, AT1G67600, AT5G07330, AT5G45690, AT5G66780, AT1G05510, AT3G58450, AT5G48850, AT5G59030, AT2G33070, AT1G36370, AT1G12030, AT4G15390, AT2G23110, AT3G50980, AT5G01300, AT5G48180, AT1G52690, AT3G17520, AT2G47770, AT5G66400, AT2G31980, AT2G40435, AT1G04560, AT1G18870, and AT3G49580.

2.4 Results

2.4.1 The Identification of Genes Uniquely Regulated in cpl1

Arabidopsis CPL1 was previously shown to regulate gene expression under osmotic stress conditions through ABA signaling (Koiwa et al., 2002; Xiong et al., 2002). To obtain insight into the regulatory networks modulated by CPL1, the global transcript profile of *cpl1-2* was determined using an Affymetrix ATH1 Gene Chip. To obtain unbiased gene expression profiles, cRNA probes were prepared from total RNA extracted from unstressed young (10-day-old) seedlings of the wild-type C24 or *cpl1-2* lines grown on medium containing 1/4 x MS salts, 0.5% sucrose, and 0.8% agar. After probe-level data normalization using the Robust Multiarray Analysis (RMA) algorithm (Fig. 2.1A), hybridization intensity data for 19597 out of 22810 probes, which were above the 20th percentile in at least one out of six hybridizations, were selected for further analysis. Next, consistency between the C24 and *cpl1-2* replicate datasets was confirmed by Principal Component Analysis (PCA). Triplicate datasets of each genotype clustered together in a three-dimensional scatter plot (Fig. 2.1.B), whereas there was a clear separation of the C24 and *cpl1-2* datasets. This is indicative of data consistency among replicate datasets for each genotype, as well as of genotype differentiation. Differentially expressed genes were then determined by evaluating fold change ($\geq$2 was considered as the cut-off) and one-way ANOVA (p <0.05 was considered significant), followed by the Tukey HSD (honestly significant difference) test and Benjamin Hochberg multiple corrections.

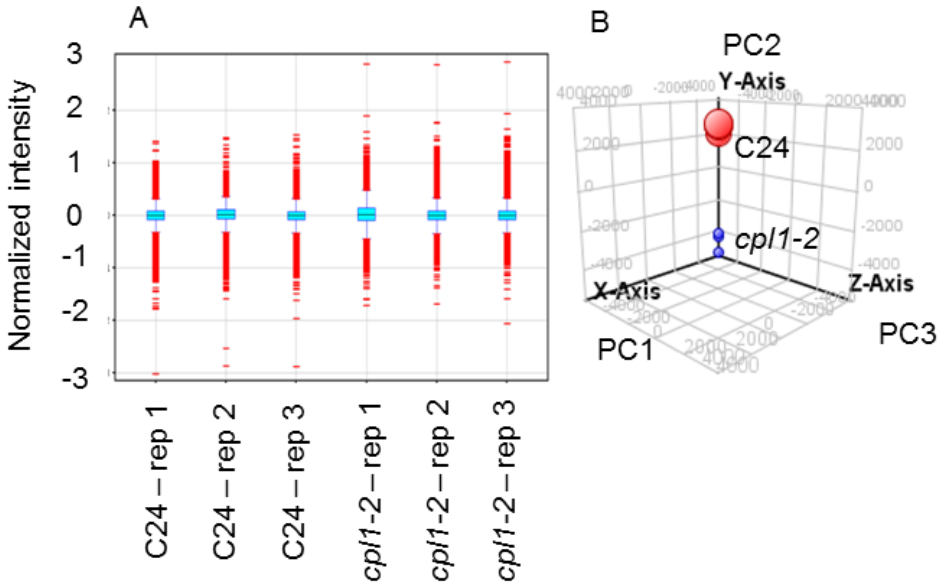

Figure 2.1. Normalization and principal component analysis of the *cpl1*-2 and C24 microarray. A, Box and whisker plots of the distributions of individual Affymetrix ATH1 Gene Chip hybridization intensities for C24 and *cpl1-2* generated after Robust Multi-array Analysis (RMA) normalization on GeneSpring GX 11.0.2. For each Gene Chip dataset, the median expression value was normalized to 0 and is shown as the horizontal line across the box. The upper and lower ends of the box indicate the first and third quartile values and the extensions show the 1.5x interquartile (IQR) range for the sample. The red lines indicate outliers whose expression level was greater or less than 1.5x IQR from the median. Triplicate datasets are shown for C24 and *cpl1-2* samples. B, Principal component analysis (PCA) of RMA-normalized Gene Chip datasets. Triplicate datasets for C24 (red) and *cpl1-2* (blue), respectively, were plotted in a 3D scatter plot. The X-axis (PC1), Y-axis (PC2), and Z-axis (PC3) components represent 42.1%, 20.34%, and 13.42%, respectively, of the total variability between the Chip datasets. Three replicates of each genotype clustered together, suggesting no significant differences between replicates, while the medians of each triplicate are well separated, suggesting that the prevalent gene expression profiles of C24 and *cpl1-2* are different.

A total of 114 and 132 genes were significantly up- and down-regulated by more than 2-fold, respectively, in the *cpl1-2* mutant datasets relative to those of the control (Supplemental dataset). To confirm the microarray data, the expression of 41 up-regulated and 22 down-regulated genes was determined by RT-qPCR analysis. The up-regulation of 36 genes and down-regulation of 15 genes was confirmed (i.e., 81% of the genes tested by RT-qPCR), indicating that the microarray results were generally reliable (Supplemental dataset). Genes that could not be confirmed as being differentially expressed were excluded in subsequent analyses. We refer to the resulting 109 genes that were up-regulated in *cpl1-2* as *CUTs* (*cpl1-Up Transcripts).*

2.4.2 CUTs Encode ABA/Osmotic Stress- and Fe Deficiency-Responsive Genes

To determine the signaling pathway in which CPL1 is involved, we screened gene expression data in the AtGenExpress and Gene Expression Omnibus databases using the list of *CUTs*. The *CUT* expression profiles of four abiotic stress/ABA treatments showed overlap with that of *cpl1-2*, and were subjected to hierarchical clustering using Pearson correlation and the average linkage rule. Clustering results showed that no single treatment profile displayed overall similarity with the *cpl1-2* profile; however, two clusters of genes were similarly up-regulated in *cpl1-2* and in plants exposed to abiotic stresses and ABA (Fig. 2.2). Genes in cluster I (27 genes) were up-regulated by hyperosmotic stress and ABA. Cluster II contains 16 genes that were strongly induced under Fe deficiency stress, including At4g19690 (*IRT1*), a major Fe transporter.

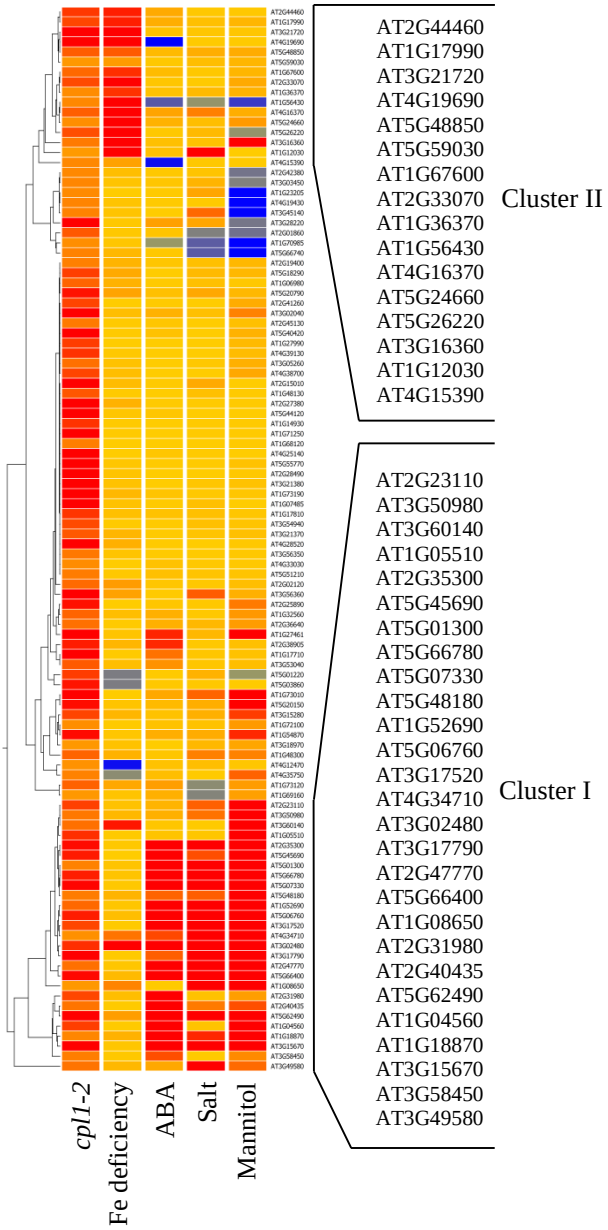

Figure 2.2. Hierarchical clustering of *CUTs* (*cpl1-Up Transcripts*) based on their differential expression during abiotic stress. The expression level of 109 *CUTs* in *cpl1-2* plants and in wild-type plants subjected to an Fe deficiency (Fe-free nutrient solution for 24 h; GEO accession GSE15189), ABA (1 µM for 3 h; NASCArray accession 176), salt (130 mM NaCl for 6 h, NASCArray accession 139), or mannitol (300 mM mannitol for 12 h, NASCArray accession 140) were subjected to hierarchical clustering using the Pearson correlation distance and average linkage rule.

The differential regulation of clusters I and II by abiotic stresses was confirmed by Gene Set Enrichment Analysis (GSEA) using GeneTrail (Backes et al., 2007; Schuler et al., 2011). As shown in Table 2.1, the genes in cluster I were significantly enriched by osmotic stress and ABA ($p<0.05$), but not by Fe deficiency. Conversely, those in cluster II were enriched only by Fe deficiency ($p<0.05$).

Table 2.1. Gene Set Enrichment Analysis (GSEA) of Cluster I and Cluster II gene sets.

Gene Set (Number of Genes in the set)	Fe deficiency 24 h[c]	1 μM ABA 3 h[d]	130 mM NaCl 6 h[e]	300 mM mannitol 12 h[e]
	***p*-value**			
Cluster I (27)	0.212	0*	0*	0*
Non-Cluster (27)[a]	0.245	0.443	0.243	0.254
Cluster II (16)	0.002*	0.183	0.192	0.524
Non-cluster (16)[a]	0.287	0.292	0.298	0.254
Reference (20)[b]	0.228	0.152	0.271	0.099

GSEA was performed against datasets obtained from GEO accession GSE15189[c], and NASCArray accessions 176[d], 139[e], and 140[e]. *Indicates a specific gene set significantly enriched ($p<0.05$) in top-ranked genes.

[a]Non-cluster gene set contains *CUTs* not classified as Cluster I or Cluster II. [b]A reference gene set contains constitutively expressed genes (Czechowski et al., 2005), and was used as a negative control.

[c]Buckhout TJ et al. (2009) Early iron-deficiency-induced transcriptional changes in Arabidopsis roots as revealed by microarray analyses. Bmc Genomics 10, 147

[d]Goda H et al. (2008) The AtGenExpress hormone and chemical treatment data set: experimental design, data evaluation, model data analysis and data access. Plant Journal 55: 526-542

[e]Kilian J et al. (2007) The AtGenExpress global stress expression data set: protocols, evaluation and model data analysis of UV-B light, drought and cold stress responses. Plant Journal 50: 347-363

To obtain deeper insight into the regulation of *CUTs* by abiotic stresses, we examined the expression level of *CUTs* in public microarray datasets designed to analyze responses to Fe deficiency (Colangelo and Guerinot, 2004; Dinneny et al., 2008; Buckhout et al., 2009; Long et al., 2010; Yang et al., 2010; Schuler et al., 2011; Ivanov et al., 2012), ABA treatment (Seki et al., 2002; Nishimura et al., 2007; Goda et al., 2008; Mizoguchi et al., 2010), and osmotic stress treatment (mannitol or drought) (Kreps et al., 2002; Seki et al., 2002; Li et al., 2006; Kilian et al., 2007). Affymetrix CEL files for each experiment were

processed as described above, and transcripts significantly up-regulated by 2 fold or more (p<0.05) were identified for each microarray experiment. Genes up-regulated in both *cpl1-2* and in wild-type plants subjected to these abiotic stress treatments were identified and grouped (Fig. 2.3; Supplemental Dataset).

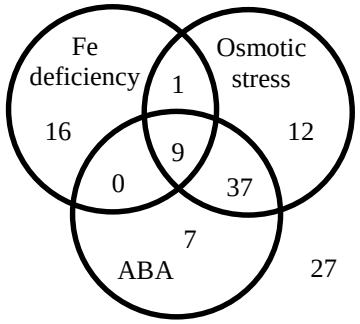

Figure 2.3. Venn diagram representing the differential regulation of *CUTs* by abiotic stresses. The expression level of *CUTs* was examined in public microarray datasets for Fe deficiency, ABA, and osmotic stress (mannitol or drought) treatments (see text and Supplemental Table S3).

In addition, the Fe-regulated genes described by Ivanov et al. (Ivanov et al., 2012) were examined for overlaps. We identified 26 and 59 *CUTs* that were up-regulated in the Fe deficiency and osmotic stress datasets, respectively (p<0.05 by GSEA, Table 2.2). Of these, 10 *CUTs* were regulated both in Fe and osmotic stress datasets. Some of the osmotically regulated *CUTs*, including nine *CUTs* regulated by Fe deficiency, were also up-regulated in ABA datasets, implying that ABA signaling plays a role in the dual regulation of some *CUTs* by osmotic stress and Fe deficiency. The remaining 27 *CUTs* were not up-regulated in either the Fe deficiency or osmotic stress experiments.

Table 2.2. Gene Set Enrichment Analysis (GSEA) of gene sets presented in Fig 2.3.

Gene Set (Number of Genes in the set)	Fe deficiency 72 h [c]	Fe deficiency 24 h [d]	Fe deficiency 24 h [e]	Fe deficiency 1 week [f]	Fe deficiency 72 h [g]	1 µM ABA 3 h [h]	0.5 µM ABA 2 days [i]	100 µM ABA 4 h [j]	300 mM Mannitol 12 h [k]	130 mM NaCl 6 h [k]	3% Mannitol 6 h [l]
	p-value										
Fe-specific (16)	$1.3x10^{-4}$*	0.008*	$7.0x10^{-5}$*	$5.0x10^{-5}$*	$2.7x10^{-4}$*	0.181	0.215	0.189	0.508	0.199	0.473*
Overlap (10)	0.049*	0.178	0.038*	0.139	$7.0x10^{-5}$*	0*	0.004*	$6.0x10^{-5}$*	0*	0*	$6.1x10^{-4}$*
Osmotic stress+ ABA (56)[b]	0.461	0.119	0.049	0.250	0.138	0*	0*	0*	0*	0*	$5.0x10^{-5}$*
Others (27)	0.649	0.344	0.285	0.206	0.357	0.392	0.673	0.409	0.064	0.053	0.290
Reference (37)[a]	0.063	0.129	0.203	0.074	0.465	0.206	0.311	0.107	0.086	0.290	0.058

GSEA was performed against datasets obtained from GEO accessions GSE10576[c], GEOD21443[d], GSE15189[e], GSE24248[f], GEOD6638[i], E-MEXP2378[j], and E-MEXP475[i], and NASCArray accessions 176[h], 139[k], and 140[k], and from Yang et al., (2010)[g]. *Indicates a specific gene set significantly enriched ($p<0.05$) in top-ranked genes. [a]A reference gene set contains constitutively expressed genes (Czechowski et al., 2005), and was used as a negative control. [b]Categories were combined due to a large degree of overlap between osmotic stress- and ABA-specific genes.

[c]Dinneny JR et al. (2008) Cell identity mediates the response of Arabidopsis roots to abiotic stress. Science 320: 942-945
[d]Long TA et al. (2010) The bHLH Transcription Factor POPEYE Regulates Response to Iron Deficiency in Arabidopsis Roots. Plant Cell 22: 2219-2236
[e]Buckhout TJ et al. (2009) Early iron-deficiency-induced transcriptional changes in Arabidopsis roots as revealed by microarray analyses. Bmc Genomics 10, 147
[f]Schuler M et al. (2011) Transcriptome analysis by GeneTrail revealed regulation of functional categories in response to alterations of iron homeostasis in Arabidopsis thaliana. Bmc Plant Biology 11
[g]Yang TJW et al. (2010) Transcriptional Profiling of the Arabidopsis Iron Deficiency Response Reveals Conserved Transition Metal Homeostasis Networks. Plant Physiol 152: 2130-2141
[h]Goda H et al. (2008) The AtGenExpress hormone and chemical treatment data set: experimental design, data evaluation, model data analysis and data access. Plant Journal 55: 526-542
[i]Nishimura N et al. (2007) ABA-Hypersensitive Germination1 encodes a protein phosphatase 2C, an essential component of abscisic acid signaling in Arabidopsis seed. Plant Journal 50: 935-949
[j]Mizoguchi M et al. (2010) Two Closely Related Subclass II SnRK2 Protein Kinases Cooperatively Regulate Drought-Inducible Gene Expression. Plant and Cell Physiology 51: 842-847
[k]Kilian J et al. (2007) The AtGenExpress global stress expression data set: protocols, evaluation and model data analysis of UV-B light, drought and cold stress responses. Plant Journal 50: 347-363
[i]Li YH et al. (2006) Establishing glucose- and ABA-regulated transcription networks in Arabidopsis by microarray analysis and promoter classification using a Relevance Vector Machine. Genome Res 16: 414-427

The *IRT1* transcript showed the highest level of up-regulation (54.6-fold) in *cpl1-2* microarray datasets, even though the plants used in the analysis were grown under Fe-sufficient conditions. Other *CUTs* in Fe-stress datasets include Fe utilization-related genes, such as *OLIGOPEPTIDE TRANSPORTER 3* (*OPT3*), *NICOTIANAMINE SYNTHASE 4* (*NAS4*), and *ISOCITRATE LYASE* (*ICL*). To confirm that the observed gene expression changes in *cpl1-2* were due to the mutation in the *CPL1* locus and not to a potential second-site mutation, the expression levels of select *CUTs* in both *cpl1-1* and *cpl1-2* alleles were determined by RT-qPCR. Of 26 *CUTs* tested, we confirmed the significant up-regulation of 19 Fe- and/or ABA/osmotic stress-regulated *CUTs* in both *cpl1-1* and *cpl1-2* plants. In addition, the expression of five more *CUTs* was significantly up-regulated in at least one *cpl1* allele (Table 2.3).

Elevated basal expression levels of Fe utilization-related genes in *cpl1-2* were unexpected, since *cpl1-2* was isolated based on altered osmotic stress responses, and *cpl1-2* does not exhibit the typical Fe deficiency symptoms (e.g., leaf chlorosis) seen in the *irt1* or *fit* mutants (Connolly et al., 2002; Vert et al., 2002; Colangelo and Guerinot, 2004; Jakoby et al., 2004).

2.4.3 CPL1 is Involved in Fe Stress Responses

To establish the causal link between *cpl1* mutations and enhanced Fe deficiency responses, we tested the basal expression level of Fe utilization-related genes (*IRT1*, *FRO2*, *FIT*, and group Ib *bHLHs*) in several independent *cpl1* mutants.

Table 2.3. Select *CUT*s confirmed as being up-regulated in *cpl1-1* and *cpl1-2*.

AGI	Class[a]	Gene	*cpl1-2*/C24		*cpl1-1*/C24
			Microarray	RT-qPCR (±SEM)	RT-qPCR (±SEM)
AT4G19690	F	Iron-responsive transporter 1 (IRT1)	54.57	57.68 (± 0.88)*	37.79 (± 0.56)*
AT3G21720	F	Isocitrate lyase, putative (ICL)	8.99	5.28 (± 0.79)*	5.98 (± 0.34)*
AT2G44460	F	Glycosyl hydrolase family 1 protein (BGLU29)	3.92	7.73 (± 0.47)*	7.36 (± 0.34)*
AT5G26220	F	ChaC-like family protein	3.46	2.64 (± 0.17)*	2.71 (± 0.06)*
AT4G16370	F	Oligopeptide transporter family protein (OPT3)	3.18	3.25 (± 0.23)*	4.08 (± 0.10)*
AT3G16360	F	HPT phosphotransmitter 4 (AHP4)	2.60	2.64 (± 0.32)*	2.81 (± 0.14)*
AT1G56430	F	Nicotianamine synthase 4 (NAS4)	2.35	1.87 (± 0.08)*	1.79 (± 0.26)
AT5G24660	F	Response to low sulfur 2 (LSU2)	2.22	1.87 (± 0.43)*	2.44 (± 0.40)*
AT1G08650	F	Phosphoenolpyruvate carboxylase kinase 1 (PPCK1)	2.03	3.43 (±0.37)*	N/D
AT1G17990	F/O	12-oxophytodienoate reductase, putative (OPR)	3.64	3.81 (± 0.21)*	6.87 (± 0.40)*
AT5G62490	F/A/O	ABA-responsive protein (HVA22b)	6.91	15.67 (±0.81)*	6.32 (±0.50)*
AT3G15670	F/A/O	Late embryogenesis abundant protein (LEA) family protein	6.32	8.89 (±0.11)*	4.29 (±0.08)*
AT2G35300	F/A/O	Late embryogenesis abundant protein 4-2 (LEA 4-2/LEA18)	4.82	5.28 (±0.52)*	3.29 (± 0.32)*
AT5G06760	F/A/O	Late embryogenesis abundatnt protein 4-5 (LEA 4-5)	4.44	4.20 (±0.38)*	4.00 (± 0.04)*
AT3G02480	F/A/O	ABA-responsive protein-related/ LEA family protein (ABAR)	4.11	3.43 (±0.40)*	2.08 (± 0.07)*
AT1G67600	F/A/O	Acid phosphatase/vanadium-dependent haloperoxidase-related protein	2.99	2.62 (± 0.32)*	1.89 (± 0.02)
AT3G60140	F/A/O	Beta glucosidase 30, dark inducible 2, senescence-related gene 2 (BGLU30/ DIN2/ SRG2)	2.81	2.35 (±0.28)*	N/D
AT4G34710	F/A/O	Arginine decarboxylase 2 (SPE2/ADC2)	2.19	3.73 (±0.27)*	3.46 (± 0.10)*
AT3G17790	A/O	Purple acid phosphatase 17 (PAP17)	5.38	7.89 (±0.04)*	7.16 (± 0.24)*
AT5G07330	A/O	unknown protein	4.93	4.26 (±0.13)*	2.68 (±0.04)*
AT5G45690	A/O	unknown protein	4.49	5.74 (±0.50)*	4.63 (± 0.23)*
AT5G66780	A/O	unknown protein	4.41	3.46 (±0.41)*	2.06 (± 0.04)*
AT1G05510	A/O	unknown protein	4.11	8.40 (±0.56)*	5.90 (±0.37)*
AT3G58450	A/O	Universal stress protein (USP) family protein/ Adenine nucleotide alpha hydrolases-like superfamily protein	2.55	6.73 (±0.62)*	5.86 (± 0.17)*

[a]Gene classes represent upregulation by Fe deficiency (F), ABA treatment (A), or Osmotic stress (O).

*$p<0.05$, Student's *t*-test between mean values of *cpl1* and C24. N/D not determined.

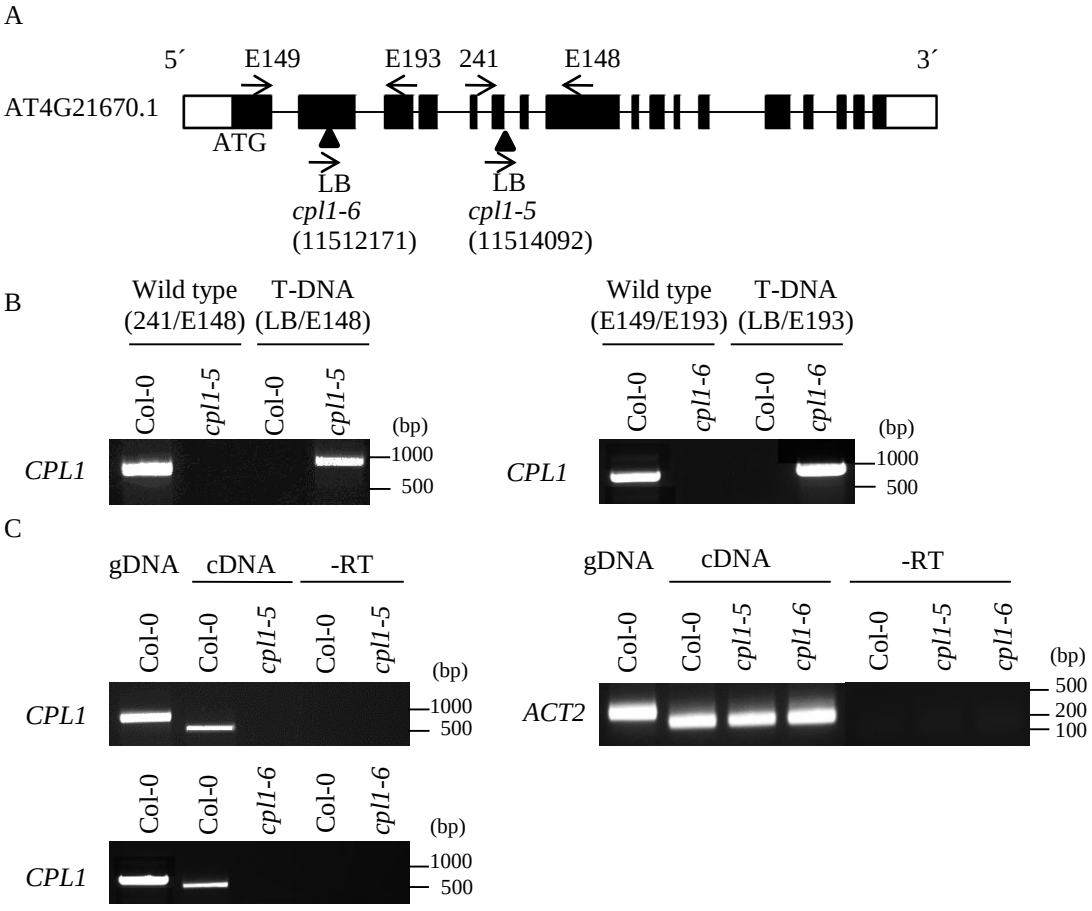

Figure 2.4. Molecular characterization of the *cpl1-5* and *cpl1-6* mutants. A, T-DNA insertion positions (triangles) in *cpl1-5* (GK-590C07) and *cpl1-6* (GK-165H09). B, Confirmation of T-DNA lines by PCR using wild-type and mutant genomic DNA as templates. The positions of specific primers are indicated by arrows in A. C, RT-PCR analysis of *CPL1* and *ACT2* transcript levels in the Col-0 wild type, *cpl1-5* and *cpl1-6*. Total RNA samples extracted from each genotype were used to prepare cDNA templates in the presence (cDNA) or absence (-RT) of reverse transcriptase. The PCR cycle number was 32.

In addition to *cpl1-1* and *cpl1-2* in the C24 background, two T-DNA insertion lines, *cpl1-5* and *cpl1-6*, in the Col-0 background, were tested. In *cpl1-5* and *cpl1-6*, T-DNAs were inserted at locus 11512171 and 11514092 of chromosome 4 (Fig. 2.4 A, B), respectively, and production of intact *CPL1* mRNA was abolished (Fig. 2.4 C). The basal expression of Fe utilization-related genes was elevated in all alleles, indicating that the *cpl1* mutations caused the gene expression phenotypes observed in these plants (Table 2.4). The phenotype was determined to be recessive, because F1 plants produced by crossing *cpl1-2* and the wild type showed a wild-type level of gene expression (Fig. 2.5). To compare the involvement of different *CPL* paralogs in this phenotype, we tested the gene expression levels in *cpl2-2* and *cpl3-1*. The expression levels of *IRT1*, *FRO2*, and *FIT* (hereafter referred to as [*IRT1, FIT, FRO2*]) in *cpl2-2 and cpl3-1* were similar to those of the wild type (Table 2.4), indicating that *CPL1* is uniquely associated with regulating Fe deficiency signaling. The above results established that the basal expression of Fe utilization-related genes was elevated in *cpl1* mutants.

Table 2.4. RT-qPCR analysis of Fe utilization-related gene expression levels in different *cpl1* alleles, *cpl2-2* and *cpl3-1*.

AGI	Gene	*cpl1-1*/C24 (±SEM)	*cpl1-2*/C24 (±SEM)	*cpl1-5*/Col-0 (±SEM)	*cpl1-6*/Col-0 (±SEM)	*cpl2-2*/Col-0 (±SEM)	*cpl3-1*/C24 (±SEM)
AT4G19690	*IRT1*	37.79 (± 0.56)*	57.68 (± 0.88)*	31.78 (± 0.42)*	35.75 (± 0.92)*	0.89 (± 0.12)	1.80 (± 0.60)
AT2G28160	*FIT1*	2.66 (± 0.10)*	2.16 (±0.18)*	1.43 (± 0.06)*	1.87 (± 0.04)*	1.15 (± 0.17)	1.64 (± 0.65)
AT1G01580	*FRO2*	6.59 (± 0.55)*	4.50 (±0.29)*	2.51 (± 0.10)*	5.10 (± 0.34)*	1.67 (± 0.54)	1.79 (± 0.76)
AT5G01600	*FER1*	0.40 (± 0.24)*	0.48 (± 0.24)*	0.94 (± 0.73)	0.13 (± 0.08)*	N.D.	N.D.
AT3G56970	*BHLH38*	2.83 (± 0.61)*	2.89 (± 0.20)*	4.89 (±0.51)*	2.04 (±0.18)*	N.D.	N.D.
AT3G56980	*BHLH39*	11.71 (± 0.31)*	13.74 (± 1.04)*	11.88 (±0.83)*	13.09 (±1.13)*	N.D.	N.D.
AT2G41240	*BHLH100*	12.13 (± 0.63)*	11.16 (± 0.85)*	18.00 (± 1.28)*	12.73 (± 0.61)*	N.D.	N.D.
AT5G04150	*BHLH101*	38.32 (± 3.87)*	24.42 (± 0.92)*	36.76 (± 1.31)*	29.04 (± 0.97)*	N.D.	N.D.

Total RNA was extracted from whole plants grown for 10 days on medium containing 1/4 x MS salts, 0.5% sucrose, and 0.8% agar. The presented expression levels are mean values (±SEM) of three biological replicates analyzed in duplicate. *$p<0.05$, Student's *t*-test between mean values of *cpl1-1/cpl1-2/cpl3-1* and C24, or *cpl1-5/cpl1-6/cpl2-2* and Col-0. N.D., not determined.

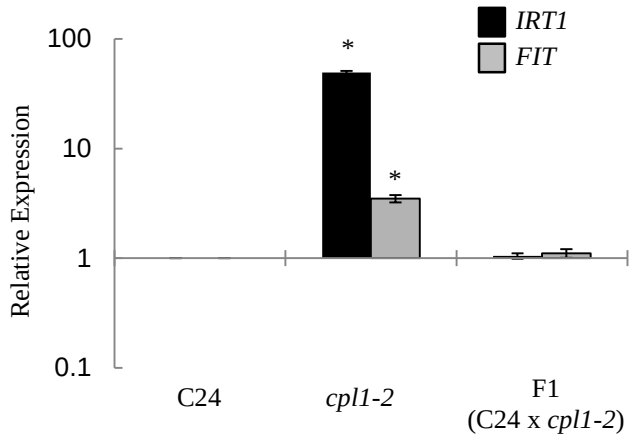

Figure 2.5. The expression levels of *IRT1* and *FIT* in F1 plants produced after crossing *cpl1-2* with the wild type. Seeds were germinated and grown on medium containing 1/4 x MS salts, 0.5% sucrose, and 0.8% agar for 7 days. The presented expression levels (relative to the C24 sample) are the mean values of three biological replicates analyzed in duplicate. Bars indicate standard errors of the mean (SEM) of three biological replicates. **p*<0.05, Student's *t*-test between mean values of *cpl1-2*/F1 and C24.

Next, we systematically analyzed the Fe deficiency responses of *cpl1-2*. For this purpose, we established Fe-sufficient conditions using basal growth medium containing 1/4x MS salts (modified to 50 µM Fe-EDTA) and 0.5% sucrose (Fig. 2.6). Fe deficiency stress was applied by transferring plants to the same medium lacking Fe-EDTA but containing 300 µM ferrozine, which chelates Fe in the medium and makes it unavailable to the plant (Colangelo and Guerinot, 2004). An increase in Fe-EDTA from 25 µM to 50 µM moderately decreased the basal expression level of Fe utilization-related genes in *cpl1-2*. Upon transfer to Fe-deficient media, *cpl1-2* showed more rapid and greater expression of [*IRT1, FIT, FRO2*] and *bHLH39* than did the wild type, as early as 12 h after transfer. The expression of *bHLH38, bHLH100,* and *bHLH101* was greater in *cpl1-2* than in the wild type, but the response kinetics of these genes in the mutant were similar to those of the wild type. *FER1* (*FERRITIN1*) was repressed in both *cpl1-2* and the wild type, albeit *cpl1-2* showed lower basal expression levels.

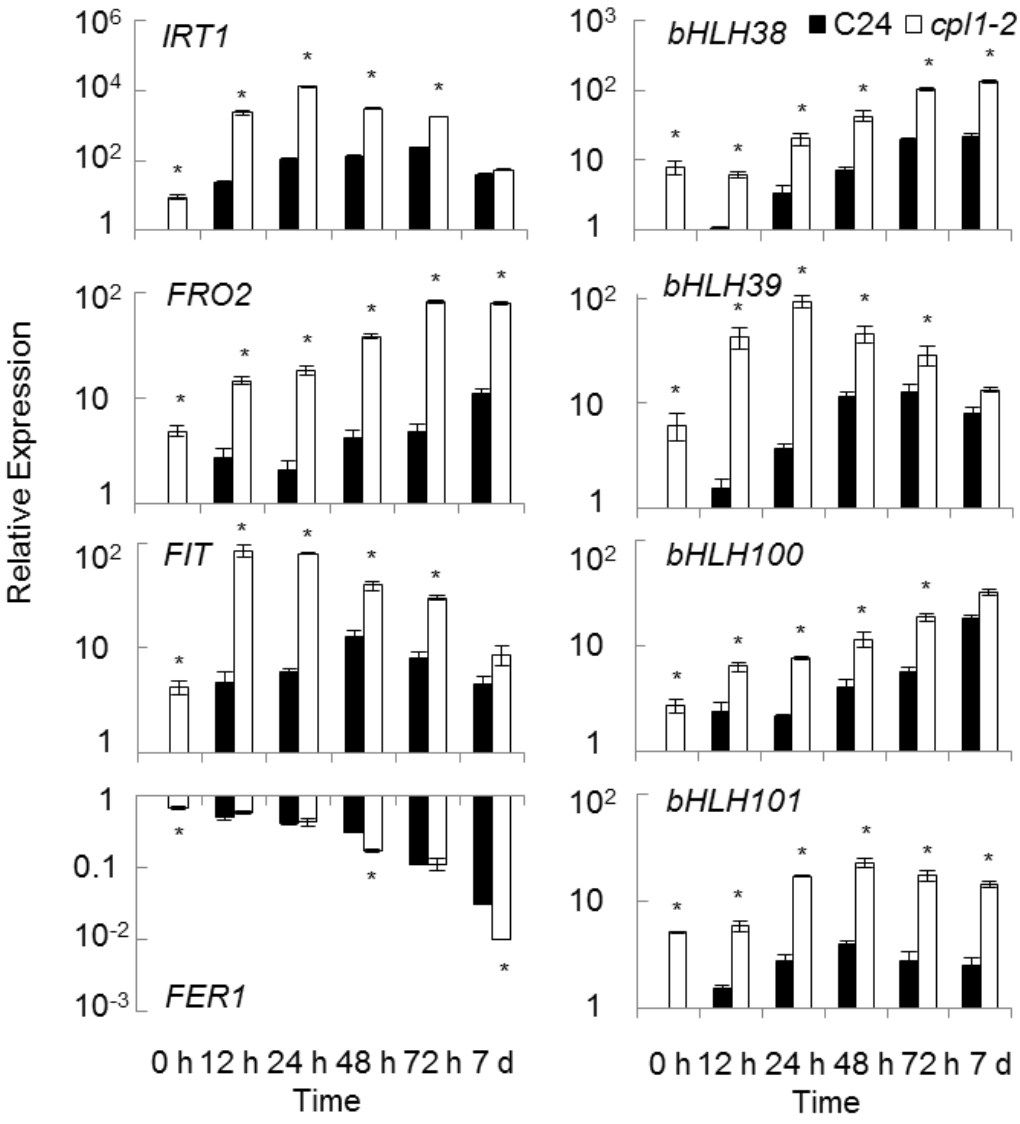

Figure 2.6. Time course analysis of expression levels of Fe utilization-related genes in the roots of *cpl1-2* and C24 under Fe deficiency (on basal medium). Plants were grown on basal medium for 7 days, and then transferred to Fe-deficient basal medium containing 300 µM ferrozine (see Materials and Methods). Root samples were collected at the time of transfer (0), or 12, 24, 48, or 72 h or 7 days after the transfer. The presented expression levels (relative to untreated C24 samples) are mean values of three biological replicates analyzed in duplicate. Bars indicate standard errors of the mean (SEM) of biological replicates. *p<0.05, Students t-test between mean values of *cpl1-2* and C24 for the same conditions.

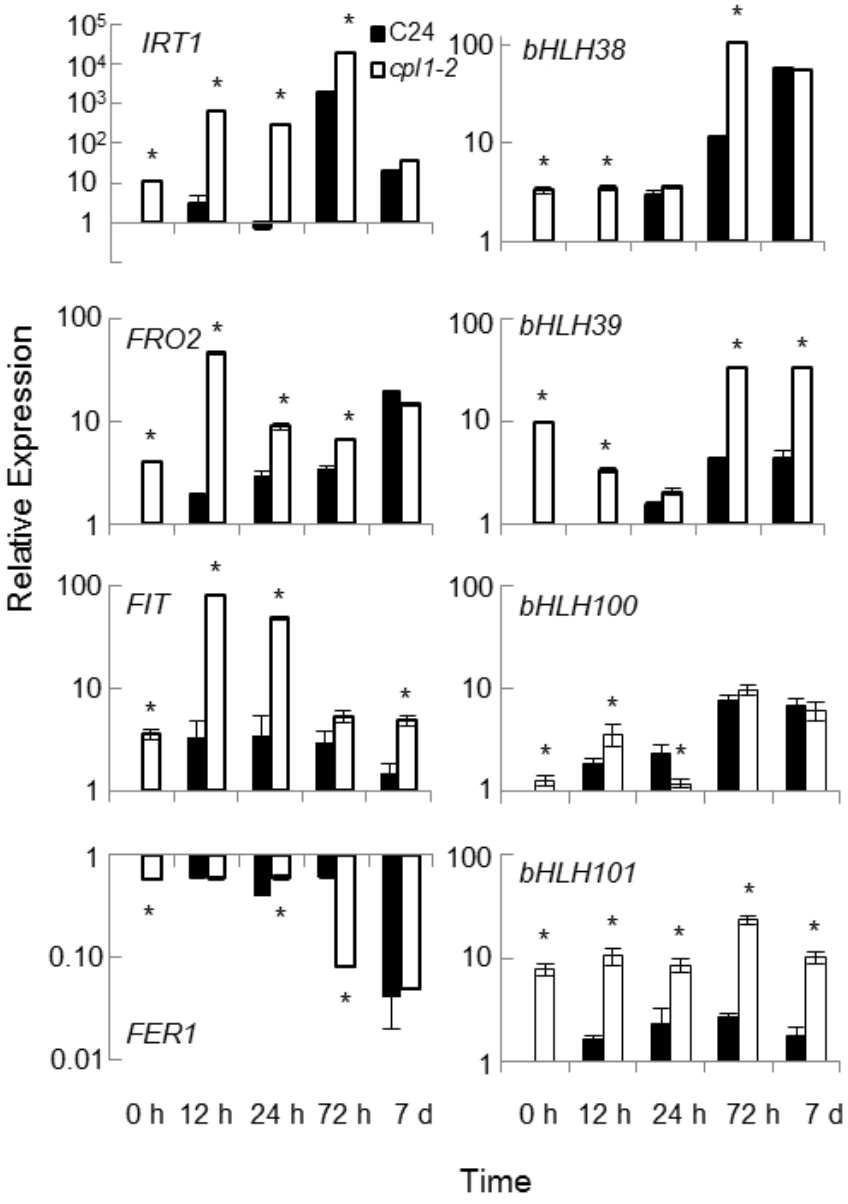

Figure 2.7. Time course analysis of expression levels of Fe utilization-related genes in the roots of *cpl1-2* and C24 under Fe deficiency (on 1 x MS medium). Plants were grown on 1x MS medium containing 3% sucrose and 1.5% agar for 7 days, and transferred to Fe-deficient medium containing 300 µM ferrozine. Roots were collected at the time of transfer (0 h), or 12, 24, and 72 hours, and 7 days after transfer. The presented expression levels (relative to untreated C24 samples) are the mean values of three biological replicates analyzed in duplicate. Bars indicate the standard errors of the mean (SEM) of three biological replicates. *p<0.05, Students t-test between mean values of *cpl1-2* and C24 for the same conditions.

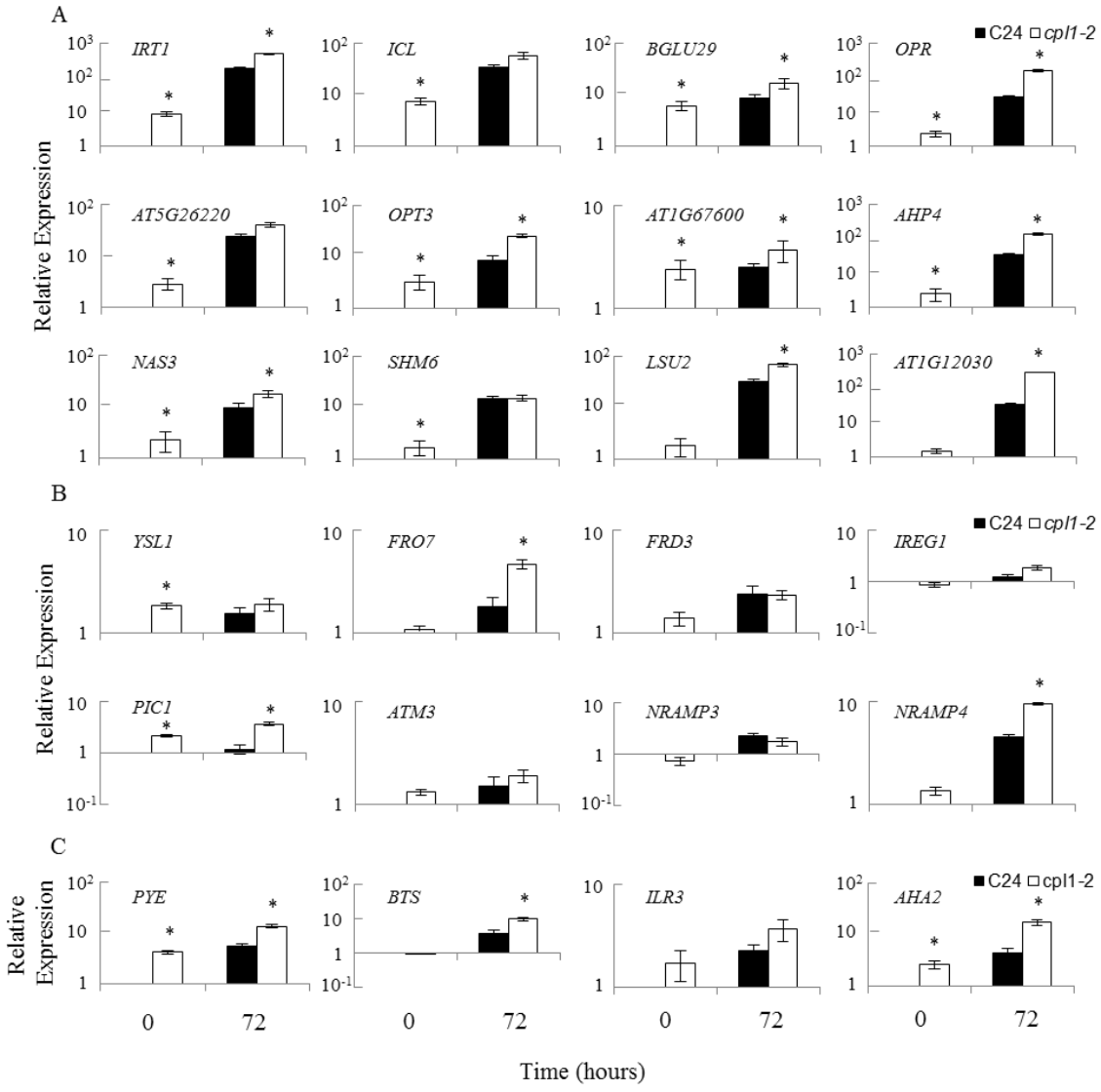

Figure 2.8. The expression of Fe utilization-related genes in roots of *cpl1-2* and C24 under Fe deficiency. Experiments were conducted as described in the legend to Figure 2.6. A. Cluster II genes. B. Fe transport genes. *YSL1*, *YELLOW STRIPE-LIKE 1* (AT4G24120); *FRO7*, *FERRIC CHELATE REDUCTASE 7* (AT5G49740*); FRD3, FERRIC REDUCTASE DEFECTIVE 3* (AT3G08040); *IREG1*, *IRON-REGULATED PROTEIN 1* (AT2G38460); *PIC1*, *PERMEASE IN CHLOROPLASTS 1* (AT2G15290); *ATM3*, *ARABIDOPSIS THALIANA ABC TRANSPORTER OF THE MITOCHONDRION 3* (AT5G58270); *NRAMP3*, *NATURAL RESISTANCE-ASSOCIATED MACROPHAGE PROTEIN 3* (AT2G23150); and *NRAMP4* (AT5G67330). C. Others. *PYE*, *POPEYE* (AT3G47640); *BTS*, *BRUTUS* (AT3G18290); *ILR3*, *IAA-LEUCINE RESISTANT 3* (AT5G54680); and *AHA2*, H^+*-ATPase 2* (AT4G30190). The presented expression levels (relative to untreated C24 samples) are the mean values of three biological replicates analyzed in duplicate. Bars indicate standard errors of the mean (SEM) of three biological replicates. **p*<0.05, Student's *t*-test between mean values of *cpl1-2* and C24 for the same condition.

Similar genotype differences were observed when 1x MS medium was used as the basal medium (Figure 2.7). Further RT-qPCR analyses confirmed the enhanced basal and/or induced expression levels of many but not all Fe-regulated/Fe utilization-related genes in *cpl1-2* (Fig. 2.8). Overall, the rapid and strong induction of [*IRT1, FIT, FRO2*] suggests that the transcriptional response of *cpl1-2* is more sensitive to Fe deficiency stress. To test this hypothesis, we determined if elevated external Fe could suppress the *cpl1-2* phenotype. Basal [*IRT1, FIT, FRO2*] expression levels were determined in plants growing on medium containing various concentrations of Fe (Fig. 2.9). *cpl1-2* maintained higher levels of [*IRT1, FIT, FRO2*], with the greatest difference between genotypes being observed at 25 µM; however, higher Fe concentrations repressed the overall expression of [*IRT1, FIT, FRO2*] in both the wild type and in *cpl1-2*. On media containing more than 100 µM Fe, the wild type and *cpl1-2* showed similar, low-level expression of [*IRT1, FIT, FRO2*]. Together, these results support the hypothesis that the Fe deficiency response in *cpl1-2* is more sensitive than that in the wild type, but is not constitutive.

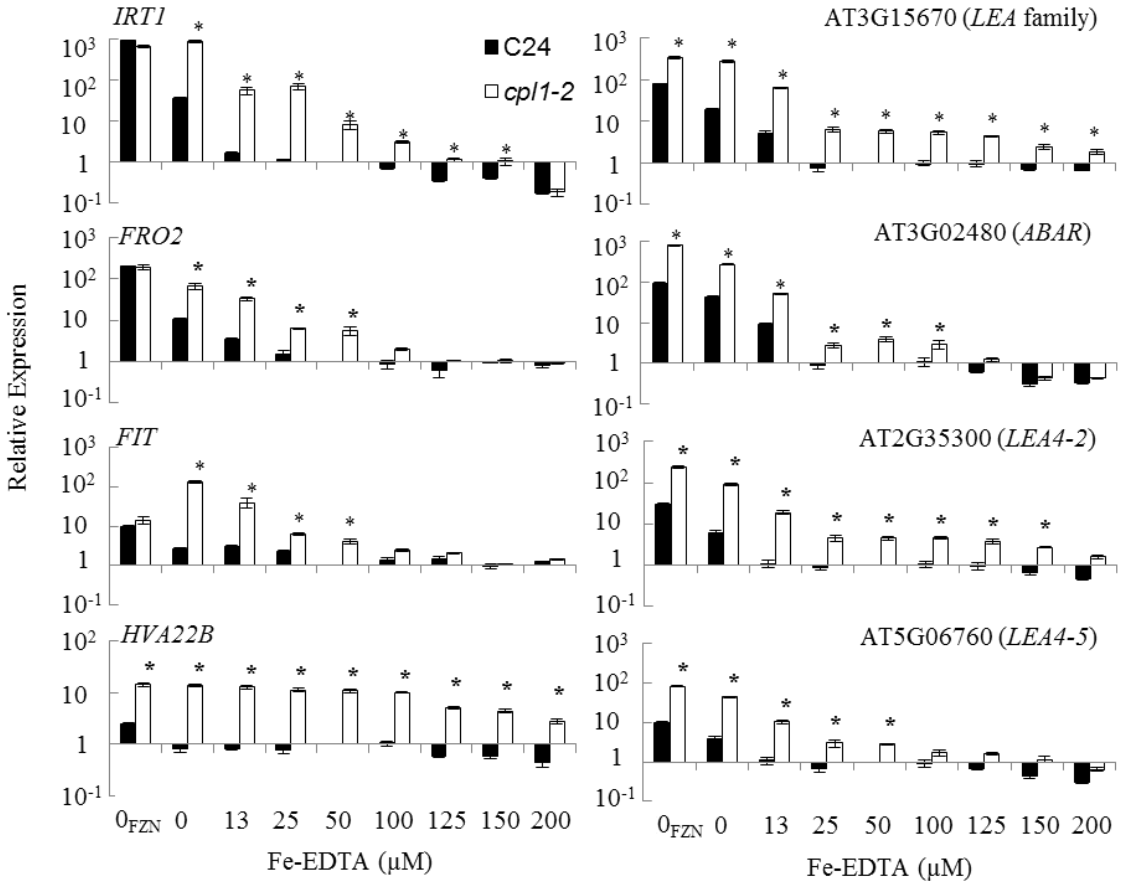

Figure 2.9. Basal expression levels of *IRT1*, *FIT*, *FRO2* and *LEA* family proteins under different Fe concentrations. Plants were grown for 10 days on medium containing 1/4 x MS salts adjusted to the indicated concentration of Fe-EDTA, 0.5% sucrose, and 1.5% agar. 0_{FZN} indicates medium without Fe-EDTA, but containing 300 μM ferrozine. Total RNA was extracted from whole plants. The presented expression levels (relative to C24 samples collected from medium containing 50 μM Fe-EDTA) are mean values of three biological replicates analyzed in duplicate. Bars indicate the SEM of biological replicates. *$p<0.05$, Student's *t*-test between mean values of *cpl1*-2 and C24 for the same conditions.

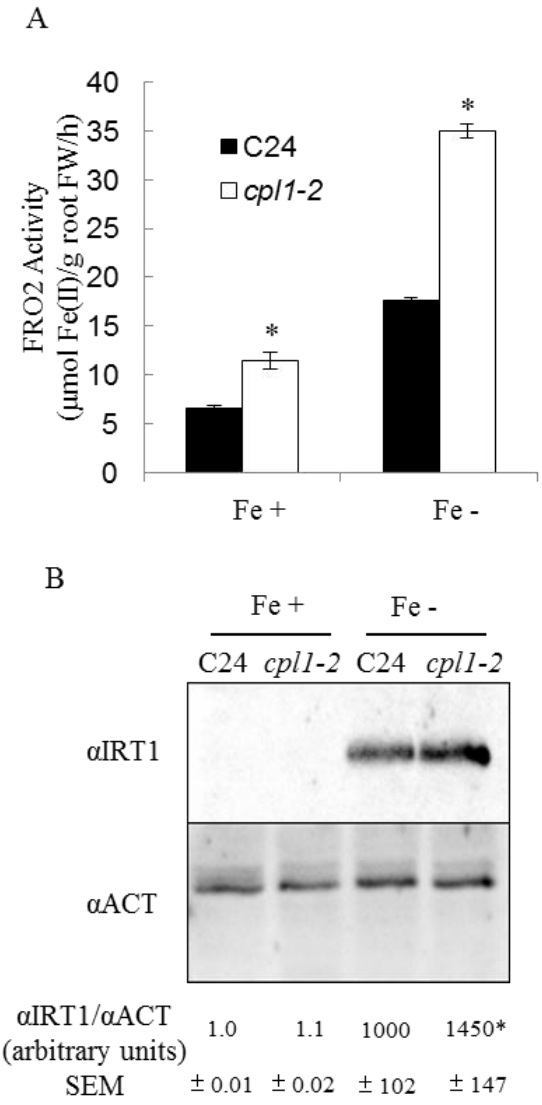

Figure 2.10. FRO activity and IRT1 protein accumulation in roots of *cpl1-2* and C24 under Fe-sufficient or -deficient conditions. Plants were grown on basal medium for 7 days, and then transferred to Fe-sufficient (Fe+, 50 µM Fe-EDTA) or Fe-deficient (Fe-, 0 µM Fe-EDTA + 300 µM ferrozine) basal medium. A, FRO2 activity after 3 days of treatment. The presented values are the means of three biological replicates, each consisting of six technical repeats. Bars indicate the SEM of biological replicates. B, IRT1 protein accumulation after 3 days of treatment. Twenty micrograms of total protein was analyzed by immunoblot using anti-IRT1 antibodies (αIRT1). An anti-actin antibody (αACT) (A2066: Sigma, MO) was used as the loading control. Average band intensities of three experiments (± SEM) are given in arbitrary units. *p<0.05, Student's t-test between mean values of *cpl1*-2 and C24 for the same conditions.

2.4.5 The cpl1-2 Mutation Affects Fe Homeostasis

To determine whether elevated *IRT1* and *FRO2* transcript levels result in an increase of the corresponding proteins in the *cpl1-2* mutant, we tested the levels of root FRO2 activity and IRT1 protein accumulation. Consistent with the transcript levels, FRO2 activity was 1.7- and 2-fold higher than in the wild type in Fe-sufficient and -deficient conditions, respectively (Fig. 2.10 A). IRT1 proteins were below the level of detection under Fe-sufficient conditions in both genotypes; however, upon exposure to Fe deficiency (0 μM Fe-EDTA + 300 μM ferrozine for 3 days), *cpl1-2* accumulated a slightly but significantly higher level of IRT1 than did the wild type (1.5 ± 0.24 fold, $p<0.05$) (Fig. 2.10 B). The small difference in IRT1 protein level between the wild-type and mutant plants is consistent with the tight regulation of IRT1 by ubiquitin-mediated protein turnover (Kerkeb et al., 2008; Barberon et al., 2011).

To determine the physiological consequence of the molecular changes in *cpl1-2*, elemental analyses were conducted for plants grown under the same conditions as described above. Roots and shoots were harvested separately and metal contents were determined by inductively coupled plasma mass spectrometry (ICP-MS). As shown in Fig. 2.11, in Fe-sufficient conditions, *cpl1-2* accumulated 34% more Fe in the roots than did the wild type, but 14% less Fe in the shoots. This suggests that although the IRT1 protein level was below our detection limit, higher basal *IRT1* expression likely contributes to enhanced Fe acquisition in *cpl1-2*. It also suggests that translocation of Fe from the roots to the shoots is impaired in *cpl1-2*. As reported previously, exposure to Fe-deficient medium induced the accumulation of zinc (Zn) and manganese (Mn) in wild-type plants (Baxter et al., 2008). Interestingly, *cpl1-2* roots accumulated 17.6% and 19.2% higher levels of Zn and Mn, respectively, under Fe-deficient conditions than did wild-type roots. Since IRT1 is likely responsible for increases in Zn and Mn uptake during Fe deficiency (Korshunova et al., 1999; Vert et al., 2002), the elevated IRT1 transcript and protein levels in *cpl1-2* are likely to be biologically relevant.

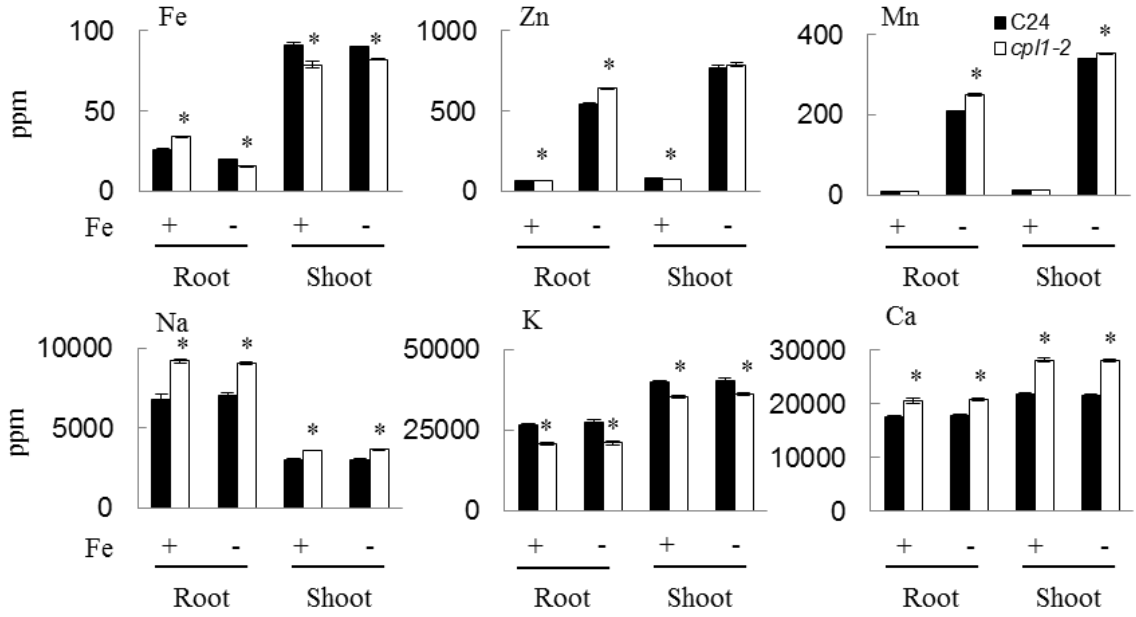

Figure 2.11. Metal contents of *cpl1-2* and C24 roots and shoots under Fe-sufficient or -deficient conditions. Plants were grown on basal medium for 7 days, and then transferred to Fe-sufficient (Fe+, 50 µM Fe-EDTA) or -deficient (Fe-, 0 µM Fe-EDTA + 300 µM ferrozine) basal medium. After 3 days, root and shoot tissues were collected separately and dried at 65ºC for 48 h, and elemental levels were determined from 100 mg of dried tissues by ICP-MS analysis. The presented elemental levels are the mean values of three biological replicates analyzed in triplicate. Bars indicate the SEM of biological replicates. **p*<0.05, Student's *t*-test between mean values of *cpl1*-2 and C24 for the same conditions.

In addition, we noted that the sodium (Na) and calcium (Ca) levels in the roots of *cpl1-2* plants grown under Fe-sufficient conditions were elevated by 35% and 17.2%, respectively, compared to the wild type, and that potassium (K) levels were reduced by 22%. Overall, the *cpl1-2* ion profile was consistent with the transcript profile of *cpl1* mutants, and was distinct from that of prototypical Fe homeostasis mutants such as *frd3,* which showed constitutive Fe deficiency stress responses and accumulated Zn and Mn even under Fe-sufficient conditions (Rogers and Guerinot, 2002).

To determine if distribution of Fe in roots is affected by *cpl1-2* mutation, Fe in root tissues was visualized by Perls staining (Fig. 2.12). Unlike previously characterized *frd3-1* mutant, which accumulates Fe in vascular tissues (Green and Rogers, 2004), root Fe profile of *cpl1-2* was indistinguishable from wild type C24 and stained predominantly root hairs.

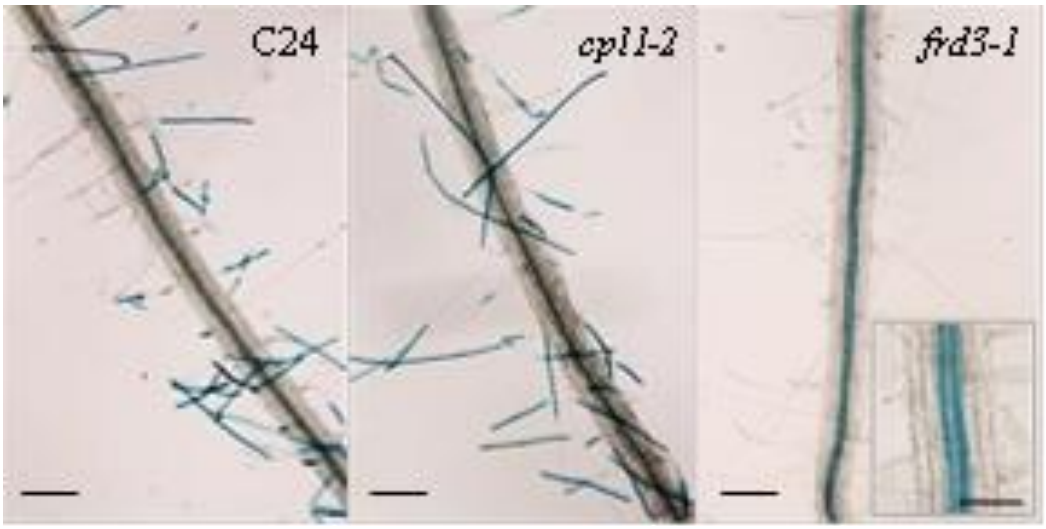

Figure 2.12. Fe deposition in *cpl1-2* and C24 roots. C24, *cpl1-2* and *frd3-1* plants were grown on basal medium for 10 days and stained with Perls stain to visualize ferric iron. Bars represent 1 mm; and 0.05 mm in inset.

The root growth response of the *cpl1* mutants to Fe deficiency stress was analyzed in vitro (Fig. 2.13). Plants were grown for 4 days on 1/4 x MS medium containing 50 µM Fe-EDTA and for another 5 days on Fe-deficient medium. Primary root growth of the wild type was inhibited by 28±3% upon transfer to Fe-deficient medium, whereas that of *cpl1-1* and *cpl1-2* was inhibited by only 13±4% and 6±2%, respectively. This indicates that the *cpl1* mutants are more tolerant to Fe deficiency than is the wild type. The intermediate tolerance in *cpl1-1* may be due to leaky expression of functional *CPL1* transcript in this allele, which contains the T-DNA insertion in the third intron (Koiwa et al., 2002).

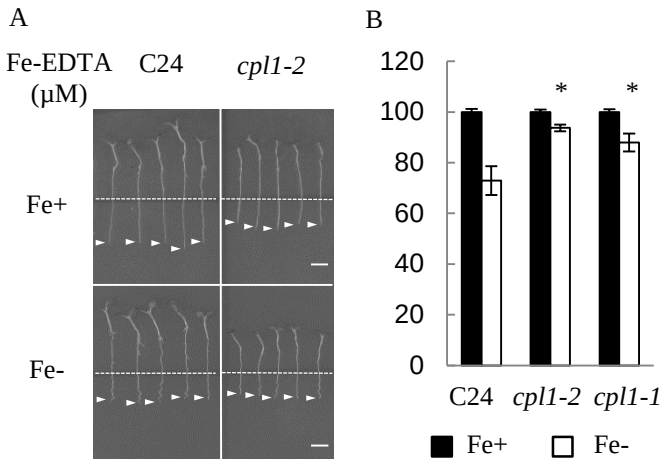

Figure 2.13. Primary root growth of C24 and *cpl1* mutants under different levels of available Fe. Four-day-old seedlings of C24, *cpl1-1*, and *cpl1-2* were subjected to Fe deficiency as described in Materials and Methods. A, Root growth after 5 days of treatment. Root tip positions are marked by arrowheads. Dashed line shows the position of the roots at the time of transfer. The scale bars represent 10 mm. Root length was quantified to calculate relative root growth of the wild type and *cpl1* mutants (B). Bars indicate SEM of three biological replicates, each consisting of 20 seedling measurements. **p*<0.05, Student's *t*-test between mean values of C24 and each mutant under Fe deficiency conditions. Fe+: 50 µM Fe-EDTA and Fe-: 0 µM Fe-EDTA +300 µM ferrozine.

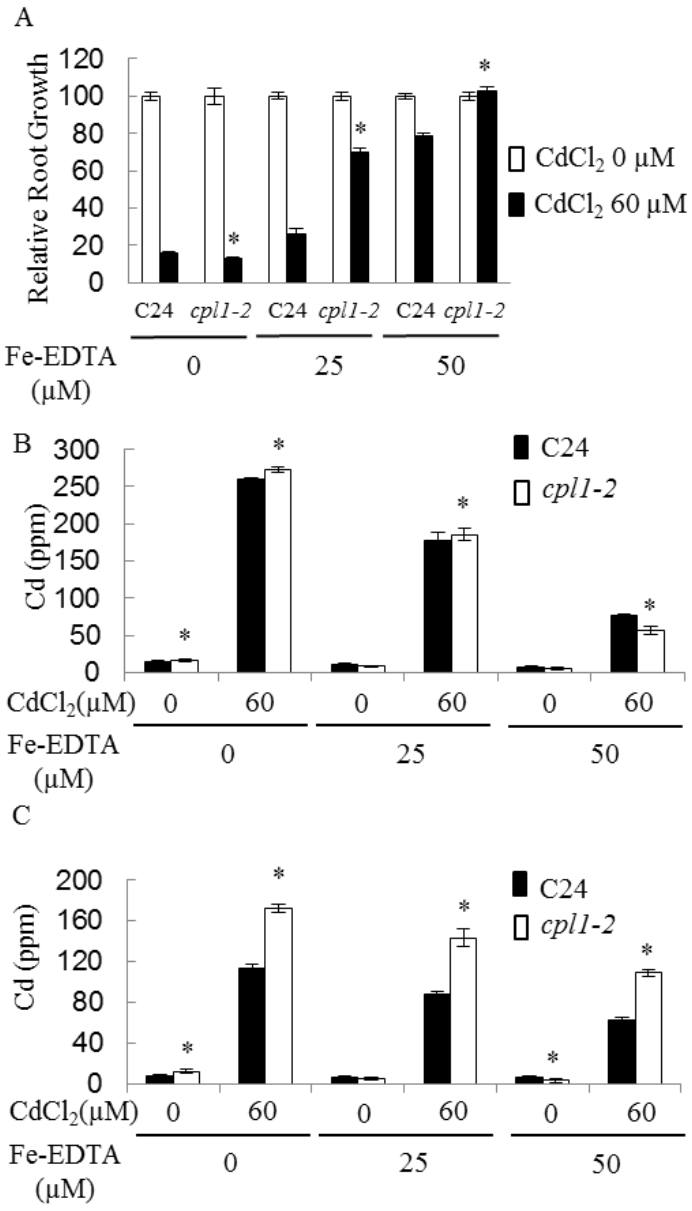

Figure 2.14. Cd resistance of *cpl1-2*. Primary root growth (A) and Cd levels in the roots (B) and shoots (C) of C24 and *cpl1-2* growing on media containing various levels of Fe and Cd. Seeds were germinated and grown for 10 days on 1/4 x MS medium adjusted to the indicated concentrations of Fe-EDTA and $CdCl_2$. The presented root lengths are the means of three biological replicates, each consisting of 20 seedlings. The presented Cd levels are the means of three biological replicates analyzed in triplicate. Bars indicate the SEM of biological replicates. *p<0.05, Student's t-test between mean values of *cpl1*-2 and C24 for the same conditions.

Since cadmium (Cd) ions can enter plant cells through Fe-uptake systems (Clemens, 2006), the *cpl1-2* mutation may affect plant tolerance to Cd. To test this possibility, the *cpl1-2* and C24 wild type were grown for 14 days on medium containing 60 µM $CdCl_2$ and various concentrations of Fe. In the absence of Fe, growth of both the wild type and *cpl1-2* was severely inhibited by the presence of cadmium (Fig. 2.14 A). With increasing amounts of Fe in the medium, both genotypes showed recovery; however, *cpl1-2* plants showed greater tolerance to Cd on medium containing 25 µM or 50 µM Fe-EDTA. In the presence of 50 µM Fe-EDTA, wild-type plants showed substantial tolerance to Cd, albeit the tolerance was weaker than that of *cpl1-2*. Root Cd contents of wild-type and *cpl1-2* plants were similar for all treatments, indicating that the basis for increased Cd tolerance in *cpl1-2* does not likely involve exclusion of Cd from the roots (Fig. 2.14 B). Surprisingly, the shoots of *cpl1-2* plants accumulated 54.2-73% more Cd than did those of the wild type, suggesting that the long-distance transport of Cd was enhanced in *cpl1-2* plants (Fig. 2.14 C).

2.4.6 Genetic Dissection of Fe Signaling Perturbation in cpl1

It has been shown that the bHLH transcription factor FIT is a central regulator of Fe deficiency signaling, and that FIT regulates its own Fe deficiency-induced expression (Colangelo and Guerinot, 2004; Jakoby et al., 2004; Wang et al., 2007). To determine whether up-regulation of Fe utilization-related genes in the *cpl1* mutants is dependent on FIT activity, the expression of these genes was analyzed in the *fit cpl1* double mutant. Since a well-characterized *fit-2* mutant is in the Col-0 genetic background (Colangelo and Guerinot, 2004), *cpl1-6* in the Col-0 background was used in this analysis. Furthermore, to quantify *FIT* expression in the *fit* mutant background, lines with a *FIT-LUC* reporter gene were prepared in the wild type (Col-0), *cpl1-6*, and *fit-2* single mutants, and in the *fit-2 cpl1-6* double mutant by genetic crossing (Fig. 2.15).

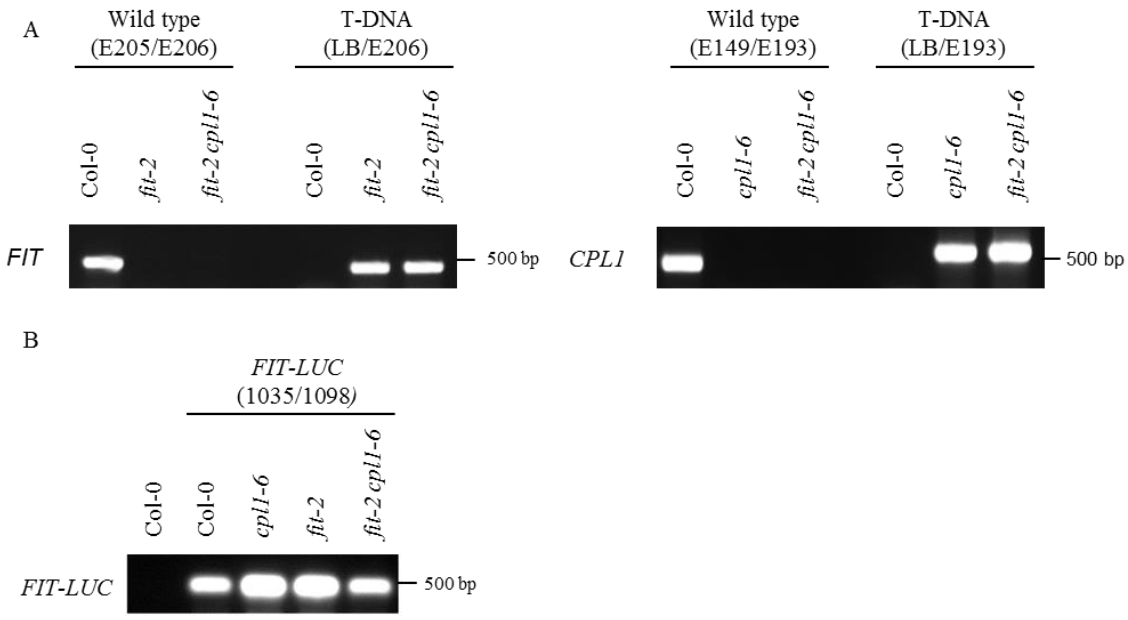

Figure 2.15. Molecular characterization of *fit-2* and *cpl1-6* mutations and the *FIT-LUC* transgene. A, Confirmation of homozygous T-DNA insertions in *fit-2* and *cpl1-6* single and *fit-2 cpl1-6* double mutant lines by PCR. Primer combinations in parenthesis were used to detect intact (wild type) and disrupted (T-DNA) *fit*-2 and *cpl1-6* loci. B, Confirmation of introgression of *FIT-LUC* in *Col-0, fit-2, cpl1-6,* and *fit-2 cpl1-6* lines. The Col-0 line without *FIT-LUC* introgression was used as the negative control.

As shown in Fig. 2.16, *FIT-LUC* and endogenous *FIT* expression were both enhanced in the *cpl1-6* mutant. On the other hand, the basal expression level of *FIT-LUC* in *fit-2* plants was 40% that of the wild-type level. In *fit-2 cpl1-6*, however, the level of *FIT-LUC* expression was similar to that of the wild type and lower than that of the *cpl1-6* single mutant. This suggests that the *cpl1-6* mutation can activate the FIT-independent signal to promote basal *FIT* expression. Furthermore, positive feedback by the FIT auto-activation mechanism likely amplifies *FIT* expression. Interestingly, Fe deficiency treatment did not induce the expression of *FIT-LUC* in the absence of functional *FIT*.

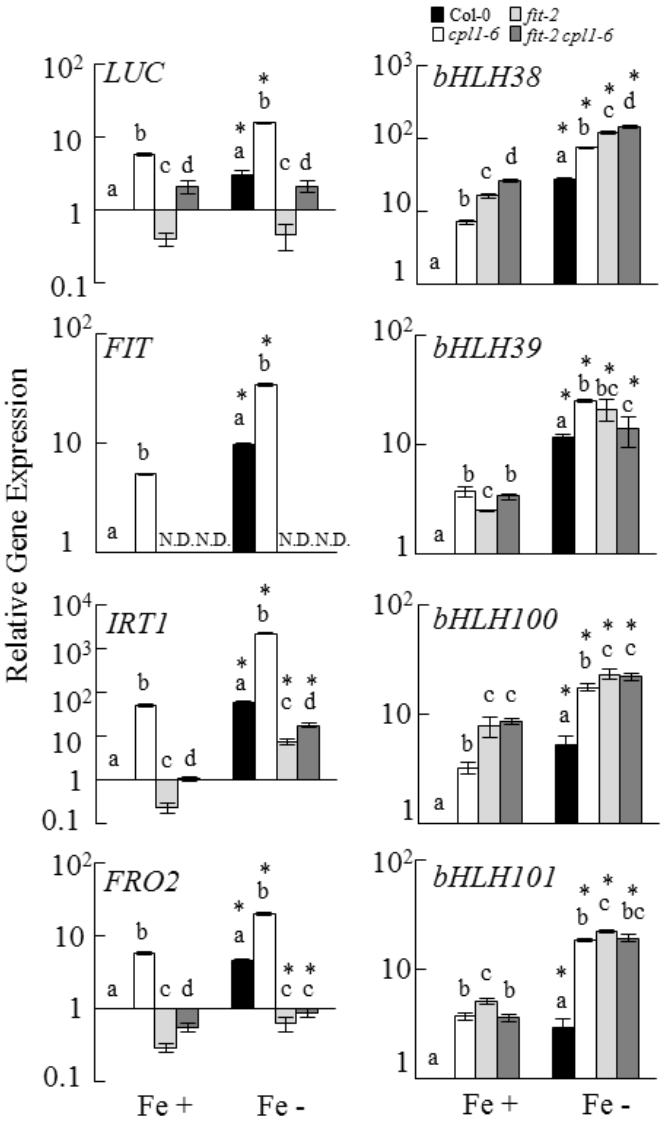

Figure 2.16. Expression levels of *FIT-LUC*, *FIT*, *IRT1*, *FRO2*, and group Ib *bHLH* transcription factors in Col-0, *cpl1-6*, *fit-2*, and *fit-2 cpl1-6* plants containing the *FIT-LUC* reporter gene. Plants were grown on basal medium for 7 days, and transferred to Fe-sufficient (Fe+, 50 µM Fe-EDTA) or -deficient (Fe-, 0 µM Fe-EDTA + 300 µM ferrozine) basal medium. Total RNA was extracted from root tissue after three days of treatment. The presented expression levels (relative to untreated Col-0 samples) are mean values of biological duplicates analyzed in duplicate. Bars indicate the SEM of biological replicates. Different letters show significant differences between genotypes under Fe+ and Fe- conditions ($p<0.05$, one-way ANOVA followed by Tukey's HSD post hoc test). *$p<0.05$, Student's *t*-test between mean values of Fe+ and Fe- for the same genotype.

This may indicate that *FIT* induction by Fe deficiency is entirely dependent on a FIT auto-regulation mechanism. However, a FIT-independent component may be activated in the *fit-2* background even during growth on Fe-sufficient medium, due to the constitutive Fe-deficient status of the mutants resulting in the lack of further activation by Fe deficiency treatment.

The expression profiles of genes downstream of FIT were similar to that of *FIT-LUC*. Under Fe-sufficient conditions, *IRT1* and *FRO2* levels were 22% and 29% lower in the *fit-2* mutant than in the wild type, respectively; however, the expression of these genes was recovered (95% and 54% of wild-type expression, respectively) in *fit-2 cpl1-6* plants. *IRT1* and *FRO2* expression levels increased in response to Fe deficiency treatment even in the *fit-2* background, indicating that a FIT-independent pathway positively regulates the expression of these genes; however, similar to *FIT-LUC*, FIT is required for the full induction of *IRT1* and *FRO2*. In contrast to [*IRT1, FIT-LUC, FRO2*], the basal and induced levels of group Ib *bHLH* expression were higher in all mutant lines tested, and their expression levels were largely similar among mutant lines other than *bHLH38*. It appears that both the enhanced Fe deficiency signals in *cpl1-6* plants and the Fe-deficient status caused by the *fit-2* mutation activate group Ib *bHLH* expression by the same FIT-independent mechanism. Together, these results indicate that *cpl1-2* likely activates Fe deficiency responses upstream of both FIT-dependent and -independent signaling pathways.

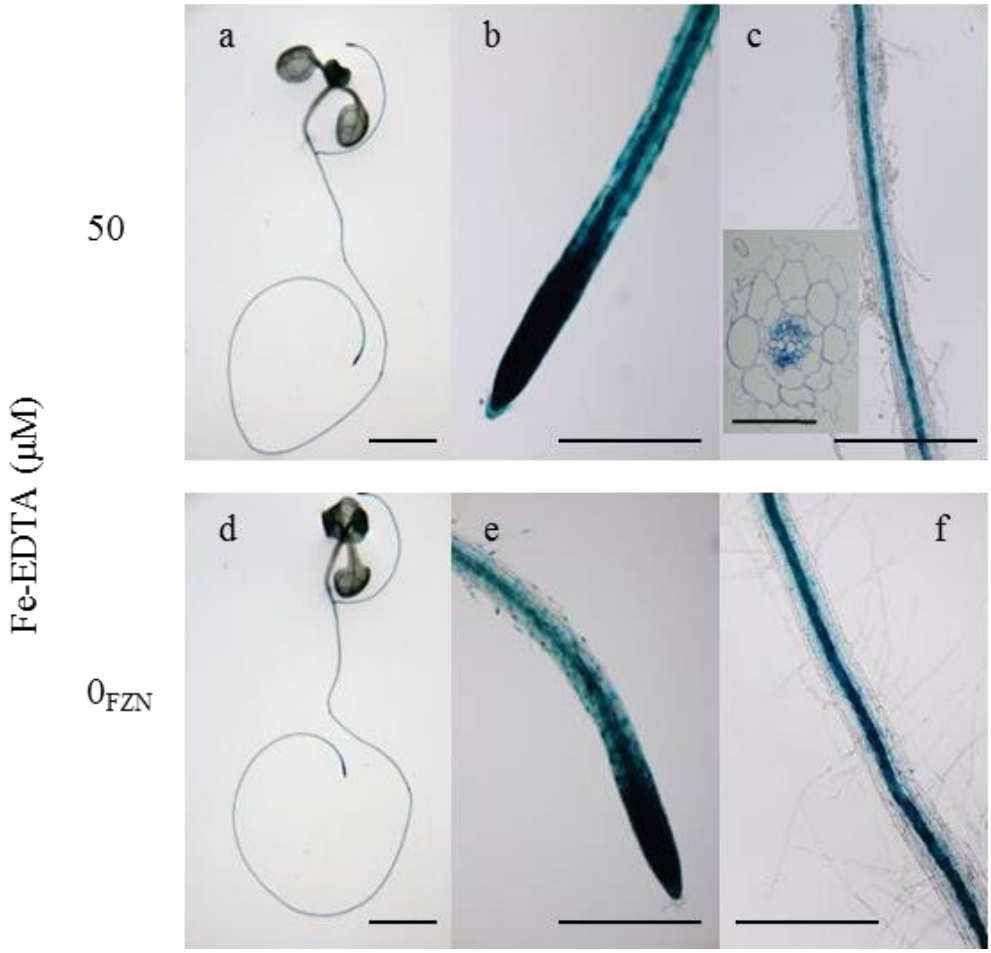

Figure 2.17. *CPL1* was expressed in the root tip and stele. Plants expressing the CPL1-GUS fusion protein were grown on basal medium for 7 days, and transferred to Fe-sufficient (50 µM Fe-EDTA) (a-c) or Fe-deficient (0 µM Fe-EDTA + 300 µM ferrozine) (d-f) basal medium. After three days, GUS activity was visualized and documented. Bars represent 10 mm in a and d; 2 mm in b,c,e, and f; and 0.05 mm in c, inset.

FIT is specifically expressed in the root epidermis (Colangelo and Guerinot, 2004); therefore, the direct regulation of *FIT* by CPL1 would require *CPL1* expression in these cells. The tissue specificity of *CPL1* expression was analyzed using a *CPL1-GUS* translational fusion construct. The *GUS* ORF was inserted in a 8.4-kbp CPL1 genomic fragment immediately before the stop codon of *CPL1* ORF, whose expression was regulated by its native regulatory sequences. The expression of the reporter gene was monitored in the roots of transgenic Arabidopsis plants (Fig. 2.17). The expression profile of *CPL1-GUS* was similar in Fe-sufficient or -deficient conditions. *CPL1-GUS* expression was high in root tips; however, in the mature part of roots, *CPL1-GUS* expression was confined to the stele, particularly in the phloem, and virtually no activity was observed in the outer layers of root cells. Overall, except for a limited area of the root tip, *CPL1* and *FIT* showed distinct tissue-specific expression patterns, suggesting that the regulation of *FIT* by CPL1 is likely indirect.

2.4.7 The cpl1-2 Mutation Promotes the Fe Deficiency-mediated Expression of ABA-/Osmotic Stress-regulated Genes

Our finding that *cpl1-2* simultaneously enhances the expression of both osmotic stress/ABA-responsive and Fe deficiency-responsive genes is somewhat contradictory to the previous report that ABA and osmotic stress inhibit Fe deficiency signaling (Seguela et al., 2008). However, an observation similar to ours was reported in rice overexpressing IDEF1 [iron deficiency element (*IDE1*)-binding factor 1] (Kobayashi et al., 2009). Because of the similarity between *IDE1* (CATGA) and the ABA signaling *cis*-element (RY-motif, CATGCATG) (Kobayashi et al., 2009), we hypothesized that CPL1 regulates a branch of Fe deficiency and osmotic stress/ABA signaling through similar *cis*-regulatory elements. While ABA treatment inhibited [*IRT1, FRO2, FIT*] expression in both the wild type and *cpl1-2* (data not shown), the expression of genes inducible by both Fe deficiency stress and ABA treatment was substantially enhanced in *cpl1-2* (Fig. 2.18).

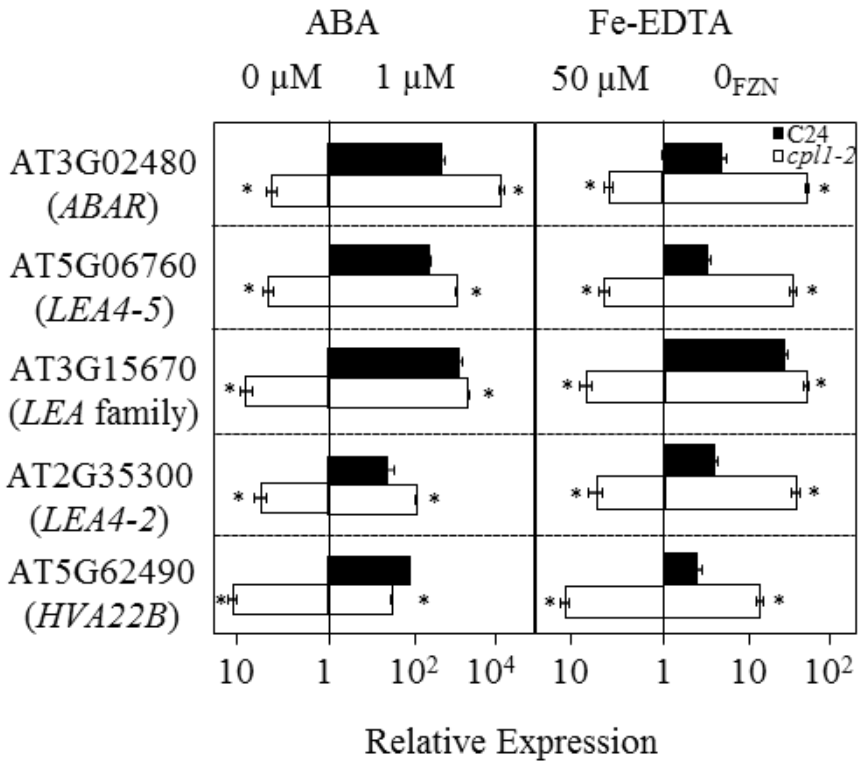

Figure 2.18. The expression of *LEA* family transcripts in response to ABA or Fe deficiency treatments. Plants were grown on basal medium for 7 days, and transferred to basal medium containing 1 µM ABA or to Fe-deficient basal medium (0_{FZN}, 0 µM Fe-EDTA + 300 µM ferrozine). The duration of treatment was 1 h for ABA and 72 h for Fe deficiency. Total RNA was extracted from roots. The presented expression levels (relative to untreated C24 samples) are mean values of biological triplicates analyzed in duplicate. Bars indicate the SEM of biological replicates. *p<0.05, Student's t-test between mean values of *cpl1-2* and C24 for the same conditions.

This indicates that some ABA-responsive genes are also regulated by Fe through a common CPL1-repressed pathway. Consistently, the presence of higher concentrations of external Fe could repress not only the expression of prototypical Fe-regulated genes [*IRT1, FRO2, FIT*], but also the enhanced expression of *LATE EMBRYONIC ABUNDANT* (*LEA)* in *cpl1-2* (Fig. 2.9). Interestingly, the repression of *LEA* expression by excess Fe (>50 µM) was less pronounced in *cpl1-2* than in the wild type, and *HVA22* expression was

largely unaffected by increased Fe, suggesting that additional Fe-independent mechanisms up-regulate *LEA* expression in *cpl1-2.* To test the state of ABA signaling in *cpl1*, the expression levels of several ABA signaling components were determined. The expression of *ABI1, ABI3,* and *AREB1/ABF2* was up-regulated 4.0-, 3.9-, and 5.4-fold in *cpl1-2* under normal growth conditions. This result was consistent with the observation that *cpl1-2* was hyperresponsive to ABA treatment (Fig. 2.18). Together, these results suggest that CPL1 regulates the signaling pathway upstream of the cross-talk between ABA and Fe signals.

2.5 Discussion

RNA metabolism regulates diverse developmental and stress response signaling pathways in plants. This study shows that an upstream component of the Fe deficiency response was regulated by an RNA metabolism factor, CPL1. Although the Fe deficiency response signaling pathway is regulated by multiple mechanisms, such as protein-protein interactions (Yuan et al., 2008), differential promoter activation (Yuan et al., 2008; Long et al., 2010), protein ubiquitination (Kerkeb et al., 2008; Li and Schmidt, 2010), and proteasomal and non-proteasomal protein degradation (Barberon et al., 2011; Lingam et al., 2011; Sivitz et al., 2011), regulation at the level of RNA metabolism has not hitherto been established. CPL1 is a plant-specific isoform of the universal pol II CTD phosphatase family of proteins, which harbor double-stranded RNA-binding motifs (DRMs) and can specifically dephosphorylate pol II CTD at Ser5-PO_4 in vitro (Koiwa et al., 2002; Xiong et al., 2002; Koiwa et al., 2004). We have shown that CPL1 localizes to the root stele and negatively regulates Fe signaling. *cpl1* mutations result in enhanced expression of *FIT* and group Ib *bHLH* genes, which are essential for Fe deficiency sensing/signaling and affect metal homeostasis. This finding is consistent with a previous report showing that Fe utilization-related genes are down-regulated in the RNA decapping-deficient mutant, *trident (tdt)* (Goeres et al., 2007).

Since alteration of the pol II phosphorylation status can potentially trigger alterations in global transcription and RNA maturation, it could be argued that the observed up-regulation of Fe utilization-related genes resulted from a pleiotropic effect of the *cpl1-2* mutation, similar to the down-regulation of Fe utilization-related genes in the *tdt* mutation (Goeres et al., 2007). However, several observations argue against the involvement of pleiotropic effects. First, in contrast to the *tdt* mutant, the *cpl1* mutants do not exhibit any major defects in growth and development. Second, *cpl1-2* affects the levels of metals associated with Fe homeostasis, i.e., Fe, Zn, Mn, and Cd. Third, *cpl1-2* affects multiple regulons in Fe deficiency signaling, i.e., FIT-dependent and -independent Fe deficiency responses and repression of the basal-level of *FER1*. Fourth, the effect of *cpl1-2* could be suppressed by increased Fe concentrations in the medium. Finally, the effect of *cpl1-2* on the expression of [*IRT1, FIT, FRO2*] likely involves intercellular communication. These findings indicate that the *cpl1* mutations affect Fe homeostasis and activate upstream signaling component(s) rather than causing mis-expression of *FIT,* regardless of the presence or absence of Fe signals. On the other hand, levels of IRT1, which are regulated post-translationally by Fe status, are affected only moderately by *cpl1* mutations under Fe deficiency stress. This suggests that CPL1 either specifically regulates branch(es) of Fe deficiency signaling, or that higher thresholds of Fe deficiency signals are required to activate post-translational Fe deficiency responses. Alternatively, the levels of IRT1 at the PM may be regulated by apoplastic Fe rather than by CPL1-mediated signaling.

How does CPL1 regulate the Fe status and deficiency responses? Our data indicate that CPL1 is strongly expressed in the root stele, and not at all in the epidermis, where FIT is expressed. It is also noteworthy that *cpl1-2* induced the expression of [*IRT1, FIT, FRO2*] under Fe-sufficient conditions, even in the presence of elevated levels of root Fe, but did repress [*IRT1, FIT, FRO2*] expression when additional Fe was supplied exogenously. One possibility is that CPL1 functions at the organ level to keep the root Fe level low, by repressing [*IRT1, FIT, FRO2*] and promoting Fe loading into the xylem (Fig. 2.19 A). This could be achieved either by promoting Fe transport from the epidermis to the xylem,

by repressing sequestration/compartmentalization of Fe in the root cells, or by repressing xylem unloading of Fe in the roots. Upon Fe deficiency, Fe starvation signals generated in the shoot overcome repression of [*IRT1, FIT, FRO2*] by CPL1. Upon mutation of *CPL1*, both repression of [*IRT1, FIT, FRO2*] and the promotion of xylem loading are impaired, resulting in elevated expression of [*IRT1, FIT, FRO2*] and accumulation of Fe in the roots. At the same time, Fe in the shoots is reduced due to decreased root-to-shoot Fe transport, which in turn generates systemic Fe deficiency signals and promotes [*IRT1, FIT, FRO2*] expression in the roots. This mutant phenotype can be ameliorated by the addition of Fe, because a basal level of xylem loading still occurs in *cpl1* mutants. The relatively large decrease in root Fe content in the *cpl1-2* mutant during Fe deficiency may be due to the continued growth of *cpl1-2* roots diluting the acquired Fe, and/or the greater mobilization of stored Fe by enhanced Fe deficiency signals. While the expression levels of *FRD3* and *IRON REGULATED 1* (*IREG1*), which likely load citrate and Fe to the xylem, respectively, do not substantially differ between the WT and *cpl1-2*, there is a moderate increase in the expression of some plastid Fe uptake genes in *cpl1-2*. This implies that CPL1 attenuates Fe compartmentalization rather than regulates xylem loading activity (Fig. 2.8 B).

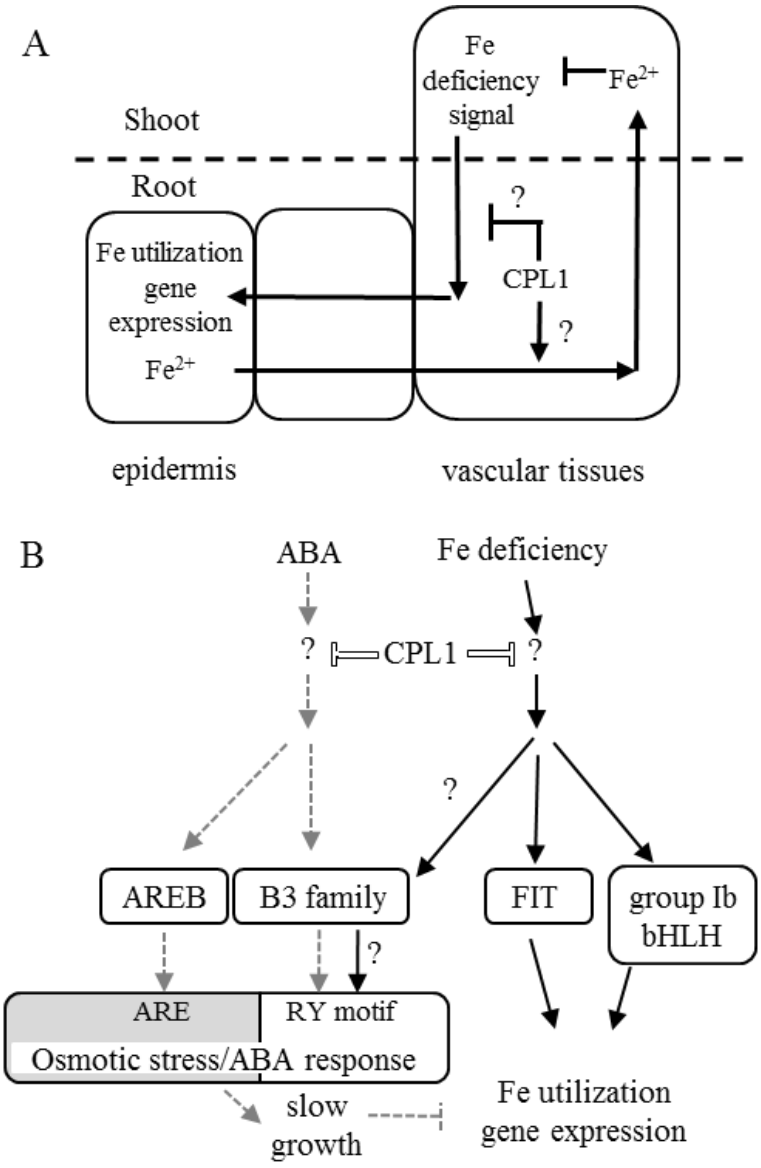

Figure 2.19. Model for the role of CPL1. A. Role of CPL1 in root-shoot Fe distribution. CPL1 in the stele likely promotes the root-to-shoot transport of Fe and attenuates the Fe deficiency signal in shoots. Communication between different cell types in shoot tissues is omitted in this model. B. Co-regulation of a subset of osmotic stress/ABA response genes by ABA and Fe deficiency signals and its attenuation by CPL1. Solid and broken arrows indicate pathways that operate during Fe deficiency or in the presence of ABA, respectively. Open bars indicate the repression activity of CPL1, which is absent in *cpl1* mutants. CPL1 attenuates the Fe deficiency signaling pathway upstream of FIT and group Ib bHLH. Direct targets of CPL1 in the pathways are currently unknown. B3 family transcription factors up-regulate the expression of a subset of osmotic stress/ABA-responsive genes through the RY motif in response to Fe deficiency and ABA signaling. ABA also promotes gene expression via the ABRE (ABA-responsive element). When ABA levels are elevated, the enhanced expression of ABA-responsive genes causes slow growth, which inhibits the expression of Fe utilization genes.

However, we cannot exclude the possibility that *cpl1-2* regulates the expression of other xylem loading Fe transporters, since *IREG1* is likely not the sole/major xylem loading Fe transporter (Morrissey et al., 2009). Furthermore, the mode of CPL1 function in this process remains to be determined. Because the physicochemical nature of intercellular Fe deficiency signaling between the shoots and roots, and the root stele and epidermal tissues remains elusive, it is difficult to address this issue. Currently, we are not able to detect significant changes in overall CTD phosphorylation status during Fe deficiency, suggesting that bulk pol II CTD phosphorylation is not involved (data not shown). The presence of the dsRNA-binding motif in CPL1 suggests that CPL1 may regulate small RNA production and/or function. It is interesting that CPL1 is strongly expressed in the stele, likely in phloem companion cells, where the expression of small RNA production machinery is enriched (Mustroph et al., 2009). Indeed, several miRNA are regulated by the Fe signal, (Kong and Yang, 2010), and the potential effect of *cpl1-2* on the mobility of small RNAs may explain the systemic nature of this mutation as well as its impact on multiple pathways.

We initially expected that the enhanced levels of IRT1 in *cpl1-2* would result in Cd oversensitivity, because IRT1 is responsible for Cd influx into root cells (Connolly et al., 2002). Instead, c*pl1-2* showed Cd tolerance, and Cd levels in *cpl1-2* roots were not greater than those in wild-type roots. Rather, *cpl1-2* showed a substantial increase in shoot Cd levels, indicating an increase in the root-to-shoot transport of Cd. Since Cd transport and tolerance involves multiple mechanisms and has not been fully elucidated, there is no simple explanation for how *cpl1-2* confers Cd tolerance. However, several genes that are up-regulated in *cpl1-2* are related to Cd tolerance.

For example, the elevated expression of Fe acquisition genes such as [*IRT1, FIT, FRO2*] and group Ib *bHLH,* and the resulting increase in root Fe levels can ameliorate toxicity of cellular Cd (Wu et al., 2012). In addition, Wu et al. (2012) also reported that co-expression of *FIT* and *bHLH38/39* activates *HMA3, MTP3, IREG2,* and *IRT2,* which can enhance the sequestration of Cd into vacuoles in the root. In addition, *OPT3* may mediate Cd tolerance

in a similar manner to the yeast homolog, ScOPT2, which transports Cd into the vacuoles (Aouida et al., 2009). However, these mechanisms in general promote sequestration of Cd into vacuoles, resulting in higher levels of Cd in the roots. In contrast, the "overflow protection mechanism" proposed for phytochelatin-mediated long-distance Cd transport from roots to shoots (Gong et al., 2003) may better explain Cd tolerance of *cpl1-2*. Similar to *cpl1* mutants, transgenic plants with root-specific expression of phytochelatin synthase have elevated levels of Cd in the shoots, but normal levels of Cd in the roots (Gong et al., 2003). However, since phytochelatin is not likely the sole chelator that mediates long-distance Cd transport (Clemens, 2006), we cannot exclude the contribution of other mechanisms.

The simultaneous up-regulation of Fe deficiency- and ABA/osmotic stress-regulated transcripts is a unique signature of the *cpl1-2* transcriptome. This may indicate that the *cpl1-2* mutation activates two distinct stress signaling pathways, and/or that these two pathways exhibit specific crosstalk. The first possibility is supported by our finding that both Fe-specific and ABA/osmotic stress-specific genes are up-regulated in *cpl1*. The increase of Na (30%) and decrease of K (23%) in *cpl1* are further indicators that *cpl1* mutants indeed experience osmotic (salt) stress under normal growth conditions. While previous studies indicate that Fe deficiency and ABA/osmotic stress pathways exhibit crosstalk (Dinneny et al., 2008; Seguela et al., 2008; Kobayashi et al., 2009), the positive co-regulation of gene expression by ABA/osmotic stress and Fe deficiency has not been studied in dicots to date. In monocots, however, specific crosstalk between ABA/osmotic stress and Fe deficiency signaling occurs, as shown with rice overexpressing IDEF1, a B3 family transcription factor (Kobayashi et al., 2009). Although an obvious IDEF1 ortholog is not present in the Arabidopsis genome, *IDE1* sequences are found in many Fe-responsive gene promoters, including those from Arabidopsis (Kobayashi et al., 2003; Kobayashi et al., 2005). Interestingly, the closest homolog of IDEF1 in Arabidopsis is ABI3, and the expression of this gene in *cpl1-2* was elevated four-fold over wild-type levels. Furthermore, the recognition sequence of IDEF1 (CATGC) overlaps with that of

ABI3/VP1-type B3 family transcription factors (CATGCA) (Kobayashi et al., 2009; Kobayashi et al., 2010). Therefore, co-regulation of genes by ABA and Fe deficiency in *cpl1-2* may be caused by a yet unidentified B3 family transcription factor(s) (Fig. 2.19 B). Another notable change in ABA signaling in *cpl1-2* was the 5.4-fold up-regulation of AREB1/ABF2. Interestingly, plants overexpressing either ABI3 or an activated AREB1-ΔQT variant show enhanced expression of the *LEA* genes identified in our *cpl1-2* microarray, and AREB1-ΔQT overexpression causes up-regulation of *bHLH38* and *bHLH39* as well (Fujita et al., 2005; Nakashima et al., 2006). It is tempting to speculate that B3 family transcription factor(s) function as an ancient form of IDEF1 in dicots and regulate both ABA and Fe deficiency signaling. However, higher-level integration of ABA and Fe signaling pathways may exist. Whereas the ABA signaling pathway and ABA-responsive promoter elements/transcription factors are well established (Hubbard et al., 2010), detailed information on specific Fe-responsive *cis*-elements in the dicot Fe deficiency-induced promoters and on the Fe signaling components that function upstream of *FIT* or group Ib *bHLH* is lacking. In addition, the role of LEA proteins in the Fe deficiency response has not been established, but some LEA proteins appear to bind metal ions and may function in metal transport (Kruger et al., 2002). Further genetic and molecular analyses are required to determine the role and the mode of action of the ABA-Fe deficiency signal crosstalk, which occurs in both strategy I and strategy II plants.

CHAPTER III

CARBOXYL-TERMINAL DOMAIN PHOSPHATASE-LIKE1 (CPL1) REGULATES THE CADMIUM DISTRIBUTION VIA OLIGOPEPTIDE TRANSPORTER8 (OPT8) IN PLANTS[2]

3.1 Summary

Toxic for most organisms, cadmium (Cd) is a widespread heavy metal contaminant in arable lands as a result of recent anthropogenic activities. It is readily absorbed by the plants and accumulates in edible parts, whereby it is introduced into the food chain; consequently, it causes severe health risks to humans. Thus, identification of Cd tolerant plants is essential for our understanding of heavy metal tolerance mechanisms. In our previous study, a knock-out mutant of *Arabidopsis thaliana CARBOXYL-TERMINAL DOMAIN (CTD) PHOSPHATASE-LIKE1 (CPL1)*, a plant-specific RNA polymerase II CTD phosphatase, showed higher tolerance to the Cd toxicity by enhancing the root-to-shoot translocation of Cd. Here we present that a Cd accumulation determinant in *cpl1-2* is a putative metal transporter, *OLIGOPEPTIDE TRANSPORTER8* (*OPT8*). *OPT8* was highly induced in *cpl1-2* roots upon exposure to Cd. Transgenic Arabidopsis expressing *GFP-OPT8* showed specific fluorescence in the plastids, indicating a role of plastids in Cd transport and accumulation. The root growth of *opt8* mutants showed higher tolerance to the Cd toxicity, and the mutants accumulated less Cd, Fe and Zn, indicating the

[2] Parts of the chapter are used with permission from **Aksoy E, Koiwa H** (2013) Function of Arabidopsis CPL1 in cadmium responses. Plant signaling & behavior **8:** e24120. http://www.landesbioscience.com/journals/psb/. Copyright Landes Bioscience.

involvement of OPT8 in the transport of these metals. Interestingly, direct regulator of *OPT8*, *DUO POLLEN1* (*DUO1*), was also responsive to Cd, and was upregulated in both the roots and the shoots of *cpl1-2* mutant. Overall, these results suggest that CPL1 regulates the Cd distribution in plants by repressing the expression of *OPT8*.

3.2 Introduction

Cadmium (Cd) is a non-essential metal that is toxic for most organisms. Massive areas of top soil in the world have been contaminated with Cd since the industrial revolution as a result of anthropogenic activities (Leitenmaier and Küpper, 2013). Among heavy metals, Cd is very phytotoxic due to its high solubility in water (Traina, 1999); thus, it promptly is absorbed by the plants, accumulated in the edible parts, and contaminates the food chain, which consequently causes severe health risks to humans (Satarug et al., 2011). Genotoxic effects of Cd in plants include competition for the binding sites of essential divalent metals such as iron (Fe^{2+}), zinc (Zn^{2+}), magnesium (Mg^{2+}) and calcium (Ca^{2+}). In addition, Cd also induces the reactive oxygen species (ROS), which in turn causes lipid peroxidation, protein degradation and genome instability (Siedlecka and Krupa, 1996; Das et al., 1997). In plants, Cd exposure induces leaf chlorosis, and inhibits photosynthesis, respiration, nitrate metabolism and overall plant growth (Yadav, 2010).

Cd enters the root cells due to the low selectivity of metal uptake systems. These include ZIP (ZRT-IRT like protein; Zinc-regulated transporter/Iron-regulated transporter-like protein) family transporters, such as *Arabidopsis thaliana* IRT1 (Cohen et al., 1998; Connolly et al., 2002; Vert et al., 2002), Noccaea *caerulescens* ZNT1/ZIP4 (Plaza et al., 2007), and *Triticum aestivum* LCT1 (Clemens et al., 1998; White and Broadley, 2003; White, 2005), and Ca channels (Verbruggen et al., 2009), and Yellow Stripe 1-like (YSL) transporters (Curie et al., 2009). Once entered the roots, Cd ions can complex with thiol and non-thiol ligands. Thiol ligands include metallothioneins (MTs), glutathione (GSH) and phytochelatins (PCs) whereas non-thiol ligands include organic acids (Küpper, 2004;

Leitenmaier and Küpper, 2013). Then, the complexes are either sequestered into the vacuole by a group of transporters including CPX/P_{1B}-type heavy metal ATPase (HMA), Cation Diffusion Facilitator (CDF), Cation Exchanger (CAX), ATP-binding cassette (ABC), and Natural Resistance-associated Macrophage Proteins (NRAMP) families (Chaffai and Koyama, 2011), or reach the stele via apoplastic and/or symplastic pathways in hyper-accumulators (Salt et al., 1995; Leitenmaier and Kuepper, 2011). In Arabidopsis, cadmium is mainly accumulated in the roots suggesting that root-to-shoot Cd translocation is restricted at the xylem loading (Thapa et al., 2012). AtHMA2/AtHMA4, PLANT CADMIUM RESISTANCE2 (PCR2) and several YSL transporters are responsible for Cd loading into the xylem (Wong and Cobbett, 2009; Lin and Aarts, 2012). HMA2 and HMA4 specifically express in the root stele, and their knock-out mutants exhibit enhanced Cd sensitivity, while overexpression of *HMA4* in Arabidopsis confers Cd tolerance (Mills et al., 2003; Eren and Argüello, 2004; Hussain et al., 2004; Verret et al., 2004; Mills et al., 2005; Verret et al., 2005; Hanikenne et al., 2008; Wong et al., 2009). HMA transporters are likely essential components in Cd hyperaccumulation system of metallophytes. AtHMA4 orthologs in Zn/Cd hyperaccumulators *A. halleri* and *N. caerulescens* confer Cd tolerance when expressed in yeast (Bernard et al., 2004; Papoyan and Kochian, 2004). In these metallophytes, hyperaccumulation and hypertolerance of Cd and Zn in *A. halleri* are related to the enhanced expression of HMA4 (Talke et al., 2006; Hanikenne et al., 2008; Lochlainn et al., 2011). Arabidopsis PCR1 and PCR2 work as Cd efflux transporters (Song et al., 2004). PCR1 is mainly expressed in the shoots, while PCR2 is highly expressed in both roots and shoots, and it can translocate Zn as well (Song et al., 2010).

Several metal transporters occur in peptide transporter-like proteins that belong to ATP-binding cassette (ABC-type) transporter or oligopeptide transporter families (Stacey et al., 2002; Lubkowitz, 2011). ABC transporters AtMRP3 (Bovet et al., 2003), AtATM3 (Kim et al., 2006) and AtPDR8 (Kim et al., 2007) are involved in long distance movement of nutrients and transition metals such as Cd and lead (Pb). OPT family proteins are highly hydrophobic, large proteins with 12 transmembrane domains (Koh et al., 2002; Wiles et

al., 2006), and are classified to two sub-families, i.e., YSL and Oligopeptide Transporter (OPT) clades (Lubkowitz, 2011). YSL family contains maize YS1, an iron–phytosiderophore-uptake transporter, and Arabidopsis YSLs that transport Fe-nicotianamine complex (Curie et al., 2001; Koh et al., 2002; Bogs et al., 2003; Zhang et al., 2004; Curie et al., 2009). OPT subfamily of proteins are also reported to play a role in metal homeostasis and distribution. OPT3 functions as a long-distance transporter of Fe-chelates, and is responsible for the seed Fe deposition in Arabidopsis (Wintz et al., 2003; Stacey et al., 2008). Expression of *AtOPT3* is induced under Fe, Cu and Mn deficiencies (Stacey, 2006; Buckhout et al., 2009). Up to date, the evidence for OPT proteins to transport heavy metals in addition to essential metals has increased. Recently, heterologous expression of *NcOPT3* in yeast increased Fe, Zn, Cu and Cd accumulation, and resulted in an increased sensitivity to Cd and Cu (Hu et al., 2012). Another OPT ortholog in *Brassica juncea* GT1, can transport glutathione and is required for the heavy-metal toxicity (Bogs et al., 2003). Moreover, both AtOPT6 and AtOPT7 can transport cadmium or cadmium-glutathione conjugates when heterologously expressed in yeast (Cagnac et al., 2004; Pike et al., 2009).

CARBOXYL-TERMINAL DOMAIN (CTD) PHOSPHATASE-LIKE1 (CPL1), a plant-specific isoform of RNA polymerase II CTD phosphatase, can specifically dephosphorylate pol II CTD at Ser5-PO4 *in vitro* (Koiwa et al., 2002; Xiong et al., 2002; Koiwa et al., 2004). CPL1 regulates the transcriptional responses to iron (Fe) deficiency and cadmium (Cd) toxicity (Aksoy et al., 2013; Aksoy and Koiwa, 2013). Fe utilization-related genes including *IRT1* is highly expressed in the roots of *cpl1* mutant, but the elevated IRT1 level in *cpl1* did not cause higher Cd level in *cpl1* roots, and the mutant roots show a higher Cd tolerance. Instead, *cpl1* accumulates more Cd in the shoots, suggesting that Cd toxicity in the *cpl1* roots is avoided by the transport of excess Cd to the shoots, which is often observed in heavy metal accumulators (Verbruggen et al., 2009).
Here we show data suggesting that OPT8 functions in Cd accumulation and is responsible for greater Cd content of *cpl1* mutant. A survey of the transcript abundance of various

metal transporters in *cpl1* roots identified that OPT8 was highly induced in *cpl1* roots upon exposure to Cd. *opt8* mutants accumulated less Cd, indicating that OPT8 is responsible for greater Cd accumulation in *cpl1*. In addition to the Cd level, *opt8* mutations also affect levels of Fe and Zn. Strong upregulation of *OPT8* together with that of global Fe-deficiency responses in *cpl1* is indicative of involvement of CPL1 in the upstream regulation of plant metal homeostasis.

3.3 Materials & Methods

3.3.1 Chemicals & Primer Information

All chemicals were obtained from Sigma. Sigma agar E was used for all plant growth experiments. Primer sequences used in this study are shown in Appendix A.

3.3.2 Plant Materials

The *Arabidopsis thaliana* ecotypes Col-0 and C24 were used in this study. *cpl1-2* (Koiwa et al., 2002; Xiong et al., 2002) and *cpl1-6* (Aksoy et al., 2013) were described previously. *opt8-1* (WiscDsLox238F10 - CS849403), *opt8-2* (SALK_033058C), *opt6* (SALK_201534C), *opt7* (SALK_113350C) and *opt9* (SALK_202456C) were obtained from the Arabidopsis Biological Resource Center (ABRC).

3.3.3 Stress Treatments

All growth experiments were performed on basal medium containing 1/4 Murashige and Skoog (MS) salts, 0.5% sucrose, and 1.5% agar. After stratification for 2 days at 4^{o}C, the plates were kept in a growth incubator under a long-day photoperiod (16 h light, 8 h darkness) at 23^{o}C.

For relative gene expression analyses, seeds were germinated and grown for 10 days on basal medium in the presence or absence of 60 µM $CdCl_2$.

For metal content analyses, seeds were germinated on basal medium for 7 days. In order to apply Cd toxicity, seedlings were transferred onto basal medium containing 60 µM $CdCl_2$. Following 3 days of treatment, root and shoot tissues were separately collected for further experiments.

To determine the cadmium sensitivity, seedlings of Col-0 wild-type and *opt8-1* and *opt8-2* mutants were grown on basal medium in the presence or absence of 40 µM and 60 µM $CdCl_2$. Seedlings were photographed after 13 days of growth and primary root lengths were analyzed using Image J software. Shoot fresh weights were determined as described (Conte et al., 2013).

3.3.4 RNA Extraction and RT-qPCR Analysis

Total RNA was isolated using TRIzol reagent (Chomczynski and Sacchi, 1987) and treated with DNase I (Promega, WI) to remove genomic DNA contamination. Total RNA samples (1 µg) were reverse-transcribed using random hexamers and GoScript™ Reverse Transcriptase (Promega, WI) in a total volume of 20 µl. One-twentieth of the reverse transcription products were analyzed using LightCycler 480 SYBR Green I Master Kit and a LightCycler 480 instrument (Roche Biochemicals, Indianapolis, IN). The amplification reaction and data analyses were performed as described (Salzman et al., 2005). Each reaction was run in technical duplicate and the melting curves were analyzed to verify that only a single product was amplified. *TUB8* (At5g23860) was used as an internal control for data normalization.

3.3.5 Preparation of P_{35S}-GFP-OPT8 Reporter Gene

p35S-GFP-OPT8 reporter gene was prepared in a Gateway LR reaction according to the manufacturer's instructions, by using full length of *OPT8* from the cDNA stock of PENTR221-AT5G53520 (Stock number of DQ447070) as entry clone and pMDC43 as the destination vector.

Transformation of *Agrobacterium tumefaciens* GV3101(pMP90RK), floral transformation of *cpl1-6*, and hygromycin selection of transformants were performed as described previously (Ueda et al., 2008).

3.3.6 Confocal Laser Scanning Microscopy

Four days-old root tissues grown on basal medium were mounted in distilled water under a coverslip. To observe the fluorescence, a FluoView FV1000 laser scanning confocal microscope (Olympus) was used. Excitation and emission of GFP were at 488 and 510–540 nm, respectively.

3.3.7 Determination of Metal Content

Tissue element analysis of Fe, Mn, Zn, and Cd using inductively coupled plasma–mass spectrometry (ICP-MS) was performed as described (Baxter et al., 2007). Briefly, shoots were washed thoroughly with distilled water. Roots were washed first in 2 mM $CaSO_4$ and 10 mM EDTA for 10 minutes, and were then rinsed twice in distilled water. Then, tissues were blot-dried, divided into three replicates of about 100 mg fresh weight, dried in a 65˚C oven for 48 h, and reweighed. The dried samples were digested completely using 0.6 ml of concentrated ultrapure grade HNO_3 (JT Baker, Netherlands) at 110˚C for 4 h. Each sample was diluted to 6 ml with nanopure water (18.2 MΩ) and analyzed on a

PerkinElmer NexION 300D ICP-MS in the reaction mode. Indium (EMD Millipore, Germany) was used as an internal standard. The National Institute of Standards and Technology traceable calibration standards (Alfa Aesar, MA) were used for the calibration. Each sample was read five times in the pulse detector mode. Three biological replicates were performed per analysis.

3.3.8 Determination of Chlorophyll Content

Total chlorophyll contents of Col-0 wild type and *opt8* mutants that were grown 13 days on basal medium in presence or absence of 60 µM $CdCl_2$ were determined according to Lichtenthaler (1987). Briefly, weighed leaves were ground with 80% (v/v) acetone, and then centrifuged at 13000 g for 5 min at 4°C. Absorbance readings of the supernatant were recorded at 470, 646.8 and 663.2 nm. Identical assay solution without plants was used as blank. Total chlorophyll content (chla + chlb) was calculated as (7.15 $A_{663.2}$ + 18.71 $A_{646.8}$)/1000/Fresh weights of leaves.

3.3.9 Bioinformatic Analyses

To identify the closest OPT8 relatives in other plant species OPT8 amino acid sequence of *A. thaliana* was used as a query in a BLASTP search against the genomes at National Center for Biotechnology Information (NCBI, http://www.ncbi.nlm.nih.gov). The protein sequences satisfied the score higher than 400 with an "E" value over e^{-120} and more than 60% similarity to *AtOPT8* sequence were assigned as significant. From each plant species, the proteins with the highest similarity (identity) to AtOPT8 were selected for the construction of the phylogenetic tree. Multiple sequence alignments of the full-length protein sequences were performed using MUSCLE (Edgar, 2004). A rooted phylogenetic tree was constructed using MEGA6.0 (Tamura et al., 2011) by the maximum likelihood method with the LG model of protein sequence substitutions (Le and Gascuel, 2008) and five discrete gamma rate categories. Bootstrap analyses were performed using 100

pseudoreplicates, and Nearest-Neighbor-Interchange (NNI) was selected as ML heuristic method.

To estimate the number and positions of transmembrane helical domains Aramemnon 8 (http://aramemnon.botanik.uni-koeln.de/) was used (Schwacke et al., 2003). The conserved domains of NPG and KIPPR among AtOPT8 homologs were identified according to Koh et al. (2002) following multiple sequence alignments of their amino acid sequences by MUSCLE. Coloring of conserved amino acids was performed using BoxShade server (http://www.ch.embnet.org/software/BOX_form.html). Membrane topology of OPT8 was drawn by the Transmembrane protein display software TOPO2 (http://www.sacs.ucsf.edu/TOPO2/) (Johns and Speth, 2010).

Comprehensive expression analysis was performed using all 9848 publicly available microarray data in Genevestigator software (Zimmermann et al., 2004). Expression levels of OPT6, OPT7, OPT8 and OPT9 were analyzed in different anatomical locations, developmental stages and perturbations. Results were presented as heat maps.

3.3.10 Statistical Analysis

Statistical analyses were performed with MINITAB 16 software (Minitab, PA). Statistical significances of differences between mean values were determined using Student's *t*-test or one-way analysis of variance (ANOVA) followed by Tukey's HSD post hoc test. Differences were considered significant when the *p*-value was less than 0.05.

3.3.11 Accession Numbers

Sequence data from this article can be found in the Arabidopsis genome initiatives under the accession numbers *CPL1*, At4g21670; *DTX1*,At2g04040; *HMA2*, At4g30110; *HMA4*, At2g19110; *NTR1.5*, At1g32450; *NRT1.8*, At4g21680; *OPT1*, AT5G55930; *OPT2*, AT1G09930; *OPT3*, AT4G16370; *OPT4*, AT5G64410; *OPT5*, AT4G26590; *OPT6*, AT4G27730; *OPT7*, AT4G10770; *OPT8*, AT5G53520; *OPT9*, AT5G53510; *DUO1*, AT3G60460; *PCR11*, AT1G68610; *GSH1*, AT4G23100; *GSH2*, AT5G27380; *PCS1*, AT5G44070; *PCS2*, AT2G37940.

3.4 Results

3.4.1 OPT8 is Constitutively Hyper-induced in cpl1 Roots

We have previously shown that the *cpl1* exhibit greater Cd accumulation in the shoots, suggesting that Cd toxicity in the *cpl1-2* roots is circumvented by the transport of excess Cd to the shoots (Aksoy et al., 2013). Various transporters are involved in root-to-shoot translocation of Cd in Arabidopsis. The expression levels of known Cd transporters (*HMA2*, *HMA4*, *NTR1.5/1.8* and *DTX1*) in *cpl1-2* were similar to those in wild-type. One exception was moderately higher expression of *OPT3*, which was recently implied in Cd accumulation because *opt3-2* mutant over-accumulates Cd (Akmakjian, Garo Zaven, 2011 MS thesis UC San Diego). Since Arabidopsis genome encode 9 isoforms of OPT, we hypothesized that other members of OPT are involved in Cd transport as well. Survey of the gene expression levels of *Arabidopsis OPT*s revealed that several OPTs are induced when plants were kept on media containing 60µM $CdCl_2$ (Table 3.1).

Table 3.1. RT-qPCR analysis of the expression levels of genes encoding for OPTs, DTX1, HMA2/4, NTR1.5/1.8, DUO1 and PCR11 in the roots and the shoots of *cpl1-2* and C24 after Cd treatment.

AGI	Gene	Cd 0 µM		Cd 60 µM	
		C24	*cpl1-2*	C24	*cpl1-2*
Roots					
AT2G04040	*DETOXIFICATION1 (DTX1)*	1	1.77 (± 0.52)	3.30 (± 0.93)	0.69 (± 0.10)*
AT4G30110	*HEAVY METAL ATPASE2 (HMA2)*	1	1.11 (± 0.05)	0.83 (± 0.04)	0.82 (± 0.08)
AT2G19110	*HEAVY METAL ATPASE4 (HMA4)*	1	0.96 (± 0.32)	0.66 (± 0.21)	0.57 (±0.23)
AT1G32450	*NITRATE TRANSPORTER1.5 (NTR1.5)*	1	1.22 (± 0.22)	0.68 (± 0.27)	0.53 (± 0.06)
AT4G21680	*NITRATE TRANSPORTER1.8 (NTR1.8)*	1	1.04 (± 0.35)	7.90 (± 0.54)	7.21 (± 0.43)
AT5G55930	*OLIGOPEPTIDE TRANSPORTER1 (OPT1)*	1	1.70 (±0.32)	1.52 (±0.28)	1.91 (±0.80)
AT1G09930	*OLIGOPEPTIDE TRANSPORTER2 (OPT2)*	1	1.77 (±0.61)	1.71 (±0.28)	6.17 (±1.26)
AT4G16370	*OLIGOPEPTIDE TRANSPORTER3 (OPT3)*	1	3.89 (±0.30)**	9.48 (±1.26)	15.08 (±2.54)
AT5G64410	*OLIGOPEPTIDE TRANSPORTER4 (OPT4)*	1	1.16 (±0.10)	9.69 (±1.41)	3.32 (± 0.61)*
AT4G26590	*OLIGOPEPTIDE TRANSPORTER5 (OPT5)*	1	1.15 (±0.09)	0.81 (±0.14)	1.52 (±0.39)
AT4G27730	*OLIGOPEPTIDE TRANSPORTET6 (OPT6)*	1	1.05 (±0.12)	0.78 (±0.04)	0.97 (±0.12)
AT4G10770	*OLIGOPEPTIDE TRANSPORTET7 (OPT7)*	1	1.23 (±0.14)	3.07 (±1.21)	4.69 (±1.02)
AT5G53520	*OLIGOPEPTIDE TRANSPORTET8 (OPT8)*	1	26.24 (±2.90) **	62.50 (±7.94)	1288.20 (±252.20) **
AT5G53510	*OLIGOPEPTIDE TRANSPORTET9 (OPT9)*	1	2.37 (±0.74)	2.42 (±0.83)	3.61 (±1.42)
AT3G60460	*DUO POLLEN1 (DUO1)*	1	3.39 (±0.23)*	2.48 (±0.06)	4.75 (±0.56)*
AT1G68610	*PLANT CADMIUM RESISTANCE11 (PCR11)*	1	2.15 (±0.11)*	3.00 (±0.47)	4.51 (±0.10)*
Shoots					
AT4G27730	*OLIGOPEPTIDE TRANSPORTET6 (OPT6)*	245.93 (±23.12)	223.80 (±24.36)	218.87 (±19.94)	319.709 (±32.75)
AT4G10770	*OLIGOPEPTIDE TRANSPORTET7 (OPT7)*	2.25 (±0.63)	2.09 (±0.28)	2.56 (±0.34)	3.65 (±0.53)
AT5G53520	*OLIGOPEPTIDE TRANSPORTET8 (OPT8)*	727.39 (±36.13)	1990.09 (±130.73)*	1117.05 (±166.31)	1844.11 (±180.90)
AT5G53510	*OLIGOPEPTIDE TRANSPORTET9 (OPT9)*	5.43 (±1.17)	23.40 (±3.45)**	12.65 (±2.31)	7.93 (±0.94)
AT3G60460	*DUO POLLEN1 (DUO1)*	11.85 (±1.67)	51.68 (±1.20)*	13.20 (±1.16)	40.10 (±3.26)*
AT1G68610	*PLANT CADMIUM RESISTANCE11 (PCR11)*	0.07 (±0.03)	0.50 (±0.09)**	0.25 (±0.02)	0.25 (±0.01)

Seeds were germinated and grown for 10 days on 1/4 x MS medium supplemented with 0.5% sucrose, 1.5% agar and indicated concentrations of $CdCl_2$. Total RNA was isolated from root and shoot tissues separately. RT-qPCR was performed as described (Aksoy et al., 2013). The presented expression levels are mean values (±SEM) of three biological replicates. *p<0.05 or **p<0.01, Student's t-test between mean values of *cpl1-2* and C24 for the same conditions.

Notably, *cpl1-2* strongly affected *OPT8* expression level in both the absence and the presence of Cd. In Cd treated plants (60µM, 10 days), the *OPT8* expression level in *cpl1-2* reached as much as 1288 fold compared to that of untreated wild type. Since previous study indicated that *OPT8* is expressed predominantly in the shoots, but not in the roots of young seedlings, we tested *OPT8* expression in the shoots. We also included *OPT6*, *7*, and *9* because of their high sequence homology to OPT8. As shown in Table 3.1, expression level of *OPT8* in the shoots was approximately 1000 fold higher than that in the roots. Interestingly, Cd did not strongly induce any of the *OPT*s tested in the shoots, and *cpl1-2* only moderately affected the expression of *OPT8* and *OPT9*. These results suggested that Cd accumulation phenotype of *cpl1-2* was caused by specific induction of *OPT8* in the roots.

As OPTs may function in Fe homeostasis, we tested the expression levels of select *OPT*s after 72 hours of Fe deficiency (Table 3.2). *OPT3*, *OPT8* and *OPT9* are induced in wild-type after Fe deficiency. *OPT8* expression in *cpl1* was not responsive to Fe deficiency, indicating the hyper-induction of *OPT8* in *cpl1* after Cd treatment is not caused by Fe deficiency.

Table 3.2. The gene expression levels of OPTs in the roots of *cpl1-2* and C24 in response to Fe deficiency.

AGI	Gene	Fe-EDTA 50 µM		0_{FZN}	
		C24	*cpl1-2*	C24	*cpl1-2*
AT4G16370	*OLIGOPEPTIDE TRANSPORTER3 (OPT3)*	1	3.96 (±0.36)*	10.79 (±1.94)	6.65 (±0.44)
AT4G27730	*OLIGOPEPTIDE TRANSPORTET6 (OPT6)*	1	1.23 (±0.25)	0.89 (±0.08)	1.95 (±0.02)*
AT4G10770	*OLIGOPEPTIDE TRANSPORTET7 (OPT7)*	1	1.39 (±0.37)	0.62 (±0.13)	0.49 (±0.07)
AT5G53520	*OLIGOPEPTIDE TRANSPORTET8 (OPT8)*	1	23.33 (±3.49)*	6.63 (±1.64)	32.88 (±3.74)*
AT5G53510	*OLIGOPEPTIDE TRANSPORTET9 (OPT9)*	1	2.06 (±0.45)	2.83 (±0.09)	2.73 (±0.28)

Plants were grown on basal medium for 7 days, and transferred to basal medium or to Fe-deficient basal medium (0_{FZN}, 0 µM Fe-EDTA + 300 µM ferrozine). After 72h for Fe deficiency treatment, total RNA was extracted from the roots, and RT-qPCR was performed as described (Aksoy et al., 2013). The presented expression levels are mean values (±SEM) of three biological replicates. *p<0.05 or **p<0.01, Student's t-test between mean values of *cpl1-2* and C24 for the same conditions.

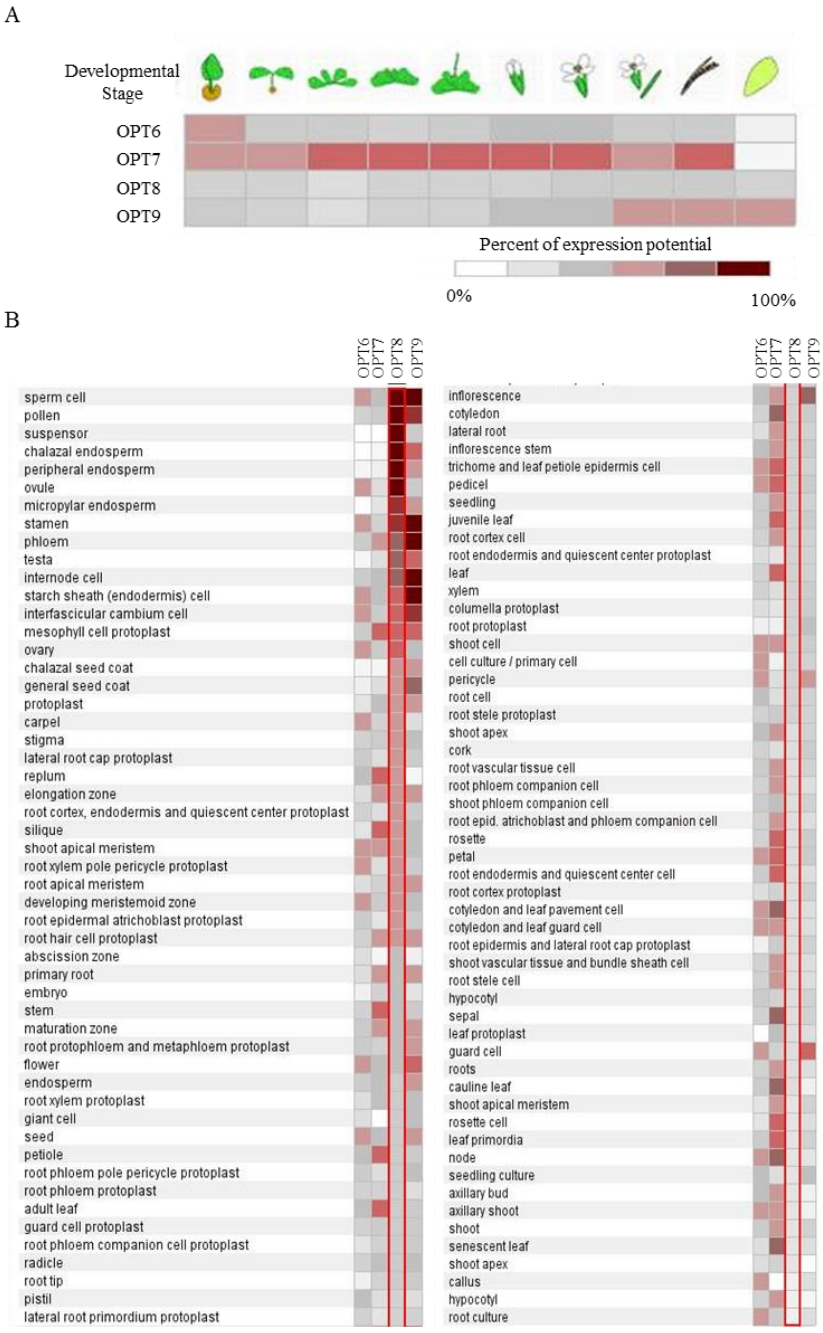

Figure 3.1. Expression profiles of Arabidopsis *OPT6*, *OPT7*, *OPT8* and *OPT9* in different stages of development and different anatomical sections. Expression profiles of 9848 microarray experiments deposited into the Genevestigator software were categorized with respect to the developmental stages that they express (A), and anatomical organs/tissues that they express (B).

Expression patterns of *OPT8* and select OPT isoforms, i.e., *OPT6*, *OPT7* and *OPT9*, in 9848 publicly available microarray data were analyzed by Genevestigator (Zimmermann et al., 2004). In these datasets, *OPT8* expression was very low in all 10 developmental stages in Arabidopsis (Fig. 3.1A). The level of the *OPT8* transcript was stable and no statistically-significant deviations were identified. On the other hand, *OPT8* and *OPT9* transcripts were commonly enriched in the sperm cell, the pollen, the endosperm, the ovule and the stamen (Fig. 3.1B). Interestingly, both *OPT8* and *OPT9* are also expressed in the phloem, which is important for the shoot-to-root translocation and seed loading of peptides and/or metals (Koike et al., 2004; Stacey et al., 2008; Aoyama et al., 2009).

The expressions of *OPT8* as well as another putative metal transporter *PLANT CADMIUM RESISTANCE11* (*PCR11*) are directly regulated by an R2R3 MYB transcription factor DUO POLLEN1 (DUO1) in sperm cells (Borg et al., 2011). We hypothesized that *DUO1* expressed in the roots and regulated the expression of *OPT8* and *PCR11* under the Cd treatment, so determined *DUO1* and *PCR11* expression. Both *DUO1* and *PCR11* were expressed higher in *cpl1-2* compared to the wild-type, and their expressions were induced by Cd. These observations suggest that *cpl1* affected the expression of *DUO1* and Cd-induction of *OPT8* and *PCR11* via the function of DUO1.

3.4.2 OPT8 is a Novel Cd Transporter in the Oligopeptide Transporter Protein Family

OPT8 belongs to the OLIGOPEPTIDE TRANSPORTER family, represented by nine members in Arabidopsis. Among OPT isoforms, AtOPT8 share high homology to AtOPT6 and AtOPT9 (with 71% and 69% homology, respectively) (Lubkowitz, 2011). While OPT family exists in other plant species, occurrence of close OPT8 homologs (>90% homology) are limited to close relatives of Arabidopsis (*Arabidopsis lyrata*, *Capsella rubella*, and *Eutrema salsugineum*), suggesting OPT8 has evolved relatively recently (Table 3.3). OPTs from monocots such as *Brachypodium distachyon*, *Triticum urartu* and Oryza sativa showed the lowest similarities.

Table 3.3. AtOPT8 homologs identified by BLASTP search.

Locus	Protein Name	E value	Identity (%)
Eudicot			
Arabidopsis thaliana			
AT5G53520.1*	ATOPT8	0	100
AT4G27730.1*	ATOPT6	0	71
AT5G53510.1*	ATOPT9	$1.90x10^{-302}$	69
AT4G10770.1*	ATOPT7	$6.50X10^{-263}$	59
Arabidopsis lyrata			
XP_002864248.1*	predicted protein	0	96
XP_002867483.1*	AlOPT6	0	74
XP_002864247.1	AlOPT9	0	71
XP_002874647.1	AlOPT7	0	61
XP_002876163.1	hypothetical protein ARALYDRAFT_906644	$5.00X10^{-15}$	70
Medicago truncatula			
XP_003601453.1*	OPT	0	63
Solanum lycopersicum			
XP_004235114.1*	oligopeptide transporter 6-like	0	64
XP_004245468.1	oligopeptide transporter 7-like	0	62
Eutrema salsugineum			
XP_006401694.1*	hypothetical protein EUTSA_v10015543mg	0	91
XP_006413036.1	hypothetical protein EUTSA_v10024519mg	0	74
XP_006401695.1	hypothetical protein EUTSA_v10016096mg	0	72
XP_006397011.1	hypothetical protein EUTSA_v10028453mg	0	62
Capsella rubella			
XP_006281558.1*	hypothetical protein CARUB_v10027665mg	0	93
XP_006285678.1	hypothetical protein CARUB_v10007142mg	0	74
Vitis vinifera			
XP_002275134.2*	oligopeptide transporter 6-like	0	69
CBI23049.3	unnamed protein product	0	69
Citrus clementine			
XP_006441174.1*	hypothetical protein CICLE_v10019012mg	0	71
XP_006439250.1	hypothetical protein CICLE_v10018971mg	0	62
Citrus sinensis			
XP_006491962.1*	oligopeptide transporter 9-like	0	71
Cucumis sativus			
XP_004138770.1*	oligopeptide transporter 6-like	0	69
XP_004163578.1	oligopeptide transporter 7-like	0	63
Theobroma cacao			
EOY23633.1*	Oligopeptide transporter 1 isoform 1	0	71
EOY23927.1	Oligopeptide transporter 7 isoform 1	0	65
Populus trichocarpa			
XP_006376657.1*	hypothetical protein POPTR_0012s02650g	0	66
Cicer arietinum			
XP_004502694.1*	oligopeptide transporter 6-like	0	67
Prunus persica			
EMJ21429.1*	hypothetical protein PRUPE_ppa002014mg	0	68

Table 3.3. Continued.

Locus	Protein Name	E value	Identity (%)
Monocots			
Oryza sativa			
EEC79904.1*	hypothetical protein OsI_21444	0	63
NP_001056665.1	Os06g0127700	0	62
BAD67732.1	putative sexual differentiation process protein isp4	0	63
Zea mays			
NP_001130398.1*	uncharacterized protein LOC100191494	0	63
NP_001167707.1	uncharacterized protein LOC100381394	0	63
Sorghum bicolor			
XP_002437735.1*	hypothetical protein SORBIDRAFT_10g001530	0	62
Hordeum vulgare			
BAJ85522.1*	predicted protein	0	62
BAJ95761.1	predicted protein	0	61
BAJ85948.1	predicted protein	0	60
Setaria italic			
XP_004964383.1*	oligopeptide transporter 7-like isoform X2	0	63
Brachypodium distachyon			
XP_003564333.1*	oligopeptide transporter 7-like	0	63
Triticum urartu			
EMS45172.1*	Oligopeptide transporter 7	0	63
Aegilops tauschii			
EMT07894.1*	Oligopeptide transporter 7	0	62
Angiosperms			
Amborella trichopoda			
ERN13351.1*	hypothetical protein AMTR_s00041p00121000	0	66

A BLASTP search was performed by using AtOPT8 amino acid sequence in the query (http://www.ncbi.nlm.nih.gov/blast). Scores higher than 400 with an ''E'' value over e^{-120} were assigned as significant, and the amino acid identities were given in percentage, with a cut off value of 60% identity. * represents the sequences used for the construction of the phylogenetic tree (Fig. 2).

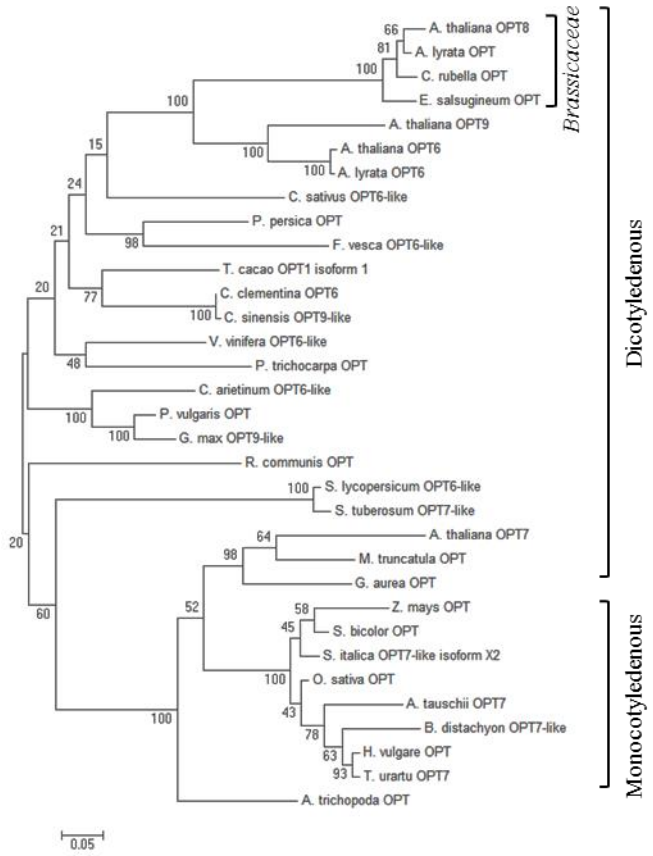

Figure 3.2. Phylogenetic relationships of *AtOPT8* homologs. Based on amino acid sequences, a phylogenetic tree of *AtOPT8* homologs in *A. thaliana* and other species was drawn according to the results generated by MEGA6.0 analysis using the neighbor-joining method with an amino acid and Poisson correction model. Bootstrap support values calculated for 1,000 replicates are indicated at corresponding nodes. Species designations and corresponding GenBank accession numbers *A. thaliana* OPT6 (AT4G27730.1), OPT7 (AT4G10770.1), OPT8 (AT5G53520.1), OPT9 (AT5G53510.1); *A. lyrata* OPT (XP_002864248.1), OPT6 (XP_002867483.1); *M. truncatula* (XP_003601453.1); *S. lycopersicum* (XP_004235114.1); *E. salsugineum (*XP_006401694.1); *C. rubella (*XP_006281558.1); *V. vinifera* (XP_002275134.2); *C. clementine* (XP_006441174.1); *C. sinensis* (XP_006491962.1); *C. sativus* (XP_004138770.1); *T. cacao* (EOY23633.1); *P. trichocarpa (*XP_006376657.1); *C. arietinum* (XP_004502694.1); *P. persica* (EMJ21429.1); *P. vulgaris* (ESW08463.1); *G. max* (XP_003522539.1); *F. vesca* (XP_004309115.1); *R. communis* (XP_002515831.1); *S. tuberosum* (XP_006350626.1); *G. aurea* (EPS60258.1); *O. sativa* (EEC79904.1); *Z. mays* (NP_001130398.1); *S. bicolor* (XP_002437735.1); *H. vulgare* (BAJ85522.1); *S. italica* (XP_004964383.1); *B. distachyon (*XP_003564333.1); *T. urartu* (EMS45172.1); *A. tauschii (*EMT07894.1); *A. trichopoda (*ERN13351.1). The scale of 0.05 represents 5% change.

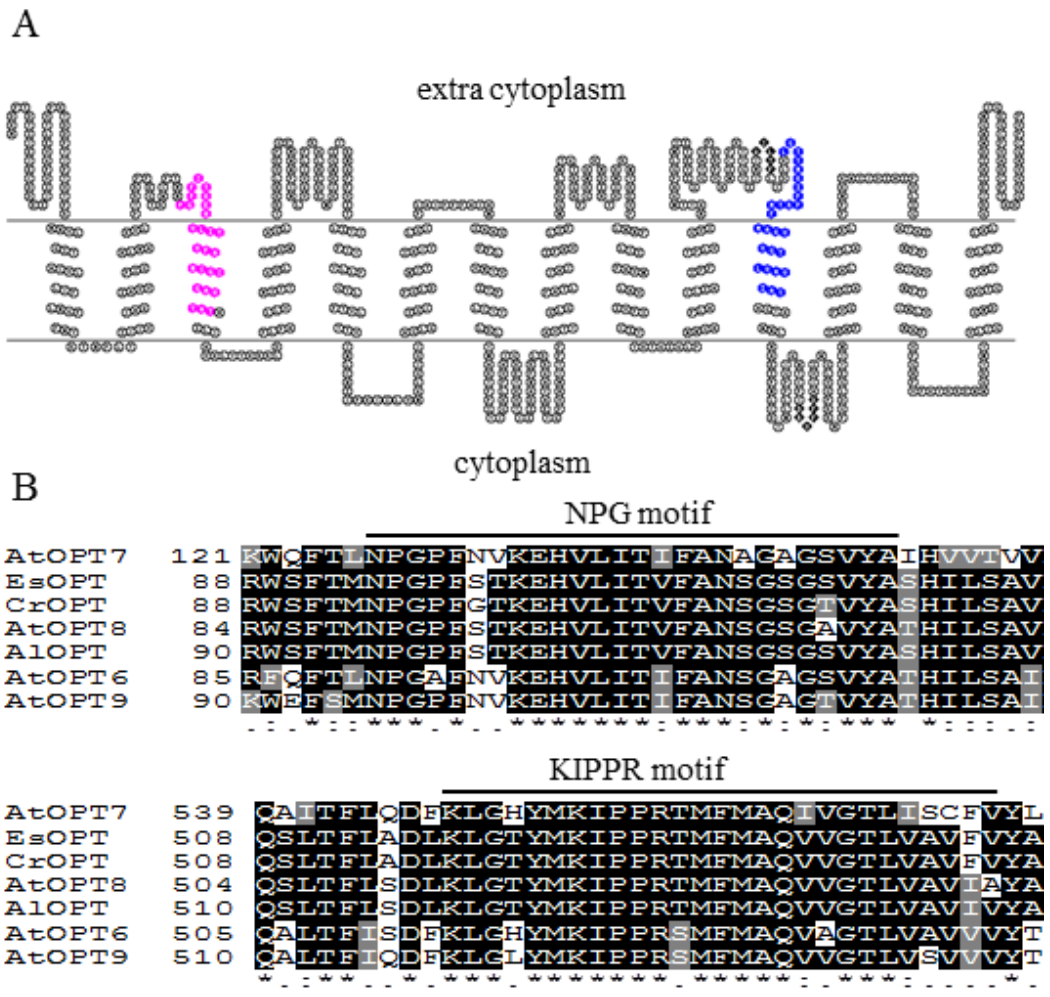

Figure 3.3. Membrane topology prediction of AtOPT8 and amino acid sequence alignment of conserved motifs of AtOPT8 homologs. A. Membrane topology prediction of AtOPT8 protein with predicted 14 transmembrane domains. Both N and C termini are predicted to be localized away from cytoplasm. 25 amino acids labelled in magenta and 26 amino acids labelled in blue represent conserved motifs of NPG and KIPPR, respectively. Amino acids designated with black diamonds represent the predicted phosphatase binding sites. The membrane topology was drawn by TOPO2. B. Sequence analysis of the AtOPT8, AlOPT, CrOPT, EsOPT, AtOPT6, AtOPT7 and AtOPT9. Two conserved motifs (NPG and KIPPR) amongst the AtOPT8 homologs were determined based on consensus of their sequences after analysis using the MUSCLE method. Colors are given in BoxShade. Black-shaded areas represent identical amino acids, and gray-shaded areas represent similar amino acids. Asterisks represent fully conserved amino acids in all OPTs.

To further confirm the phylogenetic relationship of the OPT genes, a rooted phylogenetic tree was constructed by comparing the amino acid sequences of AtOPT6/7/8/9 and the representative OPT isoform that is the most homologous to AtOPT8 from each species. As shown in Fig. 3.2, AtOPT8 is more related to OPT8 homologs from other *Brassicaceae* than other AtOPTs, indicating OPT8 is distinct from other OPTs. OPT family of proteins are very hydrophobic and likely contains 12 transmembrane (TM) domains (Koh et al., 2002; Wiles et al., 2006) (Fig. 3.3A). Alignments of amino acid sequences from AtOPT8, AlOPT, CrOPT, EsOPT, AtOPT6, AtOPT7 and AtOPT9 revealed many conserved motifs (Table 3.4 and Fig. 3.3B), two of which (NPG and KIPPR) are motifs important for the classification of PT clade of OPTs in Arabidopsis and rice (Koh et al., 2002; Vasconcelos et al., 2008). In addition to these two motifs, two potential phosphatase binding motifs as well as various phosphorylation motifs were also predicted in Eukaryotic Linear Motif (ELM) search (Dinkel et al., 2012) (Table 3.4), suggesting a possible phosphorylation-based regulation of AtOPT8 protein.

Table 3.4. Phosphorylarion-related motifs identified in OPT8 by ELM motif search after globular domain filtering, structural filtering and context filtering.

Elm Name	Instances (Matched Sequence)	Positions	ELM Description	Pattern	Probability
Phosphoprotein binding motifs					
DOC_PP1	SDRVFFD	570-576	Protein phosphatase 1 catalytic subunit (PP1c) interacting motif binds targeting proteins that dock to the substrate for dephosphorylation.	..[RK].(Ahmad et al., 2008)[VIL][^P][FW].	0.0008
LIG_BRCT_BRCA1_1	QSLTF	504-508	Phosphopeptide motif which directly interacts with the BRCT (carboxy-terminal) domain of the Breast Cancer Gene BRCA1 with low affinity.	.(S)..F	0.0019
Phosphorylation motifs					
LIG_FHA_1	DFTDTIS	3-9	Phosphothreonine motif binding a subset of FHA domains that show a preference for a large aliphatic amino acid at the pT+3 position.	..(T)..[ILV].	0.0087
	YRTNPLT	62-68			
	YATHILS	129-135			
	AKTFPIY	310-316			
	KVTSIID	329-335			
	AETGPVH	346-352			
	IITEYII	474-480			
	CDTNLLP	555-561			
LIG_FHA_2	TDTISES	5-11	Phosphothreonine motif binding a subset of FHA domains that have a preference for an acidic amino acid at the pT+3 position.	..(T)..[DE].	0.0083
MOD_CK1_1	SSVSAQI	70-76	CK1 phosphorylation site	S..([ST])...	0.0170
	SQWTCPS	564-570			
MOD_CK2_1	FTDTISE	4-10	CK2 phosphorylation site	...([ST])..E	0.0146
	DTISESE	6-12			
	GPFSTKE	107-113			
	FVASGKE	321-327			
MOD_NEK2_1	FTDTIS	4-9	NEK2 phosphorylation motif with preferred Phe, Leu or Met in the -3 position to compensate for less favorable residues in the +1 and +2 position.	[FLM][^P][^P]([ST])[^DEP][^DE]	0.0122
	LTISSV	67-72			
	FEGTRW	95-100			
	FANSGS	120-125			
	FVASGK	321-326			
	MATTNQ	463-468			
	MSQSLT	502-507			
	LCDTNL	554-559			
	FDASVI	575-580			

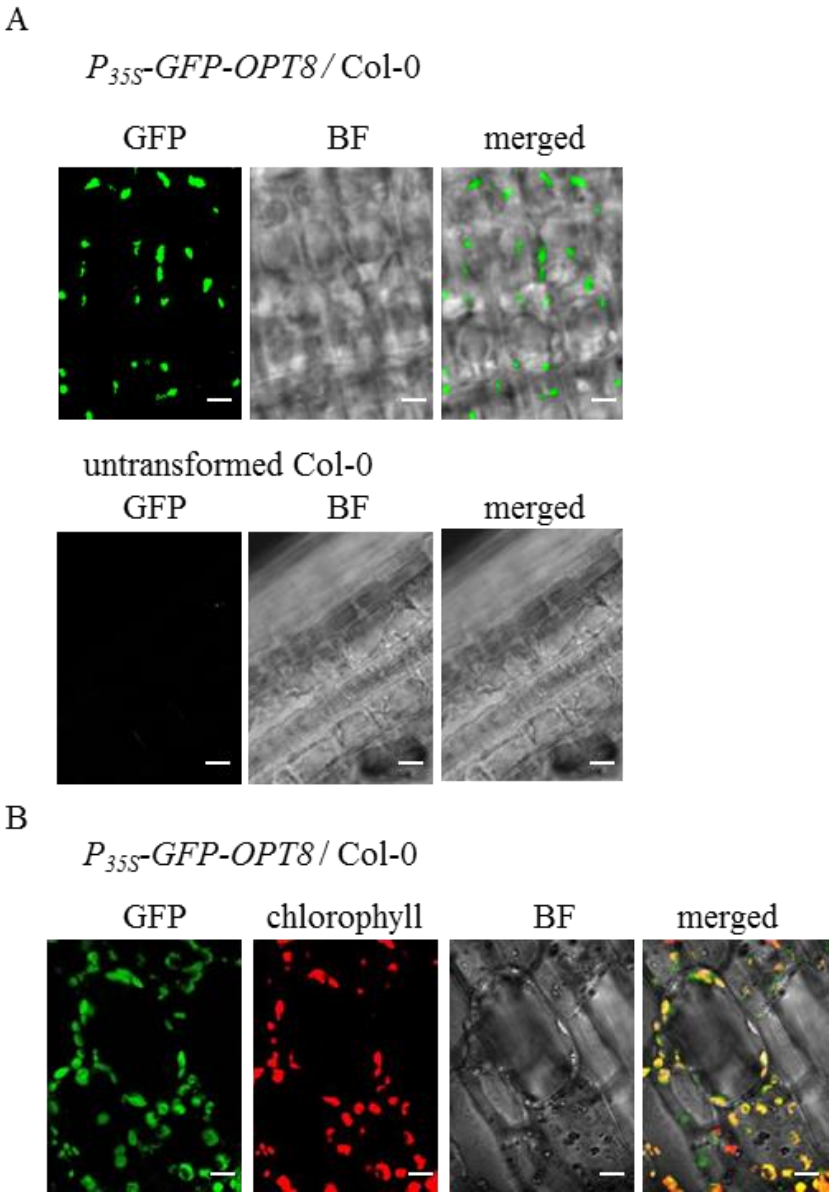

Figure 3.4. Subcellular localization of OPT8 in the roots and shoots of *cpl1-6*. Four days-old root tissues grown on basal medium were mounted in distilled water under a coverslip. GFP fluorescence was observed with a FluoView FV1000 laser scanning confocal microscope (Olympus). A. Subcellular localization of P_{35S}-*GFP-OPT8* transgene in the roots of *cpl1-6*. B. Subcellular localization of P_{35S}-*GFP-OPT8* transgene in the shoots of *cpl1-6*. Bars represent 10µm. Untransformed Col-0 seedlings were used as negative controls in both A and B. BF: Bright field image.

3.4.3 OPT8 is Localized to the Plastids

OPTs exhibit various subcellular locations including the plasma membrane, vesicles, tonoplast, plastids, and endoplasmic reticulum. Several subcellular localization prediction software programs, including SUBA (Heazlewood et al., 2007), MultiLoc (Höglund et al., 2006), Plant-mPloc (Chou and Shen, 2010), WoLF PSORT (Horton et al., 2007) and YLoc (Briesemeister et al., 2010), predicted a possible plasma membrane localization of OPT8, whereas LOCtree (Nair and Rost, 2005) predicted OPT8 as localized to the plastids. In order to empirically determine the subcellular localization of OPT8, we prepared transgenic plants expressing *GFP-OPT8* fusion protein, under the control of *35S* promoter. In the roots of *p35S-GFP-OPT8* plants, GFP fluorescence was observed in particular organelles whose sizes were 5-8 μm, similar to the plastids (Fig 3.4A). Plastid localization of OPT8 was confirmed because *GFP-OPT8* signal overlapped with chlorophyll fluorescence in the hypocotyl cells (Fig. 3.4B).

3.4.4 opt8 Mutations Affect Cd Hypersensitivity and Distribution

Constitutive elevation of the *OPT8* transcript level in the roots of *cpl1-2* mutant, as well as its induction in both wild-type and *cpl1-2* roots under Cd toxicity were unexpected, since OPT8 expression was rather constant under many conditions reported in GEO database. To clarify the involvement of OPT8 in plant Cd tolerance, we identified two T-DNA insertion lines, *opt8-1* (WiscDsLox238F10) and *opt8-2* (Salk_033058C), in the Col-0 background (Fig 3.5A). Junction sequences for both ends of the T-DNA insertion in *opt8-1* and *opt8-2* were determined (Fig 3.5B). The T-DNAs were inserted in the 5'-UTR region (Chromosome 5, at 21743422 base) in *opt8-1*, or in the third intron (at 21745104 base) in *opt8-2* T-DNA, respectively, and the production of intact *OPT8* mRNA was abolished in the mutants (Fig 3.5C and D). To determine the physiological consequence of *opt8* mutations, the root growth responses of wild-type Col-0 and *opt8* mutants to $CdCl_2$ were compared.

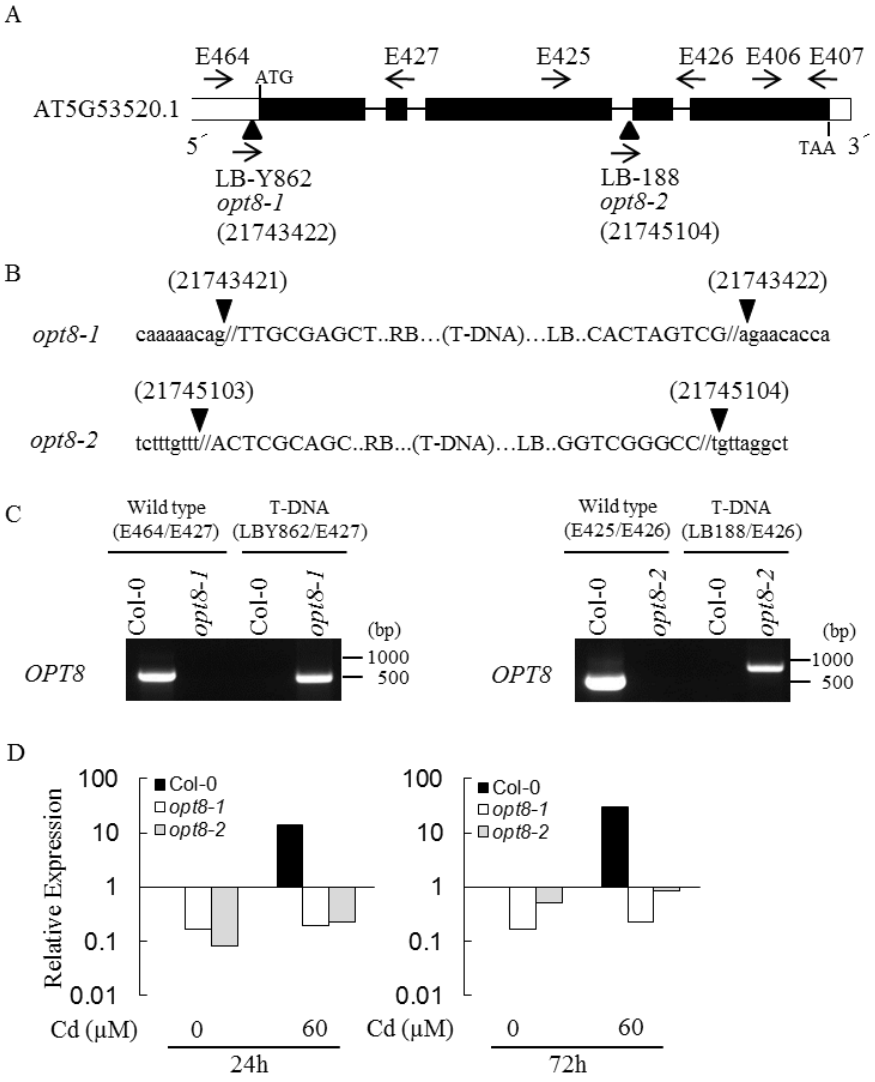

Figure 3.5. Molecular characterization of the *opt8-1* and *opt8-2* mutants. A, T-DNA insertion positions (triangles) in *opt8-1* (WiscDsLox238F10 - CS849403) and *opt8-2* (SALK_033058C). Exons and UTRs are represented by black and white boxes, respectively. Lines represent introns. B, The junction sequences of T-DNA and genomic DNA were confirmed by PCR sequencing of both ends of the T-DNA insert. Black triangles represent the T-DNA insertions. RB: Right Border, LB: Left Border of T-DNA. C, Confirmation of T-DNA lines by PCR using wild-type and mutant genomic DNA as templates. The positions of specific primers are indicated by arrows in A. C, RT-qPCR analysis of *OPT8* transcript levels in the Col-0 wild type, *opt8-1* and *opt8-2* after Cd treatment. Plants were grown on basal medium for 7 days, and then transferred to 60 µM Cd containing basal medium. Root samples were collected 24, or 72 hours after the transfer. Primers E392 and E393 were used in RT-qPCR analysis of *OPT8* transcript. The presented expression levels (relative to untreated Col-0 samples) are mean values of three biological replicates analyzed in duplicate. Bars indicate standard errors of the mean (SEM) of biological replicates. **p*<0.05, Students *t*-test between mean values of *opt8-1* or *opt8-2* and Col-0 for the same conditions.

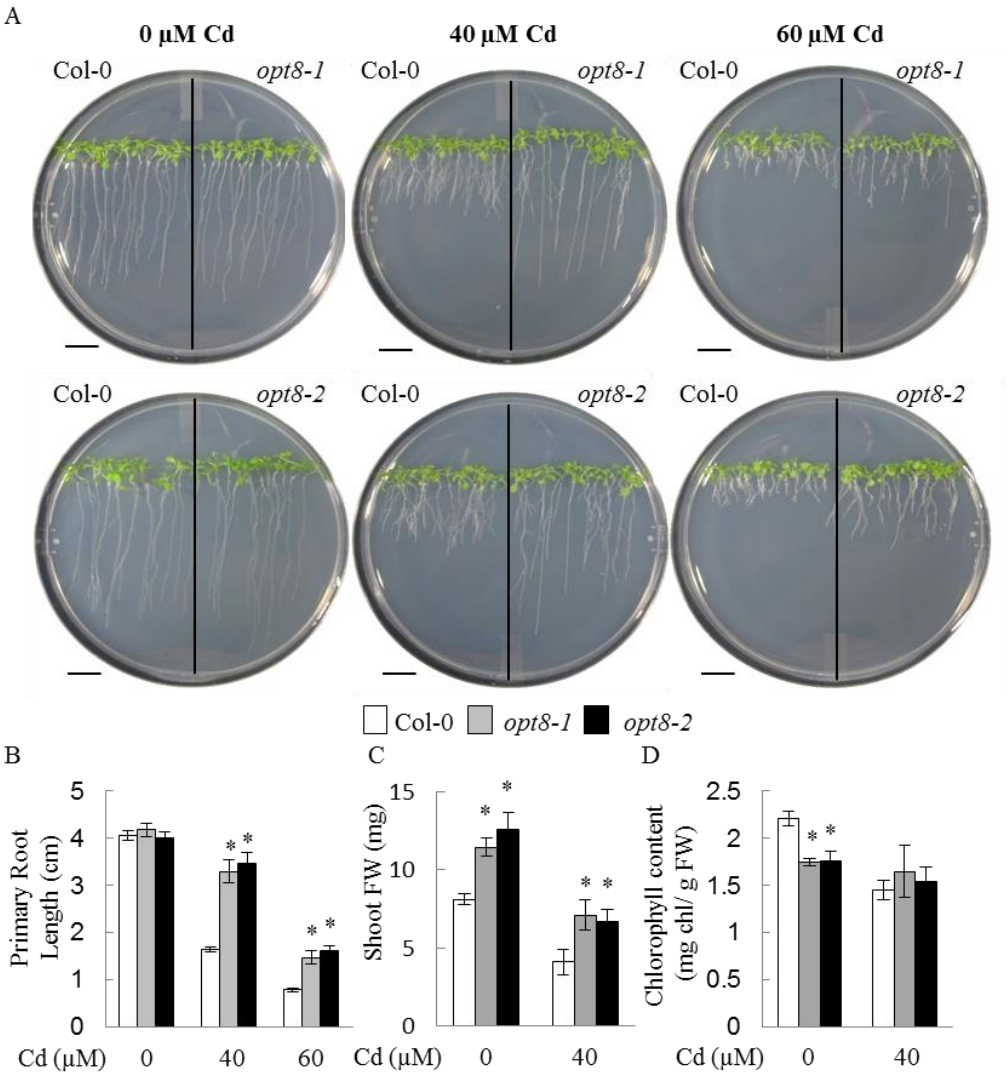

Figure 3.6. Primary root growth, shoot fresh weight and chlorophyll content of *opt8* mutants and wild-type. Seeds were germinated and grown for 13 days on ¼ x MS medium supplemented with 0.5% sucrose and 1.5% agar in presence or absence of $CdCl_2$. Final $CdCl_2$ concentrations were 40 or 60 µM. A. Representative pictures of root growth of Col-0, *opt8-1* and *opt8-2* on petri plates. The scale bars represent 1cm. B. Primary root length of Col-0 and opt8 mutants under different $CdCl_2$ concentrations. Bars indicate SEM of two biological replicates, each consisting of 20 seedling measurements. C. Shoot fresh weights (FW) of Col-0 and *opt8* mutants. Bars indicate SEM of two biological replicates. D. Total chlorophyll contents of Col-0 and *opt8* mutants. Bars indicate SEM of two biological replicates. *$p<0.05$, Student's t-test between mean values of Col-0 and *opt8-1* and *opt8-2* in each condition.

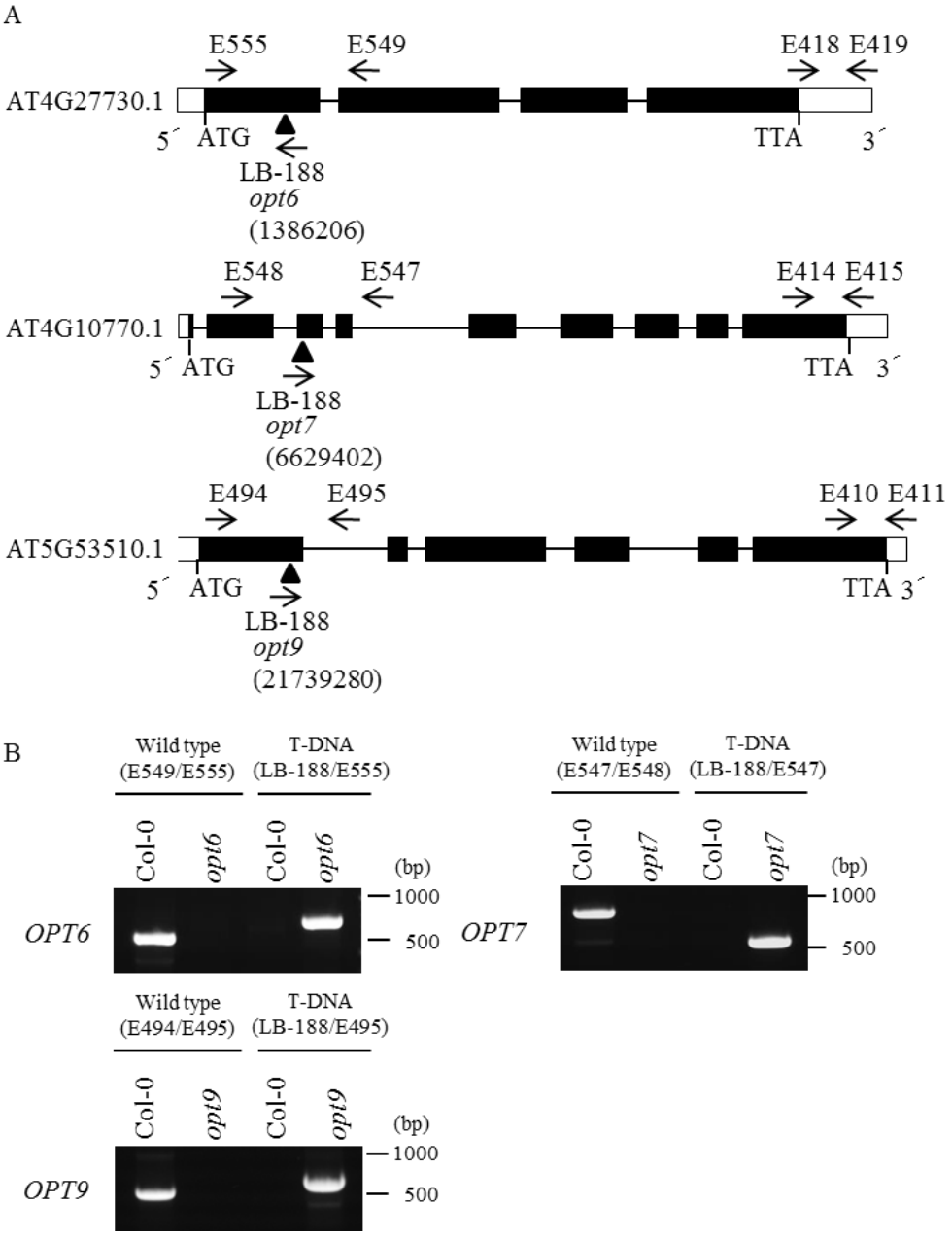

Figure 3.7. Molecular characterization of *opt6*, *opt7* and *opt9* mutants. A, T-DNA insertion positions (triangles) in *opt6* (Salk_201534C), *opt7* (Salk_113350C) and *opt9* (Salk_202456C). Exons and UTRs are represented by black and white boxes, respectively. Lines represent introns. B, Confirmation of T-DNA lines by PCR using wild-type and mutant genomic DNA as templates. The positions of specific primers are indicated by arrows in A.

As shown in Fig. 3.6, both *opt8* mutants were more tolerant to Cd than wild type. Interestingly, the growth of *opt6, 7, 9* mutants were indistinguishable from that of the wild-type (Fig. 3.7 and Fig. 3.8), indicating Cd tolerance phenotype is unique to the *opt8* mutants and is not generally associated with *opt* mutations. In addition to the root phenotype, *opt8* mutants were able to produce higher shoot biomass than wild-type regardless of the Cd condition, and higher total chlorophyll content in the absence of $CdCl_2$ (Fig. 3.6C and D). These results indicate that OPT8 has functions not only in the Cd tolerance, but also in normal plant metabolism.

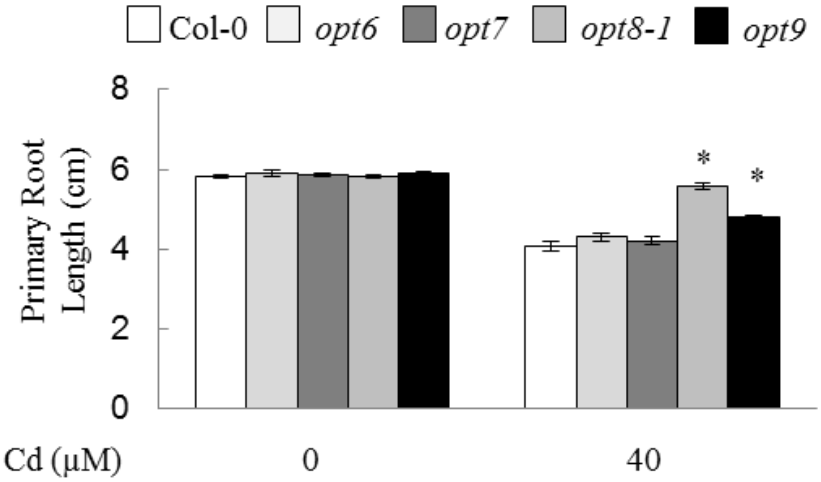

Figure 3.8. Primary root growth of *opt6, opt7, opt8-1* and *opt9* mutants and wild-type. Seeds were germinated and grown for 3 weeks on ¼ x MS medium supplemented with 0.5% sucrose and 1.5% agar in presence or absence of 40 µM $CdCl_2$. Bars indicate SEM of two biological replicates, each consisting of 20 seedling measurements. *$p<0.05$, Student's t-test between mean values of Col-0 and different *opt* mutants in each condition.

3.4.5 OPT8 Functions in Accumulation of Cd, Fe, Zn

In order to determine if the Cd tolerance phenotype of *opt8* mutants was associated with low levels of Cd and/or other metals in the mutant, we conducted elemental analyses using inductively coupled plasma mass spectrometry (ICP-MS). As shown in Fig. 3.9, *opt8-1* and *opt8-2* mutants accumulated 71.6% and 70%, respectively, less Cd in their roots than did the wild-type, and 34% and 33.7%, respectively, less Cd in the shoots. This suggests that OPT8 affects both overall uptake and root-to-shoot translocation of Cd. Notably, in wild type, cadmium is mainly accumulated in the roots because that root-to-shoot Cd translocation is restricted at the xylem loading (Thapa et al., 2012); however, the *opt8* mutants accumulated Cd to the similar levels in both roots and shoots. This suggests that OPT8 negatively regulates root-to-shoot Cd translocation.

Since Cd transport activity of metal transporters is often associated with the transport activity toward other transition metals, we tested the levels of iron (Fe), zinc (Zn), and manganese (Mn) in the *opt8* mutants. Compared to the wild-type, *opt8-1* and *opt8-2* mutants accumulated 60% and 45.5%, respectively, less Fe in their shoots even before Cd treatment. This reduction in the shoot Fe levels reached to 73.7% and 82.1% in *opt8-1* and *opt8-2*, respectively, after 3 days of Cd treatment. The low constitutive Fe level in the shoots of *opt8* plants is consistent with their chlorotic phenotype. More interestingly, constitutive Zn levels in both roots and shoots were reduced in the *opt8* mutants; however, upon Cd treatment, Zn content of wild-type and *opt8* became indistinguishable, suggesting OPT8 is responsible for Cd-sensitive Zn assimilation. On the other hand, Mn levels were not affected by *opt8* mutations.

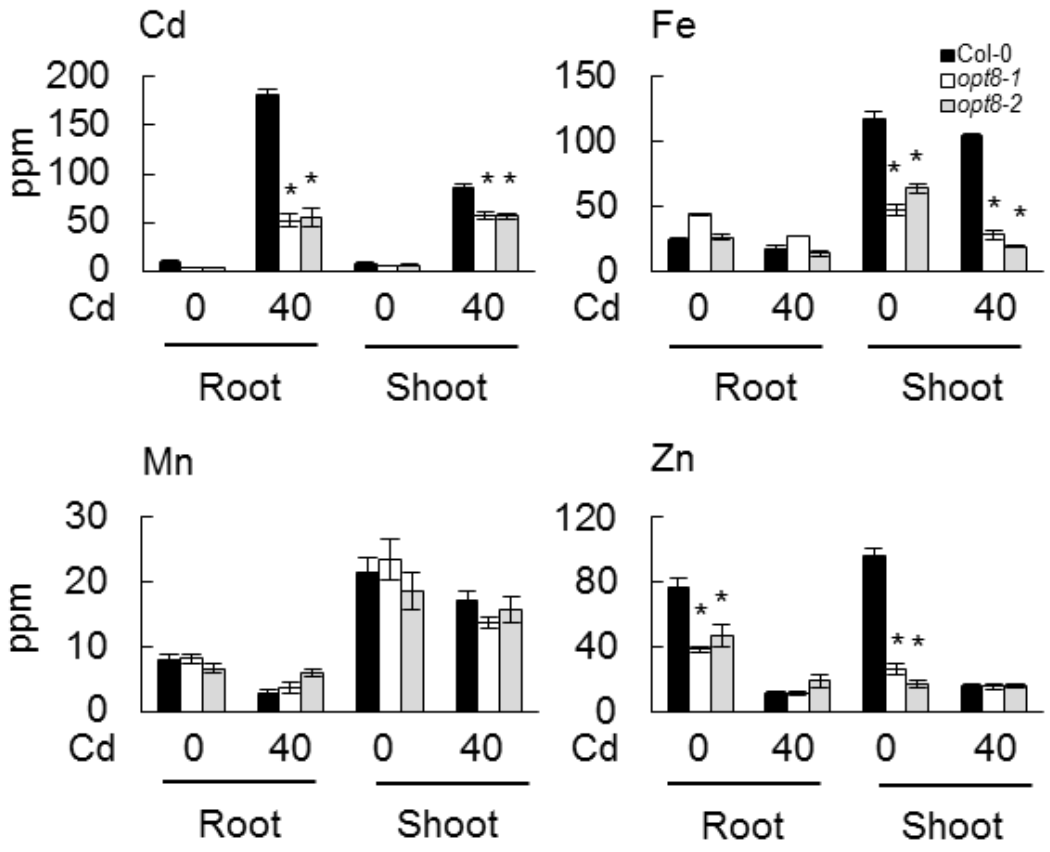

Figure 3.9. Metal contents of *opt8-1*, *opt8-2* and Col-0 roots and shoots under Cd toxicity. Plants were grown vertically for 7 days on quarter strength (¼) MS medium supplemented with 0.5% sucrose and 1.5% agar. Then, they were transferred onto medium with or without 40 µM $CdCl_2$. After 3 days, root and shoot tissues were collected separately and dried at 65ºC for 48 h, and elemental levels were determined from 100 mg of dried tissues by ICP-MS analysis. The presented elemental levels are the mean values of three biological replicates analyzed in triplicate. Bars indicate the SEM of biological replicates. **p*<0.05, Student's *t*-test between mean values of *opt8-1* or *opt8-2* and Col-0 for the same conditions.

3.4.6 Mutation in CPL1 Induces the Tolerance Mechanisms against Cd Toxicity

The above finding that loss-of-function mutations of *OPT8* confer Cd resistance is contradictory to the phenotype of *cpl1*, which exhibit higher level of OPT8 expression and Cd tolerance. Since *CPL1* can regulate the expression of a suite of genes, hyper-induction of *OPT8* in *cpl1* could be a part of coordinated-cadmium tolerance mechanisms that involve the translocation of Cd to the shoots. To test if *cpl1* mount the enhanced Cd tolerance responses, the expression levels of Cd detoxification pathway genes were analyzed (Table 3.5). We found that *cpl1* expressed significantly higher levels of *PHYTOCHELATIN SYNTHASE1* (*PCS1*), *PCS2*, and *GLUTAMATE-CYSTEINE LIGASE 1* (*GSH1*) than the wild-type in the shoots and *GSH2* in the roots. This indicated that *cpl1-2* mounted enhanced Cd detoxification pathway both in roots and shoots. From these findings we propose that the mutation in *CPL1* is unique in its nature such that it causes hyperactivation of Cd uptake, root-to-shoot translocation and tolerance mechanisms to accumulate more Cd safely in the shoots.

Table 3.5. RT-qPCR analysis of the expression levels of Cd detoxification pathway genes in the roots and the shoots of *cpl1-2* and C24 after Cd treatment.

AGI	Gene	Cd 0 µM		Cd 60 µM	
		C24	*cpl1-2*	C24	*cpl1-2*
Roots					
AT4G23100	*GLUTAMATE-CYSTEINE LIGASE1 (GSH1)*	1	1.14 (± 0.23)	1.39 (± 0.25)	1.32 (± 0.42)
AT5G27380	*GLUTAMATE-CYSTEINE LIGASE 2 (GSH2)*	1	2.45 (± 1.28)	2.42 (± 0.22)	3.87 (± 0.52)*
AT5G44070	*PHYTOCHELATIN SYNTHASE 1 (PCS1)*	1	1.40 (± 0.43)	1.62 (± 0.26)	1.27 (± 0.40)
AT1G03980	*PHYTOCHELATIN SYNTHASE 2 (PCS2)*	1	1.15 (± 0.15)	1.23 (± 0.08)	1.02 (± 0.25)
Shoots					
AT4G23100	*GLUTAMATE-CYSTEINE LIGASE1 (GSH1)*	1	1.16 (±0.35)	1.01 (±0.22)	2.48 (±0.16)*
AT5G27380	*GLUTAMATE-CYSTEINE LIGASE2 (GSH2)*	1	1.05 (±0.30)	1.67 (±0.03)	1.41 (±0.42)
AT5G44070	*PHYTOCHELATIN SYNTHASE1 (PCS1)*	1	4.86 (±0.17)**	8.08 (±0.27)	14.98 (±0.66)**
AT2G37940	*PHYTOCHELATIN SYNTHASE2 (PCS2)*	1	1.62 (±0.45)	2.68 (±0.12)	4.59 (±0.07)**

Seeds were germinated and grown for 10 days on 1/4 x MS medium supplemented with 0.5% sucrose, 1.5% agar and indicated concentrations of $CdCl_2$. RT-qPCR was performed as described (Aksoy et al., 2013). The presented expression levels are mean values (±SEM) of three biological replicates. *p<0.05 or **p<0.01, Student's *t*-test between mean values of *cpl1-2* and C24 for the same conditions.

3.5 Discussion

Cadmium (Cd) is a non-essential metal toxic for most organisms. Arabidopsis restricts xylem loading of Cd and accumulates Cd in roots, whereas hyperaccumulater species translocate large amount of Cd to shoots. Arabidopsis *cpl1* mutant appears to overcome the restriction and accumulate higher amount of Cd in the shoot tissue (Aksoy et al., 2013). Here we show that *cpl1* mutation caused overexpression of a putative metal transporter, OPT8, which affect homeostasis of Cd, Fe, and Zn in the host plants. While OPT is widely present in plants, close OPT8 homologs with >90% of similarities were present only in *Brassicaceae* species, including *Arabidopsis lyrata*, *Capsella rubella* and *Eutrema salsugineum*. The closest homologs of OPT8 in Arabidopsis, AtOPT6 and AtOPT9, showed only 71% and 69% homology, respectively, indicating OPT8 is evolved as a unique OPT in *Brassicaceae* family. Moreover, OPT8 homologs identified in either non-Brassicaceae dicots or monocots were much closer to the sequences of AtOPT6 or AtOPT7, respectively. Overall, these suggest that AtOPT8 were evolved later than AtOPT6 or AtOPT7. *AtOPT6* (AT4G27730) is found on chromosome 4 whereas *AtOPT9* (AT5G53510) and *AtOPT8* (AT5G53520) are found on chromosome 5 in tandem. It is interesting that among the proteins encoded by these three genes, *AtOP6* and *AtOPT9*, encoded on separate chromosomes, are more similar to each other than to *AtOPT8*. This suggests that the gene duplication on chromosome 5 was an earlier event than the segmental duplication across the two chromosomes, and implies that the second member of a chromosome 4 pair has subsequently been deleted. A similar type of event of gene duplication on the same chromosome followed by a segmental duplication across the chromosomes was also proposed for the evolution of heavy metal transporters, HMA2, HMA3 and HMA4 (Cobbett and Goldsbrough, 2002). Although the expression of the tandem *OPT8* and *OPT9* genes are expected to be regulated by a similar manner (Oliver et al., 2002; Liu and Moran, 2006; De and Babu, 2010; Baker et al., 2013), the expression of *OPT9* expression neither substantially responded to Cd nor was affected by *cpl1-2*. This

might indicate that *AtOPT9* has lost its function in evolution whereas *AtOPT8* has sub-functionalized to contribute to the Cd translocation in Arabidopsis.

Our data revealed novel regulation of OPT8 by Cd. Previous studies on Arabidopsis Cd-response transcriptome did not identify *OPT8* gene as Cd-responsive. Instead, a reporter gene analyses using *OPT8* promoter showed that *OPT8* are constitutively expressed in shoot vasculature and during pollen development. On the other hand, the expression level of *OPT8* in the roots is virtually undetectable in the wild-type based in these studies. Even in our analysis, the expression level of *OPT8* in the wild-type roots was only 0.1% (-Cd) or 8.5% (+Cd) of the levels observed in untreated shoots, even though there was 26-fold induction of *OPT8* by Cd treatment. In shoots, Cd treatment induced *OPT8* only by 2.7 fold. Overall, a very low expression level in roots and constant expression level in shoots likely prevented identification of OPT8 in the previous studies. The *cpl1-2* mutation strongly affected *OPT8* expression, but its effect is predominantly in the root tissue. Compared to the wild type (Cd-), the *OPT8* levels in *cpl1-2* increased to 26- (Cd-) and 1288-fold (Cd+). On the other hand, *OPT8* levels in *cpl1-2* shoots were only 2.7 fold higher than that of the wild type. It should be noted, however, that due to the low level of expression in the roots, *OPT8* levels in the shoots were always higher than those in the roots regardless of genotypes or conditions. This suggests that *OPT8* transcription is under strong CPL1-mediated repression in roots. Unlike strong activation of OPT8 in *cpl1*, the expression of the transcription factor that regulates the expression of *OPT8* and *PCR11*, another Cd transporter, i.e., *DUO1*, was only moderately activated in *cpl1*, and not regulated by Cd. It is likely that yet to be unidentified Cd-responsive transcription factor regulates vegetative expression of *OPT8*.

Yeast cells expressing OPT8 did not show clear Cd tolerance or sensitivity and no alteration of metal profile was observed, perhaps because OPT8 was expressed in endomembranes. Therefore, we can only speculate about OPT8 substrate. Substrates for OPT family proteins include diverse peptides or different metals chelated by mugineic

acids, nicotinamine, and glutathione (Curie et al., 2001; Koh et al., 2002; Bogs et al., 2003; Zhang et al., 2004). AtOPT6, but not AtOPT7, can transport glutathione and Cd-glutathione conjugate (Cagnac et al., 2004). High homology between AtOPT8 and ATOPT6 suggests that AtOPT8 may also transport Cd, as a Cd-glutathione complex. *Brassica Juncea* OPT3 homolog (BjGT1) can transport glutathione, and Cd induces its expression (Bogs et al., 2003). This implies that proposed role of OPT3 in Cd tolerance is exerted via transport of Cd-glutathione complex. Another likely form of Cd in plants is phytochelatin-Cd complex (PC-Cd). Since both OPT8 and PC likely function in translocation of Cd, OPT8 may transport PC-Cd. However, it appears rather unlikely that PC-Cd enters plastids since PC-Cd is predominantly stored in the vacuoles. Furthermore, transgenic production of PC in plastids did not alter Cd tolerance or accumulation phenotype. This contrasts with the phenotype of cytoplasmic production of PC, and is indicative that PC in plastids does not contribute to the Cd translocation processes.

Plastidic localization of OPT8 is unique among OPT isoforms, which often reside in plasma membrane (Hu et al., 2012; Hofstetter et al., 2013). Similar observation was made for Arabidopsis YSL6 and by inference, YSL4, which reside in the plastids and are involved in the extrusion of Fe from the plastids (Divol et al., 2013). Interestingly, *ysl4ysl6* double mutant hyperaccumulate Fe in the plastids whereas overexpression of *YSL4* or *YSL6* dramatically decreased the chloroplastic iron content. Since *opt8* mutations decrease shoot Fe/Zn/Cd contents, OPT8 may function in opposite direction to YSL4/YSL6, i.e., uptake of metals into the plastids. While we cannot exclude a possibility that OPT8 may function in concert with YSL4/YSL6 to regulate steady-state level of Fe/Zn/Cd in plastids, we propose it is more likely that OPT8 and YSL4/YSL6 function in distinct processes. The expression pattern of OPT8 in shoot vegetative tissues is distinct from those of YSL4/YSL6, and is restricted in the vasculature. Therefore, it is likely that OPT8 in vasculature plastids functions in long-distance transport of metals rather than storage of metals in leaf plastids.

What is the mechanism that both *opt8* loss-of-function mutant and *cpl1* that hyper-induces *OPT8* shows Cd tolerance? For *opt8* mutants, Cd levels are low both roots and shoots and this is likely cause of improved Cd tolerance. Based on this model, hyper-induction of *OPT8* in *cpl1* appears counterintuitive for its tolerance phenotype, and indeed, *cpl1* shows elevated Cd content in shoots. However, in *cpl1,* Cd tolerance can be established not by a simple regulation of Cd levels by OPT8, but by mounting multiple Cd tolerance mechanisms. Such mechanisms include improved Fe status as well as production of sulfur containing chelating compounds, such as glutathione and phytochelatins. As shown previously, *cpl1* can mount high levels of Fe uptake/utilization genes, and display improved growth when depleted of Fe supply from the media. Considering Fe-deficient phenotype of *opt8,* the elevated basal *OPT8* expression level is likely a part of *cpl1* response to the chronically-decreased shoot Fe level, even though OPT8 was not regulated by acute Fe depletion. Such a defense response to counteract Fe deficiency can protect plants from Cd toxicity. Consistently, transgenic Arabidopsis overexpressing *FIT* and *bHLH38/bHLH39* exhibited improved Cd tolerance, which was associated with upregulation of *HMA3, MTP3, IRT2* and *IREG2* involved in Cd detoxification (Wu et al., 2012). Another characteristic of Cd-related phenotype of *cpl1* is the increase of the shoot Cd level without increasing the root Cd level. Although we have not been able to determine the substrate specificity or the direction of OPT8-mediated transport, OPT8 hyper-induction in *cpl1* roots is likely responsible for this phenotype. Greater translocation of Cd from roots to shoots is a characteristic often associated with metallophytes such as *A. halleri*. However, unlike metallophytes, *cpl1* expressed higher levels of glutathione and phytochelatin biosynthetic pathway genes (Meyer et al., 2011). Since *cpl1* shoots show Cd stress symptoms, production of phytochelatin in *cpl1* shoots could be insufficient to sequester translocated Cd to vacuoles. Indeed, it requires overexpression of both phytochelatin synthase and phytochelatin conjugate transporter (ABCC1) to confer shoot Cd tolerance in wild-type Arabidopsis (Song et al., 2010). In contrast, *opt8* shoots produced greater biomass than the wild type in the presence of Cd.

Overall, the benefit of preventing distribution of Cd by *opt8* mutation likely outweighs the compromise of Fe and Zn translocation.

CHAPTER IV

CONCLUSION

RNA metabolism regulates diverse developmental and stress response signaling pathways in plants. As a RNA metabolism regulator, RNA POLYMERASE II C-TERMINAL DOMAIN (POL II CTD) PHOSPHATASE-LIKE1 (CPL1) can negatively regulate stress-responsive gene expression under various osmotic stresses. The work presented in this dissertation identifies CPL1 as a novel regulator of the Fe deficiency and Cd toxicity responses.

Chapter II explains the molecular characterization of CPL1 functions in plant Fe deficiency responses. Microarray analysis of the c*pl1* transcriptome found that both the osmotic stress/ABA response and the Fe deficiency response were activated in *cpl1*. An analysis of multiple *cpl1* alleles established that *cpl1* mutations enhanced transcriptional responses of Fe utilization-related genes, e.g. *IRON-REGULATED TRANSPORTER 1* (*IRT1*), to low Fe availability. *cpl1* mutant plants exhibited various hallmarks of the Fe deficiency response such as altered metal profiles, and increased tolerance to Fe deficiency and cadmium toxicity. Genetic data indicate that *cpl1-2* likely activates Fe deficiency responses upstream of both FE–DEFICIENCY-INDUCED TRANSCRIPTION FACTOR (FIT)-dependent and -independent signaling pathways. Moreover, CPL1 localization was found to be in the root stele. These results suggest that *CPL1* is a previously uncharacterized regulator of the Fe deficiency response. In addition, our data suggest that a subset of ABA/osmotic stress-induced genes are co-regulated by Fe deficiency signals and are targets of CPL1 regulation. Interestingly, the *cpl1-2* plants accumulated more Cd in the shoots, suggesting that Cd toxicity in the *cpl1-2* roots is circumvented by the transport of excess Cd to the shoots.

In Chapter III, the expression levels of genes encoding for known transporters function in Cd distribution were analyzed in the roots of *cpl1-2* in order to identify the major transporter(s) responsible for the Cd tolerance phenotype of *cpl1-2*. *OPT8* was found to be highly induced in *cpl1-2* roots upon exposure to Cd. OPT8 was localized to the plastids. The root growth of two alleles of *opt8* mutant showed higher tolerance to the Cd toxicity as the mutants accumulated less Cd, Fe and Zn both in shoots and roots. Interestingly, direct regulator of *OPT8, DUO POLLEN1* (*DUO1*), was also responsive to Cd, and was upregulated in both the roots and the shoots of *cpl1-2* mutant. Overall, these results point to a complex regulatory network of Cd tolerance that is under the control of RNA metabolism factor(s). Moreover, expression levels of *PCS1, PCS2* and *GSH1* were higher in the shoots of *cpl1-2* compared to the levels in the wild-type, suggesting the enhanced Cd translocation from roots to shoots in *cpl1-2* was due to the accumulation of phytochelatins. This also implies that the higher accumulation of phytochelatins in the shoots of *cpl1-2* was one of the contributors to the Cd tolerance phenotype.

Further characterization of *cpl1* and *opt8* mutants under Cd toxicity will extend our understanding of plant heavy-metal accumulation and lead to the development of new phytoremediation techniques that may prevent Cd toxicity.

REFERENCES

Ahmad P, John R, Sarwat M, Umar S (2008) Responses of proline, lipid peroxidation and antioxidative enzymes in two varieties of Pisum sativum L. under salt stress. International Journal of Plant Production **2:** 353-365

Ahner BA, Wei L, Oleson JR, Ogura N (2002) Glutathione and other low molecular weight thiols in marine phytoplankton under metal stress. Marine Ecology Progress Series **232:** 93-103

Aksoy E, Jeong IS, Koiwa H (2013) Loss of Function of Arabidopsis C-Terminal Domain Phosphatase-Like1 Activates Iron Deficiency Responses at the Transcriptional Level. Plant Physiology **161:** 330-345

Aksoy E, Koiwa H (2013) Function of Arabidopsis CPL1 in cadmium responses. Plant Signaling & Behavior **8:** e24120

Alfvén T, Elinder CG, Carlsson MD, Grubb A, Hellström L, Persson B, Pettersson C, Spång G, Schütz A, Järup L (2000) Low‐Level Cadmium Exposure and Osteoporosis. Journal of Bone and Mineral Research **15:** 1579-1586

Allison LA, Wong J, Fitzpatrick VD, Moyle M, Ingles C (1988) The C-terminal domain of the largest subunit of RNA polymerase II of Saccharomyces cerevisiae, Drosophila melanogaster, and mammals: a conserved structure with an essential function. Molecular and Cellular Biology **8:** 321-329

Alloway BJ (2013) Sources of Heavy Metals and Metalloids in Soils. *In* Brian J. Alloway, eds, Heavy metals in soils. Springer Netherlands, Vol 22: pp 3-9

Amir R, Hacham Y, Galili G (2002) Cystathionine γ-synthase and threonine synthase operate in concert to regulate carbon flow towards methionine in plants. Trends in Plant Science **7:** 153-156

Andresen E, Mattusch J, Wellenreuther G, Thomas G, Abad UA, Küpper H (2013) Different strategies of cadmium detoxification in the submerged macrophyte Ceratophyllum demersum L. Metallomics **5:** 1377-1386

Anjum NA, Umar S, Singh S, Nazar R, Khan NA (2008) Sulfur assimilation and cadmium tolerance in plants *In* Sulfur assimilation and abiotic stress in plants Springer Netherlands, pp 271-302

Aouida M, Khodami-Pour A, Ramotar D (2009) Novel role for the Saccharomyces cerevisiae oligopeptide transporter *Opt2* in drug detoxification. Biochemistry And Cell Biology **87:** 653-661

Aoyama T, Kobayashi T, Takahashi M, Nagasaka S, Usuda K, Kakei Y, Ishimaru Y, Nakanishi H, Mori S, Nishizawa NK (2009) OsYSL18 is a rice iron (III)–deoxymugineic acid transporter specifically expressed in reproductive organs and phloem of lamina joints. Plant Molecular Biology **70:** 681-692

Appenroth K-J (2010) Definition of "heavy metals" and their role in biological systems. *In* Soil heavy metals. Springer Netherlands, pp 19-29

Arnaud N, Murgia I, Boucherez J, Briat J-F, Cellier F, Gaymard F (2006) An iron-induced nitric oxide burst precedes ubiquitin-dependent protein degradation for Arabidopsis AtFer1 ferritin gene expression. Journal of Biological Chemistry **281:** 23579-23588

Arrivault S, Senger T, Krämer U (2006) The Arabidopsis metal tolerance protein AtMTP3 maintains metal homeostasis by mediating Zn exclusion from the shoot under Fe deficiency and Zn oversupply. The Plant Journal **46:** 861-879

Backes C, Keller A, Kuentzer J, Kneissl B, Comtesse N, Elnakady YA, Muller R, Meese E, Lenhof HP (2007) GeneTrail--advanced gene set enrichment analysis. Nucleic Acids Research **35:** W186-192

Baker CR, Hanson-Smith V, Johnson AD (2013) Following gene duplication, paralog interference constrains transcriptional circuit evolution. Science **342:** 104-108

Bang W, Kim S, Ueda A, Vikram M, Yun D, Bressan RA, Hasegawa PM, Bahk J, Koiwa H (2006) Arabidopsis carboxyl-terminal domain phosphatase-like isoforms share common catalytic and interaction domains but have distinct in planta functions. Plant Physiology **142:** 586-594

Bang WY, Jeong IS, Kim DW, Im CH, Ji C, Hwang SM, Kim SW, Son YS, Jeong J, Shiina T, Bahk JD (2008) Role of Arabidopsis CHL27 protein for photosynthesis, chloroplast development and gene expression profiling. Plant and Cell Physiology **49:** 1350-1363

Bang WY, Kim SW, Jeong IS, Koiwa H, Bahk JD (2008) The C-terminal region (640-967) of Arabidopsis CPL1 interacts with the abiotic stress- and ABA-responsive transcription factors. Biochemical and Biophysical Research Communications **372:** 907-912

Barberon M, Zelazny E, Robert S, Conejero G, Curie C, Friml J, Vert G (2011) Monoubiquitin-dependent endocytosis of the IRON-REGULATED TRANSPORTER 1 (IRT1) transporter controls iron uptake in plants. Proc Natl Acad Sci U S A

Baruah A, Šimková K, Hincha DK, Apel K, Laloi C (2009) Modulation of 1O2 ‐ mediated retrograde signaling by the PLEIOTROPIC RESPONSE LOCUS 1 (PRL1) protein, a central integrator of stress and energy signaling. The Plant Journal **60:** 22-32

Bashir K, Inoue H, Nagasaka S, Takahashi M, Nakanishi H, Mori S, Nishizawa NK (2006) Cloning and characterization of deoxymugineic acid synthase genes from graminaceous plants. Journal of Biological Chemistry **281:** 32395-32402

Bashir K, Ishimaru Y, Shimo H, Nagasaka S, Fujimoto M, Takanashi H, Tsutsumi N, An G, Nakanishi H, Nishizawa NK (2011) The rice mitochondrial iron transporter is essential for plant growth. Nature Communications **2:** 322

Bauer P, Ling HQ, Guerinot ML (2007) FIT, the FER-LIKE IRON DEFICIENCY INDUCED TRANSCRIPTION FACTOR in Arabidopsis. Plant Physiol Biochem **45:** 260-261

Bauer P, Thiel T, Klatte M, Bereczky Z, Brumbarova T, Hell R, Grosse I (2004) Analysis of sequence, map position, and gene expression reveals conserved essential genes for iron uptake in Arabidopsis and tomato. Plant Physiology **136:** 4169-4183

Baxter I, Ouzzani M, Orcun S, Kennedy B, Jandhyala SS, Salt DE (2007) Purdue Ionomics Information Management System. An integrated functional genomics platform. Plant Physiology **143:** 600-611

Baxter IR, Vitek O, Lahner B, Muthukumar B, Borghi M, Morrissey J, Guerinot ML, Salt DE (2008) The leaf ionome as a multivariable system to detect a plant's physiological status. Proc Natl Acad Sci U S A **105:** 12081-12086

Becher M, Talke IN, Krall L, Krämer U (2004) Cross‐species microarray transcript profiling reveals high constitutive expression of metal homeostasis genes in shoots of the zinc hyperaccumulator *Arabidopsis halleri*. The Plant Journal **37:** 251-268

Benjamini Y, Hochberg Y (1995) Controlling the False Discovery Rate - a Practical and Powerful Approach to Multiple Testing. Journal of the Royal Statistical Society Series B-Methodological **57:** 289-300

Berezin I, Mizrachy-Dagry T, Brook E, Mizrahi K, Elazar M, Zhuo S, Saul-Tcherkas V, Shaul O (2008) Overexpression of AtMHX in tobacco causes increased sensitivity to Mg2+, Zn2+, and Cd2+ ions, induction of V-ATPase expression, and a reduction in plant size. Plant Cell Reports **27:** 939-949

Bernard A (2008) Cadmium & its adverse effects on human health. Indian Journal of Medical Research **128:** 557

Bernard C, Roosens N, Czernic P, Lebrun M, Verbruggen N (2004) A novel CPx-ATPase from the cadmium hyperaccumulator Thlaspi caerulescens. FEBS Letters **569:** 140-148

Bernard DG, Cheng Y, Zhao Y, Balk J (2009) An allelic mutant series of ATM3 reveals its key role in the biogenesis of cytosolic iron-sulfur proteins in Arabidopsis. Plant Physiology **151:** 590-602

Bloß T, Clemens S, Nies DH (2002) Characterization of the ZAT1p zinc transporter from Arabidopsis thaliana in microbial model organisms and reconstituted proteoliposomes. Planta **214:** 783-791

Bogs J, Bourbouloux A, Cagnac O, Wachter A, Rausch T, Delrot S (2003) Functional characterization and expression analysis of a glutathione transporter, *BjGT1*, from *Brassica juncea*: evidence for regulation by heavy metal exposure. Plant, Cell & Environment **26:** 1703-1711

Borg M, Brownfield L, Khatab H, Sidorova A, Lingaya M, Twell D (2011) The R2R3 MYB transcription factor DUO1 activates a male germline-specific regulon essential for sperm cell differentiation in Arabidopsis. The Plant Cell **23:** 534-549

Bovet L, Eggmann T, MEYLAN‐BETTEX M, Polier J, Kammer P, Marin E, Feller U, Martinoia E (2003) Transcript levels of AtMRPs after cadmium treatment: induction of AtMRP3. Plant, Cell & Environment **26:** 371-381

Boyd RS, Davis MA, Wall MA, Balkwill K (2002) Nickel defends the South African hyperaccumulator Senecio coronatus (Asteraceae) against Helix aspersa (Mollusca: Pulmonidae). Chemoecology **12:** 91-97

Briat J-F, Ravet K, Arnaud N, Duc C, Boucherez J, Touraine B, Cellier F, Gaymard F (2010) New insights into ferritin synthesis and function highlight a link between iron homeostasis and oxidative stress in plants. Annals of Botany **105:** 811-822

Briat JF, Duc C, Ravet K, Gaymard F (2010) Ferritins and iron storage in plants. Biochimica Et Biophysica Acta-General Subjects **1800:** 806-814

Briesemeister S, Rahnenführer J, Kohlbacher O (2010) YLoc—an interpretable web server for predicting subcellular localization. Nucleic Acids Research **38:** W497-W502

Broadley M, Brown P, Cakmak I, Rengel Z, F. Z (2012) Function of Nutrients: Micronutrients. *In* P Marschner, ed, Marschner's mineral nutrition of higher plants, Ed 3rd. Academic Press, London ; Waltham, MA, pp 191–248

Buchauer MJ (1973) Contamination of soil and vegetation near a zinc smelter by zinc, cadmium, copper, and lead. Environmental Science & Technology **7:** 131-135

Buckhout TJ, Yang TJ, Schmidt W (2009) Early iron-deficiency-induced transcriptional changes in Arabidopsis roots as revealed by microarray analyses. BMC Genomics **10:** 147

Budiman M, Chang S, Lee S, Yang T, Zhang H, De Jong H, Wing R (2004) Localization of jointless-2 gene in the centromeric region of tomato chromosome 12 based on high resolution genetic and physical mapping. Theoretical And Applied Genetics **108:** 190-196

Buratowski S (2009) Progression through the RNA Polymerase II CTD Cycle. Molecular Cell **36:** 541-546

Cagnac O, Bourbouloux A, Chakrabarty D, Zhang M-Y, Delrot S (2004) AtOPT6 transports glutathione derivatives and is induced by primisulfuron. Plant Physiology **135:** 1378-1387

Cao J, Huang J, Yang Y, Hu X (2011) Analyses of the oligopeptide transporter gene family in poplar and grape. BMC Genomics **12:** 465

Cazalé A-C, Clemens S (2001) Arabidopsis thaliana expresses a second functional phytochelatin synthase. FEBS Letters **507:** 215-219

Chaffai R, Koyama H (2011) Heavy Metal Tolerance in Arabidopsis thaliana. *In* JC Kader, M Delseny, eds, Advances in Botanical Research, Vol 60, Vol 60, pp 1-49

Chaney RL, Malik M, Li YM, Brown SL, Brewer EP, Angle JS, Baker AJ (1997) Phytoremediation of soil metals. Current Opinion in Biotechnology **8:** 279-284

Chao DY, Silva A, Baxter I, Huang YS, Nordborg M, Danku J, Lahner B, Yakubova E, Salt DE (2012) Genome-Wide Association Studies Identify Heavy Metal ATPase3 as the Primary Determinant of Natural Variation in Leaf Cadmium in Arabidopsis thaliana. Plos Genetics **8**

Chapman RD, Heidemann M, Albert TK, Mailhammer R, Flatley A, Meisterernst M, Kremmer E, Eick D (2007) Transcribing RNA polymerase II is phosphorylated at CTD residue serine-7. Science **318:** 1780-1782

Chapman RD, Heidemann M, Hintermair C, Eick D (2008) Molecular evolution of the RNA polymerase II CTD. Trends in Genetics **24:** 289-296

Chen M, Shen X, Li D, Ma L, Dong J, Wang T (2009) Identification and characterization of MtMTP1, a Zn transporter of CDF family, in the Medicago truncatula. Plant Physiology and Biochemistry **47:** 1089-1094

Chen S, Sánchez-Fernández R, Lyver ER, Dancis A, Rea PA (2007) Functional characterization of AtATM1, AtATM2, and AtATM3, a subfamily of Arabidopsis half-molecule ATP-binding cassette transporters implicated in iron homeostasis. Journal of Biological Chemistry **282:** 21561-21571

Chen T, Cui P, Chen H, Ali S, Zhang S, Xiong L (2013) A KH-Domain RNA-Binding Protein Interacts with FIERY2/CTD Phosphatase-Like 1 and Splicing Factors and Is Important for Pre-mRNA Splicing in Arabidopsis. PLoS Genetics **9:** e1003875

Cheng L, Wang F, Shou H, Huang F, Zheng L, He F, Li J, Zhao F-J, Ueno D, Ma JF (2007) Mutation in nicotianamine aminotransferase stimulated the Fe (II) acquisition system and led to iron accumulation in rice. Plant Physiology **145:** 1647-1657

Cho H, Kim T-K, Mancebo H, Lane WS, Flores O, Reinberg D (1999) A protein phosphatase functions to recycle RNA polymerase II. Genes & Development **13:** 1540-1552

Chomczynski P, Sacchi N (1987) Single-step method of rna isolation by acid guanidinium thiocyanate phenol chloroform extraction. Analytical Biochemistry **162:** 156-159

Chou K-C, Shen H-B (2010) Plant-mPLoc: a top-down strategy to augment the power for predicting plant protein subcellular localization. PloS One **5:** e11335

Chu HH, Chiecko J, Punshon T, Lanzirotti A, Lahner B, Salt DE, Walker EL (2010) Successful reproduction requires the function of Arabidopsis Yellow Stripe-Like1 and Yellow Stripe-Like3 metal-nicotianamine transporters in both vegetative and reproductive structures. Plant Physiology **154:** 197-210

Clemens S (2006) Toxic metal accumulation, responses to exposure and mechanisms of tolerance in plants. Biochimie **88:** 1707-1719

Clemens S, Antosiewicz DM, Ward JM, Schachtman DP, Schroeder JI (1998) The plant cDNA LCT1 mediates the uptake of calcium and cadmium in yeast. Proceedings of the National Academy of Sciences **95:** 12043-12048

Clemens S, Kim EJ, Neumann D, Schroeder JI (1999) Tolerance to toxic metals by a gene family of phytochelatin synthases from plants and yeast. The EMBO Journal **18:** 3325-3333

Cobbett C, Goldsbrough P (2002) Phytochelatins and metallothioneins: roles in heavy metal detoxification and homeostasis. Annual review of plant biology **53:** 159-182

Cobbett CS (2000) Phytochelatins and their roles in heavy metal detoxification. Plant Physiology **123:** 825-832

Cobbett CS, May MJ, Howden R, Rolls B (1998) The glutathione‐deficient, cadmium‐sensitive mutant, cad2‐1, ofArabidopsis thalianais deficient in γ‐glutamylcysteine synthetase. The Plant Journal **16:** 73-78

Cohen CK, Fox TC, Garvin DF, Kochian LV (1998) The role of iron-deficiency stress responses in stimulating heavy-metal transport in plants. Plant Physiology **116:** 1063-1072

Cohen P (2002) The origins of protein phosphorylation. Nature Cell Biology **4:** E127-E130

Colangelo EP, Guerinot ML (2004) The essential basic helix-loop-helix protein FIT1 is required for the iron deficiency response. Plant Cell **16:** 3400-3412

Collet J-F, Stroobant V, Pirard M, Delpierre G, Van Schaftingen E (1998) A new class of phosphotransferases phosphorylated on an aspartate residue in an amino-terminal DXDX (T/V) motif. Journal of Biological Chemistry **273:** 14107-14112

Connolly EL, Campbell NH, Grotz N, Prichard CL, Guerinot ML (2003) Overexpression of the FRO2 ferric chelate reductase confers tolerance to growth on low iron and uncovers posttranscriptional control. Plant Physiology **133:** 1102-1110

Connolly EL, Fett JP, Guerinot ML (2002) Expression of the IRT1 metal transporter is controlled by metals at the levels of transcript and protein accumulation. Plant Cell **14:** 1347-1357

Conte S, Chu H, Rodriguez DC, Punshon T, Vasques K, Salt DE, Walker EL (2013) Arabidopsis thaliana Yellow Stripe1-Like4 and Yellow Stripe1-Like6 localize to internal cellular membranes and are involved in metal ion homeostasis. Frontiers in Plant Science **4**

Conte S, Stevenson D, Furner I, Lloyd A (2009) Multiple antibiotic resistance in Arabidopsis is conferred by mutations in a chloroplast-localized transport protein. Plant Physiology **151:** 559-573

Conte SS, Lloyd AM (2010) The MAR1 transporter is an opportunistic entry point for antibiotics. Plant Signaling & Behavior **5:** 49-52

Conte SS, Walker EL (2011) Transporters contributing to iron trafficking in plants. Molecular Plant **4:** 464-476

Corden JL (2013) RNA polymerase II C-terminal domain: Tethering transcription to transcript and template. Chemical Reviews **113:** 8423-8455

Cosio C, Martinoia E, Keller C (2004) Hyperaccumulation of cadmium and zinc in Thlaspi caerulescens and Arabidopsis halleri at the leaf cellular level. Plant Physiology **134:** 716-725

Curie C, Cassin G, Couch D, Divol F, Higuchi K, Jean M, Misson J, Schikora A, Czernic P, Mari S (2009) Metal movement within the plant: contribution of nicotianamine and yellow stripe 1-like transporters. Annals of Botany **103:** 1-11

Curie C, Panaviene Z, Loulergue C, Dellaporta SL, Briat J-F, Walker EL (2001) Maize yellow stripe1 encodes a membrane protein directly involved in Fe (III) uptake. Nature **409:** 346-349

Curie C, Panaviene Z, Loulergue C, Dellaporta SL, Briat JF, Walker EL (2001) Maize yellow stripe1 encodes a membrane protein directly involved in Fe(III) uptake. Nature **409:** 346-349

Czechowski T, Stitt M, Altmann T, Udvardi MK, Scheible WR (2005) Genome-wide identification and testing of superior reference genes for transcript normalization in Arabidopsis. Plant Physiology **139:** 5-17

DalCorso G, Farinati S, Maistri S, Furini A (2008) How plants cope with cadmium: Staking all on metabolism and gene expression. Journal of Integrative Plant Biology **50:** 1268-1280

DalCorso G, Manara A, Furini A (2013) An overview of heavy metal challenge in plants: from roots to shoots. Metallomics **5:** 1117-1132

Das P, Samantaray S, Rout G (1997) Studies on cadmium toxicity in plants: a review. Environmental Pollution **98:** 29-36

De S, Babu MM (2010) Genomic neighbourhood and the regulation of gene expression. Current Opinion in Cell Biology **22:** 326-333

Delhaize E, Gruber BD, Pittman JK, White RG, Leung H, Miao Y, Jiang L, Ryan PR, Richardson AE (2007) A role for the AtMTP11 gene of Arabidopsis in manganese transport and tolerance. The Plant Journal **51:** 198-210

DiDonato RJ, Jr., Roberts LA, Sanderson T, Eisley RB, Walker EL (2004) Arabidopsis Yellow Stripe-Like2 (YSL2): a metal-regulated gene encoding a plasma membrane transporter of nicotianamine-metal complexes. Plant Journal **39:** 403-414

Ding Z, Millar AJ, Davis AM, Davis SJ (2007) TIME FOR COFFEE encodes a nuclear regulator in the Arabidopsis thaliana circadian clock. The Plant Cell **19:** 1522-1536

Dinkel H, Michael S, Weatheritt RJ, Davey NE, Van Roey K, Altenberg B, Toedt G, Uyar B, Seiler M, Budd A (2012) ELM—the database of eukaryotic linear motifs. Nucleic Acids Research **40:** D242-D251

Dinneny JR, Long TA, Wang JY, Jung JW, Mace D, Pointer S, Barron C, Brady SM, Schiefelbein J, Benfey PN (2008) Cell identity mediates the response of Arabidopsis roots to abiotic stress. Science **320:** 942-945

Divol F, Couch D, Conejero G, Roschzttardtz H, Mari S, Curie C (2013) The Arabidopsis YELLOW STRIPE LIKE4 and 6 Transporters Control Iron Release from the Chloroplast. Plant Cell **25:** 1040-1055

Dräger DB, Desbrosses‐Fonrouge AG, Krach C, Chardonnens AN, Meyer RC, Saumitou‐Laprade P, Krämer U (2004) Two genes encoding Arabidopsis halleri MTP1 metal transport proteins co‐segregate with zinc tolerance and account for high MTP1 transcript levels. The Plant Journal **39:** 425-439

Driessen P, Deckers J, Spaargaren O, Nachtergaele F (2000) Lecture notes on the major soils of the world. Food and Agriculture Organization (FAO)

Duc C, Cellier F, Lobreaux S, Briat JF, Gaymard F (2009) Regulation of Iron Homeostasis in Arabidopsis thaliana by the Clock Regulator Time for Coffee. Journal of Biological Chemistry **284:** 36271-36281

Duffus JH (2002) " Heavy metals" a meaningless term?(IUPAC Technical Report). Pure and Applied Chemistry **74:** 793-807

Durrett TP, Gassmann W, Rogers EE (2007) The FRD3-mediated efflux of citrate into the root vasculature is necessary for efficient iron translocation. Plant Physiology **144:** 197-205

Duy D, Stube R, Wanner G, Philippar K (2011) The Chloroplast Permease PIC1 Regulates Plant Growth and Development by Directing Homeostasis and Transport of Iron. Plant Physiology **155:** 1709-1722

Duy D, Wanner G, Meda AR, von Wiren N, Soll J, Philippar K (2007) PIC1, an ancient permease in Arabidopsis chloroplasts, mediates iron transport. Plant Cell **19:** 986-1006

Ebbs S, Lau I, Ahner B, Kochian L (2002) Phytochelatin synthesis is not responsible for Cd tolerance in the Zn/Cd hyperaccumulator *Thlaspi caerulescens* (J. & C. Presl). Planta **214:** 635-640

Edgar RC (2004) MUSCLE: multiple sequence alignment with high accuracy and high throughput. Nucleic Acids Research **32:** 1792-1797

Egloff S, Dienstbier M, Murphy S (2012) Updating the RNA polymerase CTD code: adding gene-specific layers. Trends in Genetics **28:** 333-341

Egloff S, Murphy S (2008) Cracking the RNA polymerase II CTD code. Trends in Genetics **24:** 280-288

Egloff S, O'Reilly D, Chapman RD, Taylor A, Tanzhaus K, Pitts L, Eick D, Murphy S (2007) Serine-7 of the RNA polymerase II CTD is specifically required for snRNA gene expression. Science **318:** 1777-1779

Eide D, Broderius M, Fett J, Guerinot ML (1996) A novel iron-regulated metal transporter from plants identified by functional expression in yeast. Proc Natl Acad Sci U S A **93:** 5624-5628

Eisen MB, Spellman PT, Brown PO, Botstein D (1998) Cluster analysis and display of genome-wide expression patterns. Proceedings of the National Academy of Sciences of the United States of America **95:** 14863-14868

Ellis E (2006) Corrected Formulation for Spurr Low Viscosity Embedding Medium Using The Replacement Epoxide ERL 4221. Microscopy and Microanalysis **12:** 288-289

Eren E, Argüello JM (2004) Arabidopsis HMA2, a divalent heavy metal-transporting PIB-type ATPase, is involved in cytoplasmic Zn2+ homeostasis. Plant Physiology **136:** 3712-3723

Ernst WH (2006) Evolution of metal tolerance in higher plants. For Snow Landsc Res **80:** 251-274

Farrás R, Ferrando A, Jásik J, Kleinow T, Ökrész L, Tiburcio A, Salchert K, del Pozo C, Schell J, Koncz C (2001) SKP1–SnRK protein kinase interactions mediate proteasomal binding of a plant SCF ubiquitin ligase. The EMBO journal **20:** 2742-2756

Feng H, An F, Zhang S, Ji Z, Ling H-Q, Zuo J (2006) Light-regulated, tissue-specific, and cell differentiation-specific expression of the Arabidopsis Fe (III)-chelate reductase gene AtFRO6. Plant Physiology **140:** 1345-1354

Feng Y, Cao C-M, Vikram M, Park S, Kim HJ, Hong JC, Cisneros-Zevallos L, Koiwa H (2011) A Three-Component Gene Expression System and Its Application for Inducible Flavonoid Overproduction in Transgenic Arabidopsis thaliana. PloS One **6:** e17603

Feng Y, Kang JS, Kim S, Yun DJ, Lee SY, Bahk JD, Koiwa H (2010) Arabidopsis SCP1-like small phosphatases differentially dephosphorylate RNA polymerase II C-terminal domain. Biochemical and Biophysical Research Communications **397:** 355-360

Fergusson JE, Hayes RW, Yong TS, Thiew SH (1980) Heavy metal pollution by traffic in Christchurch, New Zealand: Lead and cadmium content of dust, soil and plant samples. NZJ Sci **23:** 293-310

Filatov V, Dowdle J, Smirnoff N, Ford‐Lloyd B, Newbury HJ, Macnair MR (2007) A quantitative trait loci analysis of zinc hyperaccumulation in Arabidopsis halleri. New Phytologist **174:** 580-590

Fuda NJ, Buckley MS, Wei W, Core LJ, Waters CT, Reinberg D, Lis JT (2012) Fcp1 dephosphorylation of the RNA polymerase II C-terminal domain is required for efficient transcription of heat shock genes. Molecular and Cellular Biology **32:** 3428-3437

Fujita Y, Fujita M, Satoh R, Maruyama K, Parvez MM, Seki M, Hiratsu K, Ohme-Takagi M, Shinozaki K, Yamaguchi-Shinozaki K (2005) AREB1 is a transcription activator of novel ABRE-dependent ABA signaling that enhances drought stress tolerance in Arabidopsis. Plant Cell **17:** 3470-3488

García-Hernández M, Murphy A, Taiz L (1998) Metallothioneins 1 and 2 have distinct but overlapping expression patterns in Arabidopsis. Plant Physiology **118:** 387-397

Garcia MJ, Lucena C, Romera FJ, Alcantara E, Perez-Vicente R (2010) Ethylene and nitric oxide involvement in the up-regulation of key genes related to iron acquisition and homeostasis in Arabidopsis. Journal of Experimental Botany **61:** 3885-3899

García MJ, Suárez V, Romera FJ, Alcántara E, Pérez-Vicente R (2011) A new model involving ethylene, nitric oxide and Fe to explain the regulation of Fe-acquisition genes in Strategy I plants. Plant Physiology and Biochemistry **49:** 537-544

Garrett RG (2000) Natural sources of metals to the environment. Human and Ecological Risk Assessment **6:** 945-963

Gendre D, Czernic P, Conéjéro G, Pianelli K, Briat JF, Lebrun M, Mari S (2007) TcYSL3, a member of the YSL gene family from the hyper‐accumulator Thlaspi caerulescens, encodes a nicotianamine‐Ni/Fe transporter. The Plant Journal **49:** 1-15

Ghosh A, Shuman S, Lima CD (2008) The Structure of Fcp1, an Essential RNA Polymerase II CTD Phosphatase. Molecular Cell **32:** 478-490

Goda H, Sasaki E, Akiyama K, Maruyama-Nakashita A, Nakabayashi K, Li WQ, Ogawa M, Yamauchi Y, Preston J, Aoki K, Kiba T, Takatsuto S, Fujioka S, Asami T, Nakano T, Kato H, Mizuno T, Sakakibara H, Yamaguchi S, Nambara E, Kamiya Y, Takahashi H, Hirai MY, Sakurai T, Shinozaki K, Saito K, Yoshida S, Shimada Y (2008) The AtGenExpress hormone and chemical treatment data set: experimental design, data evaluation, model data analysis and data access. Plant Journal **55:** 526-542

Goeres DC, Van Norman JM, Zhang W, Fauver NA, Spencer ML, Sieburth LE (2007) Components of the Arabidopsis mRNA decapping complex are required for early seedling development. Plant Cell **19:** 1549-1564

Gong JM, Lee DA, Schroeder JI (2003) Long-distance root-to-shoot transport of phytochelatins and cadmium in Arabidopsis. Proc Natl Acad Sci U S A **100:** 10118-10123

Goto F, Yoshihara T, Shigemoto N, Toki S, Takaiwa F (1999) Iron fortification of rice seed by the soybean ferritin gene. Nature Biotechnology **17:** 282-286

Green LS, Rogers EE (2004) FRD3 controls iron localization in Arabidopsis. Plant Physiology **136:** 2523-2531

Gregory BD, O'Malley RC, Lister R, Urich MA, Tonti-Filippini J, Chen H, Millar AH, Ecker JR (2008) A link between RNA metabolism and silencing affecting Arabidopsis development. Developmental Cell **14:** 854-866

Grill E, Löffler S, Winnacker E-L, Zenk MH (1989) Phytochelatins, the heavy-metal-binding peptides of plants, are synthesized from glutathione by a specific γ-glutamylcysteine dipeptidyl transpeptidase (phytochelatin synthase). Proceedings of the National Academy of Sciences **86:** 6838-6842

Gross J, Stein RJ, Fett-Neto AG, Fett JP (2003) Iron homeostasis related genes in rice. Genetics and Molecular Biology **26:** 477-497

Grotz N, Guerinot ML (2006) Molecular aspects of Cu, Fe and Zn homeostasis in plants. Biochimica Et Biophysica Acta-Molecular Cell Research **1763:** 595-608

Guan Q, Wen C, Zeng H, Zhu J (2013) A KH domain-containing putative RNA-binding protein is critical for heat stress-responsive gene regulation and thermotolerance in Arabidopsis. Molecular Plant **6:** 386-395

Guan Q, Yue X, Zeng H, Zhu J (2014) The Protein Phosphatase RCF2 and Its Interacting Partner NAC019 Are Critical for Heat Stress–Responsive Gene Regulation and Thermotolerance in Arabidopsis. The Plant Cell tpc. 113.118927

Guerinot ML (2010) Iron. *In* R Hell, R-R Mendel, eds, Cell Biology of Metals and Nutrients. Springer Science, pp 75-94

Guerinot ML, Yi Y (1994) Iron: Nutritious, Noxious, and Not Readily Available. Plant Physiology **104:** 815-820

Ha S-B, Smith AP, Howden R, Dietrich WM, Bugg S, O'Connell MJ, Goldsbrough PB, Cobbett CS (1999) Phytochelatin synthase genes from Arabidopsis and the yeast Schizosaccharomyces pombe. The Plant Cell **11:** 1153-1163

Hajheidari M, Koncz C, Eick D (2013) Emerging roles for RNA polymerase II CTD in Arabidopsis. Trends in Plant Science

Hall A, Bastow RM, Davis SJ, Hanano S, McWatters HG, Hibberd V, Doyle MR, Sung S, Halliday KJ, Amasino RM (2003) The TIME FOR COFFEE gene maintains the amplitude and timing of Arabidopsis circadian clocks. The Plant Cell **15:** 2719-2729

Haney CJ, Grass G, Franke S, Rensing C (2005) New developments in the understanding of the cation diffusion facilitator family. Journal of Industrial Microbiology and Biotechnology **32:** 215-226

Hanikenne M, Talke IN, Haydon MJ, Lanz C, Nolte A, Motte P, Kroymann J, Weigel D, Krämer U (2008) Evolution of metal hyperaccumulation required cis-regulatory changes and triplication of HMA4. Nature **453:** 391-395

Hanson B, Garifullina GF, Lindblom SD, Wangeline A, Ackley A, Kramer K, Norton AP, Lawrence CB, Pilon‐Smits EA (2003) Selenium accumulation protects Brassica juncea from invertebrate herbivory and fungal infection. New Phytologist **159:** 461-469

Hart JJ, Welch RM, Norvell WA, Sullivan LA, Kochian LV (1998) Characterization of cadmium binding, uptake, and translocation in intact seedlings of bread and durum wheat cultivars. Plant Physiology **116:** 1413-1420

Hauser M, Donhardt AM, Barnes D, Naider F, Becker JM (2000) Enkephalins are transported by a novel eukaryotic peptide uptake system. Journal of Biological Chemistry **275:** 3037-3041

Hauser M, Narita V, Donhardt AM, Naider F, Becker JM (2001) Multiplicity and regulation of genes encoding peptide transporters in Saccharomyces cerevisiae. Molecular Membrane Biology **18:** 105-112

Hausmann S, Shuman S (2002) Characterization of the CTD Phosphatase Fcp1 from Fission Yeast PREFERENTIAL DEPHOSPHORYLATION OF SERINE 2 VERSUSSERINE 5. Journal of Biological Chemistry **277:** 21213-21220

Haydon MJ, Cobbett CS (2007) A novel major facilitator superfamily protein at the tonoplast influences zinc tolerance and accumulation in Arabidopsis. Plant Physiology **143:** 1705-1719

Haydon MJ, Kawachi M, Wirtz M, Hillmer S, Hell R, Kramer U (2012) Vacuolar Nicotianamine Has Critical and Distinct Roles under Iron Deficiency and for Zinc Sequestration in Arabidopsis. Plant Cell **24:** 724-737

Heazlewood JL, Tonti-Filippini JS, Gout AM, Day DA, Whelan J, Millar AH (2004) Experimental analysis of the Arabidopsis mitochondrial proteome highlights signaling and regulatory components, provides assessment of targeting prediction programs, and indicates plant-specific mitochondrial proteins. The Plant Cell **16:** 241-256

Heazlewood JL, Verboom RE, Tonti-Filippini J, Small I, Millar AH (2007) SUBA: the Arabidopsis subcellular database. Nucleic acids research **35:** D213-D218

Hell R, Stephan UW (2003) Iron uptake, trafficking and homeostasis in plants. Planta **216:** 541-551

Henriques R, Jasik J, Klein M, Martinoia E, Feller U, Schell J, Pais MS, Koncz C (2002) Knock-out of Arabidopsis metal transporter gene IRT1 results in iron deficiency accompanied by cell differentiation defects. Plant Molecular Biology **50:** 587-597

Higuchi K, Nishizawa N, Römheld V, Marschner H, Mori S (1996) Absence of nicotianamine synthase activity in the tomato mutant 'chloronerva'. Journal of Plant Nutrition **19:** 1235-1239

Higuchi K, Suzuki K, Nakanishi H, Yamaguchi H, Nishizawa N-K, Mori S (1999) Cloning of nicotianamine synthase genes, novel genes involved in the biosynthesis of phytosiderophores. Plant Physiology **119:** 471-480

Hintermair C, Heidemann M, Koch F, Descostes N, Gut M, Gut I, Fenouil R, Ferrier P, Flatley A, Kremmer E (2012) Threonine‐4 of mammalian RNA polymerase II CTD is targeted by Polo‐like kinase 3 and required for transcriptional elongation. The EMBO Journal **31:** 2784-2797

Hirsch J, Marin E, Floriani M, Chiarenza S, Richaud P, Nussaume L, Thibaud MC (2006) Phosphate deficiency promotes modification of iron distribution in Arabidopsis plants. Biochimie **88:** 1767-1771

Hirschi KD, Korenkov VD, Wilganowski NL, Wagner GJ (2000) Expression of Arabidopsis CAX2 in tobacco. Altered metal accumulation and increased manganese tolerance. Plant Physiology **124:** 125-134

Hofstetter SS, Dudnik A, Widmer H, Dudler R (2013) Arabidopsis YELLOW STRIPE-LIKE7 (YSL7) and YSL8 Transporters Mediate Uptake of Pseudomonas Virulence Factor Syringolin A into Plant Cells. Molecular Plant-Microbe Interactions **26:** 1302-1311

Höglund A, Dönnes P, Blum T, Adolph H-W, Kohlbacher O (2006) MultiLoc: prediction of protein subcellular localization using N-terminal targeting sequences, sequence motifs and amino acid composition. Bioinformatics **22:** 1158-1165

Horton P, Park K-J, Obayashi T, Fujita N, Harada H, Adams-Collier C, Nakai K (2007) WoLF PSORT: protein localization predictor. Nucleic Acids Research **35:** W585-W587

Howden R, Goldsbrough PB, Andersen CR, Cobbett CS (1995) Cadmium-sensitive, cad1 mutants of Arabidopsis thaliana are phytochelatin deficient. Plant Physiology **107:** 1059-1066

Hsin J-P, Manley JL (2012) The RNA polymerase II CTD coordinates transcription and RNA processing. Genes & Development **26:** 2119-2137

Hsin J-P, Sheth A, Manley JL (2011) RNAP II CTD phosphorylated on threonine-4 is required for histone mRNA 3′ end processing. Science **334:** 683-686

Hu YT, Ming F, Chen WW, Yan JY, Xu ZY, Li GX, Xu CY, Yang JL, Zheng SJ (2012) TcOPT3, a Member of Oligopeptide Transporters from the Hyperaccumulator Thlaspi caerulescens, Is a Novel Fe/Zn/Cd/Cu Transporter. PloS One **7:** e38535

Hubbard KE, Nishimura N, Hitomi K, Getzoff ED, Schroeder JI (2010) Early abscisic acid signal transduction mechanisms: newly discovered components and newly emerging questions. Genes Development **24:** 1695-1708

Hussain D, Haydon MJ, Wang Y, Wong E, Sherson SM, Young J, Camakaris J, Harper JF, Cobbett CS (2004) P-type ATPase heavy metal transporters with roles in essential zinc homeostasis in Arabidopsis. The Plant Cell **16:** 1327-1339

Inoue H, Kobayashi T, Nozoye T, Takahashi M, Kakei Y, Suzuki K, Nakazono M, Nakanishi H, Mori S, Nishizawa NK (2009) Rice OsYSL15 is an iron-regulated iron (III)-deoxymugineic acid transporter expressed in the roots and is essential for iron uptake in early growth of the seedlings. Journal of Biological Chemistry **284:** 3470-3479

Irizarry RA, Bolstad BM, Collin F, Cope LM, Hobbs B, Speed TP (2003) Summaries of affymetrix GeneChip probe level data. Nucleic Acids Research **31**

Isel C, Karn J (1999) Direct evidence that HIV-1 Tat stimulates RNA polymerase II carboxyl-terminal domain hyperphosphorylation during transcriptional elongation. Journal of Molecular Biology **290:** 929-941

Ishimaru Y, Kim S, Tsukamoto T, Oki H, Kobayashi T, Watanabe S, Matsuhashi S, Takahashi M, Nakanishi H, Mori S (2007) Mutational reconstructed ferric chelate reductase confers enhanced tolerance in rice to iron deficiency in calcareous soil. Proceedings of the National Academy of Sciences **104:** 7373-7378

Ishimaru Y, Suzuki M, Tsukamoto T, Suzuki K, Nakazono M, Kobayashi T, Wada Y, Watanabe S, Matsuhashi S, Takahashi M (2006) Rice plants take up iron as an Fe3+ - phytosiderophore and as Fe2+. The Plant Journal **45:** 335-346

Itai R, Suzuki K, Yamaguchi H, Nakanishi H, Nishizawa NK, Yoshimura E, Mori S (2000) Induced activity of adenine phosphoribosyltransferase (APRT) in iron - deficient barley roots: a possible role for phytosiderophore production. Journal of Experimental Botany **51:** 1179-1188

Ivanov R, Brumbarova T, Bauer P (2012) Fitting into the harsh reality: regulation of iron-deficiency responses in dicotyledonous plants. Molecular Plant **5:** 27-42

Jakoby M, Wang HY, Reidt W, Weisshaar B, Bauer P (2004) FRU (BHLH029) is required for induction of iron mobilization genes in Arabidopsis thaliana. FEBS Letters **577:** 528-534

Jean ML, Schikora A, Mari S, Briat JF, Curie C (2005) A loss - of - function mutation in AtYSL1 reveals its role in iron and nicotianamine seed loading. The Plant Journal **44:** 769-782

Jeong IS, Aksoy E, Fukudome A, Akhter S, Hiraguri A, Fukuhara T, Bahk JD, Koiwa H (2013) Arabidopsis C-Terminal Domain Phosphatase-Like 1 functions in miRNA accumulation and DNA methylation. PloS One **8:** e74739

Jeong IS, Fukudome A, Aksoy E, Bang WY, Kim S, Guan Q, Bahk JD, May KA, Russell WK, Zhu J (2013) Regulation of Abiotic Stress Signalling by Arabidopsis C-Terminal Domain Phosphatase-Like 1 Requires Interaction with a K-Homology Domain-Containing Protein. PloS One **8:** e80509

Jeong J, Cohu C, Kerkeb L, Pilon M, Connolly EL, Guerinot ML (2008) Chloroplast Fe (III) chelate reductase activity is essential for seedling viability under iron limiting conditions. Proceedings of the National Academy of Sciences **105:** 10619-10624

Jeong J, Connolly EL (2009) Iron uptake mechanisms in plants: Functions of the FRO family of ferric reductases. Plant Science **176:** 709-714

Ji H, Kim SR, Kim YH, Kim H, Eun MY, Jin ID, Cha YS, Yun DW, Ahn BO, Lee MC (2010) Inactivation of the CTD phosphatase‐like gene OsCPL1 enhances the development of the abscission layer and seed shattering in rice. The Plant Journal **61:** 96-106

Jiang J, Wang B, Shen Y, Wang H, Feng Q, Shi H (2013) The Arabidopsis RNA Binding Protein with K Homology Motifs, SHINY1, Interacts with the C-terminal Domain Phosphatase-like 1 (CPL1) to Repress Stress-Inducible Gene Expression. PLoS Genetics **9:** e1003625

Jiang R, Ma D, Zhao F, McGrath S (2005) Cadmium hyperaccumulation protects Thlaspi caerulescens from leaf feeding damage by thrips (Frankliniella occidentalis). New Phytologist **167:** 805-814

Jin YM, Jung J, Jeon H, Won SY, Feng Y, Kang JS, Lee SY, Cheong JJ, Koiwa H, Kim M (2011) AtCPL5, a novel Ser‐2‐specific RNA polymerase II C‐terminal domain phosphatase, positively regulates ABA and drought responses in Arabidopsis. New Phytologist **190:** 57-74

Johns S, Speth R (2010) TOPO2, Transmembrane protein display software. *In*,

Johnson AA, Kyriacou B, Callahan DL, Carruthers L, Stangoulis J, Lombi E, Tester M (2011) Constitutive overexpression of the OsNAS gene family reveals single-gene strategies for effective iron-and zinc-biofortification of rice endosperm. PLoS One **6:** e24476

Kang J, Park J, Choi H, Burla B, Kretzschmar T, Lee Y, Martinoia E (2011) Plant ABC transporters. The Arabidopsis Book/American Society of Plant Biologists **9:** 1-25

Kennelly P (2003) Archaeal protein kinases and protein phosphatases: insights from genomics and biochemistry. Biochemistry J **370:** 373-389

Kerk D, Templeton G, Moorhead GBG (2008) Evolutionary radiation pattern of novel protein phosphatases revealed by analysis of protein data from the completely sequenced genomes of humans, green algae, and higher plants. Plant Physiology **146:** 351-367

Kerkeb L, Mukherjee I, Chatterjee I, Lahner B, Salt DE, Connolly EL (2008) Iron-induced turnover of the Arabidopsis IRON-REGULATED TRANSPORTER1 metal transporter requires lysine residues. Plant Physiology **146:** 1964-1973

Kilian J, Whitehead D, Horak J, Wanke D, Weinl S, Batistic O, D'Angelo C, Bornberg-Bauer E, Kudla J, Harter K (2007) The AtGenExpress global stress expression data set: protocols, evaluation and model data analysis of UV-B light, drought and cold stress responses. Plant Journal **50:** 347-363

Kim D-Y, Bovet L, Kushnir S, Noh EW, Martinoia E, Lee Y (2006) AtATM3 is involved in heavy metal resistance in Arabidopsis. Plant Physiology **140:** 922-932

Kim D, Gustin JL, Lahner B, Persans MW, Baek D, Yun DJ, Salt DE (2004) The plant CDF family member TgMTP1 from the Ni/Zn hyperaccumulator Thlaspi goesingense acts to enhance efflux of Zn at the plasma membrane when expressed in Saccharomyces cerevisiae. The Plant Journal **39:** 237-251

Kim DY, Bovet L, Maeshima M, Martinoia E, Lee Y (2007) The ABC transporter AtPDR8 is a cadmium extrusion pump conferring heavy metal resistance. The Plant Journal **50:** 207-218

Kim S, Ponka P (2003) Role of nitric oxide in cellular iron metabolism. Biometals **16:** 125-135

Kim S, Takahashi M, Higuchi K, Tsunoda K, Nakanishi H, Yoshimura E, Mori S, Nishizawa NK (2005) Increased nicotianamine biosynthesis confers enhanced tolerance of high levels of metals, in particular nickel, to plants. Plant and Cell Physiology **46:** 1809-1818

Kim SA, Guerinot ML (2007) Mining iron: Iron uptake and transport in plants. Febs Letters **581:** 2273-2280

Kim SA, Punshon T, Lanzirotti A, Li LT, Alonso JM, Ecker JR, Kaplan J, Guerinot ML (2006) Localization of iron in Arabidopsis seed requires the vacuolar membrane transporter VIT1. Science **314:** 1295-1298

Klatte M, Schuler M, Wirtz M, Fink-Straube C, Hell R, Bauer P (2009) The Analysis of Arabidopsis Nicotianamine Synthase Mutants Reveals Functions for Nicotianamine in Seed Iron Loading and Iron Deficiency Responses. Plant Physiology **150:** 257-271

Kobae Y, Uemura T, Sato MH, Ohnishi M, Mimura T, Nakagawa T, Maeshima M (2004) Zinc transporter of Arabidopsis thaliana AtMTP1 is localized to vacuolar membranes and implicated in zinc homeostasis. Plant and Cell Physiology **45:** 1749-1758

Kobayashi T, Itai RN, Ogo Y, Kakei Y, Nakanishi H, Takahashi M, Nishizawa NK (2009) The rice transcription factor IDEF1 is essential for the early response to iron deficiency, and induces vegetative expression of late embryogenesis abundant genes. The Plant Journal **60:** 948-961

Kobayashi T, Itai RN, Ogo Y, Kakei Y, Nakanishi H, Takahashi M, Nishizawa NK (2009) The rice transcription factor IDEF1 is essential for the early response to iron deficiency, and induces vegetative expression of late embryogenesis abundant genes. Plant Journal **60:** 948-961

Kobayashi T, Nakanishi H, Nishizawa NK (2010) Dual regulation of iron deficiency response mediated by the transcription factor IDEF1. Plant Signaling & Behavior **5:** 157-159

Kobayashi T, Nakanishi H, Nishizawa NK (2010) Recent insights into iron homeostasis and their application in graminaceous crops. Proceedings of the Japan Academy Series B-Physical and Biological Sciences **86:** 900-913

Kobayashi T, Nakanishi H, Takahashi M, Kawasaki S, Nishizawa N-K, Mori S (2001) In vivo evidence that Ids3 from Hordeum vulgare encodes a dioxygenase that converts 2′ -deoxymugineic acid to mugineic acid in transgenic rice. Planta **212:** 864-871

Kobayashi T, Nakayama Y, Itai RN, Nakanishi H, Yoshihara T, Mori S, Nishizawa NK (2003) Identification of novel cis-acting elements, IDE1 and IDE2, of the barley IDS2 gene promoter conferring iron-deficiency-inducible, root-specific expression in heterogeneous tobacco plants. Plant Journal **36:** 780-793

Kobayashi T, Nishizawa NK (2012) Iron uptake, translocation, and regulation in higher plants. Annual Review of Plant Biology **63:** 131-152

Kobayashi T, Suzuki M, Inoue H, Itai RN, Takahashi M, Nakanishi H, Mori S, Nishizawa NK (2005) Expression of iron-acquisition-related genes in iron-deficient rice is co-ordinately induced by partially conserved iron-deficiency-responsive elements. Journal of Experimental Botany **56:** 1305-1316

Kobor MS, Archambault J, Lester W, Holstege FC, Gileadi O, Jansma DB, Jennings EG, Kouyoumdjian F, Davidson AR, Young RA (1999) An Unusual Eukaryotic Protein Phosphatase Required for Transcription by RNA Polymerase II and CTD Dephosphorylation in S. cerevisiae. Molecular Cell **4:** 55-62

Koh S, Wiles AM, Sharp JS, Naider FR, Becker JM, Stacey G (2002) An oligopeptide transporter gene family in Arabidopsis. Plant Physiology **128:** 21-29

Koike S, Inoue H, Mizuno D, Takahashi M, Nakanishi H, Mori S, Nishizawa NK (2004) OsYSL2 is a rice metal‐nicotianamine transporter that is regulated by iron and expressed in the phloem. The Plant Journal **39:** 415-424

Koiwa H (2006) Phosphorylation of RNA polymerase II C-terminal domain and plant osmotic-stress responses. *In* Abiotic stress tolerance in plants. Springer, pp 47-57

Koiwa H, Barb AW, Xiong L, Li F, McCully MG, Lee B-h, Sokolchik I, Zhu J, Gong Z, Reddy M (2002) C-terminal domain phosphatase-like family members (AtCPLs) differentially regulate Arabidopsis thaliana abiotic stress signaling, growth, and development. Proceedings of the National Academy of Sciences **99:** 10893-10898

Koiwa H, Barb AW, Xiong L, Li F, McCully MG, Lee B-h, Sokolchik I, Zhu J, Gong Z, Reddy M, Sharkhuu A, Manabe Y, Yokoi S, Zhu J-K, Bressan RA, Hasegawa PM (2002) C-terminal domain phosphatase-like family members (AtCPLs) differentially regulate *Arabidopsis thaliana* abiotic stress signaling, growth, and development. Proc Natl Acad Sci U S A **99:** 10893-10898

Koiwa H, Barb, AW, Xiong, L, Li, F, McCully, MG, Lee, B-h, Sokolchik, I, Zhu, J, Gong, Z, Reddy, M, Altanbadralt, S, Yuzuki, M, Shuji, Y, Jian-Kang, Z, Ray, A. B, Paul, M. H (2002) C-terminal domain phosphatase-like family members (AtCPLs) differentially regulate *Arabidopsis thaliana* abiotic stress signaling, growth, and development. Proceedings of the National Academy of Sciences of the United States of America **99:** 10893–10898

Koiwa H, Hausmann S, Bang WY, Ueda A, Kondo N, Hiraguri A, Fukuhara T, Bahk JD, Yun D-J, Bressan RA (2004) Arabidopsis C-terminal domain phosphatase-like 1 and 2 are essential Ser-5-specific C-terminal domain phosphatases. Proceedings of the National Academy of Sciences of the United States of America **101:** 14539-14544

Koiwa H, Hausmann S, Bang WY, Ueda A, Kondo N, Hiraguri A, Fukuhara T, Bahk JD, Yun DJ, Bressan RA, Hasegawa PM, Shuman S (2004) Arabidopsis C-terminal domain phosphatase-like 1 and 2 are essential Ser-5-specific C-terminal domain phosphatases. Proc Natl Acad Sci U S A **101:** 14539-14544

Kong WW, Yang ZM (2010) Identification of iron-deficiency responsive microRNA genes and cis-elements in Arabidopsis. Plant Physiology And Biochemistry **48:** 153-159

Koren'kov V, Park S, Cheng N-H, Sreevidya C, Lachmansingh J, Morris J, Hirschi K, Wagner G (2007) Enhanced Cd2+-selective root-tonoplast-transport in tobaccos expressing Arabidopsis cation exchangers. Planta **225:** 403-411

Korenkov V, Hirschi K, Crutchfield JD, Wagner GJ (2007) Enhancing tonoplast Cd/H antiport activity increases Cd, Zn, and Mn tolerance, and impacts root/shoot Cd partitioning in Nicotiana tabacum L. Planta **226:** 1379-1387

Korshunova YO, Eide D, Clark WG, Guerinot ML, Pakrasi HB (1999) The IRT1 protein from Arabidopsis thaliana is a metal transporter with a broad substrate range. Plant Molecular Biology **40:** 37-44

Krämer U, Talke IN, Hanikenne M (2007) Transition metal transport. FEBS Letters **581:** 2263-2272

Kreps JA, Wu YJ, Chang HS, Zhu T, Wang X, Harper JF (2002) Transcriptome changes for Arabidopsis in response to salt, osmotic, and cold stress. Plant Physiology **130:** 2129-2141

Kruger C, Berkowitz O, Stephan UW, Hell R (2002) A metal-binding member of the late embryogenesis abundant protein family transports iron in the phloem of Ricinus communis L. Journal of Biological Chemistry **277:** 25062-25069

Kuhn JM, Schroeder JI (2003) Impacts of altered RNA metabolism on abscisic acid signaling. Curr Opin Plant Biol **6:** 463-469

Küpper H, Lombi E, Zhao F-J, McGrath SP (2000) Cellular compartmentation of cadmium and zinc in relation to other elements in the hyperaccumulator Arabidopsis halleri. Planta **212:** 75-84

Küpper H, Mijovilovich,A.,Meyer-Klaucke,W.,andKroneck,P. M. H. (2004) Tissue- and age-dependent differences in the complexation of cadmium and zinc in the Cd/Zn hyperaccumulator Thlaspi caerulescens (Gangeseco-type) revealed by X-ray absorption spectroscopy. Plant Physiology **134:** 748-757

Kushnir S, Babiychuk E, Storozhenko S, Davey MW, Papenbrock J, De Rycke R, Engler G, Stephan UW, Lange H, Kispal G (2001) A mutation of the mitochondrial ABC transporter Sta1 leads to dwarfism and chlorosis in the Arabidopsis mutant starik. The Plant Cell Online **13:** 89-100

Lan P, Li WF, Wen TN, Shiau JY, Wu YC, Lin WD, Schmidt W (2011) iTRAQ Protein Profile Analysis of Arabidopsis Roots Reveals New Aspects Critical for Iron Homeostasis. Plant Physiology **155:** 821-834

Lan P, Schmidt W (2011) The enigma of eIF5A in the iron deficiency response of Arabidopsis. Plant Signaling & Behavior **6:** 528-530

Lane TW, Saito MA, George GN, Pickering IJ, Prince RC, Morel FM (2005) Biochemistry: a cadmium enzyme from a marine diatom. Nature **435:** 42-42

Lanquar V, Lelièvre F, Bolte S, Hamès C, Alcon C, Neumann D, Vansuyt G, Curie C, Schröder A, Krämer U (2005) Mobilization of vacuolar iron by AtNRAMP3 and AtNRAMP4 is essential for seed germination on low iron. The EMBO Journal **24:** 4041-4051

Le SQ, Gascuel O (2008) An improved general amino acid replacement matrix. Molecular Biology And Evolution **25:** 1307-1320

Lee S, Chiecko JC, Kim SA, Walker EL, Lee Y, Guerinot ML, An G (2009) Disruption of OsYSL15 Leads to Iron Inefficiency in Rice Plants. Plant Physiology **150:** 786-800

Lee S, Jeon US, Lee SJ, Kim YK, Persson DP, Husted S, Schjorring JK, Kakei Y, Masuda H, Nishizawa NK, An G (2009) Iron fortification of rice seeds through activation of the nicotianamine synthase gene. Proceedings of the National Academy of Sciences of the United States of America **106:** 22014-22019

Lee S, Kim Y-Y, Lee Y, An G (2007) Rice P1B-type heavy-metal ATPase, OsHMA9, is a metal efflux protein. Plant Physiology **145:** 831-842

Lee S, Ryoo N, Jeon J-S, Guerinot ML, An G (2012) Activation of rice Yellow Stripe1-Like 16 (OsYSL16) enhances iron efficiency. Molecules and Cells **33:** 117-126

Leitenmaier B, Kuepper H (2011) Cadmium uptake and sequestration kinetics in individual leaf cell protoplasts of the Cd/Zn hyperaccumulator Thlaspi caerulescens. Plant Cell and Environment **34:** 208-219

Leitenmaier B, Küpper H (2013) Compartmentation and complexation of metals in hyperaccumulator plants. Frontiers In Plant Science **4**

Lewis MW, Leslie ME, Liljegren SJ (2006) Plant separation: 50 ways to leave your mother. Current Opinion In Plant Biology **9:** 59-65

Li L, Chen OS, Ward DM, Kaplan J (2001) CCC1 is a transporter that mediates vacuolar iron storage in yeast. Journal of Biological Chemistry **276:** 29515-29519

Li L, Cheng X, Ling H-Q (2004) Isolation and characterization of Fe (III)-chelate reductase gene LeFRO1 in tomato. Plant Molecular Biology **54:** 125-136

Li W, Santi S, Tan C, W. S (2007) Dissecting P-type H+-ATPase-mediated proton extrusion in Arabidopsis. *In* 18th International Conference on Arabidopsis Research, Beijing, China

Li W, Schmidt W (2010) A lysine-63-linked ubiquitin chain-forming conjugase, UBC13, promotes the developmental responses to iron deficiency in Arabidopsis roots. Plant Journal **62:** 330-343

Li YH, Lee KK, Walsh S, Smith C, Hadingham S, Sorefan K, Cawley G, Bevan MW (2006) Establishing glucose- and ABA-regulated transcription networks in Arabidopsis by microarray analysis and promoter classification using a Relevance Vector Machine. Genome Research **16:** 414-427

Lichtenthaler HK (1987) Chlorophylls and carotenoids: Pigments of photosynthetic biomembranes. Methods in Enzymology **148:** 350-382

Lin Y-F, Aarts MG (2012) The molecular mechanism of zinc and cadmium stress response in plants. Cellular and Molecular Life Sciences **69:** 3187-3206

Lin YF, Aarts MGM (2012) The molecular mechanism of zinc and cadmium stress response in plants. Cellular and Molecular Life Sciences**:** 1-20

Ling HQ, Bauer P, Bereczky Z, Keller B, Ganal M (2002) The tomato fer gene encoding a bHLH protein controls iron-uptake responses in roots. Proceedings of the National Academy of Sciences of the United States of America **99:** 13938-13943

Lingam S, Mohrbacher J, Brumbarova T, Potuschak T, Fink-Straube C, Blondet E, Genschik P, Bauer P (2011) Interaction between the bHLH Transcription Factor FIT and ETHYLENE INSENSITIVE3/ETHYLENE INSENSITIVE3-LIKE1 Reveals Molecular Linkage between the Regulation of Iron Acquisition and Ethylene Signaling in Arabidopsis. Plant Cell **23:** 1815-1829

Liu T, Zeng J, Xia K, Fan T, Li Y, Wang Y, Xu X, Zhang M (2012) Evolutionary expansion and functional diversification of oligopeptide transporter gene family in rice. Rice **5:** 1-14

Liu Y, Moran D (2006) Do new functions arise by gene duplication. Journal of Creation **20:** 82-89

Lobreaux S, Briat J-Fo (1991) Ferritin accumulation and degradation in different organs of pea (Pisum sativum) during development. Biochem. J **274:** 601-606

Lochlainn SÓ, Bowen HC, Fray RG, Hammond JP, King GJ, White PJ, Graham NS, Broadley MR (2011) Tandem quadruplication of HMA4 in the zinc (Zn) and cadmium (Cd) hyperaccumulator Noccaea caerulescens. PloS One **6:** e17814

Long TA, Tsukagoshi H, Busch W, Lahner B, Salt DE, Benfey PN (2010) The bHLH transcription factor POPEYE regulates response to iron deficiency in Arabidopsis roots. Plant Cell **22:** 2219-2236

Lorković ZJ, Hilscher J, Barta A (2008) Co-localisation studies of Arabidopsis SR splicing factors reveal different types of speckles in plant cell nuclei. Experimental Cell Research **314:** 3175-3186

Lubkowitz M (2006) The OPT family functions in long-distance peptide and metal transport in plants. *In* Genetic engineering. Springer, pp 35-55

Lubkowitz M (2011) The oligopeptide transporters: a small gene family with a diverse group of substrates and functions? Molecular Plant **4:** 407-415

Lubkowitz MA, Barnes D, Breslav M, Burchfield A, Naider F, Becker JM (1998) Schizosaccharomyces pombe isp4 encodes a transporter representing a novel family of oligopeptide transporters. Molecular Microbiology **28:** 729-741

Lubkowitz MA, Hauser L, Breslav M, Naider F, Becker JM (1997) An oligopeptide transport gene from Candida albicans. Microbiology **143:** 387-396

Lucena C, Waters BM, Romera FJ, García MJ, Morales M, Alcántara E, Pérez-Vicente R (2006) Ethylene could influence ferric reductase, iron transporter, and H+-ATPase gene expression by affecting FER (or FER-like) gene activity. Journal of Experimental Botany **57:** 4145-4154

Ma JF, Shinada T, Matsuda C, Nomoto K (1995) Biosynthesis of phytosiderophores, mugineic acids, associated with methionine cycling. Journal of Biological Chemistry **270:** 16549-16554

Ma JF, Taketa S, Chang Y-C, Iwashita T, Matsumoto H, Takeda K, Nomoto K (1999) Genes controlling hydroxylations of phytosiderophores are located on different chromosomes in barley (Hordeum vulgare L.). Planta **207:** 590-596

Manavella PA, Hagmann J, Ott F, Laubinger S, Franz M, Macek B, Weigel D (2012) Fast-forward genetics identifies plant CPL phosphatases as regulators of miRNA processing factor HYL1. Cell **151:** 859-870

Marschner H, Marschner P (1995) Mineral Nutrition of Higher Plants, Ed 2nd Edition. Academic Press, Boston

Marschner H, Marschner P (2011) Marschner's mineral nutrition of higher plants, Vol 89. Elsevier

Marschner H, Romheld V (1994) STRATEGIES OF PLANTS FOR ACQUISITION OF IRON. Plant and Soil **165:** 261-274

Masuda H, Usuda K, Kobayashi T, Ishimaru Y, Kakei Y, Takahashi M, Higuchi K, Nakanishi H, Mori S, Nishizawa NK (2009) Overexpression of the barley nicotianamine synthase gene HvNAS1 increases iron and zinc concentrations in rice grains. Rice **2:** 155-166

Matsuda O, Sakamoto H, Nakao Y, Oda K, Iba K (2009) CTD phosphatases in the attenuation of wound-induced transcription of jasmonic acid biosynthetic genes in Arabidopsis. Plant Journal **57:** 96-108

Mayer A, Heidemann M, Lidschreiber M, Schreieck A, Sun M, Hintermair C, Kremmer E, Eick D, Cramer P (2012) CTD tyrosine phosphorylation impairs termination factor recruitment to RNA polymerase II. Science **336:** 1723-1725

McBride MB, Richards BK, Steenhuis T, Russo JJ, Sauvé S (1997) Mobility and solubility of toxic metals and nutrients in soil fifteen years after sludge application. Soil Science **162:** 487-500

Mei H, Cheng NH, Zhao J, Park S, Escareno RA, Pittman JK, Hirschi KD (2009) Root development under metal stress in Arabidopsis thaliana requires the H+/cation antiporter CAX4. New Phytologist **183:** 95-105

Meiser J, Lingam S, Bauer P (2011) Posttranslational regulation of the iron deficiency basic helix-loop-helix transcription factor FIT is affected by iron and nitric oxide. Plant Physiology **157:** 2154-2166

Meyer C-L, Peisker D, Courbot M, Craciun AR, Cazalé A-C, Desgain D, Schat H, Clemens S, Verbruggen N (2011) Isolation and characterization of Arabidopsis halleri and Thlaspi caerulescens phytochelatin synthases. Planta **234:** 83-95

Mijovilovich A, Leitenmaier B, Meyer-Klaucke W, Kroneck PM, Götz B, Küpper H (2009) Complexation and toxicity of copper in higher plants. II. Different mechanisms for copper versus cadmium detoxification in the copper-sensitive cadmium/zinc hyperaccumulator Thlaspi caerulescens (Ganges ecotype). Plant Physiology **151:** 715-731

Mills RF, Francini A, Ferreira da Rocha PS, Baccarini PJ, Aylett M, Krijger GC, Williams LE (2005) The plant P 1B-type ATPase AtHMA4 transports Zn and Cd and plays a role in detoxification of transition metals supplied at elevated levels. FEBS Letters **579:** 783-791

Mills RF, Krijger GC, Baccarini PJ, Hall J, Williams LE (2003) Functional expression of AtHMA4, a P1B‐type ATPase of the Zn/Co/Cd/Pb subclass. The Plant Journal **35:** 164-176

Miyadate H, Adachi S, Hiraizumi A, Tezuka K, Nakazawa N, Kawamoto T, Katou K, Kodama I, Sakurai K, Takahashi H (2011) OsHMA3, a P1B‐type of ATPase affects root‐to‐shoot cadmium translocation in rice by mediating efflux into vacuoles. New Phytologist **189:** 190-199

Mizoguchi M, Umezawa T, Nakashima K, Kidokoro S, Takasaki H, Fujita Y, Yamaguchi-Shinozaki K, Shinozaki K (2010) Two Closely Related Subclass II SnRK2 Protein Kinases Cooperatively Regulate Drought-Inducible Gene Expression. Plant and Cell Physiology **51:** 842-847

Moller IM, Jensen PE, Hansson A (2007) Oxidative modifications to cellular components in plants. Annu Rev Plant Biol **58:** 459-481

Moorhead G, De Wever V, Templeton G, Kerk D (2009) Evolution of protein phosphatases in plants and animals. Biochem. J **417:** 401-409

Morel M, Crouzet J, Gravot A, Auroy P, Leonhardt N, Vavasseur A, Richaud P (2009) AtHMA3, a P1B-ATPase allowing Cd/Zn/Co/Pb vacuolar storage in Arabidopsis. Plant Physiology **149:** 894-904

Mori S, Nishizawa N (1987) Methionine as a dominant precursor of phytosiderophores in Graminaceae plants. Plant and Cell Physiology **28:** 1081-1092

Morrissey J, Baxter IR, Lee J, Li L, Lahner B, Grotz N, Kaplan J, Salt DE, Guerinot ML (2009) The ferroportin metal efflux proteins function in iron and cobalt homeostasis in Arabidopsis. Plant Cell **21:** 3326-3338

Mukherjee I, Campbell NH, Ash JS, Connolly EL (2006) Expression profiling of the Arabidopsis ferric chelate reductase (FRO) gene family reveals differential regulation by iron and copper. Planta **223:** 1178-1190

Murata Y, Ma JF, Yamaji N, Ueno D, Nomoto K, Iwashita T (2006) A specific transporter for iron (III)–phytosiderophore in barley roots. The Plant Journal **46:** 563-572

Mustroph A, Zanetti ME, Jang CJ, Holtan HE, Repetti PP, Galbraith DW, Girke T, Bailey-Serres J (2009) Profiling translatomes of discrete cell populations resolves altered cellular priorities during hypoxia in Arabidopsis. Proc Natl Acad Sci U S A **106:** 18843-18848

Nagasaka S, Takahashi M, Nakanishi-Itai R, Bashir K, Nakanishi H, Mori S, Nishizawa NK (2009) Time course analysis of gene expression over 24 hours in Fe-deficient barley roots. Plant Molecular Biology **69:** 621-631

Nair R, Rost B (2005) Mimicking cellular sorting improves prediction of subcellular localization. Journal of Molecular Biology **348:** 85-100

Nakaminami K, Matsui A, Shinozaki K, Seki M (2012) RNA regulation in plant abiotic stress responses. Biochimica Et Biophysica Acta **1819:** 149-153

Nakanishi H, Yamaguchi H, Sasakuma T, Nishizawa NK, Mori S (2000) Two dioxygenase genes, Ids3 and Ids2, from Hordeum vulgare are involved in the biosynthesis of mugineic acid family phytosiderophores. Plant Molecular Biology **44:** 199-207

Nakashima K, Fujita Y, Katsura K, Maruyama K, Narusaka Y, Seki M, Shinozaki K, Yamaguchi-Shinozaki K (2006) Transcriptional regulation of ABI3- and ABA-responsive genes including RD29B and RD29A in seeds, germinating embryos, and seedlings of Arabidopsis. Plant Molecular Biology **60:** 51-68

Nawrath C, Schell J, Koncz C (1990) Homologous domains of the largest subunit of eucaryotic RNA polymerase II are conserved in plants. Molecular and General Genetics MGG **223:** 65-75

NCM (2003) Cadmium Review. Vol 1. Copenhagen

Nishimura N, Yoshida T, Kitahata N, Asami T, Shinozaki K, Hirayama T (2007) ABA-Hypersensitive Germination1 encodes a protein phosphatase 2C, an essential component of abscisic acid signaling in Arabidopsis seed. Plant Journal **50:** 935-949

Nocito FF, Lancilli C, Dendena B, Lucchini G, Sacchi GA (2011) Cadmium retention in rice roots is influenced by cadmium availability, chelation and translocation. Plant, Cell & Environment **34:** 994-1008

Nodzon LA, Xu WH, Wang Y, Pi LY, Chakrabarty PK, Song WY (2004) The ubiquitin ligase XBAT32 regulates lateral root development in Arabidopsis. The Plant Journal **40:** 996-1006

Nordberg G (2003) Cadmium and human health: a perspective based on recent studies in China. The Journal of Trace Elements in Experimental Medicine **16:** 307-319

Nordberg GF (2009) Historical perspectives on cadmium toxicology. Toxicology and Applied Pharmacology **238:** 192-200

Nouet C, Motte P, Hanikenne M (2011) Chloroplastic and mitochondrial metal homeostasis. Trends in Plant Science **16:** 395-404

Ogawa Ki (2005) Glutathione-associated regulation of plant growth and stress responses. Antioxidants & redox signaling **7:** 973-981

Oki H, Kim S, Nakanishi H, Takahashi M, Yamaguchi H, Mori S, Nishizawa NK (2004) Directed evolution of yeast ferric reductase to produce plants with tolerance to iron deficiency in alkaline soils. Soil Science and Plant Nutrition **50:** 1159-1165

Oliver B, Parisi M, Clark D (2002) Gene expression neighborhoods. Journal of Biology **1:** 4-6

Osawa H, Stacey G, Gassmann W (2006) ScOPT1 and AtOPT4 function as proton-coupled oligopeptide transporters with broad but distinct substrate specificities. Biochemical Journal **393:** 267

Palmer CM, Guerinot ML (2009) Facing the challenges of Cu, Fe and Zn homeostasis in plants. Nat Chem Biol **5:** 333-340

Pan A, Yang M, Tie F, Li L, Chen Z, Ru B (1994) Expression of mouse metallothionein-I gene confers cadmium resistance in transgenic tobacco plants. Plant Molecular Biology **24:** 341-351

Papoyan A, Kochian LV (2004) Identification of Thlaspi caerulescens genes that may be involved in heavy metal hyperaccumulation and tolerance. Characterization of a novel heavy metal transporting ATPase. Plant Physiology **136:** 3814-3823

Patel AA (2007) Role of the Arabidopsis peptide transporter *AtOPT6* in heavy metal detoxification and plant-pathogen interaction. University of Missouri

Peiter E, Montanini B, Gobert A, Pedas P, Husted S, Maathuis FJ, Blaudez D, Chalot M, Sanders D (2007) A secretory pathway-localized cation diffusion facilitator confers plant manganese tolerance. Proceedings of the National Academy of Sciences **104:** 8532-8537

Petit J, Briat J, Lobreaux S (2001) Structure and differential expression of the four members of the Arabidopsis thaliana ferritin gene family. Biochem. J **359:** 575-582

Petit JM, van Wuytswinkel O, Briat JF, Lobreaux S (2001) Characterization of an iron-dependent regulatory sequence involved in the transcriptional control of AtFer1 and ZmFer1 plant ferritin genes by iron. J Biol Chem **276:** 5584-5590

Phatnani HP, Greenleaf AL (2006) Phosphorylation and functions of the RNA polymerase II CTD. Genes & Development **20:** 2922-2936

Pich A, Manteuffel R, Hillmer S, Scholz G, Schmidt W (2001) Fe homeostasis in plant cells: does nicotianamine play multiple roles in the regulation of cytoplasmic Fe concentration? Planta **213:** 967-976

Pich A, Scholz G (1996) Translocation of copper and other micronutrients in tomato plants (Lycopersicon esculentum Mill.): nicotianamine-stimulated copper transport in the xylem. Journal of Experimental Botany **47:** 41-47

Pietrini F, Iannelli MA, Pasqualini S, Massacci A (2003) Interaction of cadmium with glutathione and photosynthesis in developing leaves and chloroplasts of Phragmites australis (Cav.) Trin. ex Steudel. Plant Physiology **133:** 829-837

Pike S, Patel A, Stacey G, Gassmann W (2009) Arabidopsis OPT6 is an oligopeptide transporter with exceptionally broad substrate specificity. Plant and Cell Physiology **50:** 1923-1932

Pineau C, Loubet S, Lefoulon C, Chalies C, Fizames C, Lacombe B, Ferrand M, Loudet O, Berthomieu P, Richard O (2012) Natural Variation at the FRD3 MATE Transporter Locus Reveals Cross-Talk between Fe Homeostasis and Zn Tolerance in Arabidopsis thaliana. PLoS Genetics **8:** e1003120

Plaza S, Tearall KL, Zhao F-J, Buchner P, McGrath SP, Hawkesford MJ (2007) Expression and functional analysis of metal transporter genes in two contrasting ecotypes of the hyperaccumulator Thlaspi caerulescens. Journal of Experimental Botany **58:** 1717-1728

Polle A, Schützendübel A (2004) Heavy metal signalling in plants: linking cellular and organismic responses. *In* Plant responses to abiotic stress. Springer, pp 187-215

Poschenrieder C, Tolra R, Barceló J (2006) Can metals defend plants against biotic stress? Trends in Plant Science **11:** 288-295

Prasad ME, Schofield A, Lyzenga W, Liu H, Stone SL (2010) Arabidopsis RING E3 ligase XBAT32 regulates lateral root production through its role in ethylene biosynthesis. Plant physiology **153:** 1587-1596

Price N, Morel F (1990) Cadmium and cobalt substitution for zinc in a marine diatom. Nature **344:** 658-660

Programme UNE (2008) Draft Final Review of Scientific Information on Cadmium. New York

Puig S, Andres-Colas N, Garcia-Molina A, Penarrubia L (2007) Copper and iron homeostasis in Arabidopsis: responses to metal deficiencies, interactions and biotechnological applications. Plant Cell and Environment **30:** 271-290

Ramachandran V, Chen X (2008) Small RNA metabolism in Arabidopsis. Trends Plant Sci **13:** 368-374

Rampey RA, Woodward AW, Hobbs BN, Tierney MP, Lahner B, Salt DE, Bartel B (2006) An Arabidopsis basic helix-loop-helix leucine zipper protein modulates metal homeostasis and auxin conjugate responsiveness. Genetics **174:** 1841-1857

Ravanel S, Droux M, Douce R (1995) Methionine Biosynthesis in Higher-Plants. 1. Purification and Characterization of Cystathionine γ-Synthase from Spinach Chloroplasts. Archives of Biochemistry And Biophysics **316:** 572-584

Ravet K, Touraine B, Boucherez J, Briat JF, Gaymard F, Cellier F (2009) Ferritins control interaction between iron homeostasis and oxidative stress in Arabidopsis. The Plant Journal **57:** 400-412

Ravet K, Touraine B, Kim SA, Cellier F, Thomine S, Guerinot ML, Briat JF, Gaymard F (2009) Post-Translational Regulation of AtFER2 Ferritin in Response to Intracellular Iron Trafficking during Fruit Development in Arabidopsis. Molecular Plant **2:** 1095-1106

Rea PA (2007) Plant ATP-binding cassette transporters. Annu. Rev. Plant Biol. **58:** 347-375

Rellan-Alvarez R, Giner-Martinez-Sierra J, Orduna J, Orera I, Rodriguez-Castrillon JA, Garcia-Alonso JI, Abadia J, Alvarez-Fernandez A (2010) Identification of a tri-iron(III), tri-citrate complex in the xylem sap of iron-deficient tomato resupplied with iron: new insights into plant iron long-distance transport. Plant Cell Physiol **51:** 91-102

Reuß O, Morschhäuser J (2006) A family of oligopeptide transporters is required for growth of Candida albicans on proteins. Molecular Microbiology **60:** 795-812

Ricachenevsky FK, Menguer PK, Sperotto RA, Williams LE, Fett JP (2013) Roles of plant metal tolerance proteins (MTP) in metal storage and potential use in biofortification strategies. Frontiers in Plant Science **4:** 1-16

Robinson NJ, Procter CM, Connolly EL, Guerinot ML (1999) A ferric-chelate reductase for iron uptake from soils. Nature **397:** 694-697

Rodecap KD, Tingey DT, Lee EH (1994) Iron nutrition influence on cadmium accumulation by Arabidopsis thaliana (L.) Heynh. Journal of Environmental Quality **23:** 239-246

Rogers EE, Guerinot ML (2002) FRD3, a member of the multidrug and toxin efflux family, controls iron deficiency responses in Arabidopsis. Plant Cell **14:** 1787-1799

Romera FJ, García MJ, Alcántara E, Pérez-Vicente R (2011) Latest findings about the interplay of auxin, ethylene and nitric oxide in the regulation of Fe deficiency responses by Strategy I plants. Plant Signaling & Behavior **6:** 167-170

Romheld V (1987) Different strategies for iron acquisition in higher-plants. Physiologia Plantarum **70:** 231-234

Roschzttardtz H, Conejero G, Curie C, Mari S (2009) Identification of the Endodermal Vacuole as the Iron Storage Compartment in the Arabidopsis Embryo. Plant Physiology **151:** 1329-1338

Roschzttardtz H, Grillet L, Isaure MP, Conéjéro G, Ortega R, Curie C, Mari S (2011) Plant Cell Nucleolus as a Hot Spot for Iron. Journal of Biological Chemistry **286:** 27863-27866

Roschzttardtz H, Séguéla-Arnaud M, Briat JF, Vert G, Curie C (2011) The FRD3 citrate effluxer promotes iron nutrition between symplastically disconnected tissues throughout Arabidopsis development. The Plant Cell Online **23:** 2725-2737

Rudolph A, Becker R, Scholz G, Procházka Ž, Toman J, Macek T, Herout V (1985) The occurrence of the amino acid nicotianamine in plants and microorganisms. A reinvestigation. Biochemie und Physiologie der Pflanzen **180:** 557-563

Salt DE, Prince RC, Pickering IJ, Raskin I (1995) Mechanisms of cadmium mobility and accumulation in Indian mustard. Plant Physiology **109:** 1427-1433

Salvail H, Massé E (2012) Regulating iron storage and metabolism with RNA: an overview of posttranscriptional controls of intracellular iron homeostasis. Wiley Interdisciplinary Reviews: RNA **3:** 26-36

Salzman RA, Brady JA, Finlayson SA, Buchanan CD, Summer EJ, Sun F, Klein PE, Klein RR, Pratt LH, Cordonnier-Pratt MM, Mullet JE (2005) Transcriptional profiling of sorghum induced by methyl jasmonate, salicylic acid, and aminocyclopropane carboxylic acid reveals cooperative regulation and novel gene responses. Plant Physiology **138:** 352-368

Samira R, Stallmann A, Massenburg LN, Long TA (2013) Ironing out the Issues-Integrated Approaches to Understanding Iron Homeostasis in Plants. Plant Science **210:** 250-259

Sanita di Toppi L, Gabbrielli R (1999) Response to cadmium in higher plants. Environmental and Experimental Botany **41:** 105-130

Santi S, Schmidt W (2009) Dissecting iron deficiency-induced proton extrusion in Arabidopsis roots. New Phytol **183:** 1072-1084

Sasaki A, Yamaji N, Xia J, Ma JF (2011) OsYSL6 is involved in the detoxification of excess manganese in rice. Plant physiology **157:** 1832-1840

Satarug S, Baker JR, Urbenjapol S, Haswell-Elkins M, Reilly PE, Williams DJ, Moore MR (2003) A global perspective on cadmium pollution and toxicity in non-occupationally exposed population. Toxicology Letters **137:** 65-83

Satarug S, Garrett SH, Sens MA, Sens DA (2011) Cadmium, environmental exposure, and health outcomes. Ciência & Saúde Coletiva **16:** 2587-2602

Satoh-Nagasawa N, Mori M, Nakazawa N, Kawamoto T, Nagato Y, Sakurai K, Takahashi H, Watanabe A, Akagi H (2012) Mutations in rice (Oryza sativa) heavy metal ATPase 2 (OsHMA2) restrict the translocation of zinc and cadmium. Plant and Cell Physiology **53:** 213-224

Schaaf G, Honsbein A, Meda AR, Kirchner S, Wipf D, von Wirén N (2006) AtIREG2 encodes a tonoplast transport protein involved in iron-dependent nickel detoxification in Arabidopsis thaliana roots. Journal of Biological Chemistry **281:** 25532-25540

Schaaf G, Ludewig U, Erenoglu BE, Mori S, Kitahara T, von Wirén N (2004) ZmYS1 functions as a proton-coupled symporter for phytosiderophore-and nicotianamine-chelated metals. Journal of Biological Chemistry **279:** 9091-9096

Schaaf G, Schikora A, Häberle J, Vert G, Ludewig U, Briat J-F, Curie C, von Wirén N (2005) A putative function for the Arabidopsis Fe–phytosiderophore transporter homolog AtYSL2 in Fe and Zn homeostasis. Plant and Cell Physiology **46:** 762-774

Schagerlöf U, Wilson G, Hebert H, Al-Karadaghi S, Hägerhäll C (2006) Transmembrane topology of FRO2, a ferric chelate reductase from Arabidopsis thaliana. Plant Molecular Biology **62:** 215-221

Schat H, Llugany M, VOOiJS R, Hartley‐Whitaker J, Bleeker PM (2002) The role of phytochelatins in constitutive and adaptive heavy metal tolerances in hyperaccumulator and non‐hyperaccumulator metallophytes. Journal of Experimental Botany **53:** 2381-2392

Schmidke I, Stephan UW (1995) Transport of metal micronutrients in the phloem of castor bean (Ricinus communis) seedlings. Physiologia Plantarum **95:** 147-153

Schmidt W (1999) Mechanisms and regulation of reduction-based iron uptake in plants. New Phytologist **141:** 1-26

Schmidt W, Buckhout TJ (2011) A hitchhiker's guide to the Arabidopsis ferrome. Plant Physiol Biochem **49:** 462-470

Schuler M, Keller A, Backes C, Philippar K, Lenhof HP, Bauer P (2011) Transcriptome analysis by GeneTrail revealed regulation of functional categories in response to alterations of iron homeostasis in Arabidopsis thaliana. BMC Plant Biology **11:** 87-93

Schwacke R, Schneider A, van der Graaff E, Fischer K, Catoni E, Desimone M, Frommer WB, Flügge U-I, Kunze R (2003) ARAMEMNON, a novel database for Arabidopsis integral membrane proteins. Plant Physiology **131:** 16-26

Seguela M, Briat JF, Vert G, Curie C (2008) Cytokinins negatively regulate the root iron uptake machinery in Arabidopsis through a growth-dependent pathway. Plant Journal **55:** 289-300

Seki M, Ishida J, Narusaka M, Fujita M, Nanjo T, Umezawa T, Kamiya A, Nakajima M, Enju A, Sakurai T, Satou M, Akiyama K, Yamaguchi-Shinozaki K, Carninci P, Kawai J, Hayashizaki Y, Shinozaki K (2002) Monitoring the expression pattern of around 7,000 Arabidopsis genes under ABA treatments using a full-length cDNA microarray. Funct Integr Genomics **2:** 282–291

Seki M, Narusaka M, Ishida J, Nanjo T, Fujita M, Oono Y, Kamiya A, Nakajima M, Enju A, Sakurai T, Satou M, Akiyama K, Taji T, Yamaguchi-Shinozaki K, Carninci P, Kawai J, Hayashizaki Y, Shinozaki K (2002) Monitoring the expression profiles of 7000 Arabidopsis genes under drought, cold and high-salinity stresses using a full-length cDNA microarray. Plant Journal **31:** 279-292

Seo PJ, Park J, Park MJ, Kim YS, Kim SG, Jung JH, Park CM (2012) A Golgi-localized MATE transporter mediates iron homoeostasis under osmotic stress in Arabidopsis. Biochemical Journal **442:** 551-561

Shahzad Z, Gosti F, Frérot H, Lacombe E, Roosens N, Saumitou-Laprade P, Berthomieu P (2010) The five AhMTP1 zinc transporters undergo different evolutionary fates towards adaptive evolution to zinc tolerance in Arabidopsis halleri. PLoS Genetics **6:** e1000911

Shin L-J, Lo J-C, Chen G-H, Callis J, Fu H, Yeh K-C (2013) IRT1 DEGRADATION FACTOR1, a RING E3 Ubiquitin Ligase, Regulates the Degradation of IRON-REGULATED TRANSPORTER1 in Arabidopsis. The Plant Cell Online **25:** 3039-3051

Shojima S, Nishizawa N-K, Fushiya S, Nozoe S, Irifune T, Mori S (1990) Biosynthesis of Phytosiderophores In Vitro Biosynthesis of 2-Deoxymugineic Acid from l-Methionine and Nicotianamine. Plant Physiology **93:** 1497-1503

Siedlecka A, Krupa Z (1996) Interaction between cadmium and iron and its effects on photosynthetic capacity of primary leaves of Phaseolus vulgaris. Plant Physiology and Biochemistry **34:** 833-841

Singh BR, McLaughlin MJ (1999) Cadmium in soils and plants. Springer

Sivitz A, Grinvalds C, Barberon M, Curie C, Vert G (2011) Proteasome-mediated turnover of the transcriptional activator FIT is required for plant iron-deficiency responses. Plant Journal **66:** 1044-1052

Sivitz AB, Hermand V, Curie C, Vert G (2012) Arabidopsis bHLH100 and bHLH101 Control Iron Homeostasis via a FIT-Independent Pathway. PloS one **7:** e44843

Smolders EM, Jelle (2013) Cadmium. *In* Heavy Metals in Soils, Vol 22. Springer, pp 283-311

Song W-Y, Choi KS, Geisler M, Park J, Vincenzetti V, Schellenberg M, Kim SH, Lim YP, Noh EW, Lee Y (2010) Arabidopsis PCR2 is a zinc exporter involved in both zinc extrusion and long-distance zinc transport. The Plant Cell Online **22:** 2237-2252

Song W-Y, Martinoia E, Lee J, Kim D, Kim D-Y, Vogt E, Shim D, Choi KS, Hwang I, Lee Y (2004) A novel family of cys-rich membrane proteins mediates cadmium resistance in Arabidopsis. Plant Physiology **135:** 1027-1039

Song W-Y, Park J, Mendoza-Cózatl DG, Suter-Grotemeyer M, Shim D, Hörtensteiner S, Geisler M, Weder B, Rea PA, Rentsch D (2010) Arsenic tolerance in Arabidopsis is mediated by two ABCC-type phytochelatin transporters. Proceedings of the National Academy of Sciences **107:** 21187-21192

Stacey G, Koh S, Granger C, Becker JM (2002) Peptide transport in plants. Trends in Plant Science **7:** 257-263

Stacey M, Osawa, H, Patel, A, Gassmann, W, Stacey, G (2006) Expression analyses of Arabidopsis oligopeptide transporters during seed germination, vegetative growth and reproduction. Planta **223:** 291-305

Stacey MG, Koh S, Becker J, Stacey G (2002) AtOPT3, a member of the oligopeptide transporter family, is essential for embryo development in Arabidopsis. The Plant Cell Online **14:** 2799-2811

Stacey MG, Osawa H, Patel A, Gassmann W, Stacey G (2006) Expression analyses of Arabidopsis oligopeptide transporters during seed germination, vegetative growth and reproduction. Planta **223:** 291-305

Stacey MG, Patel A, McClain WE, Mathieu M, Remley M, Rogers EE, Gassmann W, Blevins DG, Stacey G (2008) The Arabidopsis AtOPT3 protein functions in metal homeostasis and movement of iron to developing seeds. Plant Physiology **146:** 589-601

Stephan UW, Scholz G (1993) Nicotianamine: mediator of transport of iron and heavy metals in the phloem? Physiologia Plantarum **88:** 522-529

Stephan UW, Scholz G, Rudolph A (1990) Distribution of Nicotianamine, a Presumed Symplast Iron Transporter, in Different Organs of Sunflower and of a Tomato Wild Type and Its Mutant *chloronerva*. Biochemie und Physiologie der Pflanzen **186:** 81-88

Stroud H, Greenberg MV, Feng S, Bernatavichute YV, Jacobsen SE (2013) Comprehensive Analysis of Silencing Mutants Reveals Complex Regulation of the *Arabidopsis* Methylome. Cell **152:** 352-364

Sun Q, Ye Z, Wang X, Wong M (2005) Increase of glutathione in mine population of *Sedum alfredii*: A Zn hyperaccumulator and Pb accumulator. Phytochemistry **66:** 2549-2556

Sun Q, Ye ZH, Wang XR, Wong MH (2007) Cadmium hyperaccumulation leads to an increase of glutathione rather than phytochelatins in the cadmium hyperaccumulator *Sedum alfredii*. Journal of Plant Physiology **164:** 1489-1498

Takagi S-i (1976) Naturally occurring iron-chelating compounds in oat-and rice-root washings: I. Activity Measurement and Preliminary Characterization. Soil Science And Plant Nutrition **22:** 423-433

Takagi Si, Nomoto K, Takemoto T (1984) Physiological aspect of mugineic acid, a possible phytosiderophore of graminaceous plants. Journal of Plant Nutrition **7:** 469-477

Takahashi M, Yamaguchi H, Nakanishi H, Shioiri T, Nishizawa N-K, Mori S (1999) Cloning two genes for nicotianamine aminotransferase, a critical enzyme in iron acquisition (Strategy II) in graminaceous plants. Plant Physiology **121:** 947-956

Takahashi R, Bashir K, Ishimaru Y, Nishizawa NK, Nakanishi H (2012) The role of heavy-metal ATPases, HMAs, in zinc and cadmium transport in rice. Plant Signaling & Behavior **7:** 1605-1607

Takahashi R, Ishimaru Y, Shimo H, Ogo Y, Senoura T, Nishizawa NK, Nakanishi H (2012) The OsHMA2 transporter is involved in root-to-shoot translocation of Zn and Cd in rice. Plant Cell and Environment **35:** 1948-1957

Talke IN, Hanikenne M, Krämer U (2006) Zinc-dependent global transcriptional control, transcriptional deregulation, and higher gene copy number for genes in metal homeostasis of the hyperaccumulator Arabidopsis halleri. Plant Physiology **142:** 148-167

Tamura K, Peterson D, Peterson N, Stecher G, Nei M, Kumar S (2011) MEGA5: molecular evolutionary genetics analysis using maximum likelihood, evolutionary distance, and maximum parsimony methods. Molecular Biology And Evolution **28:** 2731-2739

Teng Y-S, Su Y-s, Chen L-J, Lee YJ, Hwang I, Li H-m (2006) Tic21 is an essential translocon component for protein translocation across the chloroplast inner envelope membrane. The Plant Cell Online **18:** 2247-2257

Teschner J, Lachmann N, Schulze J, Geisler M, Selbach K, Santamaria-Araujo J, Balk J, Mendel RR, Bittner F (2010) A novel role for Arabidopsis mitochondrial ABC transporter ATM3 in molybdenum cofactor biosynthesis. The Plant Cell Online **22:** 468-480

Thapa G, Sadhukhan A, Panda SK, Sahoo L (2012) Molecular mechanistic model of plant heavy metal tolerance. Biometals **25:** 489-505

Thibaud M-C, Arrighi, J.-F., Bayle, V., Chiarenza, S., Creff, A., Bustos, R., Paz-Ares, J., Poirier, Y., and Nussaume, L. (2010) Dissection of local and systemic transcriptional responses to phosphate starvation in Arabidopsis. Plant Journal **64:** 775–789

Thibaud MC, Arrighi JF, Bayle V, Chiarenza S, Creff A, Bustos R, Paz-Ares J, Poirier Y, Nussaume L (2010) Dissection of local and systemic transcriptional responses to phosphate starvation in Arabidopsis. Plant J **64:** 775-789

Thomine S, Lanquar V (2011) Iron Transport and Signaling in Plants. Transporters and Pumps in Plant Signaling**:** 99-131

Thomine S, Vert G (2013) Iron transport in plants: better be safe than sorry. Current Opinion in Plant Biology

Tonks NK (2006) Protein tyrosine phosphatases: from genes, to function, to disease. Nature Reviews Molecular Cell Biology **7:** 833-846

Traina S (1999) The environmental chemistry of cadmium. *In* Cadmium in soils and plants. Springer, pp 11-37

Tsay Y-F, Chiu C-C, Tsai C-B, Ho C-H, Hsu P-K (2007) Nitrate transporters and peptide transporters. FEBS Letters **581:** 2290-2300

Ueda A, Li P, Feng Y, Vikram M, Kim S, Kang CH, Kang JS, Bahk JD, Lee SY, Fukuhara T (2008) The Arabidopsis thaliana carboxyl-terminal domain phosphatase-like 2 regulates plant growth, stress and auxin responses. Plant Molecular Biology **67:** 683-697

Ueda A, Li P, Feng Y, Vikram M, Kim S, Kang CH, Kang JS, Bahk JD, Lee SY, Fukuhara T, Staswick PE, Pepper AE, Koiwa H (2008) The Arabidopsis thaliana carboxyl-terminal domain phosphatase-like 2 regulates plant growth, stress and auxin responses. Plant Molecular Biology **67:** 683-697

Ueno D, Milner MJ, Yamaji N, Yokosho K, Koyama E, Clemencia Zambrano M, Kaskie M, Ebbs S, Kochian LV, Ma JF (2011) Elevated expression of TcHMA3 plays a key role in the extreme Cd tolerance in a Cd‐hyperaccumulating ecotype of Thlaspi caerulescens. The Plant Journal **66:** 852-862

Ueno D, Milner MJ, Yamaji N, Yokosho K, Koyama E, Zambrano MC, Kaskie M, Ebbs S, Kochian LV, Ma JF (2011) Elevated expression of TcHMA3 plays a key role in the extreme Cd tolerance in a Cd-hyperaccumulating ecotype of Thlaspi caerulescens. Plant Journal **66:** 852-862

Ueno D, Rombola A, Iwashita T, Nomoto K, Ma J (2007) Identification of two novel phytosiderophores secreted by perennial grasses. New Phytologist **174:** 304-310

Ueno D, Yamaji N, Kono I, Huang CF, Ando T, Yano M, Ma JF (2010) Gene limiting cadmium accumulation in rice. Proceedings of the National Academy of Sciences **107:** 16500-16505

Ueno D, Yamaji N, Ma JF (2009) Further characterization of ferric-phytosiderophore transporters ZmYS1 and HvYS1 in maize and barley. Journal of Experimental Botany **60:** 3513-3520

Undan J, Tamiru M, Abe A, Yoshida K, Kosugi S, Takagi H, Yoshida K, Kanzaki H, Saitoh H, Fekih R (2012) Mutation in *OsLMS*, a gene encoding a protein with two double-stranded RNA binding motifs, causes lesion mimic phenotype and early senescence in rice (*Oryza sativa L.*). Genes Genet. Syst **87:** 169-179

Usuda K, Wada Y, Ishimaru Y, Kobayashi T, Takahashi M, Nakanishi H, Nagato Y, Mori S, Nishizawa NK (2009) Genetically engineered rice containing larger amounts of nicotianamine to enhance the antihypertensive effect. Plant Biotechnology Journal **7:** 87-95

Van Trung Nguyen TK, Michels AA, Bensaude O (2001) 7SK small nuclear RNA binds to and inhibits the activity of CDK9/cyclin T complexes. Nature **414:** 322-325

Varotto C, Maiwald D, Pesaresi P, Jahns P, Salamini F, Leister D (2002) The metal ion transporter IRT1 is necessary for iron homeostasis and efficient photosynthesis in Arabidopsis thaliana. Plant Journal **31:** 589-599

Vasconcelos M, Eckert H, Arahana V, Graef G, Grusak MA, Clemente T (2006) Molecular and phenotypic characterization of transgenic soybean expressing the Arabidopsis ferric chelate reductase gene, FRO2. Planta **224:** 1116-1128

Vasconcelos MW, Li GW, Lubkowitz MA, Grusak MA (2008) Characterization of the PT clade of oligopeptide transporters in rice. The Plant Genome **1:** 77-88

Vatamaniuk OK, Mari S, Lu Y-P, Rea PA (1999) AtPCS1, a phytochelatin synthase from Arabidopsis: isolation and in vitro reconstitution. Proceedings of the National Academy of Sciences **96:** 7110-7115

Verbruggen N, Hermans C, Schat H (2009) Mechanisms to cope with arsenic or cadmium excess in plants. Current Opinion in Plant Biology **12:** 364-372

Verbruggen N, Hermans C, Schat H (2009) Molecular mechanisms of metal hyperaccumulation in plants. New Phytologist **181:** 759-776

Verret F, Gravot A, Auroy P, Leonhardt N, David P, Nussaume L, Vavasseur A, Richaud P (2004) Overexpression of AtHMA4 enhances root-to-shoot translocation of zinc and cadmium and plant metal tolerance. FEBS Letters **576:** 306-312

Verret F, Gravot A, Auroy P, Preveral S, Forestier C, Vavasseur A, Richaud P (2005) Heavy metal transport by AtHMA4 involves the N-terminal degenerated metal binding domain and the C-terminal His11 stretch. FEBS letters **579:** 1515-1522

Verrier PJ, Bird D, Burla B, Dassa E, Forestier C, Geisler M, Klein M, Kolukisaoglu Ü, Lee Y, Martinoia E (2008) Plant ABC proteins–a unified nomenclature and updated inventory. Trends in Plant Science **13:** 151-159

Vert G, Barberon M, Zelazny E, Seguela M, Briat JF, Curie C (2009) Arabidopsis IRT2 cooperates with the high-affinity iron uptake system to maintain iron homeostasis in root epidermal cells. Planta **229:** 1171-1179

Vert G, Briat JF, Curie C (2001) Arabidopsis IRT2 gene encodes a root‐periphery iron transporter. The Plant Journal **26:** 181-189

Vert G, Grotz N, Dedaldechamp F, Gaymard F, Guerinot ML, Briat JF, Curie C (2002) IRT1, an Arabidopsis transporter essential for iron uptake from the soil and for plant growth. Plant Cell **14:** 1223-1233

Visconti R, Palazzo L, Della Monica R, Grieco D (2012) Fcp1-dependent dephosphorylation is required for M-phase-promoting factor inactivation at mitosis exit. Nature Communications **3:** 894-905

von Wirén N, Klair S, Bansal S, Briat J-F, Khodr H, Shioiri T, Leigh RA, Hider RC (1999) Nicotianamine chelates both FeIII and FeII. Implications for metal transport in plants. Plant Physiology **119:** 1107-1114

Waldo GS, Wright E, Whang ZH, Briat JF, Theil EC, Sayers DE (1995) Formation of the ferritin iron mineral occurs in plastids. Plant Physiology **109:** 797-802

Walker DJ, Bernal MP (2004) The effects of copper and lead on growth and zinc accumulation of Thlaspi caerulescens J. and C. Presl: implications for phytoremediation of contaminated soils. Water, Air, and Soil Pollution **151:** 361-372

Wang HY, Klatte M, Jakoby M, Baumlein H, Weisshaar B, Bauer P (2007) Iron deficiency-mediated stress regulation of four subgroup Ib BHLH genes in Arabidopsis thaliana. Planta **226:** 897-908

Waters BM, Blevins DG, Eide DJ (2002) Characterization of FRO1, a pea ferric-chelate reductase involved in root iron acquisition. Plant Physiology **129:** 85-94

Waters BM, Chu HH, Didonato RJ, Roberts LA, Eisley RB, Lahner B, Salt DE, Walker EL (2006) Mutations in Arabidopsis yellow stripe-like1 and yellow stripe-like3 reveal their roles in metal ion homeostasis and loading of metal ions in seeds. Plant Physiology **141:** 1446-1458

Waters BM, Grusak MA (2008) Whole-plant mineral partitioning throughout the life cycle in Arabidopsis thaliana ecotypes Columbia, Landsberg erecta, Cape Verde Islands, and the mutant line ysl1ysl3. New Phytol **177:** 389-405

Waters BM, Lucena C, Romera FJ, Jester GG, Wynn AN, Rojas CL, Alcantara E, Perez-Vicente R (2007) Ethylene involvement in the regulation of the H+-ATPase CsHA1 gene and of the new isolated ferric reductase CsFRO1 and iron transporter CsIRT1 genes in cucumber plants. Plant Physiology and Biochemistry **45:** 293-301

Welch RM (1995) Micronutrient Nutrition of Plants. Critical Reviews in Plant Sciences **14:** 49-82

White JP (2012) Ion Uptake Mechanisms of Individual Cells and Roots: Short-distance Transport. *In* Marschner's Mineral Nutrition of Higher Plants, Ed 3rd. Academic Press, London ; Waltham, MA, pp 7-47

White PJ (2005) Studying calcium channels from the plasma membrane of plant root cells in planar lipid bilayers. Advances in planar lipid bilayers and liposomes **1:** 101-120

White PJ, Broadley MR (2003) Calcium in plants. Annals of Botany **92:** 487-511

White PJ, Brown PH (2010) Plant nutrition for sustainable development and global health. Annals of Botany **105:** 1073-1080

WHO (2002) The World Health Report 2002: Reducing risks, promoting healthy life. *In* A Lopez, ed. World Health Organization, Genova

Wiles AM, Cai H, Naider F, Becker JM (2006) Nutrient regulation of oligopeptide transport in Saccharomyces cerevisiae. Microbiology **152:** 3133-3145

Willems G, Dräger DB, Courbot M, Godé C, Verbruggen N, Saumitou-Laprade P (2007) The genetic basis of zinc tolerance in the metallophyte Arabidopsis halleri ssp. halleri (Brassicaceae): an analysis of quantitative trait loci. Genetics **176:** 659-674

Williams L, Miller A (2001) Transporters responsible for the uptake and partitioning of nitrogenous solutes. Annual Review Of Plant Biology **52:** 659-688

Wintz H, Fox T, Wu YY, Feng V, Chen W, Chang HS, Zhu T, Vulpe C (2003) Expression profiles of Arabidopsis thaliana in mineral deficiencies reveal novel transporters involved in metal homeostasis. J Biol Chem **278:** 47644-47653

Wirth J, Poletti S, Aeschlimann B, Yakandawala N, Drosse B, Osorio S, Tohge T, Fernie AR, Günther D, Gruissem W (2009) Rice endosperm iron biofortification by targeted and synergistic action of nicotianamine synthase and ferritin. Plant Biotechnology Journal **7:** 631-644

Wong CKE, Cobbett CS (2009) HMA P-type ATPases are the major mechanism for root-to-shoot Cd translocation in Arabidopsis thaliana. New Phytologist **181:** 71-78

Wong CKE, Jarvis RS, Sherson SM, Cobbett CS (2009) Functional analysis of the heavy metal binding domains of the Zn/Cd‐transporting ATPase, HMA2, in Arabidopsis thaliana. New Phytologist **181:** 79-88

Wu H, Chen C, Du J, Liu H, Cui Y, Zhang Y, He Y, Wang Y, Chu C, Feng Z, Li J, Ling HQ (2012) Co-overexpression FIT with AtbHLH38 or AtbHLH39 in Arabidopsis-enhanced cadmium tolerance via increased cadmium sequestration in roots and improved iron homeostasis of shoots. Plant Physiology **158:** 790-800

Wu H, Li L, Du J, Yuan Y, Cheng X, Ling H-Q (2005) Molecular and biochemical characterization of the Fe (III) chelate reductase gene family in Arabidopsis thaliana. Plant and Cell Physiology **46:** 1505-1514

Xiang C, Werner BL, E'Lise MC, Oliver DJ (2001) The biological functions of glutathione revisited in Arabidopsis transgenic plants with altered glutathione levels. Plant Physiology **126:** 564-574

Xiong L, Lee H, Ishitani M, Tanaka Y, Stevenson B, Koiwa H, Bressan RA, Hasegawa PM, Zhu J-K (2002) Repression of stress-responsive genes by FIERY2, a novel transcriptional regulator in Arabidopsis. Proceedings of the National Academy of Sciences **99:** 10899-10904

Yadav SK (2010) Heavy metals toxicity in plants: An overview on the role of glutathione and phytochelatins in heavy metal stress tolerance of plants. South African Journal of Botany **76:** 167-179

Yang TJW, Lin WD, Schmidt W (2010) Transcriptional Profiling of the Arabidopsis Iron Deficiency Response Reveals Conserved Transition Metal Homeostasis Networks. Plant Physiology **152:** 2130-2141

Yang Z, Zhu Q, Luo K, Zhou Q (2001) The 7SK small nuclear RNA inhibits the CDK9/cyclin T1 kinase to control transcription. Nature **414:** 317-322

Yen M-R, Tseng Y-H, Saier M (2001) Maize Yellow Stripe1, an iron-phytosiderophore uptake transporter, is a member of the oligopeptide transporter (OPT) family. Microbiology **147:** 2881-2883

Yeo M, Lee S-K, Lee B, Ruiz EC, Pfaff SL, Gill GN (2005) Small CTD phosphatases function in silencing neuronal gene expression. Science **307:** 596-600

Yeo M, Lin PS, Dahmus ME, Gill GN (2003) A novel RNA polymerase II C-terminal domain phosphatase that preferentially dephosphorylates serine 5. Journal of Biological Chemistry **278:** 26078-26085

Yi Y, Guerinot ML (1996) Genetic evidence that induction of root Fe(III) chelate reductase activity is necessary for iron uptake under iron deficiency. Plant Journal **10:** 835-844

Yuan L, Yang S, Liu B, Zhang M, Wu K (2012) Molecular characterization of a rice metal tolerance protein, OsMTP1. Plant Cell Reports **31:** 67-79

Yuan YX, Wu HL, Wang N, Li J, Zhao WN, Du J, Wang DW, Ling HQ (2008) FIT interacts with AtbHLH38 and AtbHLH39 in regulating iron uptake gene expression for iron homeostasis in Arabidopsis. Cell Research **18:** 385-397

Yuan YX, Zhang J, Wang DW, Ling HQ (2005) AtbHLH29 of Arabidopsis thaliana is a functional ortholog of tomato FER involved in controlling iron acquisition in strategy I plants. Cell Research **15:** 613-621

Zhai Z (2011) Identification of heavy metal transporters. Cornell university, 112 pages; 3485193, Cornell, NY

Zhai Z, Gayomba S, Jung H, Danku J, Rutzke M, Kochian L, Salt D, Vatamaniuk OK (2010) "Novel" Functions of "Old"Transporters: COPT2 and OPT3 Function in Cadmium Detoxification in *Arabidopsis thaliana*. *In* ASPB 2010, Montreal

Zhang H, Sun Y, Xie X, Kim MS, Dowd SE, Pare PW (2009) A soil bacterium regulates plant acquisition of iron via deficiency-inducible mechanisms. Plant Journal **58:** 568-577

Zhang HM, Sun Y, Xie XT, Kim MS, Dowd SE, Pare PW (2009) A soil bacterium regulates plant acquisition of iron via deficiency-inducible mechanisms. Plant Journal **58:** 568-577

Zhang M-Y, Bourbouloux A, Cagnac O, Srikanth CV, Rentsch D, Bachhawat AK, Delrot S (2004) A novel family of transporters mediating the transport of glutathione derivatives in plants. Plant Physiology **134:** 482-491

Zhang M, Yogesha S, Mayfield JE, Gill GN, Zhang Y (2013) Viewing serine/threonine protein phosphatases through the eyes of drug designers. FEBS Journal **280:** 4739-4760

Zhang X, Moréra S, Bates PA, Whitehead PC, Coffer AI, Hainbucher K, Nash RA, Sternberg MJ, Lindahl T, Freemont PS (1998) Structure of an XRCC1 BRCT domain: a new protein–protein interaction module. The EMBO Journal **17:** 6404-6411

Zhang Y, Kim Y, Genoud N, Gao J, Kelly JW, Pfaff SL, Gill GN, Dixon JE, Noel JP (2006) Determinants for dephosphorylation of the RNA polymerase II C-terminal domain by Scp1. Molecular Cell **24:** 759-770

Zhang Y, Xu YH, Yi HY, Gong JM (2012) Vacuolar membrane transporters OsVIT1 and OsVIT2 modulate iron translocation between flag leaves and seeds in rice. Plant Journal **72:** 400-410

Zhao FJ, Hamon RE, Lombi E, McLaughlin MJ, McGrath SP (2002) Characteristics of cadmium uptake in two contrasting ecotypes of the hyperaccumulator Thlaspi caerulescens. Journal of Experimental Botany **53:** 535-543

Zheng L, Cheng Z, Ai C, Jiang X, Bei X, Zheng Y, Glahn RP, Welch RM, Miller DD, Lei XG (2010) Nicotianamine, a novel enhancer of rice iron bioavailability to humans. PLoS One **5:** e10190

Zheng L, Fujii M, Yamaji N, Sasaki A, Yamane M, Sakurai I, Sato K, Ma JF (2011) Isolation and characterization of a barley yellow stripe-like gene, HvYSL5. Plant And Cell Physiology **52:** 765-774

Zhigang A, Cuijie L, Yuangang Z, Yejie D, Wachter A, Gromes R, Rausch T (2006) Expression of BjMT2, a metallothionein 2 from Brassica juncea, increases copper and cadmium tolerance in Escherichia coli and Arabidopsis thaliana, but inhibits root elongation in Arabidopsis thaliana seedlings. Journal of Experimental Botany **57:** 3575-3582

Zimmermann P, Hirsch-Hoffmann M, Hennig L, Gruissem W (2004) GENEVESTIGATOR. Arabidopsis microarray database and analysis toolbox. Plant Physiology **136:** 2621-2632

APPENDIX A

PRIMER SEQUENCES

AGI	Gene Description	Forward Primer	Reverse Primer
RT-QPCR Primers			
AT4G19690	IRON-RESPONSIVE TRANSPORTER 1 (IRT1)	(E15) ACCCGTGCGTCAACAAAGCTAAAG	(E16) TCCCGGAGGCGAAACACTTAATGA
AT2G27380	EXTENSIN PROLINE-RICH 1 (EPR1)	(E13) TGGTGGTCTTAGCCTTGTATTCC	(E14) ATGGTGGAGGACTGTTGTA
AT1G71250	GDSL-motif lipase/hydrolase family protein	(E11) TGGGTTGCATACCAGACCAA	(E12) TGGGTTGCATACCAGACCAA
AT1G73010	PHOSPHATE STARVATION-INDUCED GENE 2 (ATPS2)	(E29) GTGTCATCCCAGCCATCAAAT	(E30) TTGCGTCGCTCACTATTCTCA
AT3G21720	ISOCITRATE LYASE (ICL)	(E27) GGATTGCTAGGCTCGGATATTG	(E28) TCCTCTCCACATAAGCCAACATC
AT4G25140	OLEOSIN1 (OLEO1)	(E25) TGGTAACCGTTGCTCTCATCAT	(E26) ACTCTGCTTCCAACCTTCA
AT1G70840	MLP-like protein 31/ Bet v I allergen family protein (MLP31)	(E23) GCGAAAGCCACTCCTGACAT	(E24) CTGCCAACTTTGCCAAACTCT
AT1G73190	ALPHA-TONOPLAST INTRINSIC PROTEIN (TIP3.1)	(E339) GGTGCTCTTGTTGGAGGCAG	(E340) GCTCCAACACCTGATGCTAG
AT5G44120	12S seed storage protein (CRA1)	(E67) TATCCGTCAAAACGCAATGG	(E68) TTCCCCGTCTGTCACGTAAAG
AT5G62490	ABA-responsive protein (HVA22b)	(E59) TTTTGCTGATGTATCCACCGA	(E60) AGAAGGATGACGACTTGGGA
AT3G02040	SENESCENCE-RELATED GENE 3 (SRG3)	(E57) AGCCTATGTGGAGGAAGACA	(E58) AGCATCTTCAAGGGTACACA
AT5G55770	DC1 domain-containing protein	(E7) ATGTCGTCACCACCATCGTATC	(E8) ACAGACTCCGCAAGACCATTTT
AT2G15010	thionin, putative	(E73) GGTGCCTTAACGAGTCTCCAAA	(E74) CCTTGGTACATCGTTCAACC
AT3G15670	late embryogenesis abundant protein, putative / LEA protein, putative	(E83) AGGAGAAGACCAGTGGGATCTTG	(E84) TGCTTCACCGCATCAGTAGCT
AT3G28220	meprin and TRAF homology domain-containing protein / MATH domain-containing protein	(E341) GGTGGATACAACTGGACAC	(E342) GGAGAGTTAAGGAGTGTTGAA
AT3G17790	PURPLE ACID PHOSPHATASE 17 (PAP17)	(E343) CGTGGCTCCTTCAATCAGTC	(E344) GGAGCAGTGTAGATGTTAGAG
AT5G40420	OLEOSIN 2 (OLEO2)	(E345) GGTTATAGTCCCAGCGGCTC	(E346) GTCCCACGAAGATAGTTCATGAC
AT5G03860	MALATE SYNTHASE (MLS)	(E75) CTGATGAACTTAGTGGAAGGATCAAA	(E76) AGAGAGGCAAGACGGCGTTA
AT5G01220	SULFOLIPID SYNTHASE 2 (SQD2)/ UDP-sulfoquinovose:DAG sulfoquinovosyltransferase	(E95) GGCAAGAGAAGAGACCGAGAAA	(E96) CGCTGCACTGTACTGTTCATTG
AT1G17990	12-OXOPHYTODIENOATE REDUCTASE (OPR)	(E61) TCTGCCACCATGCCAAATC	(E62) CATTCCTCAGCCTAATGCCAAA
AT5G07990	TRANSPARENT TESTA 7 (TT7)/ FLAVONOID 3'-MONOOXYGENASE	(E347) GCACCTTACGGACACCGATG	(E348) CACACATGTTCACCAACTGGC
AT5G45820	CBL-INTERACTING PROTEIN KINASE 20 (CIPK20)	(E71) TGGCTTGCTTCACACGACAT	(E72) TCCATCATAACCTTTCTTGCCTATC
AT4G01340	CHP-rich zinc finger protein-related	(E9) TGGCTCTCTCTGGCGTCTTC	(E10) CTCTGGCTCTCTTCTCGGATTC
AT3G13950	expressed protein	(E5) CATAGAACCGCCACCACCAT	(E6) CATCATTGGCTTCCGATTCA
AT3G25820	TERPENE SYNTHASE 10 (TPS10)	(E93) ACCAATTTGGAGACCAGCAAGA	(E94) CCTGCTCATGTTTCCCCTGAT
AT3G49160	pyruvate kinase family protein	(E17) ATGGCTCTGCCTCACAGGAA	(E18) GTCTCCTCTTTCTCCCTCTAG
AT3G22740	HOMOCYSTEINE S-METHYLTRANSFERASE 3 (HMT3)	(E33) ACACCATCAGAGCCATTGCTAA	(E34) CTCCTTCCTGACATCACAAGCA
AT5G01600	FERRITIN 1 (FER1)	(E63) CGTTGCTATGAAGGGACTAG	(E64) CTGAGATAGGTGAGACGATAGG

AGI	Gene Description	Forward Primer	Reverse Primer
AT1G26250	proline-rich extensin, putative	(E87) TGGTGGTCTTAGCCTTGTATTCC	(E88) ATGGTGGAGGACTGTTGTA
AT3G27950	early nodule-specific protein, putative	(E89) TCTTCCTGCCAAAACCGTAAA	(E90) TTGGGTAGGGAGAGGTGGA
AT3G43190	SUCROSE SYNTHASE	(E99) TGCTCCAACGCATCAAACA	(E100) TCAGGAAGCAGCCGAGTGA
AT3G03060	AAA-type ATPase family protein	(E91) CACCATTCCGAAACATGATGTT	(E92) CCCGACTTCCGAGCAATCT
AT5G48000	cytochrome P450 family protein (THAH1)	(E45) GTAGCCGCTGTTGTGATTAGCA	(E46) AGAAGTCGCATGTCTCTCCGA
AT4G10270	wound-responsive family protein	(E51) GGAGACAGAAGACGAAGAGAAC	(E52) TGTGGCTCTTCTTCTCTGGTGCTT
AT1G49860	GLUTATHIONE S-TRANSFERASE (CLASS PHI) 14 (GSTF14)	(E47) GAGTCTCCTTACTTGGCTGGT	(E48) GCTACATTGGGACGTGAATAGAT
AT5G23020	2-ISOPRPYLMALATE SYNTHASE 2 (IMS2)	(E49) AGAGAGGCAAGACGGCGTTA	(E50) CTGATGAACTTAGTGGAAGGATCAAA
AT5G60950	COBRA-like protein 5 precursor	(E97) GGGCAAGGAGGTTGTTCCA	(E98) AATCGACAACTGTTGGCTTACGA
AT1G01580	FERRIC REDUCTION OXIDASE 2 (FRO2)	(E53) TGTGGCTCTTCTTCTCTGGTGCTT	(E54) TGCCACAAAGATTCGTCATGTGCG
AT2G28160	IRON-DEFICIENY INDUCED TRANSCRIPTION FACTOR 1 (FIT1)	(E55) ACCTCTTCGACGAATTGCCTGACT	(E56) TTCATCTTCTTCACCACCGGCTCT
AT5G52310	RESPONSIVE TO DESICCATION 29A (RD29A)	(E157) CAGCACCCAGAAGAAGTTGAACA	(E158) TCTTGCTCATGCTCATTGCTT
AT1G05510	unknown protein	(E103) CTCACGAGTGGGAAGTTAAAGGA	(E104) CTTGCCGTTGAATAGCTTCG
AT5G06760	LATE EMBRYOGENESIS ABUNDANT PROTEIN 4-5 (LEA 4-5)	(E115) TGGCATGGACAAAACCAAAG	(E116) TCTGAACAGGGTCTCGTGTCTTC
AT5G45690	unknown protein	(E119) TCCTAGCCGTCAGATTGAAGTC	(E120) GAGGAGTCGCAATCGTAAACAG
AT2G35300	LATE EMBRYOGENESIS ABUNDANT PROTEIN 4-2 (LEA 4-2/LEA18)	(E327) ATGCAGTCGGCGAAGGAAA	(E328)TGGTCCTTGCCATCGTCTTCT
AT5G66780	unknown protein	(E349) CCACCGTCTCGTTCTGCTC	(E350) GAATGCGACATCACGTCACC
AT5G07330	unknown protein	(E117) AGGCGACAACCGTACCAAGAT	(E118) CCTATGGAGACGTAAACTGGTG
AT3G02480	ABA-responsive protein-related/ LEA family protein	(E101) CAAGGATGCTGCTGCTTCA	(E102) GGTCTTGTCCTTGACGACAT
AT4G34710	Arginine decarboxylase 2 (SPE2/ADC2)	(E137) AACAATGTGGCGGCTTCTCT	(E138) GGCGATGCCTGCTCAGTT
AT5G06760	LATE EMBRYOGENESIS ABUNDANT PROTEIN 4-5 (LEA 4-5)	(E329) TCGGACAACCGCTCATAACAC	(E330) TTATCCAGTATATCCCCCGCC
AT3G58450	universal stress protein (USP) family protein/ Adenine nucleotide alpha hydrolases-like superfamily protein	(E135) CCGAACCAATGAGGAAAGCA	(E136) GCCTCGGCATATCTCCAATG
AT2G44460	glycosyl hydrolase family 1 protein (BGLU29)	(E127) ACTTCGAGTGGGAGCATGGA	(E128) GGATACCGTTGGAGATTGTTTTTG
AT1G67600	unknown protein	(E167) GAAACCAGACCTTTGCGTGAA	(E168) AACAAGATGACTAAGTACCCAACAAC
AT5G59030	COPPER TRANSPORTER 1 (COPT1)	(E69) CCGTGTTCTTGCCCCAAA	(E70) ATGAACGAAGGAGGAGGACATC
AT1G36370	SERINE HYDROXYMETHYLTRANSFERASE 6 (SHM6)	(E183) CATTTGCTTCTCTGGGATCTGA	(E184) CCACTTTGTTGACCGTGATATG
AT5G24660	response to low sulfur 2 (LSU2)	(E131) GAGGAGCGTCTCTGCTCACA	(E132) GAGTCTGAAGAAAGACGAGAGA
AT3G16360	HPT phosphotransmitter 4 (AHP4)	(E181) CGACGAACAATTCATGGAGTTAGA	(E182) ACTATCCAGCCGATTGAAATCA
AT1G12030	unknown protein	(E175) CGATGAAGCGAGCGGATATT	(E176) CCCTACTCACCACTTCGTTTGA
AT1G56430	nicotianamine synthase 3 (NAS3)	(E179) CGACCTCCTCGAACAAAACCTA	(E180) GAGGAAGAGGACCAGATCCAATG
AT4G16370	OLIGOPEPTIDE TRANSPORTER 3 (OPT3)	(E177) ACACCGCAGTTTGATCTGGAT	(E178) GCGAAAAGAGGGCTGAGGTA
AT1G08650	PHOSPHOENOLPYRUVATE CARBOXYLASE KINASE 1 (PPCK1)	(E185) TCGTCCATCCCTCTGTTTCG	(E186) CGTCTGAGGCTCAAAGAAGGTT
AT3G60140	glycosyl hydrolase family 1 protein (BGLU30)	(E171) GCTTGACCTCATGGGACGAA	(E172) CTCATCTCCATCGCCATTTTG
AT3G56970	BASIC HELIX-LOOP-HELIX 38 (BHLH38)	(E197) TGGTGTGTTTATCCACTAGTTCTCA	(E198) GGTCCAGATCAGTGTTAGATTCA
AT3G56980	BASIC HELIX-LOOP-HELIX 39 (BHLH39)	(E199) GGAGAGTACGACAGCTACTACCTC	(E201) CTGTAACAGCTCCATAAGTCTC
AT2G41240	BASIC HELIX-LOOP-HELIX 100 (BHLH100)	(E223) GACGACGTATCCAACACGTT	(E224) ATCACCACGGGATTGTCTAGT
AT5G04150	BASIC HELIX-LOOP-HELIX 101 (BHLH101)	(E225) CTCTCCATTTTCCTTCCTTCCT	(E226) TCTCCAAAACCACCGCTCCT

AGI	Gene Description	Forward Primer	Reverse Primer
AT3G47640	POPEYE (PYE)	(E231) CAGGACTTCCCATTTTCCAA	(E232) CTTGTGTCTGGGGATCAGGT
AT3G18290	BRUTUS (BTS)	(E227) GCTCTGGCACAAGTCAATCA	(E228) CGTTCATCAAATGCCGATAA
AT5G54680	IAA-LEUCINE RESISTANT 3 (ILR3)	(E229) AGCGCAAGGCCAAGCT	(E230) TTAAGCAACAGGAGGACGAAGGAC
AT4G30190	H(+)-ATPASE 2 (AHA2)	(E219) TGACTGATCTTCGATCCTCTCATG	(E220) GGTTTGGGAAGAGTTATGGCAAT
AT4G26080	ABA INSENSITIVE 1 (ABI1)	(E333) TGAAGAAGCGTGTGAGATGG	(E334) CTGTATCGCCAGCTTTGACA
AT3G24650	ABA INSENSITIVE 3 (ABI3)	(E260) GAGGAGGTTCTTGTCTCATC	(E261) CGATTTGGGTTTGGTTCTGC
AT5G62000	ABSCISIC ACID RESPONSIVE ELEMENTS-BINDING PROTEIN 2 (ABRBP1)/ ABSCISIC ACID RESPONSIVE ELEMENTS-BINDING FACTOR 2 (ABF2)	(Y982) AAAGAATCAGGAGACGGAGA	(Y983) AACACCTAAGTGGGATGTCA
AT3G08040	FERRIC REDUCTASE DEFECTIVE 3 (FRD3)	(E307) GGTCAGGCGATTCTGGCTTG	(E308) TTTATTGGCTGCGTTGCTGC
AT2G38460	FERROPORTIN 1 (FPN1)	(E309) GTTGCTCCCTTCTCGTGGAA	(E310) CCACCCCATTTCTAGTTATC
AT5G49740	FERRIC REDUCTION OXIDASE 7 (FRO7)	(E311) CGGTGAAGTGGAAGCAAATGG	(E312) GGTCTGGTGCCATAACGAATAG
AT4G24120	YELLOW STRIPE LIKE 1 (YSL1)	(E313) GCTCTGCCTCTTCACTGTCTC	(E314) GACAAGAAACGGAACAGCCAT
AT2G01770	VACUOLAR IRON TRANSPORTER 1 (VIT1)	(E317) GAAGTGGCAGAGATTCTGGCACA	(E318) GCTTTGTAACGCTCTTTTTGGATCAG
AT5G58270	ABC TRANSPORTER OF THE MITOCHONDRION 3 (MTA3)/ STARIK 1 (STA1)	(E319) GGACAGCACAACAGAGGCAG	(E320) CATCGCAGTGGTCAGCCTGT
AT2G23150	NATURAL RESISTANCE-ASSOCIATED MACROPHAGE PROTEIN 3 (NRAMP3)	(E321) CGTAAGAAACGAAGAGGAGG	(E322) CAAAGAGTACCCAGCAACCG
AT5G67330	NATURAL RESISTANCE-ASSOCIATED MACROPHAGE PROTEIN 4 (NRAMP4)	(E323) GAGAGCGTCCGTTATTAGCATC	(E324) GGGTCATCGTCGTAATCAGC
AT5G23860	BETA TUBULIN 8 (TUB8)	(E163) ATAACCGTTTCAAATTCTCTCTCTC	(E164) TGCAAATCGTTCTCTCCTTG
	18S ribosomal RNA	(E159) CATAAACGATGCCGACCAG	(E160) AGCCTTGCGACCATACTCC
TDNA PCR Primers			
	Allele		
	cpl1-6	(E149) GCTGATACTGAAGTGGAGAG	(E193) GAGACTGCTCGACGAATTTGA
	cpl1-5	(241) TGTATAGTAATAATAGAGTAGAAG	(E148) TCAGCCACTATAACGGCAAG
	fit-2	(E205) GTACCAAGAACATGCTCCTGA	(E206) GATCCACAGCTTCAGGTTAG
	GABI LB2	(1162) ATAACGCTGGGGACATCTAC	
	SALK LB1	(188) GCGTGGACCGCTTGCTGCAACT	
RT-PCR Primers			
AT3G18780	ACTIN 2 (ACT2)	(E161) TTCCCTCAGCACATTCCA	(E162) CCCATTCATAAAACCCCAGC
AT4G21670	C-TERMINAL DOMAIN PHOSPHATASE-LIKE 1 (CPL1)	Primer pairs of E149-E193 or 241-E148 were used for *cpl1-5* or *cpl1-6* mutants, respectively.	
FIT1 promoter		(1047)GGGAAGCTTCACCTAGATGGAATCTATAAT	(1048) CCTTCCAGATATCTGTTTTTGTCAATGAAG